CENTRAL BENZODIAZEPINE RECEPTORS IN HIPPOCAMPAL SCLEROSIS AND IDIOPATHIC GENERALISED EPILEPSIES

AND

OPIOID RECEPTORS IN READING EPILEPSY

Matthias Johannes Koepp, MD

Epilepsy Research Group,
University Department of Clinical Neurology,
National Hospital for Neurology and Neurosurgery,
Queen Square,

MRC Cyclotron Unit,
Hammersmith Hospital
DuCane Road,

London

Thesis submitted to the University of London for the
Degree of Doctor in Philosophy, 1999

ABSTRACT

Background:

Epilepsy is the most common serious disease of the brain. In order to better understand the processes and neuronal circuits involved in the pathophysiology of the epilepsies and to provide structural / functional correlations, positron emission tomography (PET) needs to be evaluated in the light of high quality MRI.

Aims:

- To determine the extent and amount of central benzodiazepine / $GABA_A$ receptor (cBZR) abnormalities in mesial temporal lobe epilepsy (mTLE) due to hippocampal sclerosis (HS)
- to quantify cBZR in idiopathic generalised epilepsy (IGE) and the effect of treatment with sodium valproate (VPA)
- to investigate dynamic changes of opioid receptors in reading epilepsy (RE) at the time of reading-induced seizures.

Methods:

^{11}C-flumazenil (FMZ)-PET scans of 37 controls, 25 candidates for temporal lobe resections with HS, and 10 patients with IGE before and after taking VPA, were analysed with statistical parametric mapping (SPM) and a partial-volume-effect (PVE) corrected regions-of-interest approach to quantify FMZ binding to cBZR.
Paired ^{11}C-diprenorphine (DPN)-PET scans of 6 control subjects and 5 patients with RE were analysed with SPM to detect significant localised reductions of DPN binding during reading-induced seizures implying a focal release of endogenous opioids.

Results:

- Using SPM, reductions of cBZR were restricted to the sclerotic hippocampus in unilateral mTLE.
- Using PVE correction loss of cBZR in HS was shown to be over and above that due to neurone loss and hippocampal atrophy.
- In-vivo ^{11}C-FMZ-PET correlated well with ex-vivo ^{3}H-FMZ autoradiography in HS.
- Subtle reductions of cBZR are seen contralaterally in unilateral mTLE in 30%.
- cBZR in IGE are increased in the cortex and thalamus, and FMZ binding is not affected by VPA.
- Endogenous opioids are released locally in the left temporo-parietal cortex at the time of reading-induced seizures.

Conclusions:

The identification of functional abnormalities of major inhibitory neurotransmitter systems, over and above structural abnormalities, has profound implications for the presurgical investigation of patients, in whom MRI does not reveal a relevant underlying lesion. Elucidation of the neurochemical and functional abnormalities underlying seizures assists the design of new anti-epileptic drugs and helps to identify neurochemical abnormalities underlying specific epilepsy syndromes.

ACKNOWLEDGMENTS

I would like first and foremost to thank all the subjects who took part in these studies. The work presented in this thesis was carried out within the MRC Cyclotron Unit, Hammersmith Hospital, London, and funded by a Project Grant from the Medical Research Council, UK, held by Professor John Duncan of the Epilepsy Research Group of the Institute of Neurology, Queen Square, London, and Professor David Brooks of the MRC Cyclotron Unit, Hammersmith Hospital London, and the work into Reading-Epilepsy co-funded by "The Welcome Clinical Epilepsy Research Stipendium 1994". The autoradiographic studies performed on hippocampal specimens from patients, who underwent temporal lobectomy, were undertaken by Professor Norman Bowery and Dr. Kieran Hand at the Department of Pharmacology, University of Birmingham.

I have been fortunate to have Professor John Duncan as my supervisor for the last 4 years. He was always ready to give advice when it was needed and has been a constant source of support and encouragement regarding my current research as well as my future career.

PET research is very much a team effort; I am grateful to Professors David Brooks and Terry Jones for their helpful guidance together with their contagious enthusiasm throughout. At the MRC Cyclotron Unit, I had the privilege to work with the best methods group and technical support staff available. In particular, the Radiochemistry section under Mr. Ian Watson, and the Blood Analysis Laboratory under Dr. Safiye Osman had provided a faultless supply of radiotracers and essential data; the Methods Section, particularly Drs. Vincent Cunningham, Roger Gunn, Ralph Myers, Simon Waters, and Leonard Schnorr had provided data analysis techniques which have made our investigations possible; and the Radiographers Andreanna Williams, Andrew Blythe, David Griffith and Hope McDewitt have provided good-humoured and excellent technical support in the scanning environment.

I have greatly enjoyed the friendship of the other neurological research fellows at the MRC Cyclotron Unit, of which the most valuable and important was with Dr. Mark Richardson. Mark "fought the same war" addressing similar problems using different strategies. We not only shared a room, hard- and software, but also solved most of these problems through lengthy discussions and mutual support. Our studies were based upon ground-breaking work by our predecessors Drs. Martin Prevett and Peter Bartenstein. I had the most challenging encounters with Dr. Claire Labbé, who developed, installed and maintained programs for partial volume effect correction (see Chapter IV to VII). Working with Claire improved my understanding of both, the Frenchs' and the physicists' world.

The PET work at the MRC Cyclotron Unit was only possible through collaborations within the Epilepsy Research Group at the National Hospital, set up, supervised and always encouraged by Professor John Duncan. Professor Simon Shorvon, Drs. Shelagh Smith, David Fish and Ley Sander of the National Hospital for Neurology generously referred patients for PET studies, most of them also had long-term video-EEG telemetry under the auspicious care of Catherine Scott. Drs. Samantha Free, Sanjay Sisodiya and Philippa Bartlett provided most of the MRI data, which had been quantified by Drs. Wim Van Paesschen and Friedrich Wörmann. Wim also performed the task of counting neurons on hippocampal specimens. I am grateful to Mr. William Harkness, who performed the surgical resections, and Drs. Maria Thom and Tomas Revesz for their neuropathological expertise in handling the specimens. Professor Norman Bowery and Dr. Kieran Hand undertook the invaluable task of validating our in-vivo PET data by performing ex-vivo autoradiography. This was the beginning of further closer collaborations and hopefully long friendships.

To Ronit, thank you for your love and care - I would never have done it without you.

AWARDS

Young Investigator Award, 21st International Epilepsy Congress, Sidney 1995
American Academy of Neurology - IAC Foreign Scholarship Award, Boston 1997
John Hopkins Prize, British Branch of the ILAE, Oxford 1997

ORIGINAL ARTICLES

1. **Koepp MJ**, Richardson MP, Brooks DJ & Duncan JS. Focal cortical release of endogenous opioids during reading induced seizures. ***Lancet*** 1998; 352: 952-955
2. **Koepp MJ,** Hand KSP, Labbé C, Richardson MP, Van Paesschen W, Baird VH, Cunningham VJ, Bowery NG, Brooks DJ Duncan JS. Flumazenil-PET correlates with ex-vivo ^{3}H-Flumazenil Autoradiography in Hippocampal Sclerosis. ***Annals of Neurology*** 1998; 43: 618-626
3. **Koepp MJ**, Hansen ML, Pressler RM, Brooks DJ, Brandl U, Guldin B, Duncan JS, Ried S. Comparison of EEG, MRI and PET in Reading Epilepsy: a case report. ***Epilepsy Research*** 1998; 29: 247-253
4. Koutroumanidis M, **Koepp MJ**, Richardson MP, Camfield C, Agathonikou A, Ried S, Duncan JS & Panayiotopoulos CP. The variants of Reading Epilepsy: a clinical and video-electroencephalographic study of 17 patients with reading-induced seizures. ***Brain*** 1998; 121: 1409-1427
5. **Koepp MJ**, Labbé C, Richardson MP, Brooks DJ, Cunningham VJ, Van Paesschen Duncan JS. Regional hippocampal 11C Flumazenil PET in Temporal Lobe Epilepsy with unilateral and bilateral hippocampal sclerosis. ***Brain*** 1997; 120: 1865-1876
6. **Koepp MJ**, Richardson MP, Labbé C, Brooks DJ, Cunningham VJ, Van Paesschen W, Revesz T, Duncan JS. 11C-Flumazenil PET, volumetric MRI and quantitative pathology in mesial Temporal Lobe Epilepsy. ***Neurology*** 1997; 49: 764-773
7. **Koepp MJ**, Richardson MP, Brooks DJ, Cunningham VJ & Duncan JS. Central benzodiazepine-$GABA_A$ receptors in idiopathic generalised epilepsy: an ^{11}C-flumazenil PET study ***Epilepsia*** 1997; 38: 1089-1097
8. Hand KSP, Baird VH, Van Paesschen W, **Koepp MJ**, Revesz T, Thom M, Harkness WFJ & Duncan JS. Central benzodiazepine receptor autoradiography in hippocampal sclerosis. ***Br J Pharamcology*** 1997; 122: 358-364
9. **Koepp MJ**, Richardson MP, Brooks DJ, Poline LB, Van Paesschen W, Friston KJ & Duncan JS. Cerebral benzodiazepine receptors in hippocampal sclerosis: an objective in vivo analysis. ***Brain*** 1996, 119: 1677-1687
10. Richardson MP, **Koepp MJ**, Brooks DJ, Fish DR & Duncan JS. Benzodiazepine in cortical dysgenesis: a 11C flumazenil PET study. ***Annals of Neurology*** 1996; 40: 188-198

TABLE OF CONTENTS

FIGURES

TABLES

ABBREVIATIONS

AED	Antiepileptic drugs
AI	Asymmetry-Index
B_{max}	Receptor density
BZ	Benzodiazepines
CAE	Childhood Absence Epilepsy
cBZR	Central benzodiazepine receptor
CFT	Carfentanil
CPS	Complex partial seizure
CSF	Cerebrospinal fluid
DPN	diprenorphine
DLPFC	dorsolateral prefrontal cortex
ESM	Ethosuximide
FBM	Felbamate
FC	Febrile convulsion
FDG	Fluoro-deoxyglucose
FGPE	Feline generalised penicillin epilepsy
FMZ	Flumazenil
FWHM	Full width at half maximum
GABA	γ-aminobutyric acid
GAD	Glutamic acid decarboxylase
GBP	Gabapentin
GM	Grey matter
GTCS	Generalised tonic clonic seizure
GVG	γ-vinyl-GABA
HCT2	Hippocampal T2 relaxation time measurement
HCV	Hippocampal volume
HS	Hippocampal sclerosis
ICV	Intracranial volume
IGE	Idiopathic generalised epilepsy
IPSP	Inhibitory postsynaptic potential
ILAE	International League against Epilepsy
JAE	Juvenile absence epilepsy
JME	Juvenile myoclonic epilepsy
LTG	Lamotrigine
LTP	longterm potentiation
MRI	Magnetic resonance imaging
mTLE	Mesial temporal lobe epilepsy
NMDA	N-methyl-D-aspartate

PET	Positron emission tomography
rCMRglu	regional cerebral glucose metabolism
RE	Reading Epilepsy
ROI	Regions of interest
SD	Standard deviation
SPM	Statistical parametric mapping
SPS	Simple partial seizure
V_d	Cerebral volume of distribution
VOI	Volume of interest
VPA	Sodium valproate
WM	White matter

CHAPTER I Introduction

1.1. Classification of Epileptic Seizures and Syndromes

Epilepsy can be classified in several ways - by clinical events, aetiology, electro-encephalographic (EEG) changes, pathophysiology, anatomy, or age. In 1969 the International League Against Epilepsy (ILAE) introduced a classification of seizure type, revised in 1981, in which EEG data are taken into account whereas aetiology, age, and anatomical site were ignored. In this scheme seizures are divided into three groups: generalised, partial and unclassifiable. Generalised seizures are further divided into tonic-clonic (GTCS), absence, myoclonic, atonic, and clonic seizures, and partial seizures into simple partial (SPS) and complex partial (CPS) categories according to the preservation or alteration of consciousness. The epileptic activity of partial seizures may spread to become generalised, in which case the seizure was said to be secondarily generalised.

An epileptic syndrome may be defined as a disorder characterised by a cluster of signs and symptoms customarily occurring together. In recognition of the fact that a seizure-type classification does not account for other aspects of the heterogeneity of epilepsy, the ILAE devised a new scheme - the classification of the epilepsies and epilepsy syndromes and related seizure disorders. This classification takes into account seizure type, EEG, and prognostic, pathophysiological, and etiological data. The two major dichotomies are into epilepsies characterised by seizures which are partial in onset and those which are generalised. The second dichotomy is between seizures which are idiopathic and those which are symptomatic. This usually devolves into those which have a genetic predisposition and those which are determined by a structural or lesional aetiology. Two new categories are added: epilepsies and syndromes undetermined, whether focal or generalised (cryptogenic), and special syndromes.

The relevant epileptic syndromes for this thesis are:

- Symptomatic localisation-related epilepsies: temporal lobe epilepsy
- Idiopathic generalised epilepsies: childhood absence epilepsy
  juvenile absence epilepsy
  juvenile myoclonic epilepsy
- Idiopathic localisation-related epilepsies: reading epilepsy

1.2. Temporal Lobe Epilepsy (TLE)

1.2.1. Introduction

Knowledge of the existence of non-convulsive epileptic attacks can be traced back to the times of Hippocrates. J.H. Jackson was the first to describe a patient with a temporal lobe tumour who had suffered from olfactory aura and "dreamy state" (Jackson, 1889). Fulton (1953) proposed the term "limbic epilepsy" because "such attacks involve not only the temporal lobe structures, but usually also the posterior orbital gyrus, the hippocampus, and the cingulate gyrus". In the present international classification temporal lobe epilepsy (TLE) is characterised by recurrent simple partial (SPS) and complex partial seizures (CPS), the principal symptoms of which are generated predominantly by mesial temporal lobe structures. Two forms of TLE are recognised:

- Mesial temporal lobe epilepsy (mTLE): a specific chronic epileptic disorder associated with hippocampal sclerosis (HS) is regarded as a discrete syndrome (Wieser, 1980; Engel, 1992). Seizures originate in the sclerotic hippocampus (Babb, 1984b) and are clinically indistinguishable from those caused by other mesial temporal lesions. It has a predictably good outcome following limited temporal lobe resections
- Neocortical temporal lobe epilepsy (ncTLE): a chronic epilepsy disorders due to specific structural epileptogenic lesions in, or immediately adjacent to, mesial temporal lobe limbic areas characterised by seizures that have the clinical features of mesial temporal ictal events.

The main focus in this thesis will be the description of clinical characteristics and the underlying pathological and neurochemical basis of mTLE.

1.2.2. Mesial temporal lobe epilepsy (mTLE)

1.2.2.1. Clinical history

The family history includes an increased incidence of epilepsy and in particular an increased incidence of febrile convulsions (FC). Patients with mTLE often have a history of complicated FC during the first year of life. Onset of non-febrile seizures is typically with CPS during the second half of the first decade or later. In particular the first seizures often become secondarily generalised, but isolated auras also occur as SPS. Anti-epileptic drugs (AED) are usually effective initially and control the CPS and secondarily generalised tonic-clonic seizures (SGTCS) for some years, but a large proportion of patients will develop a medically refractory epileptic disorder. Clinically the progression of this syndrome seems to be associated with a stronger tendency for bilateralisation and a higher incidence of secondary generalisation (Wieser, 1993).

1.2.2.2. Clinical seizure phenomenology

The ictal semiology of mTLE is relatively characteristic. Auras are frequent and typically occur in isolation. They often consist of ascending epigastric sensations, or psychic phenomena, such as memory flashbacks, deja vu, dreamy states, and complex illusions (Duncan, 1987; Wieser, 1987). Seizure symptoms include strong vegetative signs with heart rate changes, and motor arrest with motionless stare. There is slowly progressive clouding of consciousness, often associated with oro-alimentary automatisms, manual automatisms, and contralateral dystonic posturing (Kotagal, 1989). CPS have a duration of 1 to 2 min and postictal confusion or aphasia may persist for many minutes. There is variable amnesia for the entire ictal events or parts of it.

1.2.3. Neurophysiology

1.2.3.1. Inter-ictal EEG

The interictal hallmark of mTLE is the anterior temporal spike focus. Often sharp waves followed by slow waves appear in a pseudo-rhythmic fashion with a frequency of about 1/second. Interictal, dependent or independent temporal spikes may be present in about one-third of patients with medically refractory mTLE in contralateral homotopic regions (So, 1989). Morrell (1985) found evidence that a reversible, an intermediate and an irreversible stage of secondary epileptogenesis, previously documented in animals, are also present in humans. In the reversible stage of secondary epileptogenesis, the field potentials in the homotopic region mimic or reflect those of the primary focus (mirror focus). Resection of the primary focus results in cessation of the mirror focus. The intermediate stage denotes the period in which paroxysmal epileptiform discharges begin to arise from the homotopic cortex at moments when no such activity can be detected in recordings from the primary lesion; temporally independent contralateral spiking occurs. The excision of the primary focus usually leads to "running down" of the secondary focus in the intermediate stage. An independent secondary focus will not subside after resection of the primary one and may itself then behave as the primary one.

Patients with an unifocal or very strongly predominant interictal temporal spike or sharp wave have a strong likelihood of ictal onset from the same temporal region. Nevertheless, there is an error rate when interictal abnormalities are relied upon in isolation for prediction of seizure onset. The presence of an unifocal surface temporal epileptiform abnormality does not exclude the possibility of bilateral independent ictal onsets (So, 1989; Hirsch, 1991). An unifocal temporal interictal epileptiform discharge may be misleading, when in fact the typical ictal events arise from the contralateral temporal lobe or where ictal studies indicate an extra-temporal ictal onset. The

available data do not allow for an estimate of the relative occurrence of the two types of error (Quesnay, 1993).

1.2.3.2. Ictal EEG

Ictal recordings are considered to provide the best estimates of seizure onset. Auras are usually without any clear-cut scalp EEG expression, but ongoing interictal spikes cease and a slight regional or generalised attenuation of the background can be seen. With loss of awareness, the ictal scalp EEG typically shows a congruent build-up of lateralised anterior temporal (sphenoidal) sharp theta recruiting rhythms. The wave forms will evolve in terms of amplitude and frequency usually in the direction of higher amplitude, slower frequencies, and more widespread distribution over time. Finally a period of postictal alteration in the surface EEG will be noted with poly-morphic delta slowing being the most common finding encountered (Risinger, 1989).

The localising validity of surface ictal recordings has been questioned. Surface-recorded EEG wave forms provide an incomplete assessment of intracranial electrical activity. Seizures of mesial-basal origin arise in locations that are inaccessible to recording with surface or sphenoidal electrodes. Any surface ictal EEG changes must be considered to be potentially the result of some degree of ictal propagation. In intracranial recordings from stereotactic depth electrodes the discharges usually point to a mesiobasal temporal lobe origin. In densely spaced depth EEG recordings, about 65% of all seizures classified as mesiobasal limbic show high frequency tonic discharges recorded simultaneously from the hippocampal formation and the ipsilateral amygdala. Tonic discharges seen only in the hippocampal formation and not initially affecting the ipsilateral amygdala constitute another 25%. About 7% of mesiobasal seizures start in the amygdala and propagate to the hippocampal formation within 3-5 seconds. The remaining 3% show tonic discharges exclusively confined to the amygdala without spread to the hippocampus (Wieser, 1986). Given the limitations of surface EEG recordings the relatively high accuracy of these recordings may reflect the tendency for seizures of mesial temporal origin to propagate in a somewhat stereotypic fashion. Most commonly, initial propagation of the ictal discharge is to the ipsilateral temporal neocortex. Alternatively, initial propagation may be to the contralateral hippocampus. A third pattern of propagation may result in simultaneous invasion of ipsilateral neocortex and contralateral hippocampal structures (Lieb, 1986).

1.2.4. Structural Neuroimaging in TLE

1.2.4.1. Anatomical considerations

The temporal lobes can be anatomically separated into two components following the electroclinical classification with limbic and neocortical TLE:

- *mesial temporal structures:* The mesial temporal structures include the uncus, amygdala, hippocampus and parahippocampal gyrus. On coronal images the amygdala can be identified immediately posterior to the optic chiasm. More posteriorly, at the level of the basal cistern, the amygdala lies superior to the hippocampal head. The hippocampus consists of three parts: head, body, and tail. It measures about 4.5 cm in longitude and has a cylindroid structure with a medially concave curvature at the level of the body. On coronal images the posterior boundary of the hippocampal head is at the level of the red nucleus and anterior to the cerebral aqueduct. The hippocampus extends posteriorly to a level just anterior to the splenium of the corpus callosum where the tail of the hippocampus originates.
- *temporal neocortex:* Two fissures, the superior and the middle temporal fissures, divide the lateral surface of the temporal neocortex into superior, middle, and inferior temporal gyri. The superior temporal gyrus includes the temporal operculum overlying the insula. Medially, the fusiform gyrus is separated from the parahippocampal gyrus by the collateral fissure.

Neuroimaging studies are utilised in the evaluation of patients with partial epilepsy to establish the aetiology of the seizure disorder and to assist the electrophysiological studies in localising the site of seizure onset. Two structural neuroimaging modalities are used to identify potential candidates with intractable partial epilepsy for a surgical procedure: X-ray computed tomography (CT) and magnetic resonance imaging (MRI).

1.2.4.2. X-ray computed tomography (CT)

Conventional structural neuroimaging began with the introduction of X-ray CT imaging. CT is a non-invasive technique that can image intraparenchymal abnormalities directly. The radiodensity of different tissues accounts for the CT image obtained following the passage of x-rays through the head. CT studies performed after an intravenous injection of radio-opaque contrast medium increase the radiodensity of some lesions, especially vascular structures and lesions in which the blood brain barrier is disrupted. CT is very sensitive in demonstrating alterations associated with intracranial haemorrhage and calcification. The reconstructed image is usually in the axial plane and the scanning time required is only 15-20 minutes. CT scanners are widely available and the images are easy to interpret. CT has proved to be sensitive in revealing macroscopic pathological alterations, e.g. large destructive lesions and cerebral infarction (Adams, 1987); however, these studies are insensitive in imaging HS.

1.2.4.3. Magnetic resonance imaging (MRI)

MRI can provide multiplanar anatomical data without bone artefact or the use of ionising radiation. MRI rapidly replaced CT as the technique of choice in investigating patients with epilepsy. The first attempts to recognise HS with MRI concentrated on the detection of abnormal, focal high-intensity signals from the mesial structures. MRI abnormalities were detected in 65% of patients with HS using T2-weighted scans (Kuzniecky, 1987). The atrophy seen on T1-weighted images and the increased signal intensity seen in T2-weighted images of the hippocampus were critical factors for the recognition of HS. (Jackson, 1990).

The identification of hippocampal atrophy can be improved by measurement of hippocampal volumes (HCV) (Jack, 1990). Asymmetric atrophy of the resected hippocampus on MRI was associated with a good prognosis for seizure control; additional atrophy of the contralateral non-resected hippocampus was associated with a worse outcome (Jack, 1992). The validity of HCV measurement is highly dependent on the quality of images from which measures are made (Cook, 1992). The use of thin coronal images permits the precise identification of hippocampal anatomy and pathology at discrete levels. The wide normal range of absolute values largely limits the assessment to identification of asymmetry and precluded identification of bilateral HS, and lesser degrees of contralateral hippocampal damage. If the volume loss is equivalent bilaterally, no significant left to right difference will be observed and hence a normal ratio will be reported, unless HCV are corrected and normalised for head size (Free, 1995). A physiologic asymmetry in the position of the hippocampi is observed in about 40% of control subjects (Van Paesschen, 1997a) and should not be confused with HS.

In an analogous way to the quantification of hippocampal atrophy by volumetric analysis, T_2-weighted signal intensity may be quantified reproducibly by measurement of T_2 relaxation time. Hippocampal T_2 (HCT_2) relaxation times may be constructed from 16 images, with echo times from 22 msec to 262 msec (Jackson, 1993a,b; Grünewald, 1994). Subsequent studies have shown an inverse correlation between HCT_2 and neuronal density in the hippocampus (Van Paesschen, 1995). The data from healthy subjects indicate that there is a narrow range of normal HCT_2 relaxation times, resulting in the parameter being a useful measure. The main advantages of T_2 mapping are that HCT_2 relaxation times are absolute values which can be compared immediately against control values, with no gender differences, and do not need manipulations or corrections for interpretation, and can be measured within a few seconds.

A higher HCT_2 is usually observed in a more atrophic hippocampus (Van Paesschen, 1995). However, HCT_2 reflects pathology of the tissue which may be other than

sclerosis, and not necessarily accompanied by atrophy. An increased HCT_2 is associated with damage in the CA_1 subfield of the hippocampal formation and also the hilus and has probably a different neuropathological basis than HCV loss. MR-based HCV measurement and HCT_2 mapping, therefore, give complementary information in the presurgical evaluation of TLE and longitudinal studies (Van Paesschen, 1997a). Kuzniecky *et al.* (Kuzniecky, 1997) analysed the abnormalities in preoperative MRIs of 44 consecutive patients who had undergone temporal lobectomy and who had pathologic confirmation of MTS. Techniques included inversion recovery (IR), T1-weighted, volume-acquired images, HCT_2 relaxometry, volumetric assessment, and visual analysis. Sensitivity was 86% with IR, 90% with T1-weighted qualitative visual analysis, and 97% with quantitative volumetry. Pathologic prolongation of HCT_2 (>2 SD of normal) was present in 79%. Concordance between all MRI modalities was 68%. Inversion recovery and qualitative analysis lateralized the side of surgery in 93%. The combination of IR and T1-weighted images correctly identify HS in most patients. Hippocampal volumetry provided localisation in an additional small number of patients.

1.2.5. Positron Emission Tomography (PET) studies in TLE

In the field of epilepsy, PET has been used to study:

- regional cerebral glucose metabolism (rCMRglu) with ^{18}F-fluoro-2-deoxyglucose (^{18}F-FDG)
- regional cerebral blood flow (rCBF), blood volume, and oxygen metabolism with ^{15}O-O_2, ^{15}O-H_2O, ^{15}O-CO_2 and ^{13}N-NH_3
- receptor localisation and kinetics of
  central benzodiazepine receptor (cBZR) with ^{11}C-flumazenil (FMZ)
  peripheral benzodiazepine receptor with ^{11}C-PK 11195
  monoamine oxidase B (MAO-B) with ^{11}C-deuterium-L-deprenyl
  μ-opiate receptors with ^{11}C-carfentanil (CFT)
  μ- and k-opiate receptors with ^{18}F-cycloFOXY
  μ-, k-, and ∂- opiate receptors with ^{11}C-diprenorphine (DPN)
  ∂-receptors with ^{11}C-methylnaltrindole

1.2.5.1. Cerebral glucose metabolism

Interictal rCMRglu imaged with ^{18}F-FDG-PET has been the most frequently reported PET study in epilepsy. These reports indicate a 60% to 90% incidence of temporal lobe hypometabolism in medically refractory mTLE. Differences in PET technology, image analysing methodology, and in patient selection may explain this variability. Qualitative analysis of interictal ^{18}F-FDG-PET most often reveals unilateral mesial and temporal

lobe hypometabolism in mTLE. Even when amygdala or hippocampal electrophysiological ictal onsets are demonstrated on depth electrodes, many patients with mTLE have more severe lateral than mesial temporal hypometabolism on quantitative image analysis (Engel, 1990). The basis for lateral greater-than-mesial temporal interictal metabolic asymmetry in mTLE is unclear. It is possible that severe hypometabolism of epileptogenic amygdalo-hippocampal zones is partial-volume averaged with more normal metabolism of adjacent basal temporal areas, so that the epileptogenic zone metabolism itself could actually be at least as decreased as is metabolism of lateral temporal neocortex ipsilaterally. Although the metabolic pattern was different between patients with mesial and lateral temporal seizure onset, there was not a clear correlation between the location of the defined epileptogenic focus defined with EEG and the degree of hypometabolism (Hajek, 1993). In consequence ^{18}F-FDG-PET studies have been believed to be less reliable for answering the question of precise localisation of seizure onset, than for answering the question of lateralisation.

Localised neuronal loss is not the sole basis of regional interictal hypometabolism. In one study, hippocampal neurone loss was not correlated with the severity of temporal lobe hypometabolism (Henry, 1994). By contrast, recent comparisons of hippocampal atrophy and glucose metabolism in patients with temporal lobe epilepsy found that there was most marked hypometabolism in the hippocampus and temporal pole and that the degree of hippocampal atrophy correlated with the degree of hypometabolism in these structures (Semah, 1995; Gaillard, 1995).

The degree and extent of temporal lobe hypometabolism has been correlated strongly with seizure outcome following temporal lobectomy. The degree of hypometabolism in the medial, but not in the lateral temporal lobe, correlated with the chances of being rendered seizure-free by anterior temporal lobe resection (Manno, 1994). After selective amygdalo-hippocampectomy in patients with mTLE, there was an increase of rCMRglu in the ipsilateral and also in the contralateral hemisphere. There was also a trend in these patients towards a normalisation of rCMRglu in the ipsilateral temporal neocortex 12 months after surgery, implying a consequence of the removal of the epileptic focus (Hajek, 1994).

Regional hypometabolism in mTLE typically is diffuse, with gradual transition from adjacent areas of normal metabolism and with a relatively large area of hypometabolism. Frontal, parietal, thalamic, or basal ganglia hypometabolism is frequently observed in mTLE, but only ipsilateral to the temporal hypometabolism. The temporal hypometabolism is almost always more severe than any extra-temporal hypometabolism (Henry, 1990). Such extension of the abnormal metabolic zone beyond the electrically and pathologically defined seizure substrate may reflect cerebral

connectivity or different types of functional impairment than what is determined by EEG (Henry, 1994).

Interictal focal mesial temporal hypermetabolism has been rarely reported in partial epilepsies and is seen mainly in young children or in adults who do not necessarily have mTLE (Theodore, 1983). The possibility of continuous or rapidly repetitive focal mesial temporal seizures without typical electrographic ictal discharges detectable by scalp electrodes must also be considered when "interictal" temporal hypermetabolism is observed (Handforth, 1994). Ictal or peri-ictal rCMRglu increases in patients with mTLE have infrequently been reported, and are usually due to the fortuitous occurrence of partial seizures following injection of ^{18}F-FDG. In a group of patients with cryptogenic TLE, never treated with AED, Franceschi *et al.* (Franceschi, 1997) found evidence of significant interictal glucose hypermetabolism in a bilateral neural network including the temporal lobes, thalami, basal ganglia and cingular cortices. Other cortical areas, namely frontal basal and lateral, temporal mesial and cerebellar cortices had bilateral non-significant increases of glucose metabolism.

In summary, these metabolic patterns of increased or decreased glucose metabolism could represent a pathophysiological state of hyperactivity predisposing to epileptic discharge generation, neuronal activity at the site of ictal onset, in areas of ictal propagation, and in areas of postictal dysfunction or a network of inhibitory circuits activated to prevent the diffusion of the epileptic discharge.

1.2.5.2. Cerebral blood flow

Regional cerebral blood flow (rCBF) studies with ^{15}O-O_2, ^{15}O-H_2O, ^{15}O-CO_2 and ^{13}N-NH_3 PET have generally shown regional hypoperfusion of the same distribution as the regional hypometabolism observed in these patients (Bernardi, 1983). Topographic discordance between intrasubject regional hypoperfusion and regional hypometabolism has been more recently reported suggesting the possibility of complementary roles for resting interictal rCBF and rCMRglu measurements (Leidermann, 1992; Theodore, 1994)

1.2.5.3. Central benzodiazepine receptors

The earliest report of ^{11}C-flumazenil (FMZ) PET interictal imaging of central benzodiazepine receptors (cBZR) in partial epilepsies included six cases of TLE (Savic, 1988). When the data set was averaged, unilateral temporal lobe decreases in cBZR density were significantly different from normal control values, while extratemporal cBZR density apparently was normal throughout. More recently ^{11}C-FMZ-PET in definite mTLE was compared with interictal ^{18}F-FDG-PET for the same candidates for anterior temporal lobectomy, and with normal subjects' FMZ and FDG regional values

(Savic, 1993; Henry, 1993). Individual mTLE subjects had decreased anterior mesial cBZR density on the epileptogenic side, but normal cBZR density elsewhere. Eight subjects had ipsilateral mesiolateral temporal and thalamic hypometabolism and four also had other extra-temporal hypometabolism on the epileptogenic side, one had exclusively anterior mesial temporal hypometabolism on the epileptogenic side and one had normal metabolism. Nine of these patients had temporal lobectomy based on depth electrode and other studies that in each case localised ictal onsets to the same anterior mesial temporal area that decreased ^{11}C-FMZ binding.

The decrease of cBZR density appears to be restricted to the epileptogenic zone while interictal metabolic dysfunction is more variable and usually more extensive in mTLE. It seems most likely that cBZR changes reflect localised neuronal and synaptic loss in the epileptogenic zone and that the more extensive hypometabolism is a result of diaschisis. In clinical terms, it appears that ^{11}C-FMZ-PET may be superior to ^{18}F-FDG-PET for the localisation of the source of the seizure. It is not certain whether this data confers additional clinically useful information in patients with clear-cut MRI findings of HS.

1.2.5.4. Peripheral benzodiazepine receptors

PK 11195 is highly selective for the peripheral benzodiazepine receptor (BZR). In the brain, peripheral BZR are highly expressed on glia, not neurons. Autoradiographic studies revealed increased hippocampal ^{3}H-PK 11195 binding in resected temporal lobe specimens with hippocampal sclerosis (Kumlien, 1992). However, ^{11}C-PK 11195 activity was not increased in PET studies of eight patients with TLE (Kumlien, 1995).

1.2.5.5. Monoamine-oxidase B (MAO-B)

Epilepsy studies with the positron-emitting ligand for MAO-B (Kumlien, 1992) showed that binding of ^{3}H-L-deprenyl was increased in sclerotic hippocampi. Nine patients with TLE were studied with ^{11}C-deuterium-L-deprenyl and PET revealing increases in temporal lobe accumulation rate of the ligand in eight of the nine patients. Unilateral TLE was accurately lateralised, and regional ^{11}C-deuterium-L-deprenyl binding accurately distinguished bilateral TLE (ictal onsets arising independently from each side) from unilateral TLE (Kumlien, 1995).

1.2.5.6. Opiate receptors

Interictal imaging of opiate receptors in TLE has yielded divergent results in studies using ligands selective for different subtypes. ^{11}C-carfentanil (CFT) PET, which measures μ-opiate receptor density, frequently revealed marked increases over the lateral temporal neocortex. Lateral temporal glucose metabolism and ^{11}C-CFT binding showed a significant inverse relationship (Frost, 1988). Although the patients most

likely had mTLE, amygdala and hippocampal ^{11}C-carfentanil binding was less consistently increased. Only lateral temporal temporal increases on the epileptogenic side were statistically significant among group mean regional values. Later studies found decreased binding in the amygdala in TLE (Mayberg, 1991). It has been speculated that an increase in μ-opioid receptors in the temporal neocortex may be a manifestation of a tonic anti-epileptic system that serves to limit the spread of electrical activity from other temporal lobe structures. The finding of reduced signal from the amygdala may be due to partial volume effects as the amygdala is surrounded by low-binding white matter and its size is below the spatial resolution of PET (Meltzer, 1996).

^{18}F-cycloFOXY PET, which measures combined μ and k-opiate receptor binding, has shown in a few cases non-significant asymmetry of mesial temporal structures with higher binding on the epileptogenic side (Theodore, 1992). ^{11}C-diprenorphine (DPN) PET, which measures combined μ-, k-, and ∂-opiate receptor binding, has shown no asymmetry between various temporal lobe areas in TLE (Mayberg, 1991). Different opiate receptor subtypes appear to have differentially distributed alterations in binding in TLE. The different patterns of ^{11}C-CFT, ^{18}F-cycloFOXY and ^{11}C-DPN binding indicate that μ and k opioid receptors are not affected similarly in TLE. It has been speculated that loss of μ-opiate mediated inhibition in the amygdala could facilitate seizure activity (Fisher, 1991), while increased μ-opiate receptor binding in neocortical areas may be the pathophysiological basis of some chronic behavioural disturbances in TLE (Engel, 1986). Increases in μ- and ∂-receptor binding showed different regional patterns (Madar, 1997) suggesting distinct roles of different opioid-receptor subtypes in seizure phenomena.

1.2.6. Single Photon Emission Tomography (SPECT)

Interictal SPECT studies of patients with epilepsy reveal focal alterations of rCBF that may reflect a gross structural lesion or a functional deficit associated with the epileptogenic region. Interictal SPECT does not have the same value as PET in localising foci in patients with epilepsy. The major strength of SPECT is its capability for peri-ictal (ictal or early post-ictal) studies. Peri-ictal studies of epilepsy with SPECT exploit the fact that partial seizures are associated with a transient focal increase in rCBF.

SPECT is a complementary rather than a competing technology to PET. The wide availability, reduced cost, and capability of ictal imaging with SPECT make it reasonable to investigate the role of rCBF imaging by SPECT in epilepsy. Ictal SPECT studies show a characteristic pattern of unilateral temporal hyperperfusion with relatively decreased perfusion in other cortical areas, both ipsilaterally and

contralaterally (Berkovic, 1993) The temporal hyperperfusion involves both the medial and lateral cortex. Hyperperfusion of the ipsilateral basal ganglia is associated with ictal dystonia of the contralateral upper limb, which is a useful clinical sign (Newton, 1992). If ictal injection is made within the first 30s of temporal lobe seizure onset, it reportedly shows diffuse temporal lobe hyperperfusion in 100% of patients; the longer the delay, the lower the sensitivity. However, ictal injection is often not sufficiently rapid to provide functional demonstration of the location of seizure onset if the seizures propagate rapidly (Spencer, 1994). Post-ictal studies reveal correct lateralisation in 71% of cases of unilateral TLE (Rowe, 1991). There are rapid changes in the pattern of CBF distribution from the ictal to the early and late post-ictal states. The characteristic pattern of post-ictal rCBF in mTLE, which is distinct from other pathologies, consists of a focal area of relatively increased perfusion, usually in the mesial and anterior parts of the temporal lobe, with decreased perfusion in the adjacent lateral temporal cortex often extending into the parietal and frontal regions.

1.2.7. Neocortical temporal lobe epilepsy (ncTLE)

In contrast to mTLE, there is comparatively little information about ncTLE emphasising the absence of features typical of mTLE (Ebner, 1994). Epigastric auras are common in mTLE and rare in ncTLE. Ipsilateral limb automatisms, contralateral dystonic posturing, and oro-alimentary automatisms, common in mTLE, are significantly less frequent in ncTLE (Saygi, 1994). The lack of specific experiential phenomena at the onset of ncTLE may be explained by the observation that reciprocal connections between mesiobasal and lateral temporal cortex have to be activated to allow auras to enter consciousness (Gloor, 1990). Discriminating between medial and lateral onset on the basis of specific auras will be impossible if both areas must be activated for the awareness of the experience to occur. The extensive connections between medial and lateral temporal cortex suggest that spread of the ictal discharge between these regions occurs rapidly, and that a seizure onset zone in one of these regions will cause profound functional deficits on the other. The initial sensation of an aura or any other initial ictal symptom is related to the first functional area activated by the seizure that has access to consciousness. But this may not be the site of seizure origin. Psychomotor seizures may arise in silent neocortical areas lying in the extratemporal as well as in the temporal neocortex (Engel, 1992). Neocortical seizures most often arise in silent areas (Ebner, 1994). In order to produce clinical symptoms, seizure activity has to activate a symptomatogenic zone, which is defined as the area of cortex that produces the first clinical symptom. Whether this is the primary auditory cortex or the insular cortex via the mesial temporal structures, it is always already an expression of seizure activity spread. If seizure activity arises in the temporal neocortex and spreads to a neocortical symptomatogenic zone, then it is correct to label this constellation ncTLE. If, however,

the seizure activity first spreads to a symptomatogenic zone lying, for example, in the mesial structures, then it is still a ncTLE but with a different clinical manifestation.

Given the sensitivity of quantitative MRI one would expect that lack of hippocampal atrophy would readily segregate mTLE and ncTLE. However, hippocampal atrophy may reflect secondary hippocampal damage (i.e. arteriorvenous malformations or glioma), which may also occur in patients with temporal neocortical lesions, so called "dual pathology". This appears to occur in 3-20% of the patients with ncTLE, depending on definition of HS and type of lesion (Adam, 1994; Raymond, 1994). Careful analysis of resected hippocampi in patients with temporal lobe neocortical lesions reveals less impressive but still significant cell loss in most patients (Fried, 1992). Information about differences between mTLE and ncTLE has been based largely on observations made in cases of lesional ncTLE. The seizure onset zone is likely to be centred in the neocortex surrounding the lesion and therefore relatively easy to determine. However, clinical and other features of lesional cases may not be applicable to patients with non-lesional neocortical epilepsy in whom defining the seizure onset zone is especially difficult (Walczack, 1995).

Focal hypometabolism measured with ^{18}F-FDG PET involved the entire temporal lobe in 5 out of 8 ncTLE cases in one study (Henry, 1991). An unspecified number had structural lesions. In a more recent PET study medial temporal metabolism was nearly normal in patients with ncTLE, mildly depressed in patients with mesial temporal tumors, and severely depressed in patients with nonlesional mTLE (Hajek, 1993). Lateral temporal metabolism was mildly depressed in patients with mesial temporal tumours and severely depressed in both ncTLE and mTLE. Although 3 of 5 ncTLE cases had lesions, the relative lack of PET changes involving the medial temporal lobe in ncTLE is intriguing. Medial-lateral differences may be easier to detect using more specific ligands, such as ^{11}C-FMZ.

1.3. Structural and Functional Basis of TLE

The most common pathological substrate in patients with mTLE is HS. Falconer *et al.* (Falconer, 1964) first suggested that prolonged FC in infancy or early childhood lead to the development of TLE with intractable CPS (Falconer, 1974). It remains still unclear how FCs, HS and mTLE are related to each other.

1.3.1. Febrile convulsions

"A febrile seizure is an event in infancy or childhood usually occurring between 3 months and 5 years of age, associated with fever but without evidence of intracranial infection of defined cause. Seizures with fever in children who have suffered a previous non-febrile seizure are excluded. FC are to be distinguished from epilepsy, which is characterised by recurrent non-febrile seizures" (Commission on Classification and Terminology of the International League against Epilepsy, 1989).

Only children with complicated FC have a higher risk for epilepsy (Wallace, 1988). Population-based studies on patients with CPS in Rochester, Minnesota, have given strong evidence of an association between FC and CPS (Rocca, 1987). A history of FC was found in 20% (n=16) of patients with CPS but only in 2% of control subjects. FC were complicated in 14 of the 16 cases. Their material, however, does not answer the question whether CPS and FC are causally related or just have a common underlying cause. In 50 children with TLE undergoing temporal lobectomy HS was found in 20 patients, of whom 19 had a history of prolonged FC in infancy followed by a silent interval before the onset of their habitual seizures. In contrast, only one of 17 patients with tumours had a history of FC (Lindsay, 1984).

Prospective cohort studies of children with FC showed an increased risk of developing epilepsy, varying from 2% to 7% (Schmidt, 1985; Annegers, 1987). The type of subsequent seizures depends on different features of the FC. There is an increased risk for CPS when FC are lateralised, particularly for lateralised seizures of long duration (Aicardi, 1987), whereas recurrent simple FC and a family history of FC are risk factors for later generalised epilepsy (Annegers, 1987). There are no reports in the literature of patients with TLE and a history of FC who do not have HS.

1.3.2. Hippocampal sclerosis

HS has been identified in up to 67% of resected temporal lobes and is the commonest lesion found. The scarring of the medial temporal areas tends to spread out anteriorly to the amygdaloid nucleus and uncus as well as laterally into the parahippocampal gyrus

and beyond. The CA_1 field is the commonest site for severe neuronal loss and gliosis. The end folium and CA_3 field are also highly vulnerable whilst the CA_2 field, a short run of neurons lying between these two fields, is to be relatively spared. The small, dark, densely packed neurons of the dentate fascia are also often more or less.

Margerison and Corsellis (1966) found that one or both hippocampi were affected in 50-60% of cases of chronic cryptogenic epilepsy, and that unilateral damage was far the commoner. The cerebellum was damaged in 45% of the cases and the thalamus, the amygdaloid nucleus and the cerebral cortex each not necessarily together, in about 25%. Nearly all cases, in which the hippocampus was affected showed some damage elsewhere in the brain. Acute damage of this kind is rarely seen in people with longstanding cryptogenic epilepsy even if they have died shortly after an attack.

Quantitative techniques for cell counting have been applied to the hippocampus, both post mortem in patients with epilepsy of various kinds (Dam, 1980) and in temporal lobectomy specimens from patients with CPS (Babb, 1984a). Post-mortem studies show a loss of hippocampal neurons the magnitude of which is correlated with the frequency of GTCS and the total duration of epilepsy. It is most marked in the end folium, where the loss associated with normal ageing is greatly accentuated. The dentate granule cells also show significant loss. Patients with endfolium sclerosis had later onset of habitual seizures, no history of early childhood convulsions, and poorer surgical outcome compared with patients with HS (Van Paesschen, 1997b). Good postoperative outcome was associated with a predominantly anterior cell loss (Babb, 1984a). This loss was significant in the dentate fascia, in pyramidal cells in regions CA_3 and CA_1, in the prosubiculum, subiculum, and the hippocampal gyrus. When cell loss predominated in the posterior portion of the resected tissue it involved all hippocampal zones including dentate gyrus, CA_2 and CA_4, and was associated with an unsatisfactory post-operative outcome. In 95% of cases, the hippocampal nerve cell loss was patterned with a greater loss in CA_1 than any other field.

There are other ways in which the hippocampus may be damaged besides classic hippocampal sclerosis, such as an atheromateous occlusion of the posterior cerebral artery or less severely by micro-infarcts due to the degeneration of the small vessels. It is also particular prone to degenerate with the almost total loss of the CA_1 sector in senile dementia of the Alzheimer type (Meldrum, 1974). In none of these conditions are sporadic seizures particular liable to appear. It is only when hypoxic damage occurs, but does not kill during the acute stages, that the classic sclerosis will have time to develop. The degree of vulnerability of hippocampal cells is most probably age-dependant (Corsellis, 1983) and is particular prone to occur in the first years of life. HS may then be seen as part of scarring process which preferentially, but not exclusively,

affects the medial temporal grey matter and which, like scarring elsewhere in the brain, may sooner or later lead to epileptic attacks. This hypothesis does not require either that temporal lobe seizures should inevitably follow development of the scarring or that such damage should be the only determining factor.

The clinicopathological problem is further complicated by the fact that no clear-cut structural abnormality can be found in about every fifth temporal lobe that is resected. The postoperative prognosis with regard to seizures is unfavourable when no pathology or indefinite pathology is found, whereas it is particularly good when HS is identified (Babb, 1984a). This observation is sometimes presented as conclusive evidence that HS is the focal cause of the seizure activity, whereas it remains possible that HS may be an amplifier of seizure activity or is even secondary either to focal or to generalised seizure activity, and the favourable outcome arises because of the removal of epileptogenic tissue in the anterior part of the temporal lobe.

1.3.3. Animal experiments

Lesions essentially confined to the hippocampus and very closely mimicking those found in mTLE can be induced experimentally.

In primates recurrent brief seizures induced by allylglycine are followed by neuronal loss in CA_1 and the end folium, with an associated gliosis 1 to 6 weeks after induction (Meldrum, 1974). Animals with this type of lesions, however, did not have spontaneous temporal lobe seizures later on (Meldrum, 1983). As in patients with mTLE the experimental CA_1 lesions tend to be asymmetrical, whereas the endfolium lesions are symmetrical.

Purely limbic seizures can be induced in primates or rodents by focal intracerebral injections of convulsants (e.g. bicuculline or kainate) into the amygdala or hippocampus or by the systemic administration of various agents such as kainate or pilocarpine (Ben-Ari, 1980). In addition to the typical CA_1 and CA_3 lesions these models show lesions in other parts of the limbic system including the amygdala, the pyriform cortex, some thalamic nuclei, the basal ganglia and the substantia nigra. The determining factor for damage in any anatomical site appears to be the induction of sustained local seizure activity for at least 2 to 5 hours. Injection of kainic acid into the amygdala produces rapid spread of epileptiform activity from the injected amygdala to the ipsilateral hippocampus and to the contralateral amygdala. The distant effects are most probably caused by epileptiform activity and its associated convulsions, whereas the local damage occurs most probably due to a direct toxic effect of kainic acid. There is further evidence for this hypothesis in the different pattern of cell damage of the two

affected sites: massive proliferation of microglia is seen early at the site of the injection, the amygdala, whereas the distant changes in the hippocampus are less pronounced and not seen until 4 to 6 days after the injection. The histological picture of cell damage in the hippocampus resembles HS in human mTLE: the earliest changes are seen in the CA_3 region, the CA_1 region is affected, but the CA_2 region is spared. This specific distribution of nerve cell loss in HS might be due to an increase in intracellular Ca^{2+} with a limited capacity of calcium-buffering proteins of these cells (Griffiths, 1983). Calcium-buffering proteins are not present in the CA_3 region, which is rich in kainate receptors, or in the CA_1 region, which is rich in N-methyl-D-aspartate (NMDA) receptors (Sloviter, 1987).

Prolonged electrical stimulation of the perforant path may give rise in the rat to a period of limbic status epilepticus and subsequent chronic spontaneous seizures. Extended electrographic monitoring in the hippocampus revealed spontaneous recurrent paroxysmal discharges, persistent interictal spiking and fully developed electrographic seizures (Lothman, 1990). Hippocampal slices demonstrated an increased excitability relative to slices from control animals as evidenced by epileptiform bursting in increased extracellular potassium and decreased extracellular calcium (Lothman, 1990). Sustained electrical stimulation of the perforant pathway from the entorhinal cortex provides an excitant input to the dentate granule cells and leads in the rat to degenerative changes in the hilar and the CA_3 neurons (Sloviter, 1987). The perforant path from the entorhinal cortex to the dentate gyrus is the common pathway for all the inputs to the hippocampal formation from various parts of the brain, including the amygdala.

The neurons that are selectively vulnerable in the hilar region appear to be mossy cells. The mossy fibres which are axons of the dentate granule cells project to neurons in the CA_3 region. Synaptic reorganisation of mossy fibres, which might be functionally excitatory, occurs in kainate treated rats and is seen also with electrical kindling of the entorhinal cortex, amygdala or olfactory bulbs (Sutula, 1990). Epileptogenic lesions causing partial de-afferentiation of the dentate gyrus or other hippocampal structures are followed by a regenerative process of the mossy fibres, which may provide anatomically abnormal excitatory connections. (Tauck, 1985; Sutula, 1988; Ben-Ari, 1990).

The possibility that CA_1 inhibitory neurons are hypofunctional or "dormant" due to a loss of excitatory input to inhibitory cells from damaged CA_3 pyramidal cells was tested by stimulating the contralateral perforant path in order to activate the same CA_1 basket cells via different inputs. Contralateral stimulation evoked CA_1 pyramidal cell paired-pulse inhibition immediately in the previously stimulated hippocampus

(Sloviter, 1991). To demonstrate the same effect more directly, inhibitory postsynaptic potentials (IPSP) were elicited in CA_1 pyramidal cells by activation of basket cells. IPSP evoked indirectly by activation of terminals that excited inhibitory interneurons were reduced in the epileptic tissue, whereas IPSPs evoked by direct activation of basket cells, when excitatory neurotransmission was blocked, were not different from controls (Bekenstein, 1993).

So far typical HS similar to that in human mTLE has not developed in kindled animals. There is loss of polymorphic neurons in the hilus of the dentate gyrus, in addition to mossy fibre reorganisation, but not the characteristic pattern with severe cell loss in the CA_1, CA_3 and CA_4 region (Cavazos, 1990). But structural changes in the hilus induced by abnormal functional activity may just be the first step in a process that creates local circuits of increased excitability. Ultrastructural studies of vulnerable regions in the hippocampus provide important indications of the early mechanism involved (Griffiths, 1983). Seizures induce swelling of perineuronal astrocytic processes throughout the pyramidal cell layer in the hippocampus. Swollen mitochondria are seen in neuronal pericarya and in focal dendritic swellings, especially in the basal dendritics of CA_3 and CA_1 neurons. These appearances are closely similar to so-called excitotoxic changes induced by kainate and NMDA.

1.3.4. Human studies

Binding to excitatory amino acid and inhibitory amino acid receptors was compared in frozen hippocampal sections from surgical specimens resected from TLE patients with age-comparable autopsy control subjects. Binding to the NMDA recognition site and its associated glycine modulatory site was elevated by 20 to 110% in the CA_1 area and dentate gyrus of the hippocampus of the patients. Binding to these sites was unaffected in area CA_4. Binding to the quisqualate-type excitatory amino acid receptor was unchanged in all regions except the stratum lacunosum moleculare CA_1, where it was increased by 63%. $GABA_A$ and cBZR binding was reduced by 20 to 60% in CA_1 and CA_4, but unchanged in dentate gyrus (McDonald, 1991). Patients in this study had evidence of neuronal loss but not advanced HS. However, other studies in HS showed a reduction of NMDA receptor binding in CA_1, CA_3 and CA_4 (Geddes, 1990). A comparison of cell counts and autoradiography of cBZR using ^{125}I-iomazenil in resected hippocampus from patients with HS showed a significant reduction of cBZR and neuronal density in CA_1, CA_2, CA_3, CA_4 and dentate gyrus. All regions showed a tendency for the loss of receptors to be over and above the loss of cells, but this reached significance only in CA_1 and CA_3 (Johnson, 1992; Burdette, 1995).

Synaptic rearrangements due to mossy fibre sprouting appear also to occur in man (de Lanerolle, 1989). Epileptogenic lesions causing partial de-afferentiation of the dentate gyrus or other hippocampal structures are followed by a regenerative process of the mossy fibres, which may provide anatomically abnormal excitatory connections (Sutula, 1991). An enhanced and abnormal NMDA receptor response has been detected on surviving dentate granule cells in resected hippocampi of patients with chronic TLE (Isokawa-Akesson, 1989) suggesting that excitotoxic responses consequent to this might be responsible for the abnormal dendritic morphology seen in these cells.

1.4. Idiopathic Generalised Epilepsy (IGE)

1.4.1. Introduction

The generalised epilepsies are divided into those with no identifiable cause other than genetic predisposition (idiopathic) and those with a known or presumed underlying disorder of the nervous system (symptomatic or cryptogenic). Idiopathic generalised epilepsy (IGE) is characterised by generalised absence, myoclonic, and generalised tonic-clonic seizures (GTCS). Neurological examination is normal and mental retardation is absent. The background EEG is normal but shows paroxysmal, generalised and bilaterally synchronous, spike-wave discharges of around 3 Hz. In symptomatic or cryptogenic generalised epilepsy (e.g.. Lennox-Gastaut syndrome), tonic and/or atonic seizures may also be seen. There are often abnormal neurological signs and cognitive deficits. The background EEG is typically slow and the spike-wave discharges are slower at 2.5 Hz.

1.4.2. Electro-clinical features

The IGEs are subdivided on the basis of electro-clinical criteria. The ILAE currently recognises three main subgroups in which absence seizures occur: childhood absence epilepsy (CAE), juvenile absence epilepsy (JAE), and juvenile myoclonic epilepsy (JME). There is considerable overlap between the syndromes. Absence seizures and their EEG correlate, generalised spike-wave-activity, have a definite inherited tendency but it is uncertain whether CAE, JAE and JME are genetically distinct. In addition it has been suggested that patients with IGE and symptomatic generalised epilepsy may represent opposite ends of a spectrum rather than discrete entities, and that the relative contributions of genetic and acquired factors determine the clinical and EEG appearances (Berkovic, 1987).

1.4.2.1. Childhood absence epilepsy

In CAE absences begin between 3 and 12 years, most usually between age 4 and 8 years. The annual incidence is 6-8 /100,000 (Janz, 1969). Absence seizures are frequent, occurring many times a day, and last a few seconds, usually less than 15 seconds. They are often associated with marked impairment of consciousness, eye opening occurs shortly after onset of spike-wave activity and minor orofacial automatisms are frequently seen (Panayiotopoulos, 1989). 40% of patients with CAE develop GTCS, often 5-10 years after the onset of the absences. A small proportion of patients with CAE (3-8%) have been reported to have myoclonic jerks (Janz, 1969; Wolf, 1984). In CAE the EEG shows generalised, bilaterally synchronous and symmetrical 3 Hz spike and slow wave discharges that are of sudden onset and cessation and occur on normal background activity. The frequency of the spike-wave

discharge may slow to 2 Hz towards the end of a discharge, and some patients may have polyspikes. Absences become less frequent through adolescence and usually remit in adulthood.

1.4.2.2. Juvenile absence epilepsy

The onset of JAE is in the second decade of life. It has in many studies been arbitrarily set at 10 years. In contrast, Wolf and Inoue (1984) defined their patient group according to the type of seizures, and noted onset of absences at 2 to 47 years. Absence seizures are less numerous, tend to be of longer duration and are associated with less profound alteration of consciousness (Panayiotopoulos, 1989). Sixteen percent of patients with JAE have myoclonic seizures (Wolf, 1984). Up to 80% of patients with JAE develop GTCS. In some patients, the onset of GTCS precedes the onset of absences, although interpretation must be cautious as the initial absences may have passed unrecognised. Generalised spike-wave discharges with some frontal predominance occur with a frequency of 3.5-4 Hz, commonly with some slowing of the rate during a discharge. As with CAE, about 80% of patients with JAE become seizure free with medication. Both absences and GTCS may, however, persist into adulthood.

1.4.2.3. Juvenile myoclonic epilepsy

JME comprises 5-10% of cases of epilepsy. JME begins around puberty and is characterised by GTCS and myoclonic jerks which typically occur on waking. Typical absences usually appear first, at about ten years of age, followed by myoclonic jerks one to nine years later and GTCS one to two years after that. The EEG shows 4-6 Hz polyspike and slow-wave generalised discharges, that last up to 20 seconds, with normal background activity. More than 50% of patients have focal abnormalities on their EEGs, comprising focal slow waves, spikes or sharp waves, or asymmetry of generalised discharges (Panayiotopoulos, 1994). Up to 90% of patients with JME become seizure free with optimal medication. There is a very high relapse rate if medication is subsequently withdrawn, even if the patient has been seizure free for several years.

1.4.3. Treatment

The typical absences respond equally well to ethosuximide (ESM) and sodium valproate (VPA). An advantage of VPA is that it is also effective against tonic-clonic and myoclonic seizures. If VPA or ESM do not provide adequate control of absences it is appropriate to try the other, and then the two agents in combination. Second-line medications for intractable absences include: clonazepam, acetazolamide and lamotrigine. The use of the first two is often complicated by the development of

tolerance, and clonazepam use is frequently limited by drowsiness. Clobazam may be useful and phenobarbitone still has a role in the refractory case. There is anecdotal experience of lamotrigine benefiting otherwise intractable absences, especially when given with VPA (Timmings, 1992; Panayiotopoulos, 1993). Vigabatrin has been reported to worsen coexistent absences and myoclonic seizures, Gabapentin appears to be ineffective against absences (Chadwick, 1995).

1.4.4. Animal experiments

Investigation into the anatomical and neurochemical basis of absence seizures has been very dependent on the use of animal models reflecting the clinical, EEG, and pharmacological profile of absence seizures in man as near as possible. Studies in primates have proven difficult. The Singalese baboon, Papio papio, which exhibits GTCS with intermittent light stimulation has been used as a model of IGE. The EEG shows generalised spike-wave discharges prior to the GTCS but spontaneous absence seizures do not occur (Naquet, 1972). The most useful models have used small mammals and can be divided into pharmacologically induced and genetic models. Most genetic models are inbred lines of rodents in which absence-like seizures occur spontaneously (Coenen, 1992). Genetic absence epilepsy rats from Strasbourg (GAERS) and the WAG/Rij strain of rats are characterised by episodic bursts of generalised spike-wave activity with an absence like state which are suppressed by ESM and VPA. The bursts of spike-wave activity develop at about puberty and persist throughout life. In addition to these rat models, a variety of genetic mouse models have been described the best known of which is the Lethargic(lh/lh) mouse (Lin, 1993).

Systemic administration of penicillin to cats causes spike-wave activity and behavioural manifestations which resemble absence seizures. Study of this model, so called feline generalised penicillin epilepsy (FGPE), has lead to the development of many of the current concepts of absence seizures (Gloor, 1979). Systemic administration of large doses of γ-hydroxybutyrolactone (GBL) in rats and monkeys produces a picture of hypokinesia with somnolence accompanied by high amplitude spike and waves, which is suppressed by anti-absence drugs, ethosuximide and sodium valproate (Snead, 1988). Low doses (10-20 mg/kg) of pentylenetetrazol (PTZ) produce bursts of generalised spike-wave activity at 7-9 Hz and an absence-like state in rats. Intermediate doses (40-60 mg/kg) produce bursts of generalised spike-wave activity associated with clonic seizures. Both types of seizure respond to ethosuximide and sodium valproate. High doses of PTZ cause GTCS which do not respond to these drugs (Snead, 1992a).

Gibbs and Gibbs postulated that the generalised spike-wave discharge was based on a diffuse cortical abnormality (Gibbs, 1952). Bilateral application of oestrogens to the cortex resulted in generalised spike-wave discharges occurring both spontaneously and in response to hyperventilation (Marcus, 1968). Unilateral application did not result in spike-wave discharges. Section of the corpus callosum disrupted the bilateral synchrony of the spike-wave discharges, but isolation of the cortex from subcortical structures did not prevent the spike-wave activity with spike-wave activity occurring independently of subcortical structures. However, stimulation of the thalamic intraluminar nuclei of the kitten at 3 Hz also produced a generalised cortical discharge that resembled the 3 Hz spike-wave seen in man (Jasper, 1947) suggesting that generalised spike-wave activity arose from an abnormal discharge that was projected diffusely to the cortex, via the thalamus. The origin of this abnormal discharge was thought to be the brainstem reticular activating system (Penfield, 1954). This concept became known as the centrencephalic theory of IGE. Chemical and electrical stimulation of the brainstem did not produce spike-wave activity nor absences, thus making an origin in the brainstem unlikely (Kreindler, 1958; Browning, 1985).

The opposing views of a cortical versus a subcortical mechanism were combined in a unifying hypothesis proposed by Gloor in which both cortical and subcortical mechanisms are essential to the generation of spike-wave activity (Gloor, 1979). This hypothesis was derived from work on FGPE. Rather than applying convulsant substances or electrical stimulation to focal areas of the brain penicillin was administered systemically. It is known that penicillin in vitro blocks GABAergic transmission but the concentration present in the brain are not sufficiently high to cause this and its mechanism of action is unclear (Kostopoulos, 1983; Giaretta, 1987; Avoli, 1984). The spike-wave discharge generated by IM penicillin is very similar to that observed in man, although there are some differences in that it tends to be slightly faster with a more variable morphology and is best developed in parietal areas, rather than frontally. The behavioural manifestations are also similar with arrest of ongoing behaviour, bilateral eye blinking, slight pupillary dilatation, and mild bilateral myoclonic twitching of the facial muscles (Gloor, 1974).

FGPE, like the human condition, responds to ESM and VPA (Guberman, 1975). Stimulation of the midline and intralaminar thalamic nuclei prior to the administration of penicillin resulted in cortical spindles when the cat was under barbiturate anaesthesia and recruiting waves when awake. Stimulation at the same sites following IM penicillin produced generalised cortical spike-wave activity (Gloor, 1977). It was postulated that spike-wave activity represented an abnormal cortical response to normal afferent thalamo-cortical volleys, and that the primary abnormality was a diffuse cortical hyperexcitability (Gloor, 1979). It was suggested that before the administration

of penicillin the probability that thalamo-cortical volleys would excite cortical neurons sufficiently to cause action potentials was low. In the presence of penicillin, the increase in the number of action potentials with each spindle as it evolved into the spike of the spike-wave complex would trigger recurrent pathways corresponding to the slow wave of the spike-wave complex (Kostopoulos, 1983). Consecutively it has been shown that the essential input from the thalamus to the cortex was not in fact normal as was originally proposed. Spike-wave discharges oscillate between the relay nuclei of the thalamus and the cortex, and the activity in the paired individual neurons in this thalamo-cortical loop is phase locked (Avoli, 1983).

Implantation of depth electrodes in GAERS revealed spike-wave activity in cerebral cortex, thalamus and striatum but not hippocampus. In contrast to the findings in FGPE, however, cortical spike-wave never preceded thalamic spike-wave discharges, the onset being either simultaneous in the thalamus and cortex, or arising in the thalamus. In addition, spike-wave discharges were occasionally seen in the thalamus without concurrent cortical spike-wave activity but never the reverse (Vergnes, 1987). Within the thalamus, spike-wave activity was seen in the relay and reticular nuclei. It was not recorded in the midline, anterior, or ventromedial nuclei. Destruction of either the relay or the reticular nuclei suppressed cortical spike-wave discharges, whereas destruction of the midline, anterior and ventromedial nuclei was without effect (Vergnes, 1992).

These results suggested that the thalamus may be the site of a primary genetically determined abnormality which is responsible for generalised spike-wave activity. Such an abnormality could be at the level of the T-type calcium channel. However, the thalamus may not necessarily be the site of the primary abnormality and rhythmical activity in the thalamus could be initiated from elsewhere. Gloor postulated a diffuse cortical hyperexcitability on the basis of experiments in FGPE (Gloor, 1979). Both relay and reticular nuclei receive afferents from the cortex and there is some evidence that these afferents can trigger or enhance rhythmical firing in thalamus (Buzsáki, 1991; Avanzini, 1993). Thalamic nuclei also receive inputs from the brainstem. Large bilateral destructive lesions of the midbrain reticular activating formation in FGPE facilitated spike-wave activity suggesting that the brainstem has a modulatory influence (Kostopoulos, 1981). In addition, inhibition of pathways projecting from the substantia nigra to the superior colliculi have shown to suppress generalised spike-wave activity, but the path of the collicular efferents has yet to be determined (Depaulis, 1990).

1.4.5. Human studies

Animal models, both pharmacologically induced and genetic, are models of absence seizures in isolation. In humans absence seizures occur in the setting of the idiopathic generalised epilepsies in which GTCS often also occur. There have been few depth EEG studies in patients with IGE and absence seizures. Williams (1953) placed electrodes in the cortex, white matter and the thalamus of six children with typical absence seizures. 3 Hz slow wave activity was seen in the thalamus which preceded the appearance of cortical spike-wave. In a more recent study rhythmic double spike-wave complexes, which preceded cortical spike-wave-activity, were recorded in the centromedian nuclei of the thalamus in two subjects (Velasco, 1989). These two studies lend support to the theory that the thalamus plays a crucial role in the generation of spike-wave activity. Other depth EEG studies have not confirmed these findings but have been performed in heterogeneous groups of patients which have included patients with symptomatic generalised epilepsy (Niedermeyer, 1969). Bancaud studied ten patients with generalised spike-wave and absences, most of whom had atypical features such as slow or asymmetrical spike-wave activity and all were resistant to conventional therapy (Bancaud, 1974). In this particular group electrical stimulation of depth electrodes in the medial frontal cortex and to a lesser extent the anterior cingulate and frontal convexity produced generalised spike-wave discharges which were either subclinical or associated with absences. Interestingly, however, spike wave activity was recorded in the thalamus although it was not clear whether this was merely a reflection of cortical activity or whether the thalamus was playing a more active role. It is possible that an interaction between the thalamus and the cortex underlies generalised spike-wave activity in all these patients but that this mechanism is triggered by different, diffuse or focal cortical abnormalities. Patients who satisfy all the criteria for IGE may have a single common mechanism underlying generalised spike-wave activity but as the absences and EEG become more atypical and move toward the symptomatic end of the spectrum, a variety of other mechanisms such as secondary generalisation from medial frontal focus may become important.

Structural neuroimaging in patients with IGE is usually normal on visual inspection. However, a recent quantitative MRI study has revealed evidence for widespread structural changes in various IGE syndromes (Woermann, 1998a). Following semi-automatic segmentation of the cerebral hemispheres, normalised cortical and subcortical matter volumes were compared between groups of patients and controls. Patients with IGE had considerably larger cortical grey matter volumes than control subjects. Significant abnormalities of regional distribution of cortical grey matter were detected in about 40% of patients with JME and JAE suggesting the existence of structural abnormalities in patients with IGE.

1.4.6. Pathology

Pathological studies are another potential source of information but there have been few post mortem series as patients with IGE rarely die in hospital. Janz studied the pathology of JME and found evidence of microdysgenesis (Janz, 1961). Microdysgenesis has, however, been described in patients without epilepsy and without any neurological disorder and therefore the significance of this finding remained uncertain. Cohn (1968) was unable to find any abnormality in a single patient with CAE. More recently, Meencke and Janz have reported the findings at post mortem in 15 patients with idiopathic generalised epilepsy (12 with CAE or JAE and 3 with JME) (Meencke, 1984; Meencke, 1985a). All but one patient had evidence of abnormal neuronal migration with an increase in partially dystopic neurons in the stratum moleculare, white matter, hippocampus and cerebellar cortex. Blurring of the boundaries between cortex and white matter, and between lamina 1 and 2 were also seen as well as columnar arrangement of cortical neurons. Quantification of these changes has been difficult and these findings have been criticised (Lyon, 1985). However, although these changes can be physiological and have been shown to be age related, they were reported to be more severe and more frequent in patients with IGE than in control subjects (Meencke, 1985b). It was postulated that microdysgenesis may be the morphological substrate for the diffuse cortical hyperexcitability that Gloor proposed from experiments with FGPE, but until the finding of microdysgenesis is confirmed by others this hypothesis remains highly speculative.

1.5. GABAergic Transmission

1.5.1. Introduction

γ-aminobutyric acid (GABA) is the major inhibitory neurotransmitter and accounts for 30% of all synapses in the brain. The synthesis of GABA is closely linked to the excitatory amino acids aspartate and glutamate. The predominant precursor of both aspartate and GABA is glutamate which is converted to GABA by glutamic acid decarboxylase (GAD) in nerve terminals acting as a marker for GABAergic neurons. Following release from the nerve terminal into the synaptic cleft, GABA is removed from the extracellular space by sodium dependent re-uptake into neurons and uptake into glia. GABA is metabolised by GABA transaminase to succinic semialdehyde (**Figure 1**) (Krnjevic, 1974). The actions of GABA are mediated through $GABA_A$ and $GABA_B$ receptors which are distinguished by their sensitivity and insensitivity respectively to the antagonist bicuculline (Hill, 1981). Receptor mapping in rat brain has shown that $GABA_A$ receptors predominate in most areas with the exception of the molecular layer of the cerebellum and interpeduncular nucleus of the mesencephalon where $GABA_B$ receptors are more numerous (Bowery, 1989). In the thalamus numbers are approximately equal (Crunelli, 1991).

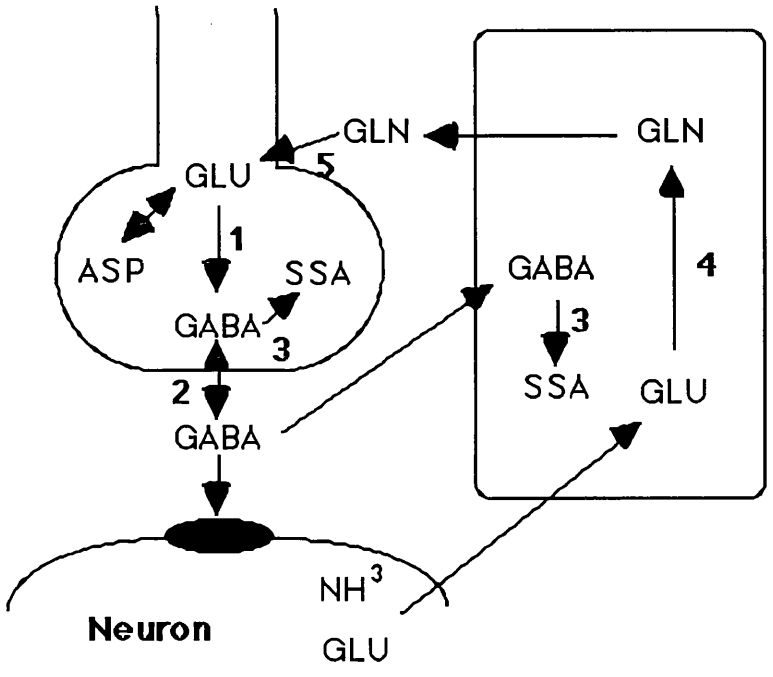

Figure 1: Metabolic pathways of GABA
1 = Gluatamate acid decarboxylase, 2 = GABA re-uptake, 3 = GABA transaminase, 4 = Gluatmine sunthetase, 5 = Glutaminase, GLU = Gluatmic acid, GLN = Succinic semialdehyde, ASP = Aspartate

1.5.2. GABA$_A$ receptors

$GABA_A$ receptors have an integral chloride channel (**Figure 2**) and $GABA_A$ agonists, such as muscimol, cause an increase in conductance and chloride resulting in rapid but brief membrane hyperpolarisation (Sivilotti, 1991). Studies in rats have shown that each receptor is composed of five subunits. Six classes of subunit (α,β,γ,δ,ε,and π) have been identified and within each class there are different subtypes (Sieghart, 1989), (Sieghart, 1992), (Wisden, 1992). In total there are at least 16 different subtypes: 6α, 4β, 3γ,1δ,1ε, and 1π. A functional $GABA_A$ receptor depends on the presence of 2α, 2β, and either a γ or δ (Verdoorn, 1990). The significance of the ε and π subtypes is not known. Differences in subunit composition result in considerable heterogeneity of the $GABA_A$ receptor and determine sensitivity to benzodiazepines and other ligands (e.g.. barbiturates, steroids, picrotoxin and zinc) which modulate GABA transmission. The α subunit determines benzodiazepine affinitiy and GABA binding to β subunit causes the chloride channel to open. The γ subunit is required for benzodiazepine binding to modulate GABA-chloride coupling and also introduces ethanol sensitivity (Pritchett, 1989). Mapping of the subunits has revealed several patterns; for example α1, β2, and γ2 have similar distribution and occur in combination to form the commonest type of $GABA_A$ receptor, while others are expressed in specific regions, such as α6 and β1 in the hippocampus and cerebellar cortex. The potential number of different $GABA_A$ receptors is vast but only relatively few seem to be of physiological significance (Wisden, 1992).

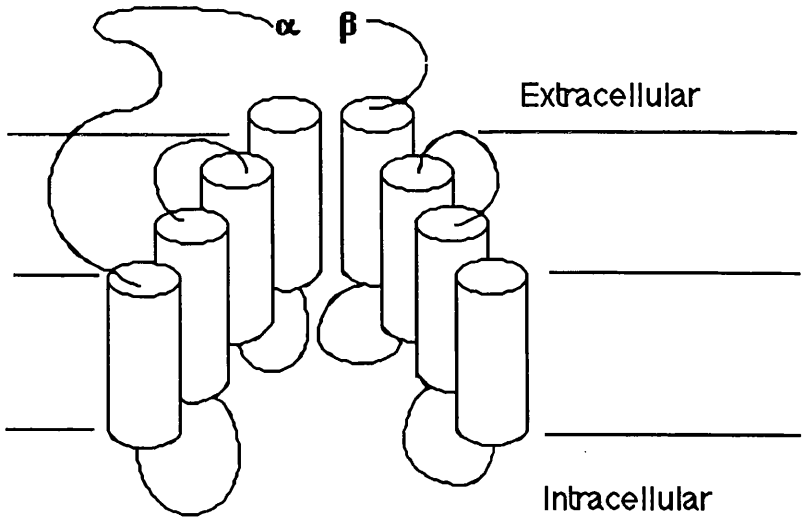

Figure 3: Structure of the $GABA_A$ receptor

The structure is based on 2α and 2β subunits (only one of each is shown for simplicity). The parts of the subunits within the cell membrane form the chloride channel while the extracellular sections form the binding sites for benzodiazepines (α subunit) and GABA (β subunit). A fifth subunit (not shown), either γ or δ, completes the structure.

1.5.3. GABA$_B$ receptors

$GABA_B$ receptors, although less numerous than $GABA_A$, are widely distributed in the CNS. Their effects on membrane conductance occur via a calcium dependent secondary messenger system involving G protein (Sivilotti, 1991). In addition they are insensitive to benzodiazepines. Many $GABA_B$ receptors are thought to have presynaptic locations and to modulate neurotransmitter release. $GABA_B$ receptors act primarily on Ca^{++} and K^+ channels. The pharmacological properties of presynaptic and postsynaptic $GABA_B$ receptor differ. At postsynaptic sites $GABA_B$ activation results in an outward K^+ flux. The consequent membrane hyperpolarisation is of slow onset, weak and relatively prolonged compared to that initiated by $GABA_A$ activation. $GABA_B$ receptors are also present at presynaptic sites where they reduce slow calcium currents and impair release of both excitatory and inhibitory neurotransmitters from vesicles. Presynaptic $GABA_B$ receptors have been found on GABAergic neurons and activation of these autoreceptors reduces GABA release. Conversely prevention of this feedback inhibition facilitates GABA release (Hill, 1981). The distribution of $GABA_A$ and $GABA_B$ receptors differs, and may be relevant to some forms of epilepsy. Within the hippocampal pyramidal cell layers, $GABA_B$ receptor-mediated feed-forward inhibition predominates in dendritic regions, whereas feedback inhibition is $GABA_A$ receptor-mediated and is most prevalent in perisomatic regions (Lacaille, 1988).

1.5.4. Benzodiazepine receptors

Benzodiazepine receptors (BZR) are divided into two groups: peripheral and central (Richards, 1984). Peripheral BZRs are found in the CNS but also at other sites including mast cells, platelets, kidney and heart. In the CNS, peripheral BZR are associated with glial tissue particularly in the olfactory bulb, medial eminence, choroid plexus and ependyma (Marangos, 1982). Their functional significance is not entirely clear but they are unlikely to be involved in the pathogenesis of epilepsy. The benzodiazepine binding site on the $GABA_A$ receptor is referred to as the central BZR (cBZR). CBZR are present at the majority of $GABA_A$ receptors and are found principally in neocortex, hippocampus and cerebellar cortex with lower densities in thalamus, basal ganglia and brainstem. There are no cBZRs in white matter unless on ectopic neurones. CBZR agonists increase the frequency of single chloride channel openings in response to a given concentration of GABA (Richards, 1984).

The classification of cBZR is controversial. Initially cBZRs were subdivided into BZ 1 BZ 2 receptors on the basis of different affinity for the triazolopyridazine, CL 218 872 (Meldrum, 1986). BZ 1 receptors are found particularly in cerebellar cortex and globus pallidus whereas BZ 2 receptors predominate in the caudate, putamen and colliculus.

Both types are present throughout the cortex and in the hippocampus. Diazepam and lorazepam bind preferentially to BZ 1 receptors, which are thought to specifically mediated the anxiolytic effects of benzodiazepines. With the discovery of different $GABA_A$ receptor subunits, it has become apparent that this classification of benzodiazepine receptors is too simplistic (Wisden, 1992). There are six α subunits each with varying affinities for different benzodiazepines. $\alpha 1$ subunits are the most abundant and are sensitive to all benzodiazepines whereas $\alpha 2$ and $\alpha 3$ subunits are relatively insensitive to CL 218 872 and diazepam. $\alpha 1$ and $\alpha 2$ subunits do not coexist within a $GABA_A$ receptor. BZ 1 receptors probably correspond to those with a $\alpha 1$ subunit and BZ2 to those with an $\alpha 2$ and/or $\alpha 3$ subunit. Flumazenil, a competitive cBZR antagonist, binds to all six α subunits, but has less affinity for $\alpha 4$ and $\alpha 6$ and binding is not influenced by GABA (Sivilotti, 1991; Wisden, 1992). Endogenous ligands (endozepines) have recently been isolated at potentially pharmacologically active concentrations. These have been shown to displace ^{3}H-flunitrazepam and positively modulate the action of GABA on chloride conductance (Rothstein, 1992).

1.5.5. GABAergic transmission and limbic seizures

Electrical stimulation and pharmacological manipulation of pathways in the normal hippocampus slice preparation in vitro can give rise to sustained hyperexcitability, which can support and give rise spontaneously to epileptiform activity. The development of a hyperexcitable hippocampus requires an imbalance between $GABA_A$-mediated inhibition and NMDA-mediated excitation. Once bursting is established, hippocampal plasticity allows bursting to be maintained even if the excitation is withdrawn (Mott, 1989; Piguet, 1993; Schneidemann, 1994). The crucial $GABA_A$ mechanisms to prevent abnormal excitability are mediated via inhibitory interneurons. These interneurons may themselves be inhibited by $GABA_B$ mechanisms, resulting in an overall increase in excitation. The net effect of baclofen, which suppressed recurrent inhibition through an action mediated by $GABA_B$ receptors, was pro-epileptic because its disinhibitory effect on the interneurons was substantially greater than its suppressive effect on synaptic excitation (Mott, 1989).

1.5.5.1. Animal models of limbic seizures

Kindling refers to the process by which repeated subconvulsive electrical stimulation to a region of the brain in a living, freely-moving animal gives rise to a sustained increase in excitability such that progressively more severe seizures arise with repeated stimulation; ultimately, spontaneous seizures may occur. In animals kindled at various sites of the limbic system the pattern of development of kindling and the nature of the seizures is very similar (McNamara, 1984). Kindling models are regarded as models of limbic, particularly hippocampal, epilepsy in man because of the occurrence of

generalised seizures of limbic origin and response to conventional anticonvulsant drugs dose-dependently suppressed generalised motor seizures in kindled rats (Löscher, 1986).

The dependence of kindling on $GABA_A$ mechanisms can be demonstrated by drug treatments in such animals. Progabide, a GABA-mimetic active at $GABA_A$ and $GABA_B$ receptors, shortened afterdischarge durations and attenuated the severity of the accompanying convulsive responses in rats previously kindled from the amygdala, frontal cortex and hippocampus, in a dose-dependent manner (Morimoto, 1993). In addition, the anticonvulsant effects of progabide were partially reversed by treatment with the antagonist of benzodiazepine receptors, flumazenil (Ro 15-1788), whereas flumazenil administration alone did not alter kindled seizures. Vigabatrin, an inhibitor of the GABA catabolic enzyme GABA-transaminase, approximately doubled the number of stimulations required for kindling development and also suppressed both generalised motor seizures and electrographic afterdischarges in previously fully kindled animals (Shin, 1986; Morimoto, 1993). After kindling decreased GABA-immunoreactive neurons in rat hippocampus (Kamphuis, 1986) and reduced GABA-stimulated chloride uptake had been observed in the hippocampus of amygdala kindled rats probably reflecting the number of reduced $GABA_A$ receptors (Tietz, 1991).

NMDA receptor function is enhanced in hippocampal dentate granule cells during kindling (Mody, 1987). CA3 pyramidal cells from kindled rats were more sensitive to NMDA than control cells (Martin, 1992). An increase in the amplitude of both the slow NMDA and fast non-NMDA receptor-mediated components of glutamatergic transmission accompanied by a decrease in $GABA_A$-mediated inhibition has been found using whole-cell current-clamp techniques (Rainnie, 1992). Further, a long-lasting decrease in the inhibitory effect of GABA on glutamate excitatory responses has been found in hippocampal pyramidal cells from a kindling model (Kamphuis, 1991). *In-vivo* microdialysis found progressive increases in glutamate release as kindling progressed (Minamato, 1992).

$GABA_A$ receptors are heteromeric protein complexes composed of multiple subunits as outlined above. Subunit composition varies in different brain regions and cell types and this confers distinct functional and pharmacological properties to the resulting receptors (Wisden 1992). This impaired GABAergic function may result, in part, from epilepsy-associated alterations in the molecular composition of the post-synaptic $GABA_A$ receptors on surviving hippocampal neurons. Such changes may result in receptors with altered functional properties that contribute to the process of epileptogenesis and compromise the efficacy of antiepileptic drugs that act at $GABA_A$ receptors. Altered transcriptional control of the production of the various $GABA_A$

receptor subunit mRNAs could result in alterations in subunit composition. Recent combined patch-clamped recordings and single-cell mRNA amplification techniques in single dentate granule cells (Brooks-Kayal, 1998) provided evidence that selective changes in $GABA_A$ receptor subunit expression precede the onset of epilepsy and thus participate in the process of epileptogenesis. Previous studies of regional changes in $GABA_A$ receptor subunit expression in epileptic dentate gyrus have demonstrated increased expression of the same subunits ($\alpha 1$ and $\alpha 2$) following kindling (Kamphuis, 1995), while in-situ hybridisation studies specifically using the pilocarpine model demonstrated increased $\alpha 5$-subunit mRNA (Rice, 1996). Some of this variability in findings between different studies may result from differences in the epilepsy model used, but another confounding factor may be the heterogeneity of cell types sampled when the entire dentate gyrus is examined. Cellular specificity may be particularly essential to the study of $GABA_A$ receptor subunit expression, which varies between neuronal subtypes and is high in glial cells (Fraser, 1995). In addition, when generalised increases in subunit expression are occurring, immunocytochemical and in situ hybridisation studies may miss changes in subunit expression relative to each other within individual neurons. Differences in $GABA_A$ receptor subunit mRNA expression between cell subtypes may also explain, at least in part, the lower levels of expression of the $\beta 2$ and $\alpha 5$ subunits in dentate gyrus single cells (Brooks-Kayal, 1998) compared with the relatively higher levels seen regionally in the dentate gyrus by in-situ hybridisation (Wisden, 1992).

1.5.5.2. Studies on human temporal lobe specimens

There has been a substantial accumulation of evidence from electrophysiological studies of tissue slices taken from hippocampus resected from patients with medically refractory TLE, indicating a functional impairment of GABAergic neurotransmission associated with increased seizure susceptibility.

Knowles *et al.* (1992) compared the *in-vitro* electrophysiology of hippocampal neurones from 14 patients with HS and hippocampal neurones from 7 epileptic patients with structural lesions near the hippocampus. No significant changes were detected in stimulus-evoked excitatory postsynaptic potentials (EPSPs) or stimulus evoked action potential bursts between the two groups but significantly fewer pyramidal neurones from the sclerotic group were found to show stimulus-evoked inhibitory postsynaptic potentials (IPSP) occurrence. Neurones from the HS group were also more likely to fire spontaneously in bursts of action potentials than hippocampal neurones from patients with structural lesions.

Masokawa *et al.* (1989) recorded from diseased hippocampal tissue, surgically removed from epileptic patients with evidence of neuronal loss and gliosis. Extracellular field

potentials were recorded from the granule cell layer of the dentate gyrus, evoked by stimulation of perforant path fibres, and compared with recordings from normal rat hippocampal slices. Application of a train of 15 stimuli at a frequency of 1 HZ resulted in a dramatic increase in the number of population spikes by as much as 8-fold thus resembling epileptiform discharges. In contrast to human epileptic hippocampal tissue, rat brain slices stimulated using an identical paradigm produced either no change or a slight decrease in the population spike evoked. Exposure of the rat brain slices to a relatively low concentration of bicuculline, however, resulted in a field potential response to the 15 train of 1 HZ simulations similar to that seen in the epileptic human hippocampi. The authors estimated that this concentration of bicuculline resulted in a blockade of only 10-20% of $GABA_A$ receptors in the rat dentate gyrus but nevertheless, a significant effect was seen on evoked neuronal discharges. These results suggested that a small decrease in $GABA_A$ receptor number or function, or a slight reduction in GABAergic neurones not readily detected using morphological techniques, may result in epilepsy *in-vivo*.

IPSPs were recorded from morphologically identified dentate granule cells in hippocampal slices, again prepared from epileptic patients by Isokawa-Akesson *et al.* (1991). In the presence of these IPSPs, multiple burst firings representative of epileptic hyperexcitatbility were rarely produced by dentate granule cells. The authors proposed that synaptic inhibition is intact and functional in chronically seizure-prone hippocampus during interictal periods, but that mechanisms of amplifying an imbalance between excitatory and inhibitory transmission may be necessary for the generation of epileptic activities.

Isokawa-Akesson *et al.* (1989) also studied inhibitory postsynaptic potentials (IPSPs) in hippocampal dentate granule cells in human TLE and the pilocarpine model of epilepsy using a whole cell patch-clamp recording in slice preparations. IPSPs were identified as $GABA_A$ mediated. High frequency (30 HZ) stimulation of the perforant path for 10 seconds resulted in a significant reduction (48%) of IPSP amplitude in human sclerotic hippocampus, an effect which was mimicked in pilocarpine-treated rats but not seen in control animals. APV, an NMDA receptor antagonist was found to effectively block the significant reduction of $GABA_A$ IPSCs in pilocarpine-treated rats and sclerotic hippocampus, confirming an involvement of NMDA receptors in this phenomenon. The author speculates that increased intracellular calcium, following activation of NMDA receptors, may result in compromised $GABA_A$ receptor channel function via phosphorylation-dephosphorylation mechanisms in chronic seizures.

Bilateral intrahippocampal microdialysis was used to test the hypothesis that an increase in extracellular glutamate may trigger spontaneous seizures. The

concentrations of glutamate and GABA were measured in microdialysates before and during seizures in six patients with complex partial epilepsy investigated before surgery. Before seizures, concentrations of glutamate were higher in the epileptogenic hippocampus, whereas GABA concentrations were lower. During seizures, there was a sustained increase in extracellular glutamate to potentially neurotoxic concentrations in the epileptogenic hippocampus. Moreover, the increase preceded the seizures. GABA concentrations were unchanged before seizures, but increased during them, with a greater rise in the non-epileptogenic hippocampus. These data suggest that a rise in extracellular glutamate may precipitate seizures and that the concentrations reached may cause cell death. Also, potentially compensatory inhibition, as measured by elevated GABA levels, is more pronounced in the non-epileptogenic hippocampus (During, 1993). In addition to elevated glutamate, other potentially excitatory amino acids have been assayed - elevations of aspartate, glycine and serine in association with seizures have also been noted with similar methods (Rooneengstrom, 1992).

1.5.6. GABAergic transmission and absence seizures

Systemic administration of both $GABA_A$ and $GABA_B$ agonists enhance spike-wave activity in GAERS, WAG/Rij rats and lethargic mice, suggesting that a diffuse increase in GABAergic activity mediated through either $GABA_A$ or $GABA_B$ receptors favours the development of absence seizures (Vergnes, 1984; Peters, 1989; Hosford, 1992). Increased spike-wave activity has been demonstrated in GAERS and WAG/Rij rats after systemic administration of γ-vinyl-GABA (GVG), which inhibits GABA transaminase and increases GABA levels (Vergnes, 1984; Peters, 1989). A similar effect was observed in rats pre-treated with GHB (Snead, 1993). Absence seizures have also been reported to be increased in patients with idiopathic generalised epilepsy taking progabide, GVG, and baclofen (Löscher, 1982; Stefan, 1988; Luna, 1989). In complete contrast, an increase in GABAergic transmission results in suppression of GTCS and partial seizures (Fariello, 1983).

Systemic administration of the $GABA_A$ antagonist, bicuculline, suppressed spike-wave activity in WAG/Rij rats (Coenen, 1992), but $GABA_A$ antagonists had little effect in GAERS (Liu, 1991) and in non-epileptic rats provoked spike-wave activity (King, 1979). The reason for this discrepancy is not clear. In vitro work has shown that blockade of $GABA_A$ inhibitory postsynaptic potentials (IPSPs) with bicuculline markedly increases $GABA_B$ IPSPs (Crunelli, 1991). This increase in $GABA_B$ activity may explain the lack of effect of $GABA_A$ antagonists in some models and possibly the enhancement of spike-wave in others. Alternatively, differences in the methodology used or in the model itself may be responsible for the apparent variability, focal administrations at critical sites will have different effects than systemic administration.

Despite some discrepancies, overall the evidence from animals and humans suggests that a global increase in GABAergic transmission at $GABA_B$ and probably $GABA_A$ receptors exacerbates spike-wave activity. These observations, although of therapeutic significance, are difficult to interpret with regard to the complex neuronal circuits that are thought to underlie generalised spike-wave activity.

Subcortical structures have been implicated in the regulation of spike-wave activity. The reticular nucleus of the thalamus is composed entirely of GABAergic neurons which project to the relay nuclei in the lateral thalamus. The reticular nucleus receives excitatory amino acid mediated input from the relay nuclei in the lateral thalamus and cortex, and cholinergic and adrenergic input from the brainstem (Avanzini, 1992; Von Krosigk, 1993). Injection of GVG and muscimol into the substantia nigra suppresses spike-wave activity in GAERS (Depaulis, 1988). There are three main inhibitory outputs from the substantia nigra: dopaminergic fibres from the pars compacta to the striatum, and GABAergic fibres from the pars reticulata to the medial thalamus and to the superior colliculi. Destruction of the superior colliculus prevented suppression of spike-wave activity suggesting that the intra-nigral muscimol is acting in the nigro-collicular pathway with consequent disinhibition of the superior colliculus (Depaulis, 1990). Studies in models of generalised convulsive seizures have reached similar conclusions (Gale, 1988), suggesting a common pathway for modulation of established seizure activity. However the nature and path of superior collicular efferents has yet to be determined.

Experiments designed to reveal abnormalities of GABAergic transmission in the pathways thought to be involved in the generation of generalised spike-wave activity have so far produced inconsistent results. No abnormality of ^{3}H-flunitrazepam binding to benzodiazepine binding site of the $GABA_A$ receptor was found in a strain of rats with spontaneous absence seizures (Hariton, 1988), but in a mouse mutant displaying absences and spike-wave discharges a reduction of ^{3}H-flunitrazepam binding was seen in all areas of the brain except hippocampus (Ortiz, 1991). In GAERS, baseline ^{3}H-flunitrazepam binding was normal (Snead, 1992b; Knight, 1992). In a recent study, however, a 20% reduction in GABA induced enhancement of ^{3}H-flunitrazepam binding was found suggesting an abnormality of coupling between the benzodiazepine and GABA binding sites on the $GABA_A$ receptor (Spreafico, 1993). No abnormalities of $GABA_B$ receptor binding have been found in GAERS using that ligand (Knight, 1992; Spreafico, 1993). A 20% increase in ^{3}H-baclofen binding has recently been demonstrated in the neocortex of lethargic mice (Lin, 1993). Receptor affinity was unchanged in the cortex and the increase in ^{3}H-baclofen binding was thought to reflect an increase in the number of receptors.

1.6. Reading Epilepsy

1.6.1. Introduction

Reading Epilepsy (RE) is presently recognised as an idiopathic localisation-related epilepsy with the following characteristics: "all or almost all seizures are precipitated by reading" (especially aloud) and are independent of the content of the text. They are simple partial motor seizures involving masticatory muscles, If the stimulus is not interrupted, SGTCS may occur. The syndrome may be inherited. Onset is typically in late puberty and the course is benign with little tendency to spontaneous seizures. Physical examination and imaging studies are normal. Ictal EEG discharges are usually brief but vary in terms of morphology and spatial distribution with a clear tendency for left-sided predominance (Commission on Classification and Terminology of the ILAE, 1989).

1.6.2. Clinical features

The age of onset is usually in late adolescence (mean age at onset of 17.7 years and only three out of 110 cases below 12 years and five beyond 25), indicating that RE is clinically manifested after the acquisition of reading skills has been completed. The male:female ratio is 1.8 in a meta-analysis of 110 cases confirming that RE is a syndrome with male preponderance (Wolf, 1992). The typical reading-induced jaw or orofacial myoclonus is by far the commonest and more constant ictal manifestation. The severity, and the frequency of the myoclonic seizures varied even in individual patients. Although ictal manifestations in RE are said to occur without impairment of consciousness, many patients described themselves as "sticking to the word" or, more frequently, reported "loss of track of the reading text" when a jaw jerk occurred that made them to restart reading from the beginning of the sentence. The phenomenon seemed to correlate with the severity of the motor manifestations. Few patients have been reported with a history of spontaneous myoclonic jerks and absences during childhood (Radhakrishnan, 1995).

An overlap of RE with JME was suggested on the basis of clinically similar findings of age at onset, bilateral myoclonic jerks, strong influence of heredity, progression to GTCS, response to sodium valproate, and persistence through life (Radhakrishnan, 1995). In RE, however, myoclonic jerks are reading-induced and involve mostly the jaw, whereas in patients with JME jerks affect the extremities and precipitation with reading has not been described (Janz, 1989; Cavenini, 1992). Furthermore absences are present in up to one-third of patients with JME (Janz, 1989), and are rare in RE.

1.6.3. Genetics

RE has a distinct genetic background. Reading-induced jaw jerking has been described in a parent and child suggesting dominant inheritance (case 9, Radhakrishnan *et al.*, 1995), as well as between monozygotic twin pairs (Forster, 1973). Furthermore, a clear inheritance of spike-and-wave reflex activation during reading has been well documented in asymptomatic family members of patients with RE (Daly, 1975). In the recent meta-analysis by Wolf (1992), 18 of 69 index patients with RE and available information on family history had first-degree relatives with epilepsy or epileptic seizures of known type; eleven of them had RE, three IGE, two febrile seizures, one GTCS since age 3, and one symptomatic localisation-related epilepsy. Radhakrishnan *et al.* (1995) found that four of the 18 patients with a known family history had first-degree relatives with epileptic seizures; one had RE while the information in the remaining three is not clear. The high incidence of RE among the first-degree relatives (11 in the review by Wolf, 1992) of the index cases with known family history reported so far reflects a specific genetic background for the syndrome but the mode of inheritance is still unclear. On the other hand, the few reported patients with RE and relatives with IGE do not suggest any clear genetic link. More substantiated hypotheses regarding the recently raised question on the possible relationship between RE and JME need a larger number of patients with reading-induced seizures and electroclinical features suggesting JME, while families with members affected by both conditions will allow molecular genetic studies. It should be noted however, that none of the so far reported patients had a family member with JME. Similarly, idiopathic localisation-related epilepsies such as benign epilepsy with centrotemporal or occipital spikes have not been reported among family members of patients with RE.

1.6.4. EEG features

1.6.4.1. Interictal findings

Of 104 patients with RE from the earlier literature11 had bilateral spike-and-wave discharges, and five paroxysmal temporal abnormalities. Nine patients were photosensitive in this review (Wolf, 1992).

1.6.4.2. Ictal findings

Of 73 available ictal traces in the literature reviewed (Wolf, 1992), 32% showed bilateral symmetrical discharges, 38% bilateral lateralised, and 30% unilateral. Lateralisation to the dominant hemisphere was noticed in 78%, to the non-dominant side in 10%, and switched between sides in 12% of patients. Unilateral or bilateral regional discharges were more often temporal-parietal (80%) than fronto-central (20%). Radhakrishnan *et al.* (1995) reported a significantly higher proportion of patients with generalised symmetrical ictal discharges (75%). Discharges were strictly lateralised to

the dominant side in only 10%, and generalised with dominant side preponderance in 15% of patients. Bilateral asymmetric and focal discharges are most often lateralised to the left than the right hemisphere. Ictal changes are not always associated with EMG potentials from the jaw muscles. Despite this obvious variability ictal EEG phenomena have been used as a major criterion on whether RE is a localisation related or a generalised syndrome (Wolf, 1992; Radhakrishnan, 1995).

1.6.5. Antiepileptic treatment and outcome

Clonazepam is particularly effective in reading-induced myoclonic seizures, but no controlled trials have been performed (Login, 1978; Hall, 1980; Murphy, 1981). VPA is considered effective in patients with the myoclonic form (Vanderzant, 1982) but failed to eliminate the reading induced seizures in three out of six patients to whom it was given, two with generalised ictal discharges.

1.7. Opioid Transmission

1.7.1. Introduction

Opiate receptors were discovered in 1973. There are several receptor subtypes and further endogenous opioids have been identified (Pleuvrey, 1991). Involvement of opiate receptors and endogenous opioids in the pathophysiology of epilepsy was first suggested in 1977 when it was shown that met-enkephalin injected directly into the lateral ventricle of rat brain resulted in epileptic activity associated with unresponsiveness and staring (Abadie, 1992). Many studies have subsequently tried to evaluate the role of endogenous opioids in epilepsy but differences in opiate receptor organisation between species and methodological problems have made interpretation difficult.

1.7.2. Endogenous opioids

Endogenous opioids are inhibitory neuropeptides. They are divided into three groups: enkephalins, endorphins and dynorphins, which are derived from three separate precursors: proenkephalin, pre-opioi-melanocortin (POMC) and prodynorphin respectively. Proenkephalin is widely distributed throughout the CNS and contains copies of the pentapeptides met-enkephalin and leu-enkephalin in a ratio of 6:1. Several of the met-enkephalin sequences may incorporate more amino acids to produce larger opioids. Enkephalins are released from nerve terminals by a potassium evoked, calcium dependent mechanism. POMC synthesising cells are found in the arcuate nucleus of the hypothalamus and to a much lesser extent in the nucleus tractus solitarius of the brainstem. POMC is made up of several different components which include β-LPH, ACTH and γ-MSH. β-endorphin is a 31 amino acid fragment of β-LPH which shares the same N-terminal structure with met-enkephalin. Release of β-endorphin from the anterior pituitary, like ACTH, is controlled by corticotropin releasing hormone and negative feedback from adrenal steroids. Release from the intermediate lobe of the pituitary is dopamine dependent. Prodynorphin, like proenkephalin, is widely distributed throughout the CNS and is the precursor of dynorphin A, dynorphin B, β-endorphin and leumorphin, all of which contain the leu-enkephalin sequence at the N-terminal. The mechanism of release of dynorphin is not known. After release from nerve terminals, endogenous opioids are rapidly degraded by a variety of amino- and carboxypeptidases (Pleuvrey, 1991; Frederickson, 1982).

1.7.3. Opiate receptors

Three main groups of opiate receptor have been identified: μ, δ and k. Both μ and δ receptors appear to be coupled to potassium channels via secondary messenger systems

involving G proteins. k-receptors are linked with calcium channels. Opiate receptors are mostly postsynaptic although presynaptic receptors have been identified in striatum and spinal cord (Pleuvrey, 1991). Although the endogenous opioids have some affinity for the μ-receptor none are selective for this site. Morphine is a selective μ-agonist and naloxone is a relatively specific antagonist. Enkephalins, especially leu-enkephalin, bind specifically to δ receptors. Enkephalins are degraded rapidly but D-Ala2-D-Leu5-enkephalin is a more stable δ agonist and naltrindole acts as an antagonist. Opiate alkaloids have low affinity for δ-receptors. Most of the products of prodynorphin bind to k-receptors. Diprenoprhine is a non-specific antagonist with similar affinity for μ- and ∂-receptors although at high doses in humans some partial agonist activity has been observed (Perry, 1980; Pleuvrey, 1991).

Autoradiography of rat brain using the non-specific ligand diprenorphine has demonstrated binding in peri-aqueductal grey, intralaminar and medial thalamic nuclei, limbic structures, layers I and II of neocortex, colliculi, and various brainstem nuclei (Pert, 1975). In human brain, studies of individual receptor types have shown that μ receptors are found predominantly in thalamus, hypothalamus, cortex and cingulate gyrus. δ-receptors are present in cortex, the extrapyramidal system and brainstem accounting for more than 50% of opiate receptors in the pons. k-receptors are the predominant subtype in the hippocampus and substantia nigra (Pfeiffer, 1982). The distribution of receptor subtypes is similar between species but k-receptors are more prevalent and δ less prevalent in human compared with rat brain (Pleuvrey, 1991).

1.7.4. Opioid transmission and partial seizures

The possibility that endogenous opioids might be involved in the pathogenesis of seizures was first suggested when β-endorphin and enkephalins injected into the lateral ventricle of rat and gerbil caused seizures characterised by staring and myoclonic twitches (Urca, 1977), which were blocked by specific δ-receptor antagonists (Haffmans, 1987). High doses of naloxone also suppressed the seizures, but at high doses naloxone is relatively non-specific. Epileptiform activity was suppressed by ethosuximide and valproate but not by phenytoin, with diazepam having no effect on opioid induced epileptiform activity (Snead, 1980). Autoradiographic studies of cerebral metabolism and subcortical EEG recordings have shown that epileptic activity following intracranially administered opioids arises from the hippocampus and then rapidly generalises to the cerebral hemispheres (Ramabadran, 1990). It was postulated that opioids mediated via ∂- and/or μ-receptors on interneurons in the hippocampus lead to disinhibition of pyramidal cells with subsequent generalisation (Zieglgänsberger, 1979).

Endogenous opioids are released at the time of GTCS causing refractoriness (Lee, 1986; Reigel, 1988; Savage, 1988). In the WAG/Rij strain of rats, pro-enkephalin levels are increased in striatum and mesencephalon (Coenen, 1992). In addition, systemic GHB has been shown to induce an increase in dynorphin concentration in the hippocampus and posterior pituitary, and to decrease levels of β-endorphin in the thalamus and hypothalamus (Lason, 1983). These findings could indicate a reduction in the release of dynorphin and an increase in the release of β-endorphin from the respective sites. Alternatively synthesis of dynorphin may be increased and β-endorphin decreased respectively.

Evidence suggests that opioid systems may play a role in inhibiting epileptiform activity (Tortella, 1985; Tortella, 1988a,b). Opioid agonists produce prolonged suppression of neuronal conductances, counteracting depolarisatory shift underlying seizure discharges (Moore, 1994), or indirectly via activation of inhibitory GABAergic neurons (Tanska, 1994). Endogenous opioids are released following partial and GTCS in man and might contribute to the post-ictal rise in seizure threshold. Increased levels of enkephalin were found in the CSF and serum of epilepsy patients (Jianguo, 1990); the anticonvulsant effects of enkephalin are reversed by naloxone (Molaie, 1989). Consistent with this finding, naloxone-sensitive displacement of binding of the opioid agonist ^{11}C-DPN evoked by high-frequency stimulation was found in the hippocampus (Neumaier, 1989).

In prior PET studies, the μ-agonist ^{11}C-CFT binding to μ-receptors was increased in lateral temporal neocortex in areas which also showed reduced glucose metabolism (Frost, 1993) speculated to be a tonic antiepileptic system that serves to limit the spread of electrical activity. The increase in ^{11}C-CFT binding to lateral temporal neocortex was confirmed and reduced binding to the amygdala was noted (Mayberg, 1991), though this may be an artefact of partial volume effect (Meltzer, 1996b). Using ^{11}C-DPN, which binds with similar affinities to μ–, k- and δ-subtypes of opioid receptors, there were no abnormalities of binding in the temporal lobe or elsewhere (Mayberg, 1991; Bartenstein, 1993). Also there was no overall asymmetry of binding of ^{18}F-cycloFOXY, which binds to μ- and k-receptors in patients with TLE (Theodore, 1992). The explanation of these findings is not clear, although either an upregulation of μ-receptors and reduction of number or affinity of non-μ-receptors, or upregulation of μ-receptors and occupation of non-μ-receptors by an endogenous opioid ligand would fit the evidence. The compensatory decrease of non-μ-receptors is more likely due to a decrease in k-receptors, since δ-receptors exist in lower concentrations in the cortex compared with k- and μ-receptors.

Significant increases in ^{11}C-methyl-naltrindole (MeNTI) binding to ∂-receptors are identified in two main regions of the temporal neocortex, the middle aspect of the inferior and the anterior aspect of the middle and superior temporal neocortex (Madar, 1997). These increases in ^{11}C-MeNTI binding in the human brain of epilepsy patients are consistent with recent reports that binding to ∂-opioid receptors is increased in the cerebral cortex and hippocampus of seizure-susceptible strains of mice with no change in affinity (Onishi, 1990). While ^{11}C-MeNTI and ^{11}C-CFT both showed increases in the temporal neocortex, there are differences in the distribution of ∂- and μ-opioid receptor increases. Significant decreases in ^{11}C-CFT binding were observed in the amygdala, while binding of ^{11}C-MeNTI was not altered. In addition, regional alterations in ^{11}C-MeNTI and ^{11}C-CFT binding in the temporal neocortex displayed different patterns of distribution. In the medial aspect of the inferior temporal neocortex, both ∂- and μ-opioid receptor bindings were increased to a similar extent, while in the anterior aspect of the middle and superior temporal neocortex, only ∂-opioid receptor binding was increases. This different distribution of regions of change may suggest distinct roles for the μ- and ∂-opioid receptor subtypes in the seizure phenomena.

Increased activity of ∂-opioid peptides and related receptors is likely responsible for mediating anticonvulsant effects. Intracellular recording have shown that ∂-opioid agonist suppress the robust depolarisatory shift underlying seizure discharges (Tanska, 1994). In view of the inhibitory action of opioid agonists, the opioid-receptor response may act as a reactive mechanism to limit epileptic discharges. Alternatively, the increased opioid activity might be secondary to reorganisation of neural circuits driven by cell loss that is caused by repeated seizures. This reorganisation involves selective loss and axonal sprouting of several neurotransmitter systems, including opioid peptides in the hippocampus and cortical areas of epilepsy patients (Swanson, 1995). In the epileptogenic hippocampus of humans and animals, mossy fibres sprouting and increases in immunoreactive sites for opioid agonists have identical anatomic patterns (Houser, 1990).

1.8. Pharmacological Mechanisms of Anti-Epileptic Drugs (AED)

1.8.1. Introduction

Sodium valproate (VPA) and benzodiazepines (BZ) are the most effective AED in IGE and are also effective in mTLE although BZ only acutely. Their pharmacological mechanisms will be discussed in relation to current concepts of the neurochemistry of partial and absence seizures and this will be followed by a brief summary of the mechanisms of other commonly used AED.

1.8.2. Sodium valproate

Valproate (di-N-propylacetate) is a branched chain fatty acid with a broad spectrum of anti-epileptic activity. It is effective in many animal models but is only weakly protective against seizures induced by excitatory amino acids. In models of partial epilepsy, VPA prevents spread of epileptic activity from the focus but has no activity against epileptiform discharges in the focus itself. In animal models of generalised epilepsy, VPA suppresses absences and GTCS. Relatively high doses are required, however, and motor toxicity occurs at levels only slightly above those necessary for the anti-epileptic effect. In man, VPA is effective against partial and SGTCS, and in IGE against absence, myoclonic and GTCS. It is well tolerated and side effects are not common in clinical practice (Rogawski, 1990). Despite this efficacy as an AED, the mechanism of action of VPA is unresolved. Three main hypotheses have been proposed:

- The first concerns GABAergic transmission. Increased CSF concentrations of GABA have been reported in patients treated with VPA suggesting that there may be enhanced GABAergic transmission in the brain (Löscher, 1984; Löscher, 1985). The mechanism by which VPA increases the concentration of GABA is not well understood. VPA has a weak inhibitory effect on GABA transaminase and enhances GAD activity but the relevance of these mechanisms at therapeutic concentrations has been questioned (McLean, 1986). One study in mice has, however, shown increased ^{3}H-flunitrazepam binding with VPA suggesting that effects of VPA on GABA metabolism may result in functionally significant effects on postsynaptic $GABA_A$ receptors (Koe, 1983). Although an increase in GABAergic transmission may be relevant to the anti-convulsant action of VPA, it would be expected to exacerbate absence seizures.
- The second hypothesis is based on the observation that VPA limits the ability of cultured neurons to generate sodium dependent action potentials at high frequency (McLean, 1986). This effect is seen at therapeutic concentrations and is similar to that seen with phenytoin and carbamazepine. It is possibly due to blockade of voltage dependent sodium channels but this has not been confirmed. Spread of

seizure activity from a focus may be limited by this mechanism but suppression of absences is unlikely. Indeed, phenytoin and carbamazepine do not suppress absence seizures (Rogawski, 1990). VPA has not been shown to bind to the same binding site as carbamazepine and phenytoin and may bind to a separate site on the sodium channel.

- VPA, at clinically relevant concentrations has also been demonstrated to invoke a modest reduction in low-threshold T-type calcium current, thought to be responsible for oscillatory bursting in thalamic neurons, which may explain its efficacy against generalised absences seizures (Kelly, 1990).

Thus, all hypotheses may account for the efficacy of VPA in partial and GTCS but neither satisfactorily explain the suppression of generalised spike-wave activity and absence seizures.

1.8.3. Benzodiazepines

Benzodiazepines (BZ) are effective in a wide variety of models including PTZ seizures and other models of absence seizures. Although effective against absence seizures in man, ESM and VPA are preferred because of sedation and development of tolerance. BZ are useful in the management of myoclonic seizures and as adjunctive treatment for GTCS (Rogawski, 1990). BZ facilitate GABA-chloride coupling at the $GABA_A$ receptor. They bind to the α subunit and in the presence of a γ subunit (Pritchett, 1989) increase the frequency of chloride channel opening for a given concentration of GABA, without affecting single channel conductance or burst duration (Richards, 1984). The six different α subunits determine the affinity for different BZ. There is high correlation between the potencies of BZ in partial and GTCS, and their affinities for the binding site *in-vivo* (Meldrum, 1986). Less than 30% receptor occupancy is required for maximum protection against seizures. The competitive BZ antagonist, flumazenil, and $GABA_A$ antagonist prevent the anti-convulsant action of BZ providing further evidence that this is the major site of action in GTCS (Nutt, 1982).

Whilst an increase in transmission at the $GABA_A$ receptor might explain the efficacy of BZ in partial and GTCS, the explanation of the suppression of absence seizures is less clear. A global increase in $GABA_A$ transmission is usually associated with exacerbation of spike-wave discharges. BZ increase GABA-chloride coupling at the $GABA_A$ receptor and yet suppress both GTCS and absence seizures. The explanation for this apparent contradiction is uncertain. In GAERS it has been shown that BZ retain their anti-absence activity despite large doses of the GABA transaminase inhibitor, GVG. It is possible that the anti-absence action of benzodiazepines is dependent on selective activation of $GABA_A$ receptors at specific sites or of certain $GABA_A$ receptor subtypes, whereas GVG causes massive non-specific activation of GABAergic

pathways (Marescaux, 1985). Alternatively, BZ are known to have other, non-GABA related, mechanism which may be relevant to their efficacy in absence seizures (Haefely, 1989). BZ are known to inhibit adenosine uptake and to block sodium and calcium channels but the importance of these actions is unknown (Haefely, 1989) and the precise way in which BZ suppress absences remains uncertain.

1.8.4. Others

The principal mode of action of phenytoin and carbamazepine is inhibition of voltage-dependent sodium channels which are responsible for the initial depolarisation of an action potential. This results in protection against spread of epileptic activity but has only minor effects on the epileptogenic focus itself. In addition to this action both drugs exhibit a variety of other effects. Other actions of phenytoin include release of endogenous opioids, and an interaction with peripheral BZRs (Rogawski, 1990). There is evidence that either drug has a direct effect against GTCS and partial seizures with no benefit against absence seizures and there are some reports suggesting that phenytoin and carbamazepine actually exacerbate seizures (Vergnes, 1982; Shields, 1983; Snead, 1985).

Of the barbiturates, phenobarbitone is the most commonly used as an AED. It has a broad spectrum of action and is effective against both GTCS and absence seizures. Several pharmacological actions have been identified but the relative importance of these to the different seizure types has not been clearly established. Phenobarbitone binds to the $GABA_A$ receptor complex and enhances the effects of GABA. It also blocks voltage-dependent calcium channels causing inhibition of neurotransmitter release. In addition, there are effects on other ion channels and excitatory amino acid transmission (Rogawski, 1990).

Vigabatrin (GVG) increases GABA levels by irreversible inhibition of GABA aminotransferase. It is effective against GTCS and partial seizures, but may exacerbate absence and myoclonic seizures (Löscher, 1982; Rogawski, 1990).

Lamotrigine (LTG) is a novel anti-epileptic drug which suppresses release of glutamate by blockade of voltage dependent sodium channels (Brodie, 1992). The anti-epileptic activity of LTG is thought to be mediated primarily via voltage-dependent sodium channels through inhibition of sustained repetitive firing. It is effective against GTCS and partial seizures but there is also some evidence that it may be useful in IGE (Timmings, 1992). In cultured rat cortical neurons, only concentration of LTG 10 times the amount needed to block Na^+ channels were found to alter Ca^+ conductances. LTG is not currently thought to have a significant action on GABAergic neurotransmission.

Topiramate has been shown to inhibit sustained repetitive firing induced by a current pulse (Coulter, 1993) suggesting a prolonged inactivation of sodium channels. Topiramate has also been shown to potentiate the effects of GABA on chloride currents in mouse cortical neurones by increasing the number of channel openings induced by GABA, possibly via a novel site on the $GABA_A$ receptor complex (Brown, 1993). In cultured rat hippocampal neurones topiramate at concentrations of 10μM produced a reversible, concentration-dependant decreases in kainate-evoked inward currents, indicating that it has antagonistic effects on the kainate/AMPA subtype of glutamate receptor. At concentrations of up to 200 μM, however, topiramate had virtually no effect on the activity of glutamate receptors of the NMDA subtype (Coulter, 1993).

Tiagabine increases GABA concentrations in the synaptic cleft via inhibition of reuptake of GABA in glial cells (Meldrum, 1996). Tiagabine is a second-line drug for partial seizures with or without secondary generalisation, but was not generally available in the UK at the time of the studies.

The exact mode of action of Gabapentin is unknown, although studies suggest that it may promote GABA synthesis (Meldrum, 1996). Gabapentin is generally viewed as being less effective than other new AEDs, although this may be because the doses initially used in clinical practice were too low. Gabapentin is not metabolised, exhibits no brain binding and does not induce hepatic enzymes. Its potential, therefore, for drug interaction is small and to date no clinical significant interactions and no serious idiosyncratic reaction have been reported.

CHAPTER II Rationale for the Use of PET in Epilepsy

PET provides a means to study local tissue physiology and neurochemistry non-invasively in humans (Frackowiak, 1989). Previously methods for gaining information about such processes relied on measurements in blood and CSF which are "biochemically distant" from the tissue being studied. Measurement of oxygen and glucose metabolism has been widely used to investigate cerebral function and disease. More recently, tracers have been developed to study a variety of neurotransmitter systems. Ligands are now available to examine the integrity of GABAergic and opioid neurotransmission. PET provides complementary information to neurophysiology and structural imaging with MRI.

2.1. ^{11}C-Flumazenil PET in Temporal Lobe Epilepsy

2.1.1. Introduction

The hallmark of an epileptogenic focus, studied interictally, is an area of reduced rCMRglu that is usually considerably larger than the pathological abnormality. Partial seizures are associated with an increase in rCMRglu in the region of the epileptogenic focus, and often a suppression elsewhere. The most likely reason for the large region of reduced metabolism is inhibition or differentiation of neurones around an epileptogenic focus (Engel, 1983; Franck, 1988). Over the last decade, some epilepsy surgery programmes have relied extensively on ^{18}F-FDG PET as a tool for localising the epileptic focus. The current place of PET needs to be re-evaluated in the light of developments in MRI as the finding of a definite focal abnormality with the latter technique, such as HS, may render an ^{18}F-FDG or ^{11}C-FMZ PET scan superfluous (Gaillard, 1995). Comparative studies of two imaging techniques, such as MRI and PET are difficult to interpret, however, because of the likelihood that the methodologies and equipment will not both be developed to the same degree in any one centre.

2.1.2. Previous studies

The binding of ^{11}C-FMZ to cBZR in epileptogenic foci was initially found to be reduced by an average of 30%, with no change in the affinity of the ligand for the receptor (Savic, 1988). Comparative studies with ^{18}F-FDG PET scans have shown the area of reduced ^{11}C-FMZ binding to be more restricted than is the area of reduced glucose metabolism in TLE (Henry, 1993; Savic, 1993). A limitation of the methodology of these previous investigations is that high resolution volumetric MRI was not always performed and co-registered with functional imaging data. This has limited the conclusions that could be drawn regarding the correlation between

underlying structural abnormalities, such as HS. In these studies the anatomical resolution of mesial temporal lobe structures has been generally suboptimal and hippocampi have not been separately identified from temporal neocortex. Further, the ROI analysis techniques that have been employed in previous investigations have largely relied upon visual placement of regions and so have been susceptible to observer bias.

The underlying pathological basis of reduced ^{11}C-FMZ binding in HS is still under study. Autoradiographic and histopathological studies of surgically removed sclerotic hippocampi have shown reduced neurone counts and cBZR densities, with a further reduction of density of cBZR per remaining neuron (Johnson, 1992). Burdette et al. (Burdette, 1995) found a highly statistically significant correlation coefficient between neurone loss and reduced cBZR binding on autoradiographic analysis of hippocampi from patients treated surgically for HS, and concluded that neurone loss was the basis of reduced 11C-FMZ binding *in-vivo*. This analysis did not exclude an additional reduction of cBZR per neurone. Further correlational studies between quantitative *in-vivo* hippocampal ^{11}C-FMZ binding, quantitative neuropathological data and autoradiographic studies, with assessment of individual cells are needed to determine whether there is an additional functional abnormality over and above the loss of BZR bearing neurones, in HS.

Absolute quantitation of PET data, however, is limited by its spatial resolution, partial volume effects particularly confounding quantitative measurements for structures smaller than twice the full width at half maximum of the scanner (Hoffman, 1979), such as the normal and the sclerotic hippocampus. Spill over of signal into surrounding white matter and cerebrospinal fluid may result in underestimations of the measured hippocampal activity due to tissue volume averaging within the hippocampal volume of interest (Müller-Gärtner, 1992; Meltzer, 1996a,b; Labbé, 1997). In addition, there is spill over of activity into mesial temporal structures from neighbouring grey matter which has a higher FMZ binding; this affects the atrophic hippocampus more than a bigger, intact hippocampus and may lead to an overestimation of cBZR density in HS. Thus, correction for partial volume effect is necessary to determine the true tissue cBZR density in the hippocampus. Furthermore, HS is generally more pronounced anteriorly rather than affecting the whole structure uniformly (Van Paesschen, 1997a). It follows that a single measurement will not detect subtle focal abnormalities. Division of the hippocampus into head, body and tail as carried out in analysis of MRI is not possible using PET, without partial volume effect correction, due to the limited spatial resolution of the latter technique. Previously published MR-based correction for partial volume effect (Müller-Gärtner, 1992; Meltzer, 1996a,b) only corrected one VOI at a time.

It seems most likely that, in addition to any functional change, cBZR changes reflect localised neuronal and synaptic loss in the epileptogenic zone and that the more extensive hypometabolism is a result of diaschisis. In clinical terms it appears that ^{11}C-FMZ PET may be superior to ^{18}F-FDG for the localisation of the source of the seizure. It is not certain, however, whether this data confers additional clinically useful information in patients with clear-cut MRI findings of unilateral HS.

2.1.3. Aims of the current study

The aims of this work were to use ^{11}C-FMZ PET to investigate the anatomical and functional basis of temporal lobe epilepsy by using state-of-the-art structural MRI and functional imaging with PET and to correlate these findings with autoradigraphically determined *ex-vivo* measurements of ^{11}C-FMZ binding in the hippocampus. The individual experiments described in chapters IV-VII had the following aims:

- to determine the extent of significant abnormalities of ^{11}C-FMZ binding in patients with mTLE due to unilateral HS in order to better understand the processes and neuronal circuits involved in the pathophysiology of TLE and to provide structural / functional correlations.
- to assess absolute changes in ^{11}C-FMZ binding corrected for partial volume effect within the head, body and tail of the hippocampus in patients with TLE and bilateral symmetrical, bilateral asymmetrical and unilateral HS in order to detect more subtle abnormalities within the inhibitory neurotransmitter system ipsi- and contralaterally to the seizure focus.
- to correlate quantitative *in-vivo* ^{11}C-FMZ binding corrected for partial volume effect with quantitative MRI and neuropathology in order to determine whether ^{11}C-FMZ binding measured *in-vivo* is reduced over and above hippocampal volume loss.
- to directly compare *in-vivo* ^{11}C-FMZ binding and *ex-vivo* ^{3}H-FMZ binding in HS from patients having anterior temporal lobe resections in order to validate our *in-vivo* findings.

2.2. ^{11}C-Flumazenil PET in Idiopathic Generalised Epilepsy

2.2.1. Introduction

Structural imaging with CT and MRI is normal in IGE and PET provides a potential means to advance our understanding of this condition. In an autoradiographic study of cerebral glucose utilisation in a rat model of spontaneous generalised absences, there was a widespread increase in cerebral glucose metabolism, compared with controls. The relationship between spike wave activity and cerebral glucose utilisation is not straightforward however, as a dose of ethosuximide that suppressed all spike-wave activity was not associated with a reduction of glucose metabolism (Nehlig, 1992; Nehlig, 1993). There have been three studies of glucose metabolism in IGE in humans. Interictal studies have been unremarkable; studies carried out when frequent absences were occurring have shown a diffuse increase in cerebral glucose metabolism of 30-300%, with greater increases being seen in children. Absence status, however, was associated with a reduction in cerebral glucose metabolism. There were no focal abnormalities and the rate of metabolism did not correlate with the amount of spike-wave activity (Engel, 1985; Theodore, 1985; Ochs, 1987).

Regional cerebral blood flow (rCBF) has been assessed using PET and bolus injections of ^{15}O-labelled water and PET, achieving a temporal resolution of < 30 seconds and a spatial resolution of 8x8x4.3 mm. Typical absences were precipitated with hyperventilation and the distribution of rCBF was compared when absences did and did not occur. During absences there was a global 15% increase in rCBF and, in addition, a focal 4-8% increase in blood flow to the thalamus. There were no focal increases in rCBF in the cortex and no focal decreases (Prevett, 1996). Spike-wave activity in typical absences oscillates in thalamo-cortical circuits and the site of primary abnormality remains uncertain. The preferential increase in thalamic blood flow is evidence to the key role of this structure in the pathophysiology of absences in man, but does not clarify whether this is the result of converging activated thalamo-cortical pathways or reflects a primary thalamic process. No significant increases in thalamic blood flow were detected in the 30 seconds prior to generalised spike-wave activity on the EEG. A focal increase in blood flow developing 5 seconds before generalised spike-wave appeared would be most unlikely to be detected with this technique.

2.2.2 Previous studies

Savic *et al.* (1990) reported a slight reduction in cortical binding of ^{11}C-FMZ to cBZR in a heterogeneous group of patients with generalised seizures, compared with the "non-focus" areas of patients with partial seizures. It was subsequently reported that, compared with normal subjects, patients with primary GTCS had an increased cBZR

density in the cerebellar nuclei and decreased density in the thalamus (Savic, 1994). Reliable identification of cerebellar nuclei is not easy on ^{11}C-FMZ PET images and these results have not been replicated. Prevett *et al.* (1995a) found no significant difference in ^{11}C-FMZ binding to cerebral cortex, thalamus or cerebellum between patients with CAE and JAE, not taking VPA, and control subjects. The volume of distribution of ^{11}C-FMZ, however, was 9% less in patients receiving VPA suggesting that this drug may result in reduced number of available cBZR. Acutely, the cerebral binding of ^{11}C-FMZ, was not affected by flurries of absences in any area of neocortex or the thalamus (Prevett, 1995b).

2.2.3. Aims

The aims of this work were to use PET to investigate the anatomical and functional basis of IGE by measuring cBZR density and to examine the effect of VPA on ^{11}C-FMZ binding to cBZR. The individual experiments described in chapter VIII aim to answer the following questions:

- to determine whether cBZR binding is normal in patients with IGE using a more sensitive scanning technique and a more objective analytical methodology than was previously available.
- to determine the effect of VPA on ^{11}C-FMZ binding in a more powerful longitudinal study design.

2.3. ^{11}C-Diprenorphine PET in Reading Epilepsy

2.3.1. Introduction

The biochemical and anatomical bases of reading epilepsy are not well understood (Wolf, 1992). Ictal EEG findings predominantly occur in the temporo-parietal cortex of the language dominant hemisphere but are also found in other hyperexcitable cortical areas that are functionally activated by reading (Radhakrishnan, 1995). Neurotransmitters are responsible for mediating human neuronal activity and, until now, PET studies of specific ligands have largely been limited to quantitation of receptor binding and availability under resting conditions (Frost, 1993). Endogenous neurotransmitter release is a pivotal event in neuroregulation, but has been very difficult to study non-invasively *in-vivo* in man (Morris, 1995). To date, PET studies of neurotransmitter release in humans have concentrated on pharmacological manipulations and measured changes in receptor availability to radioligands (Dewey, 1992). RE is an ideal model to study dynamic neurotransmitter changes in specific brain areas in relation to epileptic seizures.

2.3.2. Previous PET studies

Interictal PET studies have shown elevated μ-opiate receptor binding in the lateral temporal neocortex overlying mesial temporal foci, suggesting focal epilepsy may be associated with abnormal opioid transmission (Mayberg, 1991). Cerebral opioid release, as evidenced by displacement of ^{11}C-DPN binding, has been observed in large cerebral regions following serial absences (Bartenstein, 1993), but without any anatomical precision.

2.4.2 Aims

The aim of this study was to localise endogenous neurotransmitter release *in-vivo* at high resolution, in response to focal epileptic activity and specific cognitive activation in man. We have used ^{11}C-DPN PET studies to investigate acute changes in cerebral opioid receptor occupancy with reading induced seizures, studying the neural networks and neurotransmitter release underlying this form of epilepsy.

CHAPTER III Methodology

3.1. Basic Principles of PET

PET allows tomographic delineation of cerebral structures and measurement of local tissue concentrations of injected radioactive tracers (Phelps, 1993). PET can be performed with the subject in the resting state or during, or following a cognitive or motor task, the administration of a drug or the occurrence of a seizure. PET depends on the use of short half-life positron emitting isotopes. $^{15}0$, ^{11}C, and ^{18}F are the most commonly used isotopes and have half-lives of 2, 20 and 110 minutes respectively. In view of the short half-lives of $^{15}0$ and ^{11}C, it is necessary to have a cyclotron on site to produce these isotopes. $^{15}0$ and ^{11}C are substituted for naturally occurring elements. The use of natural elements allows labelling of compounds for use *in-vivo* without altering their biochemical properties or behaviour. These tracers are administered to the subject by intravenous injection or inhalation.

Positrons, positively charged electrons, are emitted from the unstable nuclei as they decay to more stable structures. When a positron and an electron collide (within 3mm) they annihilate releasing a pair of high energy (511 keV) photons in opposite directions, which are detected by the PET camera. The PET camera consists of multiple rings of detectors (**Figure 3**). Each ring of detectors, of which a small selection are shown (D1-D6), samples a slice of brain. Opposing detectors (D1/D2) within each ring are linked electronically to accept only those events which are recorded simultaneously from a source of activity (S1). This so called coincidence detection allows the origin of the recorded radiation within a given slice of brain to be established.

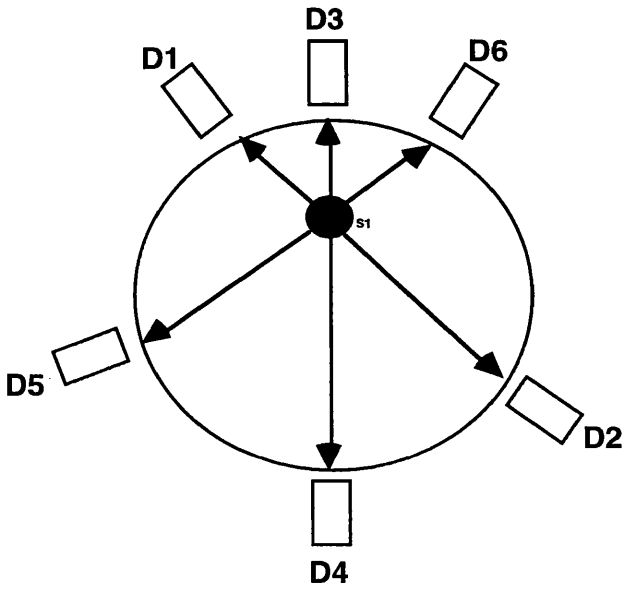

Figure 3: The principle of PET scanning

The data collected by the PET scanner may be mathematically reconstructed to produce tomographic images of tissue radioactivity concentration. The resolution of the final images is defined as the width of the distribution of counts from a single point source at half the maximum value (**Figure 4**). Two simultaneous point sources can only be distinguished if separated by > 1 full-width-at-half-maximum (FWHM).

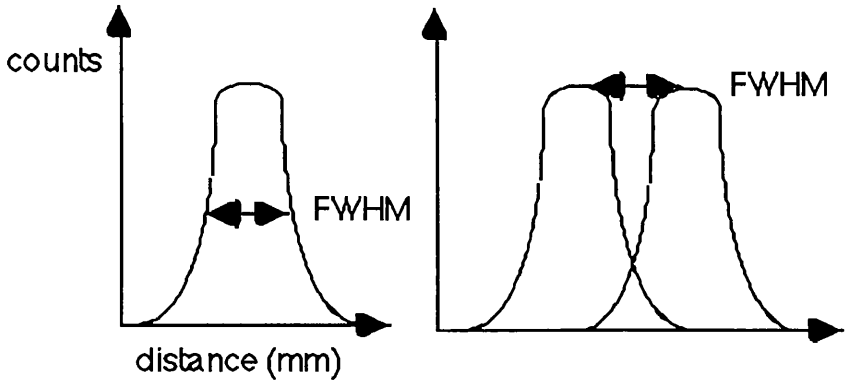

Figure 4: Full-width-at-half-maximum

3.2. Data Acquisition - PET

PET scans were performed at the MRC Cyclotron Unit at the Hammersmith Hospital. The studies were performed with a ECAT 953b scanner (CTI Siemens, Knoxville, TN) which acquires 31 simultaneous slices and has a resolution of 4.8 x 4.8 x 5.2 mm (at FWHM).

3.2.1. Head-positioning and transmission scans

In order to minimise movement artefacts during scanning subjects' heads were rested in individualised head moulds. In addition, direct observation of the alignment of marks put on the skin to projected crossed laser lines was maintained to minimise movement. Correct positioning was verified with a 2 minute transmission scan using three rotating $^{68}Ga/^{68}Ge$-rotatory line sources followed by a 10 minute transmission scan to enable emission scans to be corrected for attenuation (Bailey, 1992). Two different scanning positions were used for the studies:

- *Hippocampus - orientation:* All subjects of the studies investigating cBZR in mTLE were first positioned with the glabella-inion line parallel to the detector rings. Scans were then performed with the gantry of the scanner tilted forward 20^{o} off the glabella-inion line (**Figure 5**). Using this orientation axial images were obtained along the plane of the hippocampi, and the coronal images were orthogonal to the

hippocampus, minimising partial volume effects as has been shown in previous studies to obtain optimal MR images of hippocampal sclerosis (Jackson, 1993).

- *Standard - orientation*: All subjects for the study investigating cBZR in IGE, 10 patients and 20 healthy controls, and opioid receptors in RE, five patients and six controls, were positioned with the glabella-inion (GI) line parallel to the detector rings, so that the directly obtained transaxial images were approximately parallel to the intercommissural line (AC-PC/ GI line).

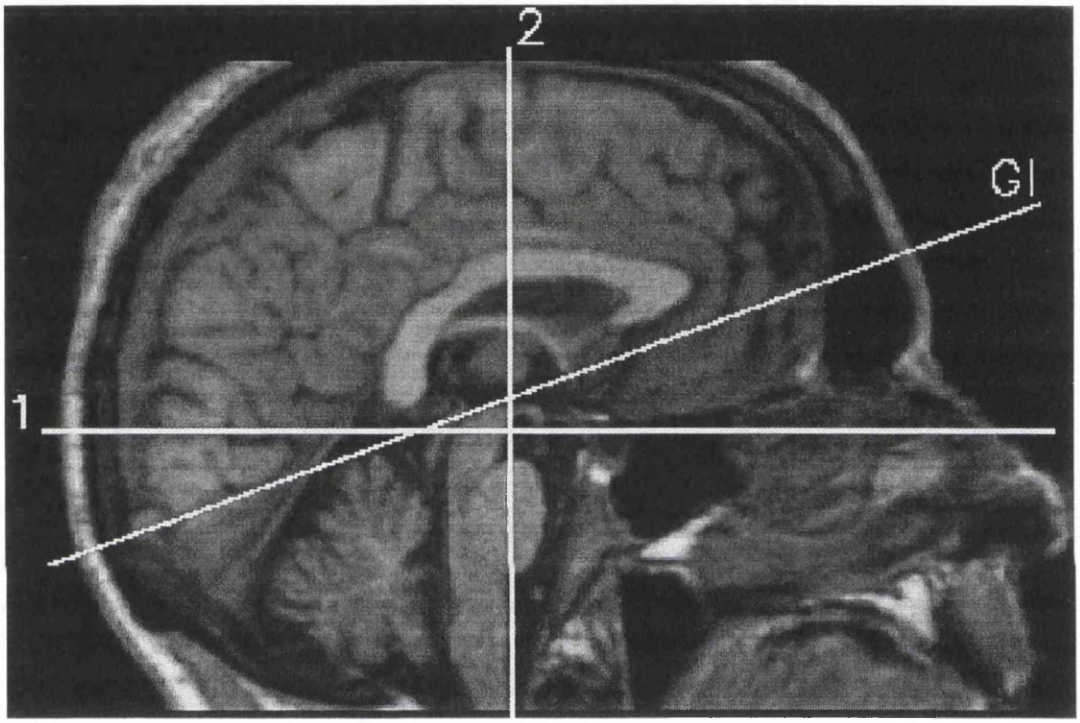

Figure 5: Hippocampus orientation
Sagittal midline view of high resolution normal MRI with GI=glabella-Inion line, 1= transaxial view and 2= coronal view of scanner orientation. Line 1 is along the long axis of the hippocampus and line 2 is orthogonal to this.

3.2.2. Continuous EEG monitoring

EEG electrodes were placed on the scalp of each subject using the 10/20 system of electrode placement. The EEG was monitored continuously during all the scans with an 8 channel Siemens Mingograph instrument. The EEG records were used to quantify the total duration of any bursts of focal or generalised spike-wave activity that occurred during the scan and for the study of opioid receptors in RE to detect sub-clinical epileptiform activity during reading activation and to monitor eye movements.

3.2.3. Arterial plasma input function

Prior to scanning, a 22 gauge cannula was inserted into the radial artery after subcutaneous infiltration with 0.5% bupivicaine. Radiolabelled metabolites appear in plasma after a short delay following intravenous injection of the parent tracer. Arterial blood sampling is essential in order to determine the availability of the radiotracer in the brain. Radioactivity in arterial blood was assayed continuously on-line (Ranicar, 1991). In order to determine how much of this total radioactivity can be attributed to the unmetabolised, available radioligand, radiolabelled metabolites in plasma are assayed in intermittent blood samples taken throughout the scanning period (Luthra, 1993). These data are used to correct the continuous measure of arterial blood radioactivity, in order to produce a time-activity curve for unchanged, available radiotracer in arterial plasma. This plasma input function was derived from the data obtained from arterial blood for subsequent kinetic analyses (Lammertsma, 1991; Lammertsma, 1993).

3.2.4. Radiotracer

The radio-isotopes were made on site in the MRC Cyclotron Unit and then incorporated into flumazenil (FMZ) and diprenorphine (DPN) respectively for injection. Each preparation was analysed by HPLC to determine the specific activity of the tracer and to ensure radiochemical purity. The tracers were injected intravenously through a 22 gauge cannula placed in an antecubital fossa vein. In accordance with ARSAC regulations, the total body dose of radiation for each subject was less than 5 mSv.

3.2.4.1. ^{11}C-Flumazenil (FMZ)

FMZ is a non-subtype specific cBZ / $GABA_A$ receptor antagonist. Clinically it is used to reverse the effects of benzodiazepines. In subjects who have not received benzodiazepines, FMZ can be administered in doses which lead to a significant degree of receptor occupation with negligible clinical effects (Hunkeler, 1981). FMZ binds to four out of six possible α subunits that may be present in $GABA_A$ receptors. These four α-subunits (α 1, 2, 3, and 5) are the most prevalent and flumazenil, therefore, acts as a good marker for the $GABA_A$ receptor (Olsen, 1990). FMZ is specifically bound exclusively in the brain with high affinity to cBZ / $GABA_A$ receptors and has low non-specific binding, it crosses the blood brain barrier easily, it is not metabolised in brain, its non-specific cerebral binding represents about 10% of the specific binding (small but not negligible), it has polar metabolites (one of which is radiolabelled) which do not cross the blood brain barrier, it dissociates from the BZ receptor rapidly (tissue half life estimates vary between 12 and 22 minutes), it reaches peak concentrations in the head by about 10 minutes and it is localised principally in cortex with some binding in hippocampus, basal ganglia, thalamus and cerebellum from which it washes out at a differential rate than from the cortex. Binding to specific receptors is reversible so that

the tracer clears slowly from the brain in its original form as the concentration in blood falls towards zero. The rate of clearance of the tracer from a given region is dependent on receptor affinity and the density of receptors at that site, clearance being most rapid from regions with least receptors.

3.2.4.2. ^{11}C-Diprenorphine (DPN)

DPN is a high affinity opiate receptor ligand with similar affinities *in-vivo* for the 3 main receptor subtypes: μ, k and ∂ (Pfeiffer, 1982). It acts predominantly as an antagonist, but at higher doses in man acts as a weak partial agonist and is associated with mild sedation. It is metabolised in the liver and metabolites rapidly accumulate in blood but they do not cross the blood brain barrier (Perry, 1980). ^{11}C-DPN has been established as a useful PET ligand and has been used in the study of normal subjects and patients (Mayberg, 1991). ^{11}C-DPN was prepared by O-methylation of 3-O-trityl, 6-desmethyl-diprenorphine. The use of the base-stable, acid labile trityl protecting group minimises the formation of byproducts and allows reproducible radiosyntheses (S. Luthra, personal communication). After intravenous injection it is rapidly taken up into the brain. The tracer then washes out slowly from areas with high receptor density and more rapidly from areas with few receptors. 90 minutes after injection of the tracer 80-90% of the remaining activity is specifically bound to receptors. High specific binding is seen in thalamus, caudate, and frontal, temporal and parietal cortex. Binding is lowest in occipital cortex and white matter (Jones, 1988).

3.2.5. Scanning protocol

As the distribution of the radioligand in the organ of interest is likely to change over the time period of the experiment, the scanning period is subdivided into a number of time intervals or "frames". The radioactivity distribution of the initial period of the experiment reflecting blood flow and ligand delivery is best imaged with a series of short, 15 seconds to 1 minute time frames. As the experiment continues the ligand will become bound and the radioactivity distribution will then, after about 60 minutes, reflect the pharmacokinetics of the ligand at the receptor. In addition, the radioactivity measurements will be affected by decay of the radioisotope which requires longer time frames towards the end of the scanning period. In the case of ^{11}C-FMZ we used a protocol of 20 frames (30 sec background, 4 x 15sec, 4 x 60sec, 2 x 150sec, 2 x 300sec, 7 x 600 sec). The scanning protocol for ^{11}C-DPN was specifically designed to detect endogenous neurotransmitter release induced by reading and reading-induced seizures from 30 to 60 minutes after tracer injection, and therefore we used very short time frames covering this 'activation' period (30 sec background, 3 x 300sec, 10 x 120sec, 5 x 300sec, 3 x 600 sec).

3.2.6. Image reconstruction and scatter correction

After completion of the scan, the raw count data was transferred onto SPARC Ultra workstations (Sun Microsystem Inc. Mountain View, CA) and reconstructed into images of radioactivity concentration using CTI software. In the past, images were obtained with lead septa separating each ring of detectors collecting each transaxial slice of data (two-dimensional or 2D imaging) and absorbing photons, which were deflected from their original trajectory, with the electronic linking of detectors to detect coincidences and mathematics of reconstruction being relatively simple. By removing the septa, three-dimensional or 3D imaging increases the numbers of counted events resulting in increased sensitivity by a factor of 6 (Bailey, 1992), but absorption of deviated photons by the lead septa no longer occurs and thereby increases the problem of scatter. With countless photons being emitted from the organ of interest, some of these photons inevitably collide with subatomic particles and are deflected from their original trajectory, or scattered. Although such photons will no longer be able to arrive coincidentally with the "partner" photon travelling in the opposite direction, by chance some scattered photns will arrive at a detector at the same moment as another photon. Because the number of photons being emitted is so huge, the proportion of photons which become scattered is not insignificant. In 2D, the scattered photons usually deviate from the possible lines of response of paired detectors and are absorbed by the septa, so scatter is not a problem in 2D. The scatter fraction varies across the field of view of the scanner due to its geometry, and also will vary depending on the local level of radioactivity in the organ of interest. Hence, scatter needs to be subtracted from the data during reconstruction in order to enable accurate radioactivity measures. This can be done by modelling scatter according to the known geometry of the camera (Bailey, 1992) or by measuring the scatter simultaneously with the unscattered data (Grootoonk, 1993). The former method is easier but cannot account for scatter from photons emitted from parts of the subject outside the field of view of the camera, which may be significant; the latter method has the advantage of allowing removal of the real scatter, rather than merely a model of it, which allows for out of field of view scatter. Measuring scatter depends upon the observation that scattered photons have lost some of their energy through a collision with another particle; it is possible to adapt the detector properties such that photons can be collected at two different "energy windows" simultaneously, one set at the level of the emitted photons (the "data window") and the other at a lower energy level appropiate for scattered photons (the "scatter window"). This is known as dual-window scatter correction.

3.3. Data Analysis - PET

3.3.1. Introduction

The dynamic image set, describing the uptake and subsequent wash-out of the tracer following intravenous injection, and the arterial plasma input function, describing the kinetic processes in the tissue, can be used to derive regional parameters of ligand binding, such as receptor density (B_{max}), receptor affinity (K_D) and volume of distribution between blood and the organ in question (V_d). These parameters are derived via modelling techniques. A tracer kinetic model provides the basis for operational equations for estimates of these physiological parameters from the acquired data (Phelps, 1993). The essential underlying assumption is that the observed time course of tissue radioactivity is the convolution of the arterial input and tissue response function, which describes the physiological process under study at each voxel.

3.3.2. Compartmental model

Compartmental models are the commonest form of a tracer kinetic model used in PET (Phelps, 1993). A compartment is a volume within which the tracer rapidly becomes uniformly distributed. For example a compartmental model describing the behaviour of a receptor ligand might include a vascular compartment and within the tissue free, non-specifically bound and specifically bound compartments. A model which is too complex results in parameter estimates with large variances. In practice, simplified models and operational equations are developed in which the number of compartments are reduced by grouping them into functional compartments that contain substructures for which no or only partial information is provided. The number, definition and inter-relationship of compartments in a compartmental model is developed from knowledge of the biological properties of the ligand in question.

3.3.2.1. Two compartment model

It has been shown that a two compartment model (Frey, 1991) adequately describes the cerebral kinetics of FMZ incorporating plasma compartment (C_P) and free, non-specific and specific compartments (C_B). K_1 and k_2 are rate constants describing exchange across the blood brain barrier. **(Figure 6).**

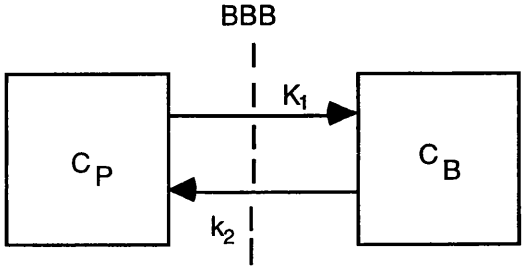

Figure 6: Example of two compartment model

3.3.2.2. Three compartment model

A three compartmental approach has been used to measure B_{max}/K_D for ^{11}C-DPN (Cunningham, 1991) with C_2 representing the free + non-specifically bound compartment, C_3 the specifically bound compartment and K_{1-4} the rate constants describing exchange between individual compartments **(Figure 7)**.

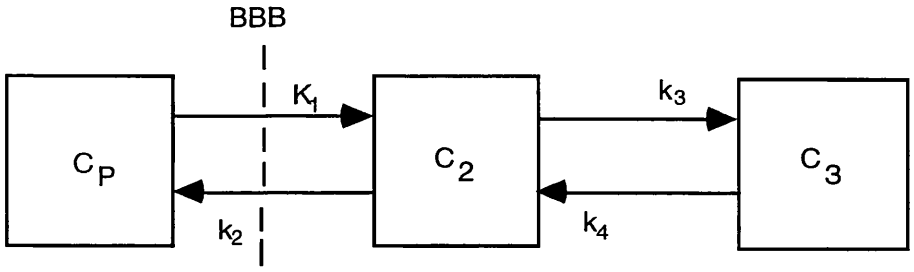

Figure 7: Example of three compartment model

A single scan with arterial sampling following a high specific activity injection of tracer can be used to derive k_3/k_4. k_3/k_4 is equal to B_{max}/K_d.

In all compartmental models a steady state is assumed. If only trace amounts of the ligand are given, a steady state of essentially zero receptor occupancy pertains throughout the study. A dynamic PET scan performed after a high specific activity injection of tracer satisfies these criteria (Koeppe, 1991). V_d represents the summed volume of distributions of free, non-specifically bound and specifically bound tracer, but because the contributions of free and non-specifically bound are relatively small, V_d correlates well with specific binding. V_d is linearly related to B_{max}/K_d, where B_{max} is the concentration of receptors available for binding and K_d is receptor affinity.

Non-steady state compartmental modelling has been used to obtain measures of B_{max} and K_d individually with two dynamic PET scans at different levels of receptor occupancy (Sadzot, 1991). Generally, a bolus injection of ^{11}C-FMZ is given at high specific activity in one study and at low specific activity in the other. In the high specific activity study, receptor occupancy by unlabelled FMZ is essentially zero throughout. During the low specific activity study, unlabelled FMZ occupies a significant number of receptors, but receptor occupancy falls as the unlabelled FMZ is cleared from the brain during the scan. The steady state assumed in compartmental analysis is thus violated.

3.3.3. Reference region model

An alternative to measuring arterial radioactivity is to use occipital cortex as a reference tissue for DPN, but not for FMZ-PET studies. If specific binding is considered to be

negligible, then the tissue to plasma ratio of radioactivity in occipital cortex equals K_1/k_2. Assuming that the ratio K_1/k_2, which describes the transport of the tracer between the plasma and tissue compartments, is the same in occipital cortex as in regions with specific binding, this value can then be used to calculate k_3/k_4 for regions with specific binding. As before, occipital cortex is not devoid of receptors and this will introduce an error. B_{max} and K_d can be derived individually but a second scan performed at a different level of receptor occupancy is necessary (Lammertsma, 1996)

3.3.4. Spectral analysis

We determined FMZ- and DPN-V_d using a single scan and spectral analysis (Cunningham, 1993) (**Figure 8**). Spectral analysis has the advantage that it makes no assumptions about the number of compartments which are needed to model the data. A large but finite number of basis functions which span the expected kinetic behaviour of the tracer in the tissue is defined. A computer algorithm is used to select and scale a small subset which best fit the data. First order kinetics lead to functions involving the convolution of the independently measured plasma/blood input function with exponentials of the form:

Equation 1.

$$\alpha e^{-\beta t}$$

where α and β are constants.

Time-activity curves are analysed without decay correction - this allows convenient limits to be placed on values of β. The slowest possible tissue response corresponds to irreversible trapping of the label and subsequent isotopic decay. Rapid transients due to label in the vasculature can be accommodated by setting the upper limit of the range $\beta = 10^0\ s^{-1}$. In the model employed in our unit n=64 basis functions are used with the values of β distributed logarithmically.

The general model takes the form:

Equation 2.

$$C_{tiss}(t) = C_m(t) \otimes \sum_{j=1}^{j=n} \alpha_j e^{-\beta_j t}$$

where $C_{tiss}(t)$ denotes tissue concentration at time t, $C_m(t)$ the measured arterial input function, $\otimes$ convolution, and α_j the contribution of the basis function $\exp(-\beta_j t)$. Variables α_j are constrained to be zero or positive. A least squares technique is used to

obtain best fit solutions for each pixel of data. Typically, most α_j are returned as zero, with only two to four positive values returned for each pixel time-activity curve. This method is sufficiently rapid for routine analysis of entire images on a pixel by pixel basis (60 - 90 minutes on a Sun SPARCclassic workstation).

For each pixel a characteristic unit impulse response function (IRF) is produced, which is the tissue response function scaled to a unit concentration value of tracer arriving at the brain simultaneously at time=zero:

Equation 3.

$$IRF(t) = \sum_{j=1}^{j=p} \alpha_j e^{-(\beta_j - \lambda)t}$$

where λ is the decay constant for the isotope and p the number of positive values of a. Having calculated the IRF for each pixel a variety of parametric images can be produced: clearance of tracer from blood to tissue (K_1), volume of distribution (V_d) of tracer in tissue relative to blood (**Figure 9**), and images constructed from the IRF at specific time points. Because the images are all constructed on the basis of response to unit impulse activity, the equivalent parametric images are directly comparable between different subjects, or in the same subject in different conditions.

In practice, the intercept K_1 is poorly defined; an index of clearance from blood to tissue is obtained by producing an image corresponding to tissue response at 2 minutes. An index of specific retention of the tracer is produced by imaging tissue response at 25 minutes. For some tracers, such images are less noisy than V_d images and may be used to identify regions of interest, which can then be mapped back onto the data set for calculation of regional V_d.

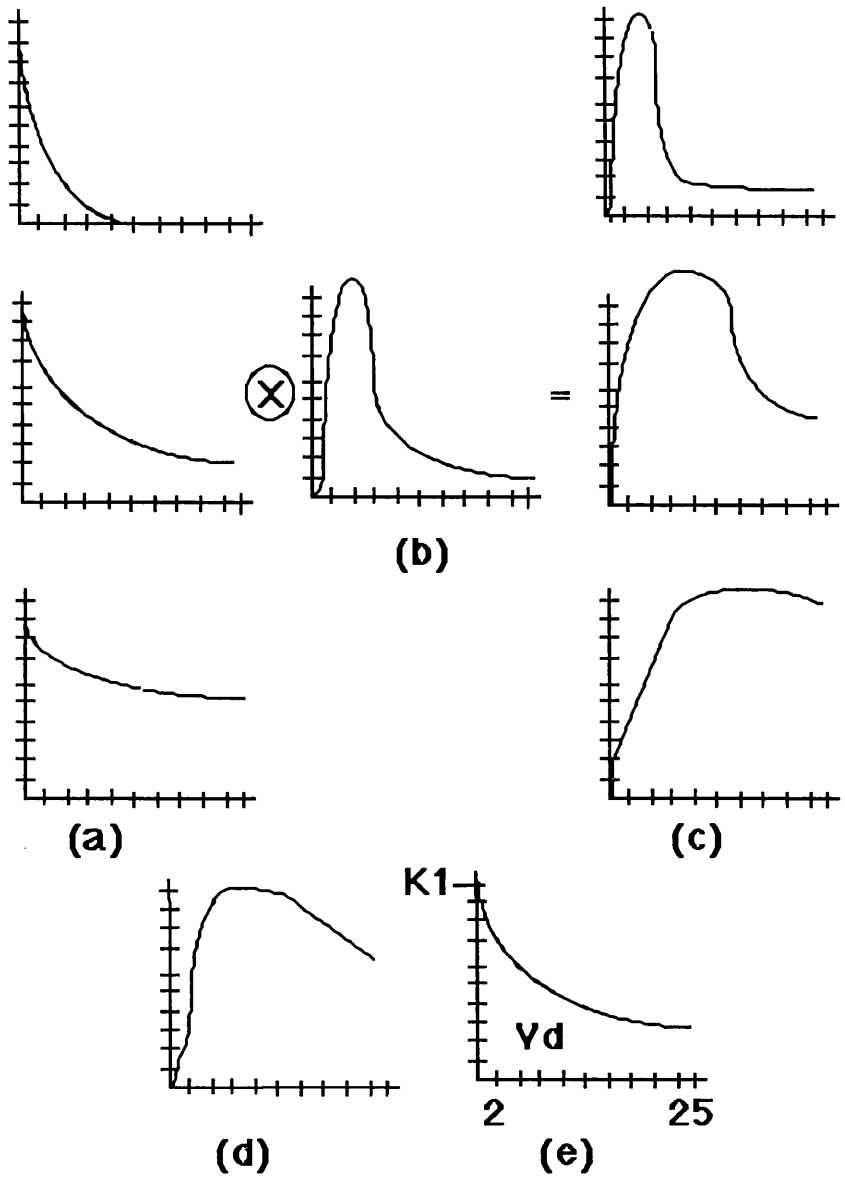

Figure 8: Principle of Spectral analysis
y-axis represents radioactivity, x-axis time in all graphs. A range of exponential basis functions (a) is defined; 3 are illustrated, 64 are used in the method. These are convolved with the measured plasma input function (b) to produce a set of convolved basis functions (c). These functions are weighted and combined by a computer algorithm to obtain a best-fit to the measured voxel time-activity curve (d). The equivalent weighted basis functions without convolution are then combined to produce the impulse function (IRF), (e) This curve can be used to derive a variety of images: K1, specific time points such as 2 mins or 25 mins, or Vd, the area under the curve extrapolated to infinity.

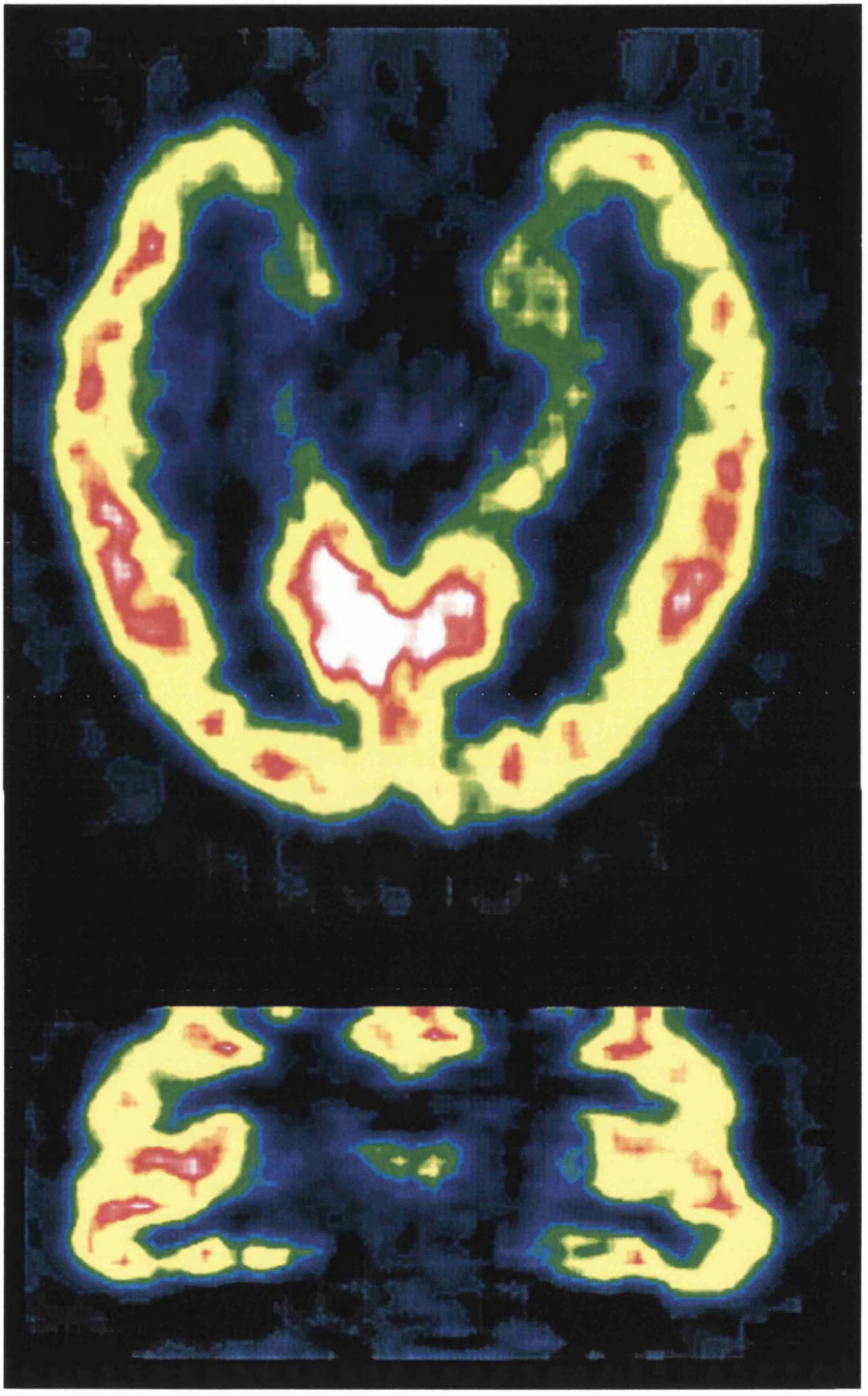

Figure 9: Transaxial and coronal ^{11}C-FMZ-V_d PET slices of a patient with right HS. Colour scale reflects step-wise increase of ^{11}C-FMZ-V_d from 1=blue to 7=white.

3.4. Region-of-Interest Based Analysis

1.4.1 Introduction

Other investigators have used a variety of techniques to define regions of interest (ROIs) (Henry, 1993; Savic, 1993). Some methods, such as outlining the ROI directly onto the PET, inevitably give rise to observer bias and partial volume effects. Placing ROIs of a predetermined shape, or anatomically configured ROIs over the structure of interest (Henry, 1993), or even defining all ROIs on a coregistered structural image such as MRI (Henry, 1993; Szelies, 1996), all lead to partial volume effects. Only 50% of the signal is recovered when using a ROI the same size as the FWHM resolution. Henry *et al.* (Henry, 1993) observed significantly greater decreases in FMZ binding (V_d) than in transport (K_1) in the affected mesial temporal lobe in TLE giving indirect evidence that decreases of receptor density are not due to atrophy alone, since K_1 and V_d should be equally affected by partial volume averaging. They addressed the importance of partial volume averaging of CSF and brain in PET by measuring the CSF content on the coregistered MRI within their anatomically configured PET ROI. This accounted for less than 20% of apparent receptor loss, and this MRI-based method does not account for the spill over of activity from neocortex. We outlined the hippocampus on optimal high quality MRI excluding, a priori, CSF from the VOI and then, during the partial volume effect correction, coregistered this with the 3D FMZ-V_d image. In order to further minimise partial volume effects both PET and MRI were acquired for patients and normal subjects in the same orientation as recommended for optimal MRI volumetric measurements with axial planes parallel to the long axis of the hippocampus (Jackson, 1993). We used Analyze™ version 7.0 (Robb, 1990) to perform image manipulation and measurements.

3.4.2. Partial volume effect correction

3.4.2.1. Introduction

Due to the limited spatial resolution of PET, the correct interpretation of PET data is obscured mainly by partial volume effects (PVE) (Hoffman, 1979; Mazziotta, 1981). An object must be greater than two times the resolution of the PET system (FWHM) in order to be recovered with its true activity. The best clinical PET systems today have a resolution of about 4 mm. Many structures in the brain including deep nuclei, hippocampi and even the cortical ribbon are smaller than twice this value, they will therefore appear less or more intense than their real activity. A cortical PET signal thus reflects the average tracer concentration of different compartments: grey matter (GM), white matter (WM) and cerebrospinal fluid (CSF). PVE are especially important in the case of cerebral atrophy, which may lead to a possible over- or underestimation of the severity of the disease. As a result it is often impossible to determine the extent to

which PET abnormalities represent changes of functional activity in the atrophic structure or purely structural changes, or possibly both together.

Thus, corrections for PVE are necessary to determine real, functional differences in PET scanning. Prior studies demonstrated PVE in small structures with simple geometric phantoms consisting of high-activity spheres within a low-activity background (Mazziotta, 1981). Assessment of PVE requires a knowledge of the size and shape of the structure of interest, of their relative position in the scanner gantry and of the presence of surrounding high or low activity (Hoffman, 1981; Kessler, 1984).

3.4.2.2. Three and four compartment algorithm

Normal PET data can be modelled by equation 4. The observed PET image (I_{PET}) is the result of the convolution ($\otimes$) of the three dimensional PET point spread function (h) with the actual radiotracer concentration in different compartments defined by MRI (I_{MRI}). I_{MRI} corresponds to the sum of the actual functional activity in grey matter (I_{GM}), white matter (I_{WM}) and cerebrospinal fluid (I_{CSF}):

Equation 4.

$$I_{PET} = I_{MRI} \otimes h = I_{GM} + I_{WM} + I_{CSF}$$

Each pixel in the three single compartments (GM, WM and CSF) is assigned a binary weight of 1 for pixels corresponding to the given pure tissue compartment and 0 otherwise (W_{GM}, W_{WM}, W_{CSF}). Their activity concentrations are denoted C_{GM}, C_{WM} and C_{CSF}. The functional image of each cerebral tissue compartment is expressed as follows:

Equation 5.

$$I_{GM} = C_{GM} \cdot W_{GM} \otimes h = C_{GM} \cdot B_{GM}$$
$$I_{WM} = C_{WM} \cdot W_{WM} \otimes h = C_{WM} \cdot B_{WM}$$
$$I_{CSF} = C_{CSF} \cdot W_{CSF} \otimes h = C_{CSF} \cdot B_{CSF}$$

where the term $W_i \otimes h = B_i$ (with i = GM, WM and CSF) representing the convolution of the segmented MR image, thus transformed into the PET resolution. By assuming that $C_{CSF} = 0$, and C_{WM} is constant, combining and arranging the *equations 4* and *5* will give the GM radiotracer concentration, the only unknown quantity to be measured:

Equation 6.

$$C_{GM} = [I_{PET} - C_{WM} \cdot B_{WM}] / B_{GM} = I_{GMobs} / B_{GM}$$

where the observed GM PET image (I_{GMobs}) is obtained by subtracting the WM contribution from the original PET images and the segmented and convolved GM MRI (B_{GM}) illustrates the degree of PVE in each pixel. However, the algebraic arrangement from *Equation 4* to *6* is only permissible, if either I_{GM} is homogeneous across the field of view or the PET resolution is perfect (e.g. h equal to a ∂ function). In reality, neither of these conditions is perfectly met, and the problem would be therefore not correctly solved.

To account for heterogeneous GM concentration (Meltzer, 1996), this algorithm has been extended by including a fourth compartment: a GM volume of interest (VOI) such that C_{VOI} differs from C_{GM}. Then, *equation 4* takes the following form:

Equation 7.

$$I_{PET} = C_{GM\text{-}VOI} \cdot B_{GM\text{-}VOI} + C_{VOI} \cdot B_{VOI} + C_{WM} \cdot B_{WM}$$

where the compartment GM-VOI is the total GM volume without the VOI. The last equation is modified to define C_{VOI}

Equation 8.

$$C_{VOI} = [I_{PET} - C_{WM} \cdot B_{WM} - \hat{C}_{GM} B_{GM\text{-}VOI}] / B_{VOI}$$

where $\hat{C}_{GM}$ is determined by the three compartment correction. The last condition can introduce error into the PET quantification of the PET signal within the VOI since in the three compartment model the GM volume includes both cortical GM and the VOI, which have different tracer radioactivity concentrations. Furthermore, cortical binding of most receptor ligands is rarely homogenous, e.g. FMZ binding is higher and DPN binding is lower in the occipital cortex than in the rest of the neocortex. In our modification of this method instead of taking the whole, total GM concentration from the three compartment model to estimate the VOI, we defined a cuboid that extended by two times the FWHM from the maximal dimensions of the VOI, to eliminate the effect of distant, occipital areas with high activity (**Figure 10**). Limitations of this four compartment algorithm are the assumptions that WM and GM activity are homogeneous throughout the brain and the concentration within these compartments can be fixed either by applying regions of interest on pure WM from PET images or by the three compartment model leading to an accumulated error in the corrected VOI activity. Only one VOI at a time could be processed. Furthermore a threshold was used for MRI segmentation into GM, WM and CSF introducing a bias as the PVE correction depend on accurate segmentation.

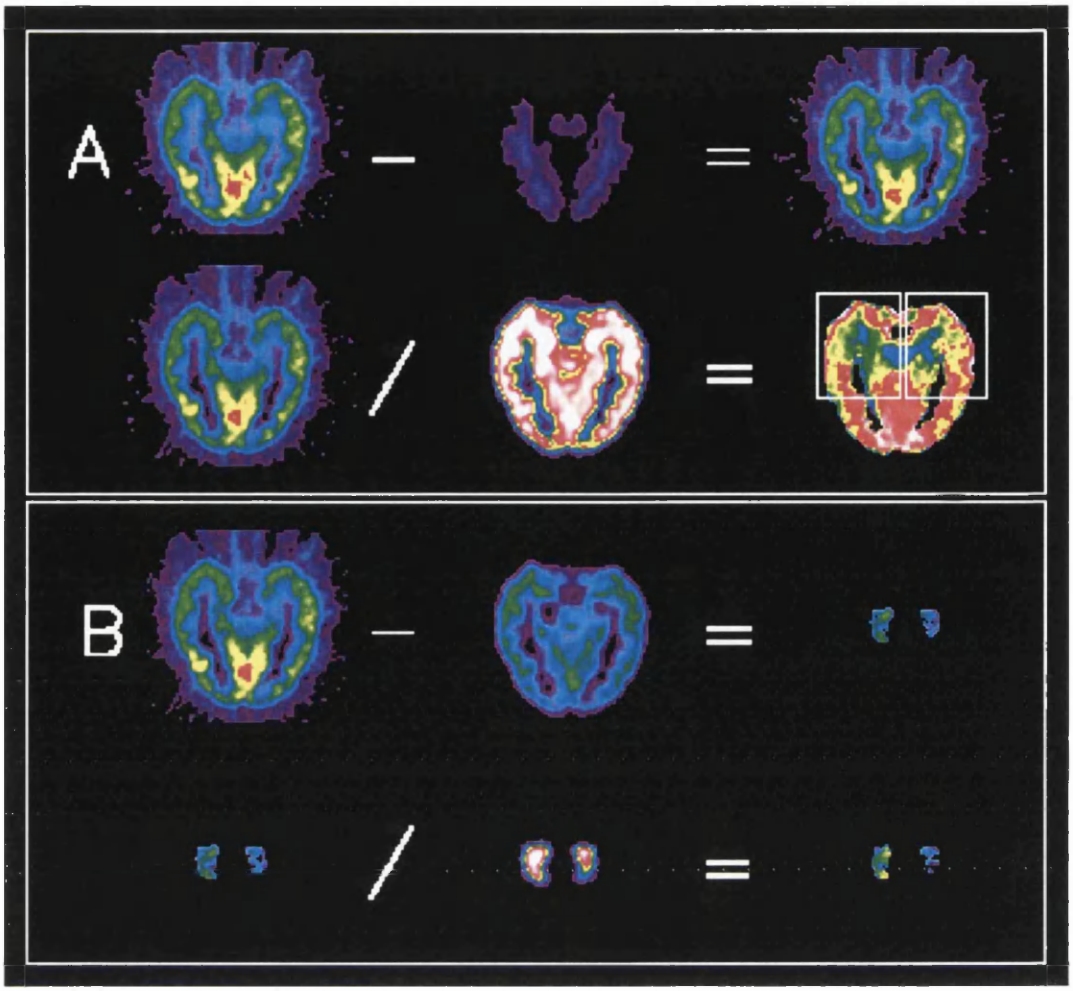

Figure 10: Principle of three- and four-compartment model for PVE correction
A: Three-compartment method to correct grey matter (GM) activity for PVE:
The observed GM PET image (upper right) was created by subtracting the WM contribution (upper middle) from the observed PET image (upper left). The PVE corrected GM PET image (lower right) was then obtained by dividing the observed GM PET image (lower left) by the binarised and convolved GM MRI (lower middle, scaled from 0 to 1).

B: Four-compartment method to correct hippocampal volume-of interest (VOI) activity for PVE:
The observed VOI PET image (upper right) was created by subtracting the GM-VOI contribution (upper middle) from the observed GM PET image (upper left). The GM activity concentration had been calculated within a cuboid around each hippocampus on the corrected GM PET image (white box in lower right of figure 1A) using the three-compartment correction. The PVE corrected VOI PET image (lower right) was then obtained by dividing the observed VOI PET (lower left) by the binarised and convolved VOI MRI (lower middle, scaled from 0 to 1).

3.4.2.3. Linear least squares - model

As the improved four compartment model still relies on several constraints, which are not met in reality, we therefore developed a new, algebraic correct method for PVE-correction based on a linear least square sense (LLS) in functional imaging data which allows to measure an unlimited number of homogeneous VOI. VOI can be delineated on high contrast MRI and be either within GM, WM or CSF. Although the inclusion of multiple additional compartments might be approached through an iterative algorithm, propagation of errors limits the utility of this model since the interaction of several adjacent regions with different radioactivity values creates a more complex situation. We have solved this problem by using a new approach that permits the inclusion of as many VOI as necessary, and without making any assumptions of radioactivity concentration in any single compartment, including WM and CSF. The only assumption made is that each VOI has a homogeneous radioactivity concentration. We can express *equation 4* for each pixel (i,j) with a set of linear algebraic equations:

Equation 9.

$$\left.\begin{aligned} PET_{11} &= GM - VOI_{11} \cdot C_{GM\text{-}VOI} + WM_{11} \cdot C_{WM} + VOI_{11} \cdot C_{VOI} \\ PET_{21} &= GM - VOI_{21} \cdot C_{GM\text{-}VOI} + WM_{21} \cdot C_{WM} + VOI_{21} \cdot C_{VOI} \\ &\cdots \\ PET_{ij} &= GM - VOI_{ij} \cdot C_{GM\text{-}VOI} + WM_{ij} \cdot C_{WM} + VOI_{ij} \cdot C_{VOI} \\ &\cdots \\ PET_{NN} &= GM - VOI_{NN} \cdot C_{GM\text{-}VOI} + WM_{NN} \cdot C_{WM} + VOI_{NN} \cdot C_{VOI} \end{aligned}\right\}$$

where the coefficients PET_{ij}, $GM\text{-}VOI_{ij}$, WM_{ij} and VOI_{ij} with i=1,2...,N and j=1,2,...,N are known values corresponding to PET and convolved GM-VOI, WM and VOI images, respectively. $C_{GM\text{-}VOI}$, C_{WM}, C_{VOI} are the 3 unknown values to be solved which are related to NxN equations. Since there are many more equations than unknowns, the linear set can be solved in single precision (32 bit floating) without resorting to sophisticated methods. *Equation 9* can be written in matrix form as

Equation 10.

$$A = B \cdot x$$

with:

$$A = \begin{bmatrix} PET_{11} & PET_{21} & \cdots & PET_{2N} \\ PET_{21} & PET_{22} & \cdots & PET_{2N} \\ \vdots & & & \vdots \\ PET_{i1} & PET_{i2} & \cdots & PET_{iN} \\ \vdots & & & \vdots \\ PET_{N1} & PET_{N2} & \cdots & PET_{NN} \end{bmatrix} = \begin{bmatrix} PET_{11} \\ PET_{21} \\ \vdots \\ PET_{ij} \\ \vdots \\ PET_{NN} \end{bmatrix}; B = \begin{bmatrix} GM - VOI_{11} & WM_{11} & VOI_{11} \\ GM - VOI_{21} & WM_{21} & VOI_{21} \\ \vdots & \vdots & \vdots \\ GM - VOI_{ij} & WM_{ij} & VOI_{ij} \\ \vdots & \vdots & \vdots \\ GM - VOI_{NN} & WM_{NN} & VOI_{NN} \end{bmatrix}; x = \begin{bmatrix} C_{GM\text{-}VOI} \\ C_{WM} \\ C_{VOI} \end{bmatrix}$$

where :

- A is the matrix of PET values from PET images of NxN matrix size and the element pet_{ij} denotes its row, the second index its column. We resized the matrix of PET images, segmented and convolved MRI into one column each of NxN elements for reasons of simplicity;
- B = [GM-VOI WM VOI] representing the segmented and convolved MRI images of GM-VOI, WM and VOI, respectively;
- x is the column vector containing the unknown concentrations to be determined (e.g. C_{GM}, C_{WM} and C_{VOI}) .

The best compromise solution of the matrix equation A = B.x is the one which comes closest to satisfying all equations simultaneously. If this is defined in the least square sense, i.e. that the sum of the squares of the differences between the left and right-hand sides of equation A= B.x be minimised, then the linear set problem reduces to a solvable linear least-squares (LLS) problem. The computation of $x = A. B^{-1}$ was done using singular value decomposition (Press, 1988). To minimise interactions between small VOIs of distant areas and to reduce the effect of heterogeneity within large VOI, we solved the set of equations within a cuboid around the VOI to be measured, as we also implemented this for the 4-compartment method.

3.4.3. Cluster analysis

A prerequisite for PVE correction is the availability of MRI for each individual and the presence of a structural abnormality. To determine interindividual and, in paired scans, intraindividual differences of FMZ binding in patients with IGE and normal MRI, we used an entirely objective method, gaussian clustering, to define region boundaries of cerebral cortex, cerebellum and thalamus. Two different FMZ-images of the same dynamic FMZ PET scan - an early, blood flow weighted and a late, receptor weighted image of FMZ binding - were used as "multi-spectral" images and segmented using gaussian clustering. This automated algorithm allocates each voxel into three different clusters:

(1) high initial activity (= high blood flow) and high FMZ-V_d

(2) high blood flow and moderate FMZ-V_d

(3) low blood flow and low FMZ-V_d.

These clusters correspond to:

(1) cerebral cortex

(2) cerebellar cortex, thalamus and basal ganglia

(3) white matter and CSF, respectively.

The gaussian clustering technique calculates means and standard deviations for each cluster, and then models the clusters' probability distribution as a gaussian function with these parameters. Each voxel is then classified by calculating the probability that it belongs to a particular cluster. A voxel was included in one cluster if it lies within five standard deviations from the cluster's centre. An automated post-processing iterative relaxation technique smoothes the segmentation, so that classification of voxels which are of uncertain cluster membership will be influenced by adjoining voxels and no voxel is left unclassified (**Figure 11**). Cerebral cortex was defined over 17 consecutive axial planes in each subject, starting 3 planes below the AC-PC line, thalamus over 7 planes and cerebellum over 6 planes.

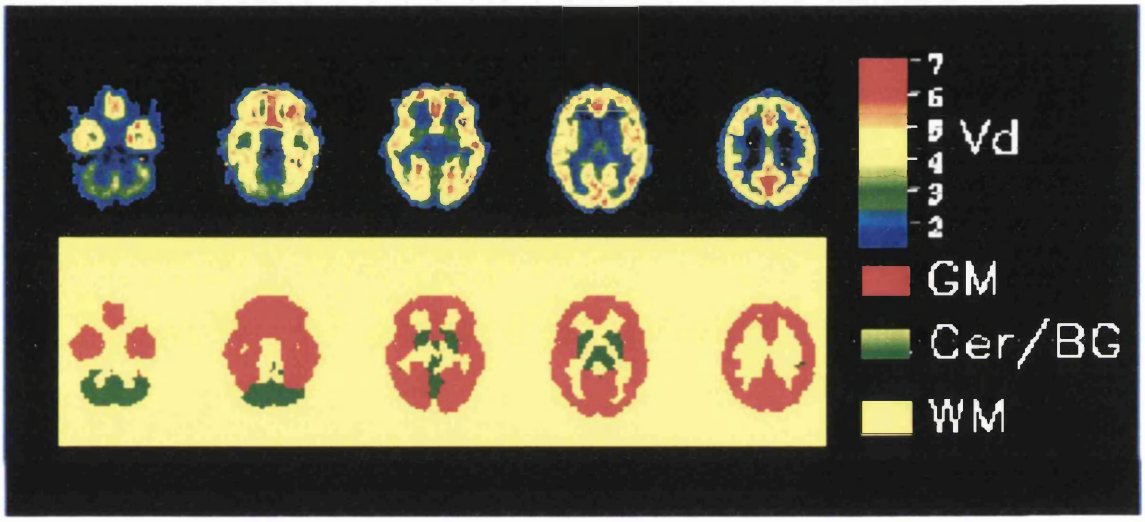

Figure 11: Principle of gaussian clustering
Top: Selection of axial FMZ-V_d images from one patient.
Bottom: Segmentation of FMZ-V_d images into three clusters: (1) red = cerebral cortex; (2) green = cerebellar cortex / basal ganglia; (3) yellow = white matter / CSF

3.5. Voxel-Based Analysis

3.5.1. Statistical Parametric Mapping - the general model

Statistical parametric mapping (SPM) is an approach that is predicated on functional specialisation and is used to characterise physiology or pathology in terms of regional specific responses. It does this characterisation by treating each voxel separately and by performing voxel-wise statistical analyses in parallel creating an image of a statistic. SPM refers to the construction of spatially extended statistical processes to test hypotheses about regionally specific effects. SPMs are image processes with voxel values that are, under the null hypothesis, distributed according to a known probability density function (usually gaussian). These statistical parametric maps are 3D projections of statistical functions that are used to characterise significant regional brain differences in imaging parameters. Corrections for the implicit multiple comparisons, when making inferences based upon the statistical parametric map, are confounded by spatial correlations. The theory of Gaussian fields is used to provide p values that are corrected for the brain volume analysed (Friston, 1991; Friston, 1995b; Worsley, 1992).

SPM is a framework, subsuming the general linear model and the theory of Gaussian fields, that allows for a diverse interrogation of functional imaging data. One analyses each and every voxel using any standard statistical test. The same ideas and implementation can accommodate approaches ranging from simple unpaired t-test to multifactorial ANCOVA. The resulting statistical parameters are assembled into an image - the SPM. SPMs are interpreted as spatially extended statistical processes by referring to the probabilistic behaviour of stationary gaussian fields. "Unlikely" excursions of the SPM are interpreted as regionally specific effects, attributable to a sensorimotor or cognitive process that has been manipulated experimentally. This characterisation of physiological responses appeals to functional segregation as the underlying model of brain function. Functional segregation implies that the brain consists of a great many modules that process information more or less independently of each other. One could regard all applications of SPM as testing some variant of the functional segregation hypothesis.

The experimental design and the model used to test for specific neurophysiological responses are embodied in a mathematical structure called the design matrix. The design matrix is partitioned according to whether the effect is interesting (e.g. an activation) or not (e.g. nuisance effect like global activity). The contribution of each effect to the observed physiological responses is estimated using the general linear model and standard least squares. These estimated contributions are known as parameter estimates and can be as simple as the mean activity associated with a particular condition or as complicated as an interaction term in a multifactorial

experiment. Regionally specific effects are framed in terms of differences among these parameter estimates and are specified using linear compounds or contrasts. The significance of each contrast is assessed with a statistic whose distribution has Student's t distribution under the null hypothesis. For each contrast or differences in parameter estimates, a t statistic is computed in parallel for each and every voxel to form a SPM{t}. For convenience the SPM{t} is transformed to Gaussian field or SPM{Z}. Statistical inferences are then made about local excursions of the SPM{Z} above a specified threshold using distributional approximations from the theory of Gaussian fields. These distributions pertain to simple characterisations of the "blobs" of activation, namely their maximal value and their spatial extent. The resulting P values can be considered corrected for the volume of brain tested. By specifying different contrasts one can test for a variety of effects.

The following represents a summary of the stages required for an analysis of PET studies. The stages of analysis include spatial normalisation, spatial smoothing, voxel-wise statistical analysis using the general linear model, and statistical inference based on the spatial extent and maxima of thresholded foci that ensue.

3.5.2. Spatial normalisation

To implement voxel-based analysis of imaging data, data from different subjects must derive from homologous parts of the brain. Spatial transformations are therefore applied that move and "warp" the images such that they all conform (approximately) to some idealised or standard brain. This normalisation facilitates inter subject averaging. The normalising transformations can be computed on the basis of the PET data themselves (for example FMZ add-images or FMZ-V_d images with enough anatomical details) or on the basis of co-registered high resolution anatomical MRI scans (ideally for DPN images, as opioid binding in the occipital cortex is very low).

For the purposes of statistical analysis of a group of patients, the FMZ-V_d images of patients with left sided hippocampal sclerosis were flipped, so that the hippocampal sclerosis was on the right side in all patients. The images were then transformed into a standard anatomical space (Friston, 1991), which was created for studying TLE on the basis of five individual controls scanned in the hippocampal orientation. The procedure involves linear 3-dimensional transformation, using a set of smooth basis functions that allow for normalisation at a finer anatomical scale. The MRI scans for each patient were coregistered with the FMZ-V_d PET for that individual. The coregistered MRIs were then transformed into the standard space using the transformation parameters calculated for the volumetric normalisation of that individual's FMZ-V_d PET. These coregistered and volumetrically normalised MRI scans were then combined on a pixel-

by-pixel basis to produce an average transformed MRI **(Figure 12)**, as a quality control of the normalisation process.

Figure 12: Normalised MRI template
Transaxial and coronal view of an average transformed MRI of 12 patients with unilateral hippocampal sclerosis. The sclerotic hippocampus is on the left side of the image. For the statistical analysis, images of patients with left hippocampal sclerosis were flipped, so hippocampal sclerosis was on one side in all patients.

3.5.3. Spatial smoothing

Convolving the data with a smoothing kernel has several important objectives. First, it generally increases signal relative to noise. Second, convolving with a Gaussian kernel conditions the data in the sense that the data conform more closely to a Gaussian field model. The final reason for smoothing is specific to intersubject averaging. For example, at a scale of 100 μm it is highly unlikely that even with perfect spatial normalisation the functional anatomy and organisation of cortex in two subjects will show meaningful homologies. However, at an anatomical scale of 8mm they do.

3.5.4. Statistical analysis

This stage corresponds to modelling the data in order to partition observed responses into components of interest, confounds of no interest and error term. The analysis of regionally specific effects uses the general linear model to assess differences among parameter estimates specified in a contrast in a univariate sense, by referring to the error variance. This assessment is in terms of a t value for each and every voxel, the SPM$\{t\}$. The SPM$\{t\}$ is transformed to the unit normal distribution to give a Gaussian field or parametric maps of the Z-statistic (SPM{Z}).

The aim of the analysis was to identify focal areas of cerebral ligand binding that were significantly different in the patients compared with controls. Significant differences between patients and control subjects were estimated according to the general linear model at each and every voxel (Friston, 1995b). Comparing individual patients with a group of normal subjects the design matrix designated global cerebral FMZ activity differences as a confounding factor covariate and this analysis can therefore be regarded as an ANCOVA (Friston, 1990). Comparison between patients and controls as groups was performed without ANCOVA. Linear contrasts were used to test the hypotheses for specific focal effects. The resulting set of voxel values for each contrast constitute a statistical parametric map of the t statistic SPM {t}.

3.5.4. Statistical inference

Statistical inference about specific regional changes requires statistical parametric mapping. With an anatomically constrained hypothesis about effects in a particular brain region a priori (e.g. the hippocampus) the Z-value in that region in the SPM{Z} can be used to test the hypothesis. With an anatomically open hypothesis (i.e. null hypothesis that there is no effect anywhere in the brain), a correction for multiple non-independent comparisons is required. The theory of Gaussian fields provides a way of computing a corrected P value. The resulting foci of significant differences are characterised in terms of spatial extent (k) and peak height (μ). The significance of each regional difference is estimated using distributional approximations from the theory of Gaussian Fields. This characterisation is in terms of the probability that a region of the observed number of voxels (or bigger) could have occurred by chance [P(nmax > k)], or that the peak height observed (or higher) could have occurred by chance [P(Zmax > μ)] over the entire volume analysed (i.e. a corrected p-value) (Friston, 1995a; Friston, 1995b). The threshold chosen for P (nmax>k) and P (Zmax>μ) was $P<0.05$.

3.6. Principles of Quantitative MRI

MRI depends on the behaviour of certain anatomic nuclei when placed in orthogonal magnetic and radiofrequency fields. Image parameters of importance include repetition time, echo time, field of view, slice thickness, and plane, among others. Selection of some degree determines the sensitivity of the study to abnormalities in epilepsy patients. The basic epilepsy MRI protocol employed for the patients in these studies is:

- Volume acquisition T_1-weighted coronal data set that covers the whole brain in 0.9 - 1.5 mm thick slices. This sequence produces approximately cubic voxels, allowing for reformatting in any orientation, subsequent measurement of hippocampal morphology and volumes, and for 3D reconstruction and surface rendering. The sequences used is MPRAGE (Siemens), which provides good contrast between grey and white matter.
- Oblique coronal inversion recovery sequence, that is heavily T_1-weighted and orientated perpendicular to the long axis of the hippocampus, to best demonstrate the internal structure and T_1-weighted signal intensity of the hippocampus.
- Oblique coronal fast spin echo (GE) or double-echo STIR (Siemens) sequence, that is heavily T_2-weighted and orientated perpendicular to the long axis of the hippocampus, to demonstrate any increase in T_2-weighted signal intensity. Quantitation of hippocampal T_2 relaxation times may also be obtained using a Carr Purcell Meiboom Gill multiecho sequence, with 16 echo times ranging from 22 to 262 msec.

To minimise partial volume effects the hippocampus is best visualised in two planes: along the long axis and perpendicular to the structure. These imaging planes are readily determined on a sagittal scout image: the axial plane being in the line joining the base of the splenium of the corpus callosum to the inferior, posterior border of the frontal lobe and the coronal plane being perpendicular to this, parallel to the anterior border of the brainstem.

MR images were obtained for each control subject and patient on a 1T Picker scanner using a gradient echo sequence protocol which generated 128 contiguous 1.3 mm thick sagittal images. These high resolution volume acquisition MRI scans were coregistered with the parametric images of FMZ-V_d (Woods, 1993).

Hippocampal T2 relaxation time measurements (HCT_2s) were obtained for all patients on a 1.5T Siemens SP63 Magnetom scanner using a 16 echo sequence, as previously described (Jackson, 1993). We used 108 msec as the upper limit of normal, which is 2 standard deviations above mean control HCT_2.

All patients also had images for hippocampal volumetric studies that were obtained on a 1.5T Siemens SP63 Magnetom scanner using a 3D Magnetisation Prepared Rapid Gradient Echo (MPRAGE) sequence 10/4/200/1 (TR/TE/TI/NEX), flip angle 12 degrees, matrix size 256x256, and 128 sagittal partitions in the third dimension. The MPRAGE dataset was reformatted into 1 mm thick contiguous slices in a tilted coronal plane that was perpendicular to the long axis of the hippocampus. Hippocampal cross-sectional areas were outlined manually with hippocampal boundaries as described by Watson *et al.* (Watson, 1992) and measured on consecutive images. The sum of the hippocampal cross-sectional areas times partition thickness gave total hippocampal volume (HCV). Intracranial volume (ICV) was measured on the sagittal 1mm unreformatted MPRAGE dataset. HCV of 22 control subjects correlated with ICV ($r=0.66$; $p<0.001$). Correction for ICV allows detection of bilateral abnormalities in HCV (Free, 1995). Mean control HCV corrected for ICV was 5180 (SD=401mm$^{3)}$. The lower limit of normal total HCV corrected for ICV was 4378mm^3 (-2 SD).

Hippocampal volume ratio (HCVR) was determined as the volume of the hippocampus with higher HCT2 divided by the volume of the hippocampus with lower HCT2. The control HCVR was 0.96 (SD=0.03), with 0.90 (-2 SD) as the lower limit of normal of the HCVR (Cook, 1992).

3.7. Principles of Quantitative Neuropathology

Quantitative pathology with measurements of neuronal cell densities (ND) was only possible in 14 patients with an MRI diagnosis of unilateral HS due to tissue damage during surgical removal in three cases. Six control hippocampi of persons (three men and three women, median age 31 years, range: 14 to 52) who had died from non-neurological causes were obtained at autopsy.

Quantitative neuropathology with measurements of ND in different subregions (CA_1, CA_2, CA_3, CA_4 and the dentate gyrus) was performed by one investigator (WVP) in all patients and controls using a three dimensional counting method (Williams, 1988).

Hippocampi were removed en bloc during surgery and were fixed immediately in formalin. After fixation both the temporal lobe and the hippocampus were cut in approximately 3 to 5 mm thick slices. Twenty µm thick sections of each slice were stained with luxol fast-blue/cresyl violet (LFB/CV) methods. A direct 3-D counting method was used with a 90x90x10 µm counting box. The bottom plane of the counting box was 5 µm above the bottom plane of the tissue section. Fifty counting boxes were used to count one hippocampal subregion. Sampling and counting was carried out in a random, systematic and unbiased way. By focusing from the bottom to top plane of the counting box, cells that came into focus were counted according to established counting rules (Williams, 1988). Cell nuclei completely inside the counting box were counted, and cell nuclei completely outside the counting box were not counted. Cell nuclei that touched the forbidden planes i.e. bottom, front and left side of the counting box were also excluded. Cell nuclei that touched the top, right side and back side of the counting box were counted, provided they did not touch any of the forbidden planes, in- or outside the counting box.

A neuron was defined as a large cell, pyramidal-shaped in the CA_1 to CA_3 and multipolar or triangular-shaped in the hilus, with Nissl substance in the cytoplasm and a vesicular nucleus containing a prominent nucleus. For the definition of the neuron containing layers of the hippocampus, descriptions of Lorente de Nô (Lorente de Nô, 1934) were used. ND were determined for the pyramidal cell layer of CA_1, CA_2, CA_3, CA_4 and the dentate gyrus. A section of the body of the hippocampus with the characteristic C-shaped appearance of the cell layers was used.

3.8. Principles of Saturation Autoradiography

The receptor autoradiography protocol used was based upon the methodology published by Houser and colleagues (Houser, 1988). On the day of the assay, slides were allowed to reach room temperature and prewashed twice for 30 minutes at 0-4°C in buffer containing 170mM Tris-HCl at pH 7.4. Incubation was for 60 minutes at 0-4°C in fresh assay buffer containing one of six concentrations of ^{3}H-FMZ (75.17Ci/mmol) ranging from 0.25nM to 20nM. Non specific binding was determined in the presence of 2μM clonazepam. Following incubation, slides were vacuum-aspirated, rinsed twice for 1 minute in fresh ice-cold buffer, briefly dipped into distilled water and dried under a stream of cold air. Slides were then apposed to ^{3}H-sensitive Hyperfilm in X-ray cassettes and co-exposed with ^{3}H-impregnated plastic standards for 21 days at room temperature.

Binding was assessed in at least two sections per concentration (usually four sections) and non-specific binding in one or two sections per concentration, depending on tissue availability, and the mean values were used for subsequent analysis. Hippocampal subregions were identified in sections stained with cresyl violet following autoradiography and optical density values for the cross-section of the hippocampus were obtained by computer-assisted densitometry, using a Quantimet 970 image analysis system for direct comparison with *in-vivo* ^{11}C-FMZ PET measurements of cBZR binding. Concentration of bound radioactivity was determined from a standard curve generated from film optical densities produced by the ^{3}H-impregnated plastic standards, corrected for tissue quenching. Receptor availability (B_{max}) and receptor affinity (K_d) values were determined by non-linear regression with an iterative curve-fitting package using a standard two-variable Langmuir equation.

3.9. Subject Recruitment

Many of the practical aspects of patient recruitment and data collection were common to all the experiments and to avoid repetition they are described in this section. Methods specific to each experiment are included in the relevant chapters. Patients with mTLE and IGE were identified from EEG reports at the National Hospitals for Neurology and Neurosurgery (Queen Square, Maida Vale Hospital and National Society for Epilepsy at Chalfont St. Peter). Clinical data and results of CT / MRI scans were obtained from the hospital notes. Any patients with clinical or imaging features not in keeping with a diagnosis of mTLE or IGE, or who were under the age of 18 years were excluded at this stage. Patients with mTLE who were treated with benzodiazepines, barbiturates, vigabatrin or sodium valproate within two months of the PET examination were not included in the FMZ studies. Patients, in whom the clinical, EEG and imaging data were all consistent with mTLE or IGE, were approached in writing and invited to take part, permission having been first obtained from their consultants and general practitioners.

Normal volunteers to act as controls were recruited from colleagues and friends at the National Hospital and Hammersmith Hospital. Subjects did not consume alcohol within 48 hours preceding the PET scan. Written informed consent according to the declaration of Helsinki (BMJ 1991) was obtained in all cases and the approvals of local ethical committees and of the UK Administration of Radiation Substances Advisory Committee (ARSAC) were obtained. In accordance with the regulations of the Administration of Radioactive Substances Committee of the United Kingdom (ARSAC), both male and female patients were studied but all normal volunteers were male. Only female patients in whom there was felt to be no risk of pregnancy were scanned.

Chapter IV Cerebral benzodiazepine receptors in hippocampal sclerosis: an objective *in-vivo* analysis

4.1. Summary

Rationale: To objectively delineate the extent of abnormalities in ^{11}C-FMZ binding to cBZR in patients with mTLE due to unilateral HS.
Methods: We studied 12 patients with mTLE associated with unilateral HS, who underwent presurgical evaluation and subsequent temporal lobe surgery, and compared parametric 3D-images of regional cerebral ^{11}C-FMZ-volume of distribution (V_d) obtained for individual and groups of patients with ^{11}C-FMZ-V_d for a group of 17 healthy controls using SPM.
Results: ^{11}C-FMZ-V_d was significantly reduced ($p<0.001$) in the affected hippocampus in the group of 12 patients with unilateral HS. Analysis of individual patients reflected the group finding and there was no significant abnormality of cBZR outside the hippocampus in any patient.
Conclusions: We conclude that SPM is an useful objective method for detecting changes in regional cerebral ^{11}C-FMZ binding and that in patients with mTLE and unilateral HS reduction of cBZR is restricted to the area of HS with no abnormalities being detected in the temporal neocortex or elsewhere in the neocortex.
(published in ***Brain*** 1996, 119: 1677-1687)

4.2. Introduction

Previous ^{11}C-FMZ PET studies in TLE have reported decreased cBZR density in the region of the epileptogenic zone while studies of interictal rCMRglu using ^{18}F-FDG PET have generally shown more extensive hypometabolism (Henry, 1993; Savic, 1993; Sadzot, 1994). A limitation of the methodology of previous investigations using ^{11}C-FMZ PET is that high resolution volumetric MRI was not always performed and co-registered with functional imaging data. This has limited the conclusions that could be drawn regarding the correlation between underlying structural abnormalities, such as HS or cortical dysplasia, and any functional abnormality. In these studies the anatomical resolution of mesial temporal lobe structures has been generally suboptimal and hippocampi have not been separately identified from temporal neocortex. Further, the ROI analysis techniques that have been employed in previous investigations have largely relied upon visual placement of regions and so have been susceptible to

observer bias. Improvement of anatomical resolution and an entirely objective method of data analysis would clearly be advantageous.

4.3. Methods

4.3.1 Subjects

We studied 12 patients (7 female, 5 male) who were recruited from the epilepsy clinic of the National Hospital for Neurology and Neurosurgery, Queen Square, London. The median age at onset of habitual epilepsy was 7 years (range: 2-30 years), the median duration of epilepsy prior to PET examination was 16 years (range: 5-42 years) and the median age at PET examination was 27 years (range: 18-47 years). Five of our patients had a history of prolonged febrile convulsions in early childhood. The antiepileptic medication was mono- or polytherapy with carbamazepine (11 patients), lamotrigine (6), phenytoin (2), gabapentin (1), or felbamate (1) (**Table 1**). Seventeen healthy volunteers (16 male, 1 female) with a median age of 32 years (range: 23-54 years), who were on no medication, had no history of neurological or psychiatric disorder, normal EEGs and MRI studies, served as controls.

4.3.2 Electroencephalography

All 12 patients had prolonged video-EEG recordings with scalp electrodes. Ictal events were captured for all 12 patients and an unilateral anterior temporal epileptogenic focus ipsilateral to the side of HS was identified.

4.3.3. Epilepsy surgery and histopathology

Eleven of the 12 patients have undergone an anterior temporal lobe resection to date. In all cases the histopathologic findings of the removed mesial structures (including hippocampus, part of the amygdala, and anterior 2 to 3 cm of lateral temporal neocortex) verified the MRI finding of HS. No pathological abnormalities were detected in the resected anterior temporal cortical tissue, apart from an increased number of neurones in the resected white matter of one patient (no. 3), suggestive of microdysgenesis.

4.3.4 PET and MRI methodology

PET scans were performed at the MRC Cyclotron Unit at the Hammersmith Hospital on a ECAT 953b scanner (CTI Siemens, Knoxville, TN) which acquires 31 simultaneous slices and has a resolution of 4.8 x 4.8 x 5.2 mm (at FWHM).

Table 1: Clinical and EEG, quantitative MRI and [^{11}C]FMZ PET findings in 12 patients with TLE and unilateral HS

	Age / Sex	PFC	Age of onset (years)	AEDs	EEG focus	inter CPS /PET (days)	CPS per year	MRI	L HCT2 (msec)	R HCT2 (msec)	L HCV (mm^3)	R HCV (mm^3)	HCV Ratio	Path	FMZ-V_d focus	max Z score	red (%)
Normal range									<108	<108	>4378	>4378	>0.90				
1	18/ F	yes	8	CBZ	R temp ant	5	12	R HS	104	129*	5661	4131*	0.71	HS	R temp	2.99	33
2	22 / F	yes	7	CBZ, LTG	R temp ant	30	12	R HS	103	125*	5748	3864*	0.68	HS	R temp	3.94	47
3	44 /M	no	2	LTG, PHT	R temp ant	4	48	R HS	98	113*	4415	1986*	0.68	HS+MD	R temp	4.12	49
4	47 /M	no	7	CBZ	R temp ant	14	36	R HS	102	123*	5065	3736*	0.73	HS	R temp	3.32	42
5	24 /F	yes	7	CBZ, FBM	L temp ant	300	1	L HS	114*	98	3706*	5506	0.66		L temp	4.16	57
6	22 / M	no	2	CBZ, PHT	R temp ant	2	150	R HS	109	142*	5801	4351*	0.68	HS	R temp	4.5	58
7	40 / M	no	5	CBZ, LTG	R temp ant	7	52	R HS	113*	134*	5421	3889*	0.73	HS	R temp	4.17	53
8	35 / M	no	30	CBZ	L temp ant	7	48	L HS	128*	101	2689*	4694	0.58	HS	L temp	3.9	53
9	27 / F	no	14	CBZ, LTG	R temp ant	2	180	R HS	97	118*	6286	3732*	0.59	HS	R temp	3.59	42
10	25 / F	yes	2	CBZ, LTG	L temp ant	30	12	L HS	129*	97	2522*	4718	0.53	HS	L temp	3.04	33
11	27 / F	yes	11	CBZ, GBP	L temp ant	1	180	L HS	116*	102	3384*	5090	0.64	HS	L temp	2.17	19
12	26 / F	no	2	CBZ, LTG	R temp ant	5	12	R HS	104	125*	5133	4035*	0.75	HS	R temp	4.09	45

* >2 SD above normal HCT2 or >2 SD below normal HCV

L=left; R=right; AED=Antiepileptic drugs; CBZ=Carbamazepine; LTG=Lamotrigine; PHT=Phenytoin; FBM=Felbamate; GBP=Gabapentin; CPS=complex partial seizure; inter CPS/PET=interval between last CPS and PET scan; temp=temporal; ant=anterior; HS=hippocampal sclerosis; HCT2=hippocampal T2; HCV=hippocampal volume corrected for intracranial volume; HCVR=hippocampal volume ratio (volume of hippocampus with higher HCT2 divided by volume of hippocampus with lower HCT2); FMZ-V_d focus=site of reduced ^{11}C-flumazenil volume of distribution; SPM=statistical parametric mapping; FMZ-V_d reduction= % reduction of FMZ-Vd at the voxel with the highest Z-score compared with 17 normal subjects; SD=standard deviation

Scans were performed with axial images obtained along the the long axis of the hippocampus and coronal images orthogonal to it. High specific activity ^{11}C-FMZ tracer (370MBq) was injected intravenously and arterial blood was sampled continuously in order to determine a metabolite-corrected arterial input function. Voxel-by-voxel parametric images of ^{11}C-FMZ-V_d, reflecting binding to cBZR, were produced from the brain uptake and plasma input functions by using spectral analysis.

MR images were obtained for each control subject and patient on a 1T Picker scanner using a gradient echo sequence protocol which generated 128 contiguous 1.3 mm thick sagittal images. These high resolution volume acquisition MRI scans were coregistered with the parametric images of ^{11}C-FMZ-V_d. (see chapters 3.2., 3.3.4., 3.5. and 3.6.)

4.4. Results

The patients' clinical data, EEG findings, drug treatment, quantitative MRI findings with HCT2 and HCV, and FMZ PET findings for the patient group are summarised in **Table 1**. All patients had unilateral HS, characterised by decreased HCV and increased HCT2.

4.4.1. Group to group comparison

A comparison of all patients and normal controls as groups showed that there was a highly significant reduction of FMZ binding to cBZR in the patient group, that was confined in its extent to the hippocampus on the epileptogenic side with its maximum in the anterior portion (corrected $p<0.001$) (**Figure 13**).

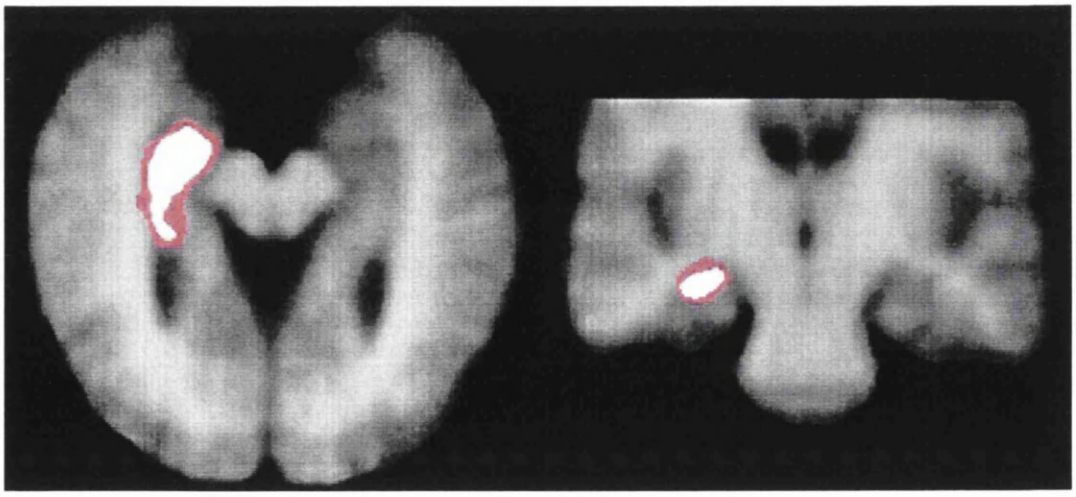

Figure 13: Group-to-group SPM comparison
SPM-result of group comparison superimposed on an average transformed MRI showing a highly significant reduction of ^{11}C-FMZ-V_d (white=$p<0.001$, red=$p<0.01$).

The mean maximum reduction of ^{11}C-FMZ binding in this group of voxels in the patients compared with the controls was 44%. There was no voxel detected outside the sclerotic hippocampus showing either a significant decrease or increase in ^{11}C-FMZ binding. We repeated the analysis with a 10 times lower threshold (uncorrected $p<0.01$) to check whether other areas of the brain may also be different from controls albeit at a less significant level. Even applying a ten times lower threshold no other regions of significant reduction of ^{11}C-FMZ binding became apparent. The only change was that the size of the volume of reduced ^{11}C-FMZ binding increased from 4448mm^3 (corrected $p<0.001$) to 8496mm^3 (uncorrected $p<0.01$). Considering the spatial resolution of PET, this volume is still in accordance with the area of reduced binding being within the hippocampus. ^{11}C-FMZ-V_d in temporal neocortex and elsewhere in the neocortex of the patients did not differ significantly from the control subjects.

Testing for the effect of covariates of interest: age (lowest corrected p-value found in entire 3D volume $p=0.997$), sex ($p=0.390$), occurrence of prolonged early childhood convulsions ($p=0.979$), duration of epilepsy ($p=0.996$), frequency of seizures ($p=0.581$), time between scan and last seizure ($p=1.0$), HCV ratio ($p=0.999$), and HCT2 ($p>1.0$), none of them had any effect on ^{11}C-FMZ-V_d.

4.4.2. Single case analysis

Comparison of each normal subject with the 16 other normal volunteers did not reveal any significant differences anywhere in the brain at a corrected $p<0.05$. A comparison of each individual patient with the group of 17 controls showed that each patient had a reduction of cBZR density in the volume of the sclerotic hippocampus. This reduction was highly significant ($Z > 3.09$; $p < 0.001$) in nine out of 12 patients, in two cases p was <0.01 and in the remaining one patient p was <0.05. No significant changes were seen outside of the hippocampus.

4.5. Discussion

The main finding of this study was that ^{11}C-FMZ binding to cBZR was significantly reduced in the hippocampus in patients with unilateral HS and did not involve adjacent or distant cortical structures. Changes were most prominent in the anterior part of the hippocampus, with a mean maximum reduction of 44 %. SPM of ^{11}C-FMZ-V_d images coregistered with high resolution MRI provided an entirely objective means of assessing the extent of significant changes in cBZR in the hippocampi, neocortex and thalamus of patients with mTLE.

4.5.1. Methodological considerations

This is the first study to use SPM to investigate changes in cBZR binding. The analysis of ^{11}C-FMZ PET data was completely automated and so without any observer bias. SPM is based on the application of the general linear model and is equivalent to performing unpaired t-tests at each and every voxel. It has been applied successfully to various kinds of data as $H_2{}^{15}O$ (Friston, 1990) and FDG (Kennedy, 1995) PET to show statistical differences between two series of 2D or 3D volumes. Weeks *et al.* (Weeks, 1997) compared ^{11}C-DPN binding in patients with Huntingdon's disease and Tourette's syndrome using a standard ROI approach and SPM. SPM not only replicated the ROI results of receptor loss in caudate and putamen, but also detected significant abnormalities in cortical areas which would have been difficult to identify accurately using ROIs.

While the SPM approach is free from observer bias, it does suffer from limited spatial resolution due to the 1cm smoothing applied for comparing individual patients with a group of controls, resulting in a final spatial resolution of 13mm x13mm x11mm at FWHM. In the group to group comparison no smoothing was necessary and the decrease of FMZ binding was evident to behind the posterior edge of the brainstem, which is as far as the MRI can identify hippocampal atrophy. The head of the hippocampus, however, cannot be easily separated from the amygdala due to the limited spatial resolution of PET.

The agreement of our finding with previous ROI based analyses of ^{11}C-FMZ binding in patients with mTLE (Henry, 1993; Savic, 1993; Sadzot, 1994) provides further validations of the SPM technique. The assumptions about the data implicit in using SPM are that the data are approximately normally distributed, however this distribution does not have to have a uniform variance over the brain. This is because SPM uses a local estimate of error variance. Our data represent independent observations from 29 different subjects; we have no reason to assume that these data are not normally distributed. Furthermore, the data were smoothed and this ensures that the parametric assumption holds, by virtue of the central limit theorem. The observation that receptor density varies across regions is a further reason for using SPM which is essentially a univariate technique and treats each brain region separately.

Patients, who were treated with AED that potentially interact with the cBZR complex, such as BZ, phenobarbitone, GVG or VPA, were not included in this study. Whilst AEDs may result in a global reduction of cerebral blood flow and glucose metabolism (Leiderman, 1991) we analysed changes in FMZ-V_d, which is independent of blood flow effects (Frey, 1991). Furthermore the lack of differences of ^{11}C-FMZ V_d in the cerebral neocortex, thalamus and cerebellum between patients and normal volunteers

suggest that AEDs like carbamazepine, phenytoin, LTG, felbamate (FBM) or gabapentin, do not affect cBZR density in these structures. FBM has been recently suggested to have a positive allosteric effect at $GABA_A$ receptors (Rho, 1994). Results for the patient (no. 5) taking FBM were, however, not different from the others.

In the current study, we acquired PET data for patients and normal subjects in the same orientation as recommended for optimal MRI volumetric measurements with axial planes parallel to the long axis of the hippocampus in order to minimise partial volume effects (Cook, 1992; Jackson, 1993). Mean global ^{11}C-FMZ-V_d for patients and normal subjects were not different and so the use of ANCOVA to detect focal ^{11}C-FMZ-V_d changes in individual patients was valid. Coregistration with high quality MRI precisely revealed the anatomical and structural correlation of any abnormalities of ^{11}C-FMZ binding to cBZR that were detected.

4.5.2. Clinical considerations

Previous studies of temporal lobe glucose metabolism in patients with TLE have shown hypometabolism throughout the temporal lobe and so have been useful for lateralising rather than localising the seizure focus (Abou-Khalil, 1987; Theodore, 1988; Henry, 1990). A recent study comparing FDG PET with volumetric MRI suggested an association between temporal cortical glucose metabolism and hippocampal volume (Gaillard, 1995). An important finding of our study was that there was no focal abnormality of $GABA_A$-BZR densities in the neocortical temporal lobe and the rest of the brain in patients with unilateral hippocampal sclerosis. These findings suggest that neuronal integrity is preserved in the neocortex and so further support the hypothesis that diaschisis (Feeney, 1986; Henry, 1993) explains the hypometabolism that commonly extends beyond the mesial temporal structures in ^{18}F-FDG PET studies of patients with mTLE (Gaillard, 1995).

The concordance of MRI abnormality and reduced ^{11}C-FMZ binding to cBZR in this group contrasts to findings in patients with cortical dysplasia in whom abnormal FMZ binding is frequently more extensive than the abnormality revealed by MRI (Richardson, 1996). The outcome of surgical treatment for HS is markedly better than it is for cortical dysplasias and it seems likely that the reason underlying this is that in the former the structural and functional abnormality may be completely removed.

Our study suggests that both volumetric MRI and ^{11}C-FMZ PET are sensitive means of detecting hippocampal sclerosis. If high resolution MRI, however, identifies an unilateral hippocampal sclerosis with no abnormalities found elsewhere and which is concordant with clinical and EEG data, ^{11}C-FMZ PET does not confer additional,

clinically useful information. ^{11}C-FMZ PET may prove to be clinically useful in preoperative epilepsy evaluation when high resolution MRI, including quantification, does not reveal a significant single focal structural abnormality. It is of note in this regard that in patients with malformations of cortical development, ^{11}C-FMZ PET has shown more extensive abnormalities than were demonstrated with MRI (Richardson, 1996). This PET technique may also delineate the true extent of functional neuronal abnormality, which cannot be done with either ^{18}F-FDG-PET or HMPAO-SPECT as diaschisis leads to widespread changes.

CHAPTER V ^{11}C-Flumazenil PET, volumetric MRI and quantitative Pathology in mesial Temporal Lobe Epilepsy

5.1. Summary

Background: Using SPM and ^{11}C-FMZ PET we have shown reduction of cBZR binding restricted to the hippocampus in mTLE due to HS (see Chapter IV). The limited spatial resolution of PET, however, results in partial volume averaging that affects quantitative analysis of cBZR density.
Method: We determined HCV loss and reduction in cBZR binding using an MRI based method for partial volume effect correction of ^{11}C-FMZ-V_d in 17 patients with refractory mTLE and an MRI diagnosis of HS which was subsequently histologically verified in all cases. Quantitative neuropathology was performed with assessment of neurone density (ND) in 14 of the 17 patients. Absolute ^{11}C-FMZ-V_d and asymmetry indices (AI) were compared before and after partial volume effect correction with MRI-determined HCV, HCT2 measurements and, if available, neuronal cell densities.
Results: Compared with 15 age-matched healthy volunteers, significant reductions of absolute hippocampal ^{11}C-FMZ-V_d were found before correction for partial volume effects in 11 out of 17 patients (65%) and only abnormal ^{11}C-FMZ-AI in the other six patients. After partial volume effect correction all 17 patients (100%) showed both significant unilateral reductions of absolute ^{11}C-FMZ-V_d and abnormal AI. There was no correlation between corrected absolute ^{11}C-FMZ-V_d and HCV or ND. After correction for partial volume effects we found a mean 38% reduction of ^{11}C-FMZ-V_d in the sclerosed hippocampus over and above the mean 32% reduction of HCV.
Conclusion: Correction for partial volume effects allows absolute quantitation of ^{11}C-FMZ-PET and increases its sensitivity for detecting abnormalities in mTLE due to HS. The lack of correlation between cBZR binding and neuronal density implies that atrophy with neurone loss is not the sole determinant of reduced cBZR binding patients with mTLE and HS.
(published in ***Neurology*** 1997; 49: 764-773)

5.2. Introduction

Comparisons of ^{18}F-FDG PET with volumetric MRI have shown a correlation between mesio-temporal hypometabolism and loss of hippocampal volume (Gaillard, 1995; Semah, 1995). Autoradiographic and histopathologic studies of temporal lobectomy

specimens from TLE patients have revealed reduced neuronal cell counts and $GABA_A$ / cBZR densities in sclerotic areas, with further reductions of $GABA_A$ / cBZR throughout the hippocampal formation (Johnson, 1992; Burdette, 1995). Correlational analysis of autoradiography and quantitative neuropathology in resected hippocampi have also revealed a reduction of ^{3}H-FMZ binding over and above than that due to reduced neuronal cell density in the CA_1 subregion (Hand, 1997).

The limited spatial resolution of PET affects the accuracy of quantitative PET, especially for structures smaller than twice the FWHM resolution (Hoffman, 1979), which include the normal and the sclerotic hippocampus. Surrounding white matter (WM) and cerebrospinal fluid (CSF) may lead to underestimation of the measured activity due to tissue volume averaging within the hippocampal VOI (Müller-Gärtner, 1992; Labbé, 1996; Meltzer, 1996b). In addition, there is spill over of activity into mesial temporal structures from neighbouring grey matter (GM) which has a higher ^{11}C-FMZ binding; this affects the sclerotic hippocampus more than a bigger, intact hippocampus and may lead to an overestimation of cBZR density in HS. Thus, corrections for partial volume effects are necessary to determine the true tissue cBZR density in the hippocampus.

We used a MRI-based correction for partial volume effects (Labbé, 1996; Meltzer, 1996b), to assess changes in cBZR binding within the hippocampus in patients with unilateral HS. We correlated quantitative *in-vivo* ^{11}C-FMZ-PET corrected for partial volume effects with HCV and HCT2 measurements and, if available, neuronal cell densities in the resected hippocampus. The main aims of this study were:

- to determine the importance of partial volume effect correction on ^{11}C-FMZ binding within the hippocampus;
- to determine whether cBZR binding measured *in-vivo* with ^{11}C-FMZ PET is reduced over and above HCV loss and
- to assess the sensitivity of optimal, partial volume effect corrected ^{11}C-FMZ-PET in the investigation of patients with refractory mTLE compared to high quality, quantitative MRI.

5.3. Methods

5.3.1. Subjects

We studied 17 patients (10 female, 7 male) who were recruited from the epilepsy clinics of the National Hospital for Neurology and Neurosurgery, Queen Square, London. The median age at onset of habitual epilepsy was 7 years (range: 1-27 years), the median duration of epilepsy prior to PET examination was 22 years (range: 12-41

Table 2: Clinical and EEG data, quantitative MRI findings in 17 patients with TLE and unilateral HS

	Age / Sex	PFC	Age of onset (years)	AEDs	EEG	inter CPS / PET (days)	CPS per years	MRI	L HCT2 (msec)	R HCT2 (msec)	L HCV (mm^3)	R HCV (mm^3)	HCV Ratio
Normal range									<108	<108	>4378	>4378	>0.90
1	26 / F	no	2	CBZ, LTG	R temp ant	5	12	R HS	104	125*	5133	4035*	0.75
2	49 / F	yes	11	CBZ, GBP	L temp ant	1	20	L HS	131*	103	24078	5273	0.46
3	22 / F	yes	5	CBZ	L temp ant	3	72	L HS	127*	104	2753*	4803	0.58*
4	25 / F	yes	2	CBZ, LTG	L temp ant	30	12	L HS	129*	97	2522*	4718	0.53
5	38 / F	no	23	CBZ, LTG	R temp ant	4	95	R HS	102	140*	4544	3454*	0.76*
6	47 /M	no	7	CBZ	R temp ant	14	36	R HS	102	123*	5065	3736*	0.73
7	19 / F	yes	7	CBZ	R temp ant	5	144	R HS	103	125*	5713	3829*	0.67*
8	44 /M	no	2	LTG, PHT	R temp ant	4	48	R HS	98	113*	4415	1986*	0.68
9	33 / F	yes	21	GBP, PHT	R temp ant	4	144	R HS	104	126*	4511	3706*	0.82*
10	27 / F	no	14	CBZ, LTG	R temp ant	2	180	R HS	97	118*	6286	3732*	0.59
11	26 / F	yes	2	CBZ, LTG	R temp ant	5	336	R HS	104	125*	5142	4077*	0.79*
12	38 / M	no	1	CBZ, PHT	L temp ant	14	72	L HS	125*	101	3207*	4632	0.70*
13	28 / F	yes	1	LTG, PHT	L temp ant	7	144	L HS	105	103	3314*	4240	0.78*
14	22 / M	no	2	CBZ, PHT	R temp ant	2	150	R HS	109	142*	5801	4351*	0.68
15	27 / F	yes	11	CBZ	L temp ant	2	120	L HS	102	101	4350	5746	0.76*
16	31 / F	yes	7	GBP, PHT	R temp ant	3	4	R HS	101	113*	5379	4175	0.78*
17	22 / F	no	4	CBZ, LTG	R temp ant	10	24	R HS	99	102	4035*	2278*	0.56*

* >2 SD above normal HCT2 or >2 SD below normal HCV

L=left; R=right; AED=Antiepileptic drugs; CBZ=Carbamazepine; LTG=Lamotrigine; PHT=Phenytoin; GBP=Gabapentin; CPS=complex partial seizure; inter CPS/PET=interval between last CPS and PET scan; temp=temporal; ant=anterior; HS=hippocampal sclerosis; HCT2=hippocampal T2; HCV=hippocampal volume corrected for intracranial volume; HCVR=hippocampal volume ratio (volume of hippocampus with higher HCT2 divided by volume of hippocampus with lower HCT2)

years) and the median age at PET examination was 27 years (range: 19-49 years). Nine patients had a history of prolonged FC in early childhood. The antiepileptic medication was mono- or polytherapy with carbamazepine (12 patients), lamotrigine (8), phenytoin (6) or gabapentin (4) (**Table 2**).

Using accepted qualitative and quantitative MRI criteria (Cook, 1992; Jackson, 1993b) 13 patients had a clear MRI diagnosis of unilateral diffuse HS with unilaterally reduced HCV corrected for ICV, abnormal HCV-AI and increased HCT2. Three patients (pat. 14 -16) had unilateral anterior hippocampal atrophy on longitudinal HCV measurements and one patient (pat. 17) had a marked HCV-AI with diffuse HS concordant with the EEG focus, but also anterior hippocampal atrophy in the contralateral hippocampus.

Fifteen healthy volunteers (13 male, 2 female) with a median age of 30 years (range: 23-54 years), who were on no medication, had no history of neurological or psychiatric disorder, normal EEGs and MRI studies, were studied for comparison.

5.3.2. Electroencephalography

All 17 patients had prolonged video-EEG recordings with scalp electrodes. Ictal events were captured for all patients and an unilateral anterior temporal epileptogenic focus ipsilateral to the side of HS was identified.

5.3.3. Epilepsy surgery and histopathology

In all cases the histopathologic findings of the removed mesial structures (including hippocampus, part of the amygdala, anterior 2 until 3 cm of lateral temporal neocortex) verified the MRI finding of HS. No pathological abnormalities were detected in the resected anterior temporal cortical tissue, apart from an increased number of neurones in the resected white matter in seven patients (**Table 3**).

5.3.4. Quantitative neuropathology

Quantitative pathology with measurements of neuronal cell densities was only possible in 14 patients with an MRI diagnosis of unilateral hippocampal sclerosis due to tissue damage during surgical removal in three cases. Six control hippocampi of persons (three men and three women, median age 31 years, range: 14 to 52) who had died from non-neurological causes were obtained at autopsy (**Table 3**) (see chapter 3.7.).

Table 3: Histopathology and quantitative neuropathology with neuronal cell density

	Histology	ND CA1 (cells x $10^3/mm^3$)	ND CA2	ND CA3	ND CA4	ND DG	Follow up (years)	Outcome (Grade)
Normal mean		20.3	30.2	16.4	12.0	482		
Normal range		15.6 - 23.4	25.7 - 38.0	15.6 - 25.9	8.6 - 14.9	295 - 635		
1	HS	3.46	n.a.	n.a.	4.94	205	2	I
2	HS	1.99	16.46	4.94	0.99	180	1.5	I
3	HS	n.a.	n.a.	n.a.	n.a.	n.a.	1	I B
4	HS	1.73	n.a.	n.a.	0.99	150	2	I B
5	HS	1.48	22.22	14.32	10.37	530	1.5	I
6	HS	4.20	n.a.	n.a.	0.99	255	2.5	III
7	HS	2.96	20.25	3.80	1.48	138	2	I
8	HS+MD	5.66	22.96	n.a.	1.98	195	2	I
9	HS+MD	2.96	19.26	3.46	1.48	170	1.5	I
10	HS+MD	3.46	n.a.	n.a.	4.94	110	2	I
11	HS+MD	2.47	16.30	3.95	2.47	220	1	I
12	HS+MD	2.25	20.76	6.42	2.81	170	1	I
13	HS	n.a.	n.a.	n.a.	n.a.	n.a.	1	I
14	HS+MD	3.46	n.a.	n.a.	1.48	164	2.5	I
15	HS	n.a.	n.a.	n.a.	n.a.	n.a.	1.5	I
16	HS	2.94	13.30	11.05	4.24	198	1	I
17	HS+MD	3.46	21.24	8.40	6.42	130	1	I

ND= neuronal cell density; DG= dentate gyrus; HS= hippocampal sclerosis; L= left; R= right; MD= microdysgenesis; n.a.= not available for quantitative pathology; temp ant= temporal anterior

5.3.5. PET and MRI methodology

PET scans were performed at the MRC Cyclotron Unit at the Hammersmith Hospital on a ECAT 953b scanner (CTI Siemens, Knoxville, TN) which acquires 31 simultaneous slices and has a resolution of 4.8 x 4.8 x 5.2 mm (at FWHM). Scans were performed with axial images obtained along the the long axis of the hippocampus and coronal images orthogonal to it. High specific activity ^{11}C-FMZ tracer (370MBq) was injected intravenously and arterial blood was sampled continuouslyin order to determine a metabolite-corrected arterial input function. Voxel-by-voxel parametric images of ^{11}C-FMZ-V_d, reflecting binding to cBZR, were produced from the brain uptake and plasma input functions by using spectral analysis. (see chapters 3.2., 3.3.4.)

MR images were obtained for each control subject and patient on a 1T Picker scanner using a gradient echo sequence protocol which generated 128 contiguous 1.3 mm thick sagittal images. These high resolution volume acquisition MRI scans were coregistered with the parametric images of ^{11}C-FMZ-V_d (see chapter 3.6.).

5.3.6. Methodology for partial volume effect correction

The aim was to quantify authentic decreases in hippocampal FMZ binding after correction for partial volume effects due to hippocampal atrophy. We used a MRI-based four-compartment, three-dimensional correction of human PET data (Müller Gartner, 1992). In summary, the hippocampus as the VOI was first outlined on high resolution MRI using accepted criteria (Van Paesschen, 1995). The high resolution volume acquisition MRI scans were then automatically segmented into neocortical GM, WM, and CSF using a clustering, maximum likelihood "mixture model" algorithm (Hartigan, 1975). This algorithm assumes that the MR image consists of a number of distinct tissue types (clusters) from which every voxel has been drawn. All segments, GM, WM, and VOI were coregistered with the parametric images of FMZ-V_d (Woods, 1993). After superimposition of MRI and PET data, the MR images were blurred to result in the same spatial resolution as PET. This was achieved by convolving the MRI with the 3D PET point spread function (PSF), as previously described (Labbé, 1996) (see Chapter 3.4.2.2.).

5.3.7. Intra-rater test-retest repeatability of correction for partial volume effects

Partial volume corrected ^{11}C-FMZ-V_d was determined twice for cortical GM and hippocampal VOIs for five controls and five patients with an interval of weeks to months. The repeatability coefficient, i.e. 2 SD of the mean difference between repeated measurements was 17% for absolute ^{11}C-FMZ-V_d. This repeatability study indicated that 5% of individual cBZR measurements were different from the first measurement by more than 17%.

5.3.8. Statistical analysis

As several comparisons were made the normal limit for all observations was defined as 2.5 SD below or above the normal control mean. Statistical analysis was performed using StatsView (Haycock, 1992). Pearson's correlation coefficients (r), Fisher's Exact test, Mann-Whitney U test, Student's t test and ANOVA were used where indicated.

5.4. Results

5.4.1. Control subjects

The 30 hippocampal ^{11}C-FMZ-V_d values were normally distributed before and after partial volume effect correction in the 15 control subjects examined. There was no significant difference between mean left and right, or mean larger and smaller hippocampus. Before correction the mean control hippocampal ^{11}C-FMZ-V_d was 3.94

(SD = 0.33; range: 3.12 to 4.76) and after correction 4.74 (SD = 0.48; range: 3.54 to 5.94). The uncorrected ^{11}C-FMZ-Vd AI (^{11}C-FMZ-Vd of bigger hippocampus divided by ^{11}C-FMZ-Vd of smaller hippocampus) was 1.02 (SD = 0.05; range: 0.94 to 1.10), similar to the corrected ^{11}C-FMZ-AI with 1.04 (SD = 0.05; range: 0.97 to 1.18). Before and after partial volume effect correction all control values, absolute ^{11}C-FMZ-Vd and AI, lay within 2.5 SD with the exception of one control who showed a non-significant relative increase of ^{11}C-FMZ-Vd in the smaller hippocampus resulting in a AI marginally above 2.5 SD of the control mean. An absolute hippocampal ^{11}C-FMZ-Vd of < 3.12 or > 4.76 before and < 3.54 or > 5.94 after partial volume effect correction or an uncorrected AI of < 0.90 or > 1.14 and a corrected AI of < 0.92 or > 1.16 were considered as abnormal.

5.4.2. Patients with unilateral hippocampal sclerosis

Hippocampal ^{11}C-FMZ-V_d before and after correction for partial volume effects

Before partial volume effect correction the patients' mean ^{11}C-FMZ-V_d on the side of the HS was 2.96 (SD = 0.47; range: 2.21 to 3.98). After partial volume effect correction absolute ^{11}C-FMZ-V_d within the HS was 2.79 (SD = 0.55; range: 1.51 to 3.50) representing a mean 38% reduction from control values. The corrected ^{11}C-FMZ-AI was highly significantly lower than the uncorrected (0.62 vs. 0.76; $p < 0.0001$). Before partial volume effect correction 11 of the 17 patients (65%) had an abnormally reduced hippocampal ^{11}C-FMZ-V_d, with one patient (pat. 6) showing reductions in the contralateral hippocampus marginally below 2.5 SD. The remaining six patients showed only an abnormal AI. After correction for partial volume effects all 17 patients (100%) had both significant unilateral reductions of absolute ^{11}C-FMZ-V_d in the epileptogenic hippocampus, and an abnormal AI. No abnormalities contralateral to the epileptogenic hippocampus were observed. (**Table 4**)

Comparison of partial volume corrected FMZ-V_d with quantitative MRI

Thirteen patients had a clear MRI diagnosis of diffuse unilateral HS with reduced HCV measurements affecting the whole length of the epileptogenic hippocampus and increased HCT_2. The remaining four patients all had marked HCV-AI, but in three patients (pat. 14 - 16) hippocampal atrophy was confined only to the anterior hippocampus and in the fourth patient (pat. 17) HCV contralateral to the diffusely involved, epileptogenic hippocampus was also reduced, albeit only marginally below 2.5 SD. All 17 patients had both significant unilateral reductions of ^{11}C-FMZ-V_d and abnormal AI after correction for partial volume effects. Examining the relationship between quantitative ^{11}C-FMZ binding and quantitative MRI measurements in all 34 patients' hippocampi there was a highly significant correlation between absolute hippocampal ^{11}C-FMZ-V_d and HCV (Pearson $r = 0.778$; $p < 0.0001$), and between

^{11}C-FMZ-V_d and HCT_2 ($r = -0.864$; $p<0.0001$). However, no correlation was found between absolute ^{11}C-FMZ-V_d and HCV in the epileptogenic hippocampus ($r = 0.433$; $p = 0.082$), but still a significant inverse correlation between absolute ^{11}C-FMZ-V_d and HCT_2 ($r = -0.66$; $p = 0.004$). There was a significant correlation between ^{11}C-FMZ-AI and HCV-AI ($r = 0.578$, $p = 0.015$).

Table 4: *Hippocampal FMZ PET results before and after correction for partial volume effect*

No.	before PVE-correction			after PVE-correction		
	FMZ-V_d left HC	FMZ-V_d right HC	FMZ-AI	FMZ-V_d left HC	FMZ-V_d right HC	FMZ-AI
Normal mean(SD)	3.94 (0.33)		1.02 (0.05)	4.74 (0.48)		1.04 (0.05)
Normal range	3.12 - 4.76		0.90 - 1.14	3.54 - 5.94		0.92 - 1.16
1	2.73*	3.40	0.80*	2.75*	4.12	0.67*
2	2.64*	3.91	0.68*	2.10*	4.77	0.44*
3	2.53*	3.84	0.66*	1.91*	4.30	0.44*
4	2.84*	4.23	0.67*	2.11*	4.85	0.44*
5	3.51	2.69*	0.77*	3.79	2.11*	0.53*
6	3.09*	2.21*	0.72*	4.12	2.76*	0.67*
7	3.72	2.92*	0.79*	4.79	3.31*	0.69*
8	3.95	2.81*	0.71*	5.05	2.94*	0.58*
9	4.67	3.28	0.83*	4.84	3.28*	0.68*
10	3.96	2.84*	0.72*	4.73	3.22*	0.68*
11	4.03	2.99*	0.74*	4.76	2.92*	0.61*
12	3.33	4.27	0.78*	2.77*	4.61	0.60*
13	3.41	3.94	0.87*	3.39*	4.23	0.80*
14	3.96	2.59*	0.65*	4.13	1.98*	0.48*
15	3.30	3.73	0.89*	3.39*	4.54	0.78*
16	4.72	3.98	0.84*	4.89	3.50*	0.73*
17	4.20	3.16	0.75*	4.68	2.90*	0.62*

* > 2.5 standard deviations (SD) below normal FMZ-V_d or below normal FMZ-AI
PVE = partial volume effects; FMZ-V_d = flumazenil volume of distribution; FMZ-AI = FMZ asymmetry index (FMZ-V_d of smaller HCV divided by FMZ-V_d of bigger HCV); HC = hippocampus

Comparison of partial volume corrected FMZ-V_d with quantitative neuropathology
Neurone cell densities for CA_1, CA_4 and the dentate gyrus (DG) were measured in all available 14 specimens, whereas the CA_2 and CA_3 regions were preserved for quantitative analysis only in nine and eight patients, respectively. In the patients neurone cell density was reduced compared to the control mean values in the CA_1,

CA_2, CA_3, CA_4 and DG by 85%, 30%, 57%, 73% and 57% respectively. In the patient group there was no correlation between hippocampal ^{11}C-FMZ-V_d corrected for partial volume effects and neurone cell density within CA_1 (r = 0.305), CA_2 (r = -0.269), CA_3 (r = -0.299), CA_4 (r = -0.085) or DG (r=-0.328). (**Table 3**)

5.4.3. Clinical correlations

Age of onset of habitual seizures and age at the time of PET scanning, duration of epilepsy, frequency of seizures, interval between last seizure and time of PET scanning, and occurrence of prolonged FC during early childhood did not correlate with reductions of ^{11}C-FMZ-V_d before and after correction for partial volume effects.

5.5. Discussion

The main finding of this study was that in patients with unilateral mTLE absolute ^{11}C-FMZ binding to cBZR was significantly reduced in the sclerosed hippocampus over and above the loss of volume. Correction for partial volume effects increased the yield of FMZ-PET from 65% to 100% compared to uncorrected data. The reduction of neurone cell density in the resected hippocampus was not correlated with the reduction of ^{11}C-FMZ-V_d, but this analysis was confined to a population of severely affected cases. The use of ^{11}C-FMZ PET coregistered with high quality MRI and corrected for partial volume effects provides a quantitative and objective means of measuring cBZR density in the hippocampi of patients with TLE.

5.5.1. Methodological considerations

This is the first study that has used a MRI-based method for partial volume effect correction to quantitate changes of cBZR binding in HS. Using SPM reductions of cBZR binding are restricted to the sclerosed hippocampus without any decreases or increases of cBZR elsewhere in the cerebral neocortex (Koepp, 1996a). While the SPM approach is completely automated and so free from observer bias, it also suffers from partial volume averaging due to the limited resolution of PET and the specific anatomical orientation of mesial temporal structures. Partial volume effects are especially relevant, if structures are smaller than twice the FWHM of the scanner resolution (with our PET scanner smaller than 16x16x8 mm^3) (Hoffman, 1979). Before correction for partial volume effects the higher adjacent activity in mesio-basal temporal and frontal neocortex led to an overestimation of hippocampal cBZR binding, which was more marked for the smaller, sclerosed hippocampus. In contrast, underestimation of true cBZR density through loss of signal into CSF and white matter

was more pronounced within the bigger, unaffected hippocampus. Uncorrected ^{11}C-FMZ-V_d thereby underestimated the severity of the disease in terms of both absolute reductions of ^{11}C-FMZ-V_d and AI.

Other investigators have used a variety of techniques to define ROI (Henry, 1993; Savic, 1993). Some methods, such as outlining the ROI directly onto the PET, inevitably give rise to observer bias and partial volume effects. Placing ROIs of a predetermined shape, or anatomically configured ROIs over the structure of interest (Henry, 1993), or even defining all ROIs on a coregistered structural image such as MRI (Henry, 1993; Szelies, 1996), all lead to partial volume effects. Only 50% of the signal is recovered when using a ROI the same size as the FWHM resolution. Henry *et al.* (1993) observed significantly greater decreases in FMZ binding (V_d) than in transport (K_1) in the affected mesial temporal lobe in TLE giving indirect evidence that decreases of receptor density are not due to atrophy alone, since K_1 and V_d should be equally affected by partial volume averaging. They addressed the importance of partial volume averaging of CSF and brain in PET by measuring the CSF content on the coregistered MRI within their anatomically configured PET ROI. This accounted for less than 20% of apparent receptor loss, and this MRI-based method does not account for the spill over of activity from neocortex, as observed in our study. We outlined the hippocampus on optimal high quality MRI excluding, a priori, CSF from the VOI and then, during the partial volume effect correction, coregistered this with the 3D FMZ-V_d image. In order to further minimise partial volume effects both PET and MRI were acquired for patients and normal subjects in the same orientation as recommended for optimal MRI volumetric measurements with axial planes parallel to the long axis of the hippocampus (Jackson, 1993a,b).

The importance of partial volume effect correction for the analysis of functional imaging data has recently been reported in a series of patients with Alzheimer disease using ^{11}F-FDG PET data (Meltzer, 1996a). The authors used a three-compartment method (Meltzer, 1990), which assumed homogenous cortical activity and incompletely corrected cortical VOI when local tissue concentrations were highly heterogeneous (Meltzer, 1996b). This method may lead to undercorrection of small structures such as the hippocampus, where spill-in of activity from surrounding structures greatly influences the apparent tracer concentration. The same group recently described a four-compartment method (Meltzer, 1996b) which permits the accurate determination of the true tissue concentration in one specific VOI defined by MRI accounting for the influence of heterogeneous activity distribution between this structure and the rest of the cortex. Combining this four-compartment method with our own developments (Labbé, 1996) we further improved this partial volume effect correction. We accounted for spatial differences of the PET PSF in all three-dimensions and for the heterogeneity

of cBZR density in the neocortex by using a cuboid centred on the hippocampus for the determination of the corrected GM ^{11}C-FMZ-V_d around the hippocampal VOI.

5.5.2. Clinical considerations

Greater reductions of ^{11}C-FMZ binding have been reported in patients with frequent seizures, in comparison to those with less frequent seizures (Savic, 1996). It is not yet clear whether this finding represents the cause or consequence of epileptic activity. In this study we could not find any correlations between ^{11}C-FMZ-V_d and clinical parameters, such as frequency of seizures, time since last seizure, duration of epilepsy or treatment with specific AED. Patients, who were treated with AED that potentially interact with the cBZR complex, such as benzodiazepines, phenobarbitone, sodium valproate or vigabatrin, were not included in this study. Four patients were treated with gabapentin (GBP), which increases cerebral GABA concentrations (Petroff, 1996). Treatment with GBP, therefore, theoretically could affect global $GABA_A$ / cBZR density due to increased GABA in these four patients. However, ^{11}C-FMZ-V_d in the contralateral hippocampus for the patients taking GBP were not significantly different from the other patients and the controls. Whilst AEDs may result in a global reduction of cerebral blood flow and glucose metabolism (Leidermann, 1992) changes in ^{11}C-FMZ-V_d are independent of blood flow effects (Frey, 1991) so this will not have been a confounding factor.

The utility of ^{11}C-FMZ PET in the clinical investigation of patients with refractory partial seizures and unremarkable high quality MRI is currently under investigation. Comparisons of this nature, however, clearly depend on the relative sophistication of the instruments and methodologies used. In six patients with frontal lobe epilepsy, reduction in cBZR binding was demonstrated with ^{11}C-FMZ PET that was consistent with clinical and EEG data (Savic, 1995). Using SPM we have demonstrated significant changes of hippocampal ^{11}C-FMZ-V_d in six out of eight patients with TLE and normal quantitative MRI (Koepp, 1996b). SPM has also detected areas of abnormal cortical FMZ binding, both decreases and increases, in 12 out of 17 patients with extra-temporal lobe epilepsy and normal high quality MRI (Richardson, 1996). In both studies SPM showed the spatial extent of significant abnormalities, absolute quantification of these changes with correction for partial volume effects, however, has not yet been performed.

We noted a significant correlation between HCT_2 and absolute ^{11}C-FMZ-V_d and between asymmetry indices of HCV and ^{11}C-FMZ-V_d. Absolute measurements of HCV and ^{11}C-FMZ-V_d correlated in the whole group, but not when the affected hippocampi were considered in isolation. Quantitative MRI and ^{11}C-FMZ-PET are

both sensitive means to detect an underlying disease with ^{11}C-FMZ PET reflecting structural and functional abnormalities. Although MRI has made a considerable difference to the evaluation of patients with refractory seizures who are candidates for surgical treatment, other investigations are not redundant. ^{11}C-FMZ-PET corrected for partial volume effects may be clinically useful in preoperative epilepsy evaluation when quantitative MRI does not reveal a single abnormality that is concordant with other data.

CHAPTER VI Regional hippocampal ^{11}C-Flumazenil PET in Temporal Lobe Epilepsy with unilateral and bilateral Hippocampal Sclerosis

6.1. Summary

Background: Using SPM and ^{11}C-FMZ PET we have shown reduction of cBZR binding restricted to the hippocampus in mTLE due to unilateral HS. Bilateral hippocampal pathology, however, can be present in up to 50% of patients with mTLE. Additionally, the limited spatial resolution of PET results in partial volume averaging that affect quantitative analysis of cBZR and can mask hippocampal dysfunction.
Method: We analysed changes in ^{11}C-FMZ-V_d before and after correction for partial volume effect in six patients with refractory mTLE and a quantitative MRI diagnosis of bilateral HS, which appeared either symmetrical on MRI (bil-sym-HS; three patients) or bilateral, but asymmetrical (asym-HS; three patients), with refractory mTLE and unilateral HS on MRI (uni-HS; nine patients) that was subsequently histologically verified. Fifteen healthy controls were also studied for comparison.
Results: Before correction for partial volume effect significant unilateral reductions of ^{11}C-FMZ-V_d were found in one of three patients with bil-sym-HS, in one of the three asym-HS patients and in six of the nine uni-HS patients. No significant bilateral reductions of hippocampal ^{11}C-FMZ-V_d were detected. After correction for partial volume effect all three patients with bil-sym-HS showed significant bilateral reductions of ^{11}C-FMZ-V_d, and these were asymmetrical in two. All three patients with asym-HS and all nine patients with uni-HS on MRI showed unilateral reductions of ^{11}C-FMZ-V_d concordant with the side of the EEG focus. In addition one of the three patients with asym-HS and three of the nine patients with uni-HS showed significant reductions of ^{11}C-FMZ-V_d in the hippocampus contralateral to the side of the EEG focus.
Conclusion: Absolute quantitation of ^{11}C-FMZ-PET, corrected for partial volume effect within multiple hippocampal VOI was necessary in order to detect bilateral changes of cBZR in mTLE due to HS with optimal sensitivity. This ^{11}C-FMZ-PET approach was able to demonstrate subtle contralateral abnormalities in one third of patients thought to have unilateral or bilateral-asymmetric HS on MRI. Reduction of cBZR binding was consistently over and above loss of HCV indicating that atrophy is not the sole determinant of cBZR loss in mTLE.
(published in ***Brain*** 1997; 120: 1865-1876)

6.2. Introduction

The majority of patients with refractory mTLE have HS (Babb, 1987). Cell loss is usually asymmetrical but present, to some degree, in both hippocampi in the majority of patients. As many as 25% of HS patients in one pathological study had symmetrical damage (Margerison, 1966). HS may also coexist with other temporal or extra-temporal lesions (Levesque, 1991; Raymond, 1994).

Absolute quantitation of PET data is limited by its spatial resolution, partial volume effects particularly confounding quantitative measurements for structures smaller than twice the FWHM (Hoffman, 1979), such as the normal and the sclerotic hippocampus. Spill over of signal into surrounding WM and CSF may result in underestimations of the measured hippocampal activity due to tissue volume averaging within the hippocampal VOI (Müller-Gärtner, 1992; Rousset, 1995; Labbé, 1996; Meltzer, 1996a; Meltzer, 1996b; Labbé, 1997). We have shown in chapter V that correction for partial volume effects is essential if tissue cBZR density in the hippocampus is to be determined (Koepp, 1997).

HS is generally more pronounced anteriorly rather than affecting the whole structure uniformly (Van Paesschen, 1997). It follows that a single measurement will not detect subtle focal abnormalities. Division of the hippocampus into head, body and tail as carried out in analysis of MRI is not possible using PET, without partial volume effect correction, due to the limited spatial resolution of the latter technique. Previously published MR-based correction for partial volume effect (Müller-Gärtner, 1992; Meltzer, 1996b) only corrected one VOI at a time. We have now implemented a partial volume effect correction method based on a linear least squares algorithm which can accurately correct multiple VOIs of any size. We have used this correction method to assess changes in cBZR within the head, body and tail of the hippocampus in patients with mTLE and bilateral symmetrical, bilateral asymmetrical and unilateral HS, as defined using MRI.

6.3. Methods

6.3.1. Subjects

We studied 15 patients (9 female, 6 male) who suffered from drug-resistant mTLE (Wieser, 1987). Using accepted qualitative and quantitative MRI criteria (Cook, 1992;Jackson, 1993; Van Paesschen, 1997) three patients had an MRI diagnosis of bilateral symmetrical HS (bil-sym-HS) with bilaterally reduced HCV normalised to ICV, bilaterally increased HCT2, but normal HCV symmetry (HCV-AI) (pat. 1 - 3,

table 1 and 2). Three patients (pat. 4 - 6) had bilateral asymmetrical HS (asym-HS) with abnormal HCV-AI, but bilateral reduced HCV (pat. 5), bilateral increased HCT2 (pat. 6) or in one case focal anterior HS contralateral to the EEG focus evident on the display of hippocampal crossectional areas (pat. 4) (Van Paesschen, 1997). Nine patients (pat. 7 - 15) had an unequivocal MRI diagnosis of unilateral HS (uni-HS) with unilateral reduction of HCV, increase of HCT2 and abnormal HCV-AI. (**Table 5**)

The median age at onset of habitual epilepsy was 5 years (range: 2 - 12 years) for the bil-sym-HS group, 4 years (range: 1 - 5 years) for the asym-HS group and 7 years (range: 1 - 23 years) for the uni-HS group. The median duration of epilepsy prior to PET examination was 35 years (range: 20 - 43 years) for the bil-sym-HS group, 27 years (range: 18 - 35 years) for the asym-HS group and 20 years (range: 12 - 37 years) for the uni-HS group. The median age at PET examination was 37 years (range: 32 - 48 years) for the bil-sym-HS group, 28 years (range: 22 - 40 years) for the asym-HS group and 27 years (range: 19 - 49 years) for the uni-HS group. None of the bil-sym-HS, one of the asym-HS (33%) and five of the uni-HS (55%) patients had a history of prolonged FC in early childhood. The antiepileptic medication was mono- or polytherapy with carbamazepine (12 patients), lamotrigine (7), phenytoin (5), gabapentin (3), topiramate (1) and valproate (1) (**Table 5**). Patients who were treated with benzodiazepines, barbiturates or vigabatrin within two months of the PET examination were not included in the study.

Fifteen healthy volunteers (13 male, 2 female) with a median age of 30 years (range: 23 - 54 years), who were on no medication, had no history of neurological or psychiatric disorder, normal EEGs and MRI studies, were studied for comparison. Subjects did not consume alcohol within 48 hours preceding the PET scan.

6.3.2. Electroencephalography

Bil-sym-HS. Every patient had repeated long-term scalp EEG monitoring which exhibited bilateral temporal interictal epileptiform activity consisting of sharp and slow wave complexes in all patients. In addition one patient (pat. 3) had prolonged video-EEG recordings with scalp electrodes. Interictal recordings revealed independent bitemporal spikes with a left sided preponderance. Two clinically similar seizures were recorded for this patient with unilateral EEG changes occurring 17 and 25 seconds after clinical seizure onset which consisted of a rhythmic discharge over the left temporal lobe.

Asym-HS. All three patients had prolonged video-EEG telemetry recordings. Ictal events were captured for all patients and an unilateral anterior temporal epileptogenic

focus ipsilateral to the side of the most atrophic hippocampus was identified. Scalp EEGs exhibited clear, strictly unilateral anterior temporal paroxysmal activity consisting of sharp and slow wave complexes in two patients. One patient (pat. 6) had bilateral independent, temporal interictal epileptiform activity with a lateralised preponderance (ratio left:right: 2:1). Depth EEG recordings using a combination of stereotactically implanted electrodes and a subdural strips covering temporal neocortex, both hippocampi and amygdalae revealed the seizure onset in two recorded habitual seizures consistently in the right hippocampus.

Uni-HS. All nine patients had several days of video-EEG telemetry recordings with scalp electrodes including surface sphenoidal electrodes. Ictal and interictal epileptiform activity were detected and an unilateral anterior temporal epileptogenic focus ipsilateral to the side of HS was identified in all patients. Two patients (pat. 7, 8) had bilateral temporal interictal epileptiform activity with a lateralised preponderance (ratios: 10:1, 8:1), but no independent bilateral discharges. (**Table 5**)

6.3.3. Epilepsy surgery, histopathology and outcome

Bil-sym-HS. None of these patients have undergone hippocampectomy to date.

Asym- and uni-HS. All 12 patients have had an anterior temporal lobe resection. In all cases the histopathologic findings of the removed mesial structures (including hippocampus, part of the amygdala, anterior 2 to 3 cm of lateral temporal neocortex) verified the MRI finding of HS. No pathological abnormalities were detected in the resected anterior temporal cortical tissue, apart from an increased number of neurones in the resected white matter in four patients. (**Table 5**). The median post-surgical follow-up period was 1.5 years (range 1 to 3 years). Outcome was classified in all patients as Grade 1 according to the Engel criteria (Engel, 1987) with two patients still experiencing simple partial seizures (auras only).

6.3.4. PET and MRI methodology

PET scans were performed at the MRC Cyclotron Unit at the Hammersmith Hospital on a ECAT 953b scanner (CTI Siemens, Knoxville, TN) which acquires 31 simultaneous slices and has a resolution of 4.8 x 4.8 x 5.2 mm (at FWHM). Scans were performed with axial images obtained along the the long axis of the hippocampus and coronal images orthogonal to it. High specific activity ^{11}C-FMZ tracer (370MBq) was injected intravenously and arterial blood was sampled continuously in order to determine a metabolite-corrected arterial input function. Voxel-by-voxel parametric

images of ^{11}C-FMZ-V_d, reflecting binding to cBZR, were produced from the brain uptake and plasma input functions by using spectral analysis. (see chapters 3.2., 3.3.4.)

MR images were obtained for each control subject and patient on a 1T Picker scanner using a gradient echo sequence protocol which generated 128 contiguous 1.3 mm thick sagittal images. These high resolution volume acquisition MRI scans were coregistered with the parametric images of ^{11}C-FMZ-V_d. (see chapter 3.6.)

6.3.5. Methodology of partial volume effect correction

The aim was to differentiate authentic decreases in hippocampal FMZ binding from that due to partial volume averaging of neighbouring signal with hippocampal atrophy. Our method corrects multiple VOIs for partial volume effect, without requiring any prior assumptions concerning radioactivity concentration in given compartments, such as white matter and CSF. The only assumption made is that each VOI contains a homogeneous radioactivity concentration.

In summary, the hippocampus was first delineated using accepted criteria (Cook, 1992) and then divided from anterior to posterior into three parts of equal length. The high resolution volume acquisition MRI scans were then automatically segmented into probability images of neocortical GM, WM, and CSF using a clustering, maximum likelihood "Mixture Model" algorithm (Hartigan, 1975). This algorithm assumes that the MR image consists of a number of distinct tissue types (clusters) from which every voxel has been drawn. All probability MR images, GM, WM, and VOIs were coregistered with the parametric images of FMZ-V_d (Woods, 1993). After superimposition of MRI and PET data, the MR images were "blurred" to result in the same spatial resolution as PET. This was achieved by convolving the MR images with the 3D PET point spread function (PSF) (Labbé, 1996). For further details see chapter 3.4.2.3.

6.3.6. Intra-rater test-retest repeatability of correction for partial volume effects

Corrected cBZR densities were determined twice for cortical GM and hippocampal VOI including outlining the hippocampus of five controls and five patients again after an interval of weeks to months. The coefficient of repeatability (Bland, 1986) , i.e. 2 SD of the mean difference between repeated measurements was 6.8% for absolute cBZR density measurements. This repeatability study indicated that only 5% of individual cBZR measurements would differ from the first measurement by more than 6.8%.

Table 5: Clinical and EEG data, quantitative MRI findings in 15 patients with refractory TLE

	Age / Sex	PFC	Age of onset (years)	AEDs	EEG (interictal; ictal)	inter CPS PET (days)	CPS per year	MRI	L HCT2 (msec) <108	R HCT2 (msec) <108	L HCV (mm^3) >4378	R HCV (mm^3) >4378	HCV Ratio >0.90	histology
Normal range														
1	32 / F	no	12	CBZ, LTG	L temp ant; L temp ant	48	10	bil HS	125*	121*	3016*	3286*	0.91	n.o.
2	48 / M	no	5	CBZ, PHT	bil temp L>R; no ictal	2	35	bil HS	100	105	3602*	3466*	0.96	n.o.
2	48 / M	no	5	GBP, PHT	ind bil temp L>R (30:1)	36	21	bil HS	120*	117*	3356*	3703*	0.91	n.o.
4	28 / F	yes	1	LTG, PHT	L temp ant; L temp ant	7	144	as HS	105	103	3314*	4240	0.78*	HS
5	22 / F	no	4	CBZ, LTG	R temp ant; R temp ant	10	24	as HS	99	102	4035*	2278*	0.56*	HS+MD
6	40 / M	no	5	CBZ, LTG	ind bil temp L>R (2:1)	48	7	as HS	113*	134*	5386	3854*	0.72*	HS
7	27 / F	no	7	CBZ, LTG	R>L (10:1); R temp ant	480	2	R HS	97	118*	6249	3695*	0.59*	HS+MD
8	49 / M	no	12	CBZ, GBP	L>R (8:1); L temp ant	48	7	L HS	131*	103	2407*	5273	0.46*	HS
9	26 / F	yes	2	CBZ, LTG	R temp ant; R temp ant	5	336	R HS	104	125*	5142	4077*	0.79*	HS+MD
10	38 / M	no	1	CBZ, PHT	L temp ant; L temp ant	14	72	L HS	125*	101	3207*	4632	0.70*	HS+MD
11	22 / M	yes	5	CBZ	L temp ant; L temp ant	72	3	L HS	127*	104	2753*	4803	0.58*	HS
12	31 / F	yes	7	LTG, VPA	R temp ant; R temp ant	24	7	R HS	108	126*	4492	2622*	0.59*	HS
13	38 / F	no	23	CBZ, LTG	R temp ant; R temp ant	4	95	R HS	102	140*	4544	3454*	0.76*	HS
14	19 / F	yes	7	CBZ	R temp ant; R temp ant	5	144	R HS	103	125*	5713	3829*	0.67*	HS
15	27 / F	yes	11	CBZ, GBP	L temp ant; L temp ant	120	1	L HS	116*	102	3345*	5051	0.66*	HS

* >2 SD above normal HCT2 or >2 SD below normal HCV

L=left; R=right; AED=Antiepileptic drugs; CBZ=Carbamazepine; LTG=Lamotrigine; PHT=Phenytoin; GBP=Gabapentin; VPA=Sodium Valproate; CPS=complex partial seizure; inter CPS/PET=interval between last CPS and PET scan; temp=temporal; ant=anterior; bil=bilateral; as=asymmetrical; HS=hippocampal sclerosis; MD=microdysgenesis; HCT2=hippocampal T2; HCV=hippocampal volume corrected for intracranial volume; HCVR=hippocampal volume ratio (volume of hippocampus with higher HCT2 divided by volume of hippocampus with lower HCT2); bil temp L>R (ratio) = bilateral synchronous temporal spikes more on the left than on the right side; ind bil temp L>R (ratio) = independent bilateral temporal spikes more on the left than on the right side; temp = temporal; ant = anterior; bil = bilateral; HS = hippocampal sclerosis; MD = microdysgenesis; n.o. = not operated

6.4. Results

6.4.1. Control subjects

Temporo-frontal neocortex (GM)

The 30 temporo-frontal GM ^{11}C-FMZ-V_d values were normally distributed before and after correction for partial volume effect in the control subjects. Before correction the mean control GM ^{11}C-FMZ-V_d was 4.09 (SD = 0.38). There was no difference between left and right or side of bigger and smaller hippocampus with a mean GM ^{11}C-FMZ-AI (defined as GM FMZ-V_d on the side of the smaller hippocampus divided by GM ^{11}C-FMZ-V_d on the side of the larger hippocampus) of 1.01 (SD = 0.02). Therefore an absolute GM ^{11}C-FMZ-V_d of < 3.14 and > 5.04 was considered as abnormal before correction for partial volume effect. After correction GM ^{11}C-FMZ-V_d was significantly higher (mean 6.48; SD = 0.45; $P < 0.001$).

Total hippocampus

The 30 hippocampal ^{11}C-FMZ-V_d values were normally distributed before and after partial volume effect correction in the control subjects. There was no significant difference between mean left and right, or mean larger and smaller hippocampus. Absolute hippocampal ^{11}C-FMZ-V_d and AI (^{11}C-FMZ-V_d of bigger hippocampus divided by ^{11}C-FMZ-V_d of smaller hippocampus) were almost identical before and after correction for partial volume effects. The normal range of absolute hippocampal ^{11}C-FMZ-V_d was 3.12 to 4.76 before and 3.36 to 4.56 after correction. An uncorrected ^{11}C-FMZ-AI of less than 0.90 or higher than 1.14 and a corrected AI of less than 0.82 or higher than 1.22 were considered as abnormal. (**Table 6**)

Multiple hippocampal VOI

Mean values of ^{11}C-FMZ-V_d within the head, body and tail of the hippocampus were calculated after partial volume effect correction. The 30 ^{11}C-FMZ-V_d values within each VOI were normally distributed in the control subjects. The mean ^{11}C-FMZ-V_d for the head of the hippocampus was 3.24 (SD = 0.31) while those for the hippocampal body were 4.23 (SD = 0.5) and tail 3.99 (SD = 0.6) respectively. The normal range of absolute ^{11}C-FMZ-V_d was defined as 2.5 SD below and above mean control value (hippocampal head: 2.47 - 4.02; body: 3.11 - 5.35; tail: 2.49 - 5.48). (**Table 7**)

6.4.2. Patients with bilateral symmetrical hippocampal sclerosis (bil-sym-HS)

Temporo-frontal neocortex (GM)

Absolute ^{11}C-FMZ-V_d were all within normal limits.

Table 6: Uncorrected and PVE corrected absolute FMZ-V_d and FMZ-AI in the total hippocampus

	MRI	before PVE-correction			after PVE-correction		
		FMZ-V_d left HC	FMZ-V_d right HC	FMZ-AI	FMZ-V_d left HC	FMZ-V_d right HC	FMZ-AI
Normal mean(SD)		3.94 (0.33)		1.02 (0.05)	3.96 (0.24)		1.02 (0.08)
Normal range		3.12 - 4.76		0.90 - 1.14	3.36 - 4.56		0.82 - 1.22
1	bil HS	3.23	2.72*	1.19*	2.10*	1.63*	1.28*
2	bil HS	3.50	3.68	1.05	2.70*	2.09*	0.77*
3	bil HS	3.56	3.57	0.99	3.08*	3.02*	1.02
4	as HS	3.41	3.94	0.87*	2.80*	3.78	0.74*
5	as HS	4.20	3.16	0.75*	3.95	2.25*	0.57*
6	as HS	4.65	3.68	0.79*	4.26	2.95*	0.74*
7	R HS	3.96	2.84*	0.72*	4.07	2.53*	0.62*
8	L HS	2.64*	3.91	0.68*	1.14*	4.05	0.28*
9	R HS	4.03	2.99*	0.74*	3.98	2.20*	0.55*
10	L HS	3.33	4.27	0.78*	1.68*	3.65	0.46*
11	L HS	2.53*	3.84	0.66*	1.21*	3.78	0.32*
12	R HS	4.59	3.88	0.85*	4.12	2.74*	0.66*
13	R HS	3.51	2.69*	0.77*	3.41	1.31*	0.38*
14	R HS	3.72	2.92*	0.79*	3.92	2.80*	0.71*
15	L HS	2.73*	3.40	0.80*	2.13*	3.58	0.59*

* > 2.5 standard deviations (SD) below normal FMZ-V_d or below normal FMZ-AI
PVE = partial volume effects; FMZ-V_d = flumazenil volume of distribution; FMZ-AI = FMZ asymmetry index (FMZ-V_d of smaller HCV divided by FMZ-V_d of bigger HCV); HC = hippocampus

Total hippocampus

Before correction for partial volume effect one patient (pat. 1) had significant unilateral reduction on the side of the bigger hippocampus and an abnormally increased ^{11}C-FMZ-AI. (Table 7) After correction all three patients showed significant bilateral reductions of absolute ^{11}C-FMZ-V_d, which were asymmetrical in two (pat. 1, 2). (**Table 6**)

Multiple hippocampal VOI

^{11}C-FMZ binding was bilaterally reduced in the head of the hippocampus in all three patients. One patient (pat. 1) showed bilateral reductions of ^{11}C-FMZ-V_d in the head and the body and unilateral reductions in tail of the hippocampus. In one patient (pat. 2) the head was affected bilaterally and symmetrically and the tail bilateral asymmetrically and in one patient (pat. 3) only the head of the hippocampus was affected bilaterally and symmetrically (**Table 7**).

Table 7: PVE corrected absolute FMZ-V_d in multiple hippocampal VOI

	MRI	HC head		HC body		HC tail	
		left	right	left	right	left	right
Normal mean(SD)		3.24 (0.31)		4.23 (0.5)		3.99 (0.6)	
Normal range		2.47 - 4.02		3.11 - 5.35		2.49 - 5.48	
1	bil HS	0.98*	0.71*	2.51*	2.06	3.04	1.93*
2	bil HS	1.66*	1.63*	3.62	3.15	2.28*	1.21*
3	bil HS	2.01*	2.17*	3.63	3.34	3.10	2.59
4	as HS	2.83	2.63	2.59*	3.4	2.46*	4.47
5	as HS	4.08	2.09*	3.04*	2.62*	3.09	1.26*
6	as HS	3.10	2.20*	4.15	3.00*	4.64	3.46
7	R HS	3.86	2.67	3.43	1.89*	4.23	2.48*
8	L HS	0.68*	2.97	1.56*	3.88	0.58*	5.74
9	R HS	4.08	2.09*	4.08	2.62*	3.09	1.26*
10	L HS	1.10*	2.23*	1.56*	3.88	1.31*	4.17
11	L HS	1.30*	3.08	1.33*	3.51	1.35*	4.42
12	R HS	3.23	1.22*	4.72	3.9	3.47	2.28*
13	R HS	2.30*	1.20*	3.60	1.13*	3.44	2.30*
14	R HS	2.96	1.76*	4.23	3.20	4.52	3.56
15	L HS	1.91*	2.33*	3.06	3.83	1.06*	3.45

* > 2.5 standard deviations (SD) below normal FMZ-V_d or below normal FMZ-AI
PVE = partial volume effects; FMZ-V_d = flumazenil volume of distribution; FMZ-AI = FMZ asymmetry index (FMZ-V_d of smaller HCV divided by FMZ-V_d of bigger HCV); HC = hippocampus

6.4.3. Patients with bilateral asymmetrical hippocampal sclerosis (asym-HS)

Temporo-frontal neocortex (GM)

Absolute ^{11}C-FMZ-V_d were all within normal limits.

Total hippocampus

Before partial volume effect correction none of the asym-HS patients had any reductions of absolute hippocampal ^{11}C-FMZ-V_d, but all three patients showed abnormal ^{11}C-FMZ-AI. After partial volume effect correction all three patients' hippocampal ^{11}C-FMZ-V_d were unilaterally reduced with abnormal ^{11}C-FMZ-AI concordant with the EEG focus. (**Table 6**)

Multiple hippocampal VOI

^{11}C-FMZ binding was reduced in the head of the hippocampus of two of the three patients (pat. 5, 6) using multiple hippocampal VOI analysis. One patient (pat. 5) had bilateral changes with asymmetrical reductions of ^{11}C-FMZ-V_d in the body of the

hippocampus. In the other two patients the body of the hippocampus was affected unilaterally. Significant reductions in the tail of the epileptogenic hippocampus were found in two patients (pat. 4, 5). (**Table 7**)

6.4.4. Patients with unilateral hippocampal sclerosis (uni-HS)

Temporo-frontal neocortex (GM)

Absolute ^{11}C-FMZ-V_d were all within normal limits.

Total hippocampus

Before partial volume effect correction seven of the nine uni-HS (78%) patients had unilateral reductions of absolute hippocampal ^{11}C-FMZ-V_d while the remaining two patients showed abnormal ^{11}C-FMZ-AI, but normal absolute values. After correction all nine patients' corrected hippocampal ^{11}C-FMZ-V_d were unilaterally reduced with abnormal ^{11}C-FMZ-AI concordant with the EEG focus. (**Table 6**)

Multiple hippocampal VOI

Abnormalities of ^{11}C-FMZ binding were found in the head of the hippocampus of all patients bar one (pat. 7) using multiple hippocampal VOI analysis. Three patients (pat. 10, 13, 15) had bilateral anterior changes with asymmetrical reductions of ^{11}C-FMZ-V_d. The body of the hippocampus was affected unilaterally in six of the nine patients. Significant reductions in the tail of the epileptogenic hippocampus were found in all patients except one (pat. 14) who only showed reductions of absolute ^{11}C-FMZ-V_d in the head of the hippocampus. 33% of patients with unilateral HS on MRI had abnormally low ^{11}C-FMZ binding in the head of the hippocampus contralateral to their EEG focus. (**Table 7**)

6.4.5. Clinical correlations

Age of onset of habitual seizures, duration of epilepsy, age at the time of PET scanning, frequency of seizures and interval between last seizure and time of PET scanning did not differ significantly between patients of the three MRI-defined subgroups. A history of prolonged FC during early childhood was obtained for one asym-HS and five uni-HS patients but in none of the patients with bilateral HS. None of these factors, however, or the occurrence of bilateral symmetrical interictal temporal spikes on EEG recordings correlated in any way with reductions of partial volume effect corrected ^{11}C-FMZ-V_d.

6.5. Discussion

The main findings of this study were that, after correction for partial volume effect, absolute hippocampal ^{11}C-FMZ binding was bilaterally reduced in all patients (100%) with mTLE and bilateral symmetric HS on MRI and 33% of mTLE patients with unilateral HS. The reductions were over and above the loss of hippocampal volume. Compared to uncorrected data, correction for partial volume effect dramatically increased the sensitivity of ^{11}C-FMZ-PET for detecting abnormalities of hippocampal ^{11}C-FMZ-V_d. Using multiple VOIs ^{11}C-FMZ-PET corrected for partial volume effect detected significant abnormalities of FMZ binding contralateral to the EEG focus in one third of patients with bilateral asymmetrical or unilateral HS on quantitative MRI that was subsequently histologically verified. The use of partial volume corrected ^{11}C-FMZ-PET coregistered with high quality MRI within multiple VOI therefore provides a quantitative and objective means of delineating regional cBZR abnormalities in the hippocampi of patients with mTLE and uni- or bilateral HS.

6.5.1. Methodological considerations

We used an MRI-based method for partial volume effect correction to quantitate cBZR density in the hippocampi. With uncorrected datasets SPM detected bilateral abnormalities in none of the 12 patients with bilateral asymmetrical or unilateral HS (Koepp, 1996). While the SPM approach is completely automated and so free from observer bias, it is subject to partial volume effect due to the limited resolution of PET and the specific anatomical orientation of mesial temporal structures. SPM analysis could only be performed on image data that was not corrected for partial volume effect, as our correction method calculates the true concentration within a given VOI, but does not create a "partial volume effect corrected" PET image. SPM localises significant changes in patients relative to controls but does not allow absolute quantification of functional imaging data. The analysis of covariance (ANCOVA) in SPM minimises the variance in a group dataset whereas partial volume effect correction increases the variance in functional data but reduces the bias due to structural volume changes. Despite this increase in variance, differences between patients and controls became more obvious after partial volume effect correction. As SPM is voxel-by-voxel based, it can be used in a complementary role to the VOI-based partial volume effect correction method: SPM can guide the placement of VOIs followed by partial volume effect correction to quantify receptor density.

Using an established correction method based on four-compartments (GM, WM, CSF, VOI) (Meltzer, 1996b), we have previously shown that in patients with unilateral HS failure to correct for partial volume averaging leads to an underestimation of the

severity of the disease (Koepp, 1997a) (see Chapter V). This four-compartment method permitted the accurate determination of the true tissue concentration in one specific VOI but makes several assumptions, which are not met in reality. The most important assumption is that one can measure activity within pure WM in order to correct GM activity. The "corrected" GM activity is then used to correct activity within the VOI, leading to a possible accumulation of errors. We have therefore now implemented a method to correct for partial volume effect based on a linear least square method, which allowed measurements of true tracer radioactivity concentration within multiple VOIs of any size and shape, independently of the activity within each of these VOI.

6.5.2. Clinical considerations

The main advantage of the correction method used in the current study was the ability to correct for partial volume effect within multiple VOIs. This allowed for the first time detection of subtle abnormalities of cBZR along the length of the hippocampus and differentiation between diffuse and anterior hippocampal pathology. HS may be of varying severity along the length of the hippocampus or confined to the anterior part of the head. The head of the hippocampus was nearly always and sometimes exclusively affected in patients with TLE when assessed by longitudinal HCV and HCT2 measurements (Van Paesschen, 1997a). Two patients, however, had more marked reductions of FMZ binding in mid to posterior hippocampus raising the possibility that, in some cases, cBZR may be lost more in the mid to posterior hippocampus. FMZ-PET findings are complementary to comprehensive and quantitative MRI studies. In combination they could provide better presurgical information for tailored resections, leaving parts of unaffected mesial-temporal structures intact and by this means possibly reducing the risk of memory impairment after anterior temporal lobe resection (Miller, 1993).

It remains unclear whether bilateral HS reflects bilateral consequences of an initial epileptogenic insult, such as prolonged febrile convulsions or cerebral infection, or whether one epileptogenic hippocampus can induce functional and structural changes in the contralateral hippocampus (Babb, 1987). As has been found in MRI studies (Van Paesschen, 1997a) duration of epilepsy was longer and age of onset of habitual seizures was lower in the patients with bilateral HS compared to strictly unilateral cases. Seizure frequency did not appear to correlate with reduction of hippocampal ^{11}C-FMZ-V_d. A prospective, longitudinal study is necessary to determine if there is progression of HS during the course of TLE.

6.5.3. Pathological and pathophysiological considerations

Quantitative ^{11}C-FMZ-PET analysis with partial volume effect correction identified bilateral abnormalities in 33% of patients in whom high resolution quantitative MRI only revealed unilateral abnormalities. Autopsy studies of HS from patients with long-standing TLE have revealed that the degree of cell loss is usually asymmetrical, but present, to some degree, on both sides in the majority of patients (Babb, 1987). We detected significant bilateral ^{11}C-FMZ-V_d abnormalities in three of nine unilateral HS patients with histologically proven HS. Our patient selection, however, was based on MRI findings and post-operative histological verification of HS and this would bias our observations to underdetection of bilateral HS.

In patients with severe unilateral HS, endfolium sclerosis was noted in the contralateral hippocampus (Margerison, 1966). Unilateral perforant path stimulation in rats occasionally produces bilateral endfolium sclerosis (Sloviter, 1994). Endfolium sclerosis is difficult to detect by MRI (Van Paesschen, 1995). The bilateral changes in cBZR we detected in patients with histologically proven HS using corrected ^{11}C-FMZ-PET might reflect endfolium sclerosis in the contralateral hippocampus. It is uncertain whether these changes may reflect reversible functional disturbances rather than permanent structural abnormalities and their clinical importance has to be assessed by correlation with post-surgical outcome, and by re-scanning patients after surgery.

Two of three patients with bilateral, albeit asymmetric HS had no abnormalities in ^{11}C-FMZ binding contralaterally. In contrast, three out of nine patients with a MRI diagnosis of unilateral HS had bilateral abnormalities of hippocampal cBZR. These five patients with slightly discordant MRI and PET results have been operated so far and typical HS has been histologically verified. At present the interval since surgery is too short (at 1 to 3 years) to assess the clinical significance of these contralateral functional and structural abnormalities.

Chapter VII *In-vivo* ^{11}C-Flumazenil-PET and *ex-vivo* ^{3}H-Flumazenil Saturation Autoradiography in Hippocampal Sclerosis

7.1. Summary

Background: Using FMZ-PET we have shown that reductions of cBZR are restricted to the hippocampus in mTLE due to unilateral HS. Receptor autoradiographic studies on resected hippocampal specimens from the same patients demonstrated loss of cBZR in CA1, over and above loss of neurons.

Rationale: To directly compare *in-vivo* cBZR binding with ^{11}C-FMZ-PET and *ex-vivo* binding using ^{3}H-FMZ autoradiography.

Methods: We applied an MRI based method for partial volume effect correction to the PET images of ^{11}C-FMZ-V_d obtained for 10 patients with refractory mTLE due to unilateral, histologically verified HS. Saturation autoradiography was performed on the hippocampal specimens obtained from the same patients allowing calculation of receptor availability (^{3}H-FMZ-B_{max}).

Results: After correction for partial volume effect ^{11}C-FMZ-V_d in the body of the epileptogenic hippocampus was reduced by a mean of 42.1% compared to normal controls. ^{3}H-FMZ-B_{max}, determined autoradiographically from the same hippocampal tissue, was reduced by a mean of 42.7% compared with control hippocampi. Absolute *in-vivo* and *ex-vivo* measurements of cBZR binding for the body of the hippocampus were significantly correlated in each individual ($r=0.496$, $p=0.023$).

Conclusions: Our study demonstrates that reduction of available cBZR on remaining neurons in HS can be reliably detected *in-vivo* using ^{11}C-FMZ-PET following correction for partial volume effect.

(published in ***Annals of Neurology*** 1998; 43: 618-626)

7.2. Introduction

Autoradiographic and histopathologic studies of temporal lobectomy specimens from mTLE patients have revealed reduced neuronal cell counts and cBZR density in sclerotic areas with further reductions of cBZR density in all subregions of the hippocampal formation (Johnson, 1992; Burdette, 1995). Correlational analysis of autoradiography and quantitative neuropathology in resected sclerotic hippocampi have also revealed a reduction of ^{3}H-FMZ binding over and above that due to reduced neuronal cell density in the CA1 subregion (Hand, 1997). The aim of this study was to directly compare *in-vivo* ^{11}C-FMZ binding and *ex-vivo* ^{3}H-FMZ binding in HS from patients having anterior temporal lobe resections (**Figure 14**).

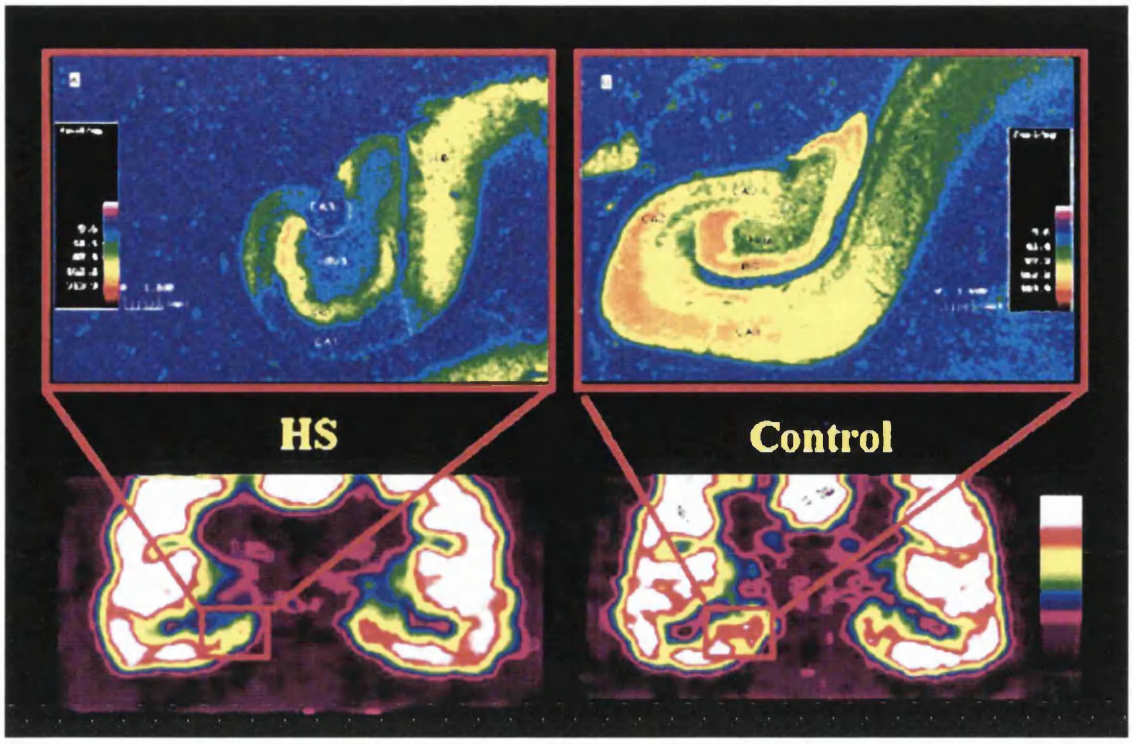

Figure 14: Comparison of *in-vivo* ^{11}C-FMZ-PET and *ex-vivo* ^{3}H-FMZ autoradiography.

Cross-sectional views of the hippocampal body with ^{3}H-FMZ autoradiography (upper row) and coronal views through the hippocampal body with ^{11}C-FMZ PET (lower row) from a patient with HS (left) and a normal control (right). The colourscale in the upper row reflects FMZ B_{max}, in the lower row FMZ-V_d.

7.3. Methods

7.3.1. Subjects

We studied 10 patients (7 female, 3 male) who suffered from drug-resistant mTLE. The median age at onset of habitual epilepsy was 5 years (range: 1-21 years), the median duration of epilepsy prior to PET examination was 24 years (range: 12-46 years) and the median age at PET examination was 33 years (range: 21-48 years). Seven patients had a history of prolonged febrile convulsions in early childhood. The antiepileptic medication was mono- or polytherapy with carbamazepine (9 patients), phenytoin (4), lamotrigine (3), topiramate (2), gabapentin (2) or sodium valproate (1) (**Table 8**). Patients who were treated with benzodiazepines, barbiturates or vigabatrin within two months of the PET examination were not included in the study.

All patients had a clear MRI diagnosis of unilateral HS with unilaterally reduced HCV corrected for ICV, abnormal HCV-AI and / or increased HCT2. Two patients (pat. 1 and 2) had predominantly focal anterior HS with abnormal HCV but normal HCT2.

Fifteen healthy volunteers (13 male, 2 female) with a median age of 30 years (range: 23-54 years), who were taking no medication and had no history of neurological or psychiatric disorder, with normal EEGs and MRI studies, were studied for comparison. Subjects did not consume alcohol within 48 hours preceding the PET scan.

7.3.2. Electroencephalography

All ten patients had prolonged video-EEG recordings with scalp and surface sphenoidal electrodes. Scalp EEGs exhibited clear, strictly unilateral, anterior temporal interictal epileptiform activity consisting of sharp and slow wave complexes in all patients. Seizures were recorded in all patients. Unilateral anterior temporal ictal EEG changes, at or before clinical seizure onset, were recorded in all cases, ipsilateral to the side of HS. One patient (pat. 3) had bilateral independent, temporal interictal epileptiform activity with a lateralised preponderance (ratio left:right: 2:1). Subsequent depth EEG recordings revealed the seizure onset consistently in the right hippocampus; another patient (pat. 4) had bilateral temporal interictal epileptiform activity with a lateralised preponderance (ratios: 5:1), but unilateral ictal onset. (**Table 8**)

7.3.3. Epilepsy surgery, histopathology and outcome

In all cases the histopathologic findings of the removed mesial structures (including hippocampus, part of the amygdala and anterior 3 cm of lateral temporal neocortex) verified the MRI finding of HS. No pathological abnormalities were detected in the resected anterior temporal cortical tissue, apart from an increased density of neurons in the resected white matter in four patients (pat. 4 - 7) (**Table 8**). Median post surgical follow-up was 1 year (range 0.8 to 2 years) and outcome was grade 1A in eight patients according to the Engel classification and two patients (pat. 8 and 9) still experiencing simple partial seizures (auras only).

7.3.4. Quantitative neuropathology

see chapter 3.7. For two specimens (pat. 8 and 10, **Table 8**) it was not possible to obtain density measurements for all subregions in two patients, particularly CA2 and CA3, due to damage during the resection procedure, and adequate neuronal density data were not available for one of the control hippocampi and one of the epilepsy specimens (pat. 1).

Table 8: Clinical and EEG data, quantitative neuropathological findings in 10 patients with refractory TLE

	Age / Sex	PFC	Age of onset (years)	AEDs	EEG (interictal; ictal)	inter CPS /PET (days)	CPS per year	MRI	ND CA1	ND CA2	ND CA3	ND CA4	ND DG	histology
									(neuronal cells x $10^3/mm^3$)					
Normal mean									20.3	30.2	16.4	12.0	482	
Normal range									15.6 - 23.4	25.7 - 38.0	15.6 - 25.9	8.6 - 14.9	295 - 635	
1	31 / F	yes	7	LTG, VPA	R temp ant; R temp ant	24	7	R HS	n.a.	n.a.	n.a.	n.a	n.a	HS
2	31 / F	yes	7	GBP, PHT	R temp; R temp ant	24	3	R HS	2.94	13.30	11.05	4.24	198	HS
3	40 / M	no	5	CBZ, LTG	ind bil temp L>R (2:1)	48	7	as HS	2.58	10.08	3.38	0.65	161	HS
4	33 / F	yes	21	GBP, PHT	R>L (5:1) bil; R temp ant	144	4	R HS	2.96	19.26	3.46	1.48	170	HS+MD
5	38 / M	no	1	CBZ, PHT	L temp ant; L temp ant	14	72	L HS	2.25	20.76	6.42	2.81	170	HS+MD
6	22 / F	no	4	CBZ, LTG	R temp ant; R temp ant	10	24	as HS	3.46	21.24	8.40	6.42	130	HS+MD
7	26 / F	yes	2	CBZ, LTG	R temp ant; R temp ant	5	336	R HS	2.47	16.30	3.95	2.47	220	HS+MD
8	22 / M	yes	5	CBZ	L temp ant; L temp ant	72	3	L HS	1.00.	n.a.	n.a.	n.a.	n.a.	HS
9	40 / F	yes	2	CBZ, TOP	R temp ant; R temp ant	520	2	R HS	1.71	22.61	6.35	1.66	309	HS
10	48 / F	yes	2	CBZ, TOP	L temp ant; L temp ant	48	5	L HS	3.84	n.a.	n.a.	1.34	207	HS

* >2 SD above normal HCT2 or >2 SD below normal HCV

L=left; R=right; AED=Antiepileptic drugs; CBZ=Carbamazepine; LTG=Lamotrigine; PHT=Phenytoin; GBP=Gabapentin; VPA=Sodium Valproate; CPS=complex partial seizure; inter CPS/PET=interval between last CPS and PET scan; temp=temporal; ant=anterior; bil=bilateral; as=asymmetrical; HS=hippocampal sclerosis; MD=micordysgenesis; bil temp L>R (ratio) = bilateral synchronous temporal spikes more on the left than on the right side; ind bil temp L>R (ratio) = independent bilateral temporal spikes more on the left than on the right side; temp = temporal; ant = anterior; bil = bilateral; HS = hippocampal sclerosis; MD = microdysgenesis; ND = neuron cell density; CA = cornu ammonis; DG = dentate gyrus; n.a. = not available

7.3.5. Saturation autoradiography

Temporal neocortex and hippocampi from each patient were resected en bloc and frozen within 10-20 minutes on dry ice, surrounded with Lipshaw embedding matrix and stored at -80°C. Control tissue was obtained at autopsy from patients with no history of neurological disease. The median post mortem interval until autopsy was 17 hours (range 5.5 to 28 hours). The receptor autoradiography protocol used was based upon the methodology published by Houser and colleagues (Houser, 1988). For further details see chapter 3.8.

7.3.6. PET and MRI methodology

PET scans were performed at the MRC Cyclotron Unit at the Hammersmith Hospital on a ECAT 953b scanner (CTI Siemens, Knoxville, TN) which acquires 31 simultaneous slices and has a resolution of 4.8 x 4.8 x 5.2 mm (at FWHM). Scans were performed with axial images obtained along the the long axis of the hippocampus and coronal images orthogonal to it. High specific activity ^{11}C-FMZ tracer (370MBq) was injected intravenously and arterial blood was sampled continuously in order to determine a metabolite-corrected arterial input function. Voxel-by-voxel parametric images of ^{11}C-FMZ-V_d, reflecting binding to cBZR, were produced from the brain uptake and plasma input functions by using spectral analysis.

MR images were obtained for each control subject and patient on a 1T Picker scanner using a gradient echo sequence protocol which generated 128 contiguous 1.3 mm thick sagittal images. These high resolution volume acquisition MRI scans were coregistered with the parametric images of ^{11}C-FMZ-V_d. (see chapters 3.2., 3.3.4., 3.5. and 3.6.)

7.4. Results

7.4.1. ^{11}C-FMZ-V_d for the body of the hippocampus

Control subjects. Mean values of ^{11}C-FMZ-V_d within the body of the hippocampus after partial volume effect correction were 4.23 (SD = 0.5). The normal range of ^{11}C-FMZ-V_d in the hippocampal body was 3.23 to 5.23. (**Table 9**)

Patients with unilateral hippocampal sclerosis. Abnormally low ^{11}C-FMZ binding in the hippocampal body was found unilaterally in seven patients and bilaterally but asymmetrically in two further patients (pat. 6 and 9). One patient (pat. 1) with an MRI diagnosis of unilateral focal anterior HS showed significant asymmetry of ^{11}C-FMZ binding with lower values in the epileptic hippocampal body, but absolute ^{11}C-FMZ-V_d values lay within the normal range (**Table 9**).

Table 9: Comparison of partial volume corrected ^{11}C-FMZ-PET with ^{3}H-FMZ autoradiography

No.	EEG	PVE corrected ^{11}C-FMZ-V_d HC body	reduction (%)	^{3}H-FMZ Autoradiography B_{max} (fmol/mg)	reduction (%)	K_d (nM)
Normal mean		4.23		297.5		1.79
Normal range		3.23 - 5.23		186.3 - 408.2		1.03 - 2.55
		left / right				
1	Right	4.72 / 3.94	6.9	204.5	31.3	0.74*
2	Right	4.80 / 2.64*	37.6	191.2	35.7	1.18
3	Right	3.43 / 1.23*	70.9	102.8*	65.5	1.22
4	Right	5.15 / 2.33*	44.9	158.4*	46.8	1.73
5	Left	2.36* / 4.13	44.2	169.8*	43.1	1.04
6	Right	3.04* / 2.58*	39.1	139.4*	53.1	1.51
7	Right	3.83 / 2.72*	35.7	181.2*	39.1	1.13
8	Left	3.11* / 4.13	26.5	201.8	32.2	1.50
9	Right	2.92* / 1.74*	59.9	181.2*	39.1	0.99*
10	Left	1.86* / 3.89	56.0	175.8*	40.9	1.19

* > 2 standard deviations
PVE = partial volume effect; HC = hippocampus; reduction = percentage reduction compared to the normal control mean; B_{max} = receptor availability; K_d = receptor affinity

7.4.2. ^{3}H-FMZ B_{max} and K_d for the body of the hippocampus

The mean hippocampal B_{max} for the six control subjects was 297.5 fmol/mg (SD: 55.6 fmol/mg) with all control values lying within 2 SD. All individual HS patient values were lower than the controls; seven lay more than 2 SD below the normal control mean. The mean control hippocampal K_d was 1.79 nM (SD: 0.39 nM), all control values lay within 2 SD of the control mean. Individual values of two out of 10 patients (pat. 1 and 9) fell more than 2 SD below the normal control mean.

7.4.3. Correlations between in-vivo ^{11}C-FMZ-V_d and ex-vivo ^{3}H-FMZ-B_{max}

^{11}C-FMZ-V_d, corrected for partial volume effect, was reduced in the body of the hippocampus of the patients compared to controls by a mean of 42.1% (SD: 18%; $p<0.0001$). Mean B_{max} for FMZ in the mid hippocampal body of the patients was reduced by 42.7% compared with six controls ($p<0.0001$). Individual absolute ^{11}C-FMZ-V_d for the body of the hippocampus measured *in-vivo* for the patients was highly correlated with B_{max} for FMZ at that section of the body of the hippocampus measured *ex-vivo* ($r=0.496$, $p=0.023$) (**Figure 15**).

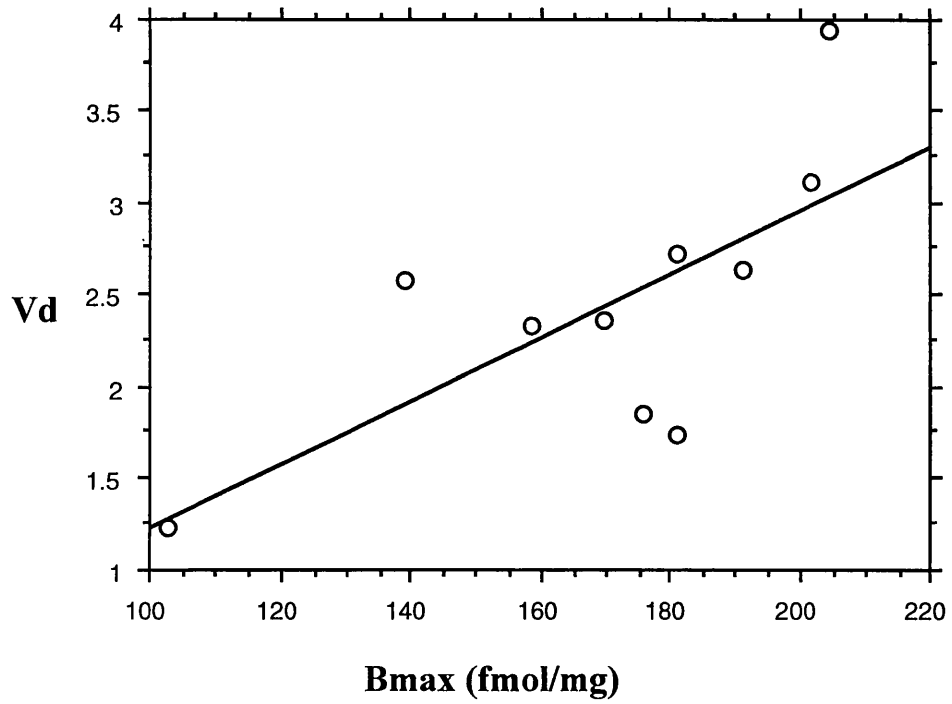

Figure 15: Correlation of absolute ^{11}C-FMZ-V_d and ^{3}H-FMZ B_{max} for the body of the hippocampus.

7.4.4. Correlations between in-vivo ^{11}C-FMZ-V_d and neuronal densities

There was no correlation between individual patient ^{11}C-FMZ-V_d values for the body of the hippocampus and neuronal densities in the hippocampal CA1 ($r = 0.25$, $p = 0.17$) or other subregions.

7.5. Discussion

The main finding of this study was that *in-vivo* ^{11}C-FMZ PET measurements of hippocampal cBZR binding, when corrected for partial volume effects, were highly correlated with *ex-vivo* ^{3}H-FMZ autoradiographical findings in patients with mTLE and histologically verified HS. Hippocampal ^{11}C-FMZ-V_d *in-vivo* was reduced by a mean 42.1% in the body of the sclerosed hippocampi, over and above hippocampal volume loss, compared with a mean 42.7% reduction of ^{3}H-FMZ B_{max} *ex-vivo* in hippocampal slices taken from the same part of this structure.

7.5.1. Methodological considerations

We developed a new, algebraically more rigorous correction method based on linear least squares, which allows measurement of true activity concentration within multiple VOIs of any size and shape independent of the activity concentration within each VOI (Labbé, 1997). Using this new method we have previously shown regional changes of cBZR binding along the length of the hippocampus with higher binding in the middle compared with the anterior or posterior portions in normal subjects (Koepp, 1997b). Using this technique, one third of patients with an MRI diagnosis of unilateral HS showed additional reductions of cBZR binding in the contralateral anterior hippocampus concordant with the results of previous pathology studies (Margerison, 1966). In the current study we replicated these findings by detecting bilateral abnormalities in the body of the hippocampus in two out of 10, highly selected patients with mTLE. Five of the 10 patients with unilateral HS defined on MRI in the current study were included in a comparison group in a study evaluating bilateral HS with ^{11}C-FMZ PET (Koepp, 1997b).

As the distribution of cBZR binding varies throughout the length of the hippocampus our new method was of particular importance as it allowed comparisons of *in-vivo* measurements of cBZR binding in the hippocampus at the same location as in *ex-vivo* specimens. For our correlational analysis we chose the middle third of the hippocampus as our PET VOI (about 10mm thick), which incorporates the 10μm thick slices of the hippocampal body used for autoradiographic analysis. The mean reduction of cBZR binding for our group of HS patients compared with controls was similar *in-vivo* and *ex-vivo*, however both data sets showed a considerable coefficient of variation. This was partly due to partial volume effect corrections increasing the variance in functional data, but reducing the bias due to structural volume changes.

A number of limitations in the use of human tissue for B_{max} measurements must be considered when interpreting these results, particularly concerning the control tissue. It is not possible to be sure about the influence of factors such as age and post-mortem interval upon the parameters we measured. Although Burdette et al (Burdette, 1995) detected a trend towards increased muscimol binding with post-mortem delay, suggestive of post-mortem increased ambient GABA concentration, others have reported no influence of post-mortem delay, age or gender on ^{3}H-GABA membrane binding (Lloyd, 1979) or ^{3}H-flunitrazepam binding (Zezula, 1988) in human brain. In our previous quantitative neuropathology and autoradiography study, hippocampal subregions were outlined on coronal sections and B_{max} and K_d values obtained for each subregion. These subregions are beyond the resolution of PET and so in this study we estimated B_{max} values for the whole hippocampal cross-section, sampling areas similar in size to the hippocampal body PET outlined on *in-vivo* MR images.

Inevitably, control data for PET and autoradiographic studies come from different individuals and no autoradiographic data for the contralateral hippocampus was available, from either the patients or the controls. We, therefore, calculated the percentage reduction of the patient data compared to the normal control mean and found almost identical reductions for both *in-vivo* and *ex-vivo* measurements. The influence of chronic medication on receptor binding and affinity must also be considered when interpreting data obtained from human studies.

Although the patients selected for this study were receiving chronic anti-epileptic medication not thought to act at the cBZR complex, it is possible that cBZR density and / or affinity may have been affected indirectly by the anti-epileptic actions of these drugs. However, FMZ-B_{max} and K_d are reported to be unaffected by the presence of GABA agonists and allosteric modulators at the $GABA_A$ complex (Möhler, 1981). Low non-specific binding, lack of sensitivity to modulation by endogenous GABA and selectivity for neuronal cBZR make ^{3}H-FMZ an extremely useful and appropriate ligand for receptor autoradiography studies of this type.

Our *in-vivo* PET measurements could also be affected by changes in endozepine binding to the cBZR, thereby reducing the number of available receptors, and which would not affect autoradiography of cBZR. As reductions in cBZR measured with PET and autoradiography were the same, however, we do not infer endozepin binding to have a major effect on *in-vivo* measurements. We only performed a single PET scan and so could not determine B_{max} and K_d separately but only their ratio. Previous studies of ^{11}C-FMZ PET have shown reductions of B_{max} but no change in K_d (Savic, 1994; Prevett, 1995b). As Flumazenil has negligible non-specific binding, FMZ-V_d is closely related to B_{max} / K_d. Despite these methodological limitations we were able to validate our PET findings using autoradiography. Our results illustrate the importance of and validated the applicability of partial volume effect correction when assessing small structures such as sclerotic hippocampi, with PET.

7.5.2. Pathophysiological considerations

The underlying pathological basis of reduced ^{11}C-FMZ binding in HS is still under study. *In-vitro* autoradiographic and histopathologic studies of temporal lobectomy specimens from TLE patients show diminished number of receptors per neuron in CA_1, as well as neuron loss. Although changes in cell densities correlate with alteration in cBZR subtypes in specimens from patients with mTLE, the percent receptor changes are always of greater magnitude than those of cell densities (Johnson, 1992). McDonald *et al.* (1991) found reduced $GABA_A$ and cBZR binding in CA_1 and CA_4 of the hippocampal formation in patients with TLE. Burdette *et al.* (1995) reported a

significant correlation between loss of neurons and autoradiographic findings of cBZR binding in hippocampi from 11 patients with mTLE treated surgically and suggested that neuron loss was the predominant cause of reduced ^{11}C-FMZ binding in the hippocampus *in-vivo*. We found a trend towards a correlation of ^{11}C-FMZ-V_d with neuronal density in the CA_1 subregion, but not in other hippocampal subregions. In our autoradiographic study we concluded that cBZR density was reduced over and above neuronal loss in the CA_1 region in HS associated with TLE (Hand, 1997).

Reduced cBZR density on surviving neurons in the CA_1 region in particular, may indicate a functional deficit of GABAergic inhibitory transmission in the hippocampus of patients with mTLE. Immunocytochemical studies have demonstrated preservation of GAD-immunoreactive neurons in TLE despite significant losses of other cell types (Babb, 1989). It has been proposed that these preserved inhibitory GABAergic basket cells are deprived of their excitatory input due to the loss of hilar mossy cells and CA_3 pyramidal neurons associated with HS, thus rendering them dormant and ineffective in preventing seizure propagation (Sloviter, 1994). However, the issue of whether a preceding pathological change in hippocampal neurotransmission, such as a functional deficit of GABAergic inhibition at the post-synaptic level, may result in the initial loss of the GABAergic basket cell excitatory input neurons, is currently unresolved.

It is also unclear at present whether the changes in cBZR binding seen in HS are a cause or consequence of epileptogenesis. Long lasting changes in the expression of mRNA for various subunits of the $GABA_A$ receptor have been demonstrated in the kindling model of TLE (Kamphuis, 1995) and a loss of the $GABA_A$ $\alpha 1$ subunit has been demonstrated immunohistochemically in epileptic human hippocampus, although this has been proposed to occur as a result of neuronal loss (Wolf, 1994). Using a combination of single cell patch-clamp and mRNA amplification techniques Brooks-Kayal *et al.* (Brooks-Kayal, 1998) described a decrease in $\alpha 1$ and $\beta 1$ subunits relative to other α and β subunits and an increase in δ and ε subunits weeks before the animals demonstrated spontaneous seizure activity. However, $GABA_A$ receptors increased much later, after spontaneous seizures have occurred. From the timing of these changes, one might view the later increase in $GABA_A$ receptors as a compensatory reaction to the high level of excitation associated with the seizures, but not as a seizure mechanism itself. This altered subunit configuration of the $GABA_A$ receptor in surviving hippocampal neurons might also reflect the 60% decrease in ^{3}H-FMZ K_d, which we found in the dentate gyrus of our temporal lobe specimens (Hand, 1997).

Chapter VIII ^{11}C-flumazenil PET in Idiopathic Generalised Epilepsy

8.1. Summary

Background: Previous ^{11}C-FMZ PET investigations in patients with IGE have found either non-significant global cortical decreases in cBZR binding, or focal decreases in the thalamus and increases in the cerebellar nuclei with no changes in cerebral cortex. Lower ^{11}C-FMZ binding in cerebral cortex has been reported in IGE patients treated with VPA compared with controls.
Rationale: Using high resolution 3D ^{11}C-FMZ PET studies in a large number of subjects, to detect differences in cBZR between IGE patients and controls and, using a powerful longitudinal design, to determine the functional effect of VPA.
Methods: Comparison of parametric images of ^{11}C-FMZ-V_d in 10 IGE patients, before and after the addition of VPA, and in 20 normal subjects.
Results: Mean ^{11}C-FMZ-V_d was significantly higher in the cerebral cortex (11%; p=0.009), thalamus (14%; p=0.018) and cerebellum (15%; p=0.027) of the 10 IGE patients compared with 20 normal controls. No significant areas of focal abnormality of ^{11}C-FMZ-V_d were detected using SPM. The addition of VPA was not associated with a significant change of mean ^{11}C-FMZ-V_d in any brain area.
Conclusions: Our finding of an increased ^{11}C-FMZ-V_d in IGE could reflect microdysgenesis or a state of cortical hyperexcitability. Our data suggest that short-term VPA therapy does not affect the number of available cBZR in patients with IGE.
(published in ***Epilepsia*** 1997; 38: 1089-1097)

8.2. Introduction

In contrast to the effects of GABAergic drugs in localisation-related epilepsy, GABA agonists enhance spike-wave activity in IGE at the thalamic level (Peters, 1989), while GABA antagonists at this site reduce the occurrence of spike-wave discharges. Savic *et al.* (Savic, 1990) found a non significant 15% reduction of ^{11}C-FMZ binding in cerebral cortex in a heterogeneous group of patients with generalised seizures who were receiving anti-epileptic medication but not VPA. The same authors subsequently reported no changes in cBZR density in the cerebral and cerebellar cortex, but increased cBZR density in the cerebellar nuclei and decreases in the thalamus (Savic, 1994). In a recent cross-sectional study a mean 9% reduction of ^{11}C-FMZ-V_d was found in patients with CAE and JAE receiving VPA, while patients not on VPA showed a non-

significant trend towards increased ^{11}C-FMZ binding in the occipital and parietal lobe (Prevett, 1995a).

VPA is the treatment of choice in most IGE. The mode of action of clinically effective doses of VPA is uncertain. It has been reported to increase CSF GABA levels in animals at high doses but not at doses normally given in humans (Johnston, 1984). Löscher and Siemes (Löscher, 1984), however, found significantly increased CSF GABA levels in children with epilepsy treated with VPA compared to children treated with other drugs and normal controls. VPA has also been reported to have anticonvulsant activity without any measurable increase in GABA levels (Kerwin, 1981).

A limitation of the methodology of previous investigations using ^{11}C-FMZ PET is that detection of abnormalities has relied upon a priori ROI-analysis and so has been susceptible to observer bias. It is also questionable how reliably small structures, such as cerebellar nuclei, can be identified with PET. We used an entirely objective method, gaussian clustering, to define region boundaries so as to determine interindividual and, in paired scans, intraindividual differences of ^{11}C-FMZ binding in cerebral cortex, cerebellum and thalamus. In addition we used SPM to detect focal changes, either increases or decreases of ^{11}C-FMZ binding, in cortical and subcortical structures. Using a more sensitive scanning technique (3D acquisition) and a more objective analytical methodology than was previously available to us, the aim of this study was first to determine whether cBZR binding is normal in patients with IGE and secondly to determine the effect of VPA on this binding in a longitudinal design.

8.3. Methods

8.3.1. Subjects

We studied 10 patients (8 male, 2 female) who were recruited from the epilepsy clinics of the National Hospital for Neurology and Neurosurgery, Queen Square, London (**Table 10**). All patients suffered from absences and GTCS, six of them from myoclonic jerks. The epilepsy syndromes were classified according to the 1989 International Classification of Epilepsies. Five patients were diagnosed as having JME, three as JAE and two as CAE. MRI scanning did not show any abnormalities. The median age at onset of habitual epilepsy was 14 years (range: 3-17 years), the median duration of illness prior to PET examination was 18 years (range: 8-43 years) and the median age at PET examination was 30 years (range: 21-58 years). The anti epileptic medication at the time of the first PET scan was in eight patients mono- or polytherapy of carbamazepine (6 patients), lamotrigine (1), phenytoin (1) and gabapentin (1).

Table 10: Clinical data of 10 patients with IGE

No.	age / gender	seizure type / age of onset (years)	estimated number of absences per month	Syndrome	AEDs (mg/day) at 1st scan	VPA dosage (mg/day)/ VPA level (µmol/l) at 2nd scan	scan interval (weeks)	seizures on VPA (frequency per month)
1	30/M	ABS/14, GTCS/14	16	JAE	CBZ/800	2000 / 327	6	ABS (8)
2	23/F	ABS/12, GTCS/14, MJ/14	1	JME	CBZ/800	800 / 447	8	ABS (1)
3	58/M	ABS/15, GTCS/33	1	JAE	no	1000 / 277	9	no
4	23/M	ABS/10, MJ/10, GTCS/13	4	JME	CBZ/800	1000 / 321	13	no
5	30/M	ABS/3, GTCS/15	20	CAE	no	500 / 256	12	ABS (8),1 GTCS
6	25/M	ABS/15, GTCS/16, MJ/16	3	JME	CBZ/1600	1500 / 227	16	ABS (1)
7	21/F	ABS/6, GTCS/18, MJ/20	30	CAE	CBZ/1400, LTG/400	1000 / 342	15	no
8	39/M	ABS/14, GTCS/14, MJ/16	3	JME	CBZ/1600	1500 / 312	16	ABS (1), 1 GTCS
9	37/M	ABS/17, GTCS/17	1	JAE	PHT/400	1000 / 321	18	no
10	33/M	ABS/15, GTCS/15, MJ/15	30	JME	GBP/900	1000 / 296	24	ABS (12)

F = female, M = male, ABS = absence, MJ = myoclonic jerks, GTCS = generalised tonic clonic seizure, JME = juvenile myoclonic epilepsy, JAE = juvenile absence epilepsy, CAE = childhood absence epilepsy, AED = antiepileptic drugs, CBZ = carbamazepine, LTG = lamotrigine, PHT = phenytoin, GBP = gabapentin, VPA = sodium valproate

One patient had never been treated with AED before and another patient had not had any AED for the six months prior to his first FMZ PET scan. Treatment with VPA was started immediately after the first PET scan and a second scan was performed after they had taken VPA for a minimum of six weeks (VPA dose: 500-2000mg; scan interval: 6 - 24 weeks). Concomitant medication was kept unchanged during this period. Twenty normal subjects of similar age (median: 32 years; range: 23-61 years) who had no evidence of neurological disorder and were on no medication were also studied. Patients or normal volunteers who had received benzodiazepines or barbiturates within two months prior to the PET examination were not included in the study. No subject consumed alcohol within the 48 hours preceding the PET scan.

8.3.2. PET methodology

PET scans were performed at the MRC Cyclotron Unit at the Hammersmith Hospital on a ECAT 953b scanner (CTI Siemens, Knoxville, TN) which acquires 31 simultaneous slices and has a resolution of 4.8 x 4.8 x 5.2 mm (at FWHM). Subjects were positioned with the glabella-inion line parallel to the detector rings so that the directly obtained transaxial images were parallel to the intercommissural line (AC-PC line). Correct positioning of the patient in the scanner was verified with a two minute transmission scan. High specific activity ^{11}C-FMZ tracer (370MBq) was injected intravenously and arterial blood was sampled continuously in order to determine a metabolite-corrected arterial input function. Voxel-by-voxel parametric images of ^{11}C-FMZ-V_d, reflecting binding to cBZR, were produced from the brain uptake and plasma input functions by using spectral analysis. (see chapter 3.2.1.2 and 3.3.4.)

We determined whether there were global differences of ^{11}C-FMZ binding in the cortex, thalamus and cerebellum between control subjects and patients before and after starting VPA. ROI were defined with gaussian clustering using the multi-spectral voxel classification feature of Analyze^{TM} version 7.5. (see chapter 3.4.3., figure 11). Mean values for FMZ-V_d of the cerebral cortex, thalamic and cerebellar voxels were calculated from the FM-V_d image. The efficacy of the segmentation was assessed by comparing the numbers of voxels allocated to each cluster inter-individually between patients and controls, and intra-individually before and after treatment with VPA.

8.3.3. Statistical analysis

Two-tailed analysis of variance (ANOVA) was used to assess group differences of mean FMZ-V_d and to assess the effect of VPA in pairs of ^{11}C-FMZ PET scans in patients with IGE. A regression analysis was performed to examine if there was a relationship between subject's age, age of onset of habitual epilepsy, treatment

response, VPA serum concentration, scan interval and FM-V_d. Amount of spike-wave activity on EEG recorded during PET scanning was compared using Wilcoxon Test. SPM was used to identify focal areas of ^{11}C-FMZ binding that were significantly different in the patients compared with controls (see chapter 3.5.).

8.4. Results

Ten patients with IGE had a first ^{11}C-FMZ PET scan before additional treatment with VPA was started and a second scan after they had been taking VPA for at least 6 weeks. The patients' clinical data, seizure types, drug treatment and treatment response are summarised in **Table 11**.

Table 11: Comparison of mean FMZ-V_d in 10 patients with IGE before and after taking VPA, comprising 5 patients with JME and 5 patients with CAE or JAE, versus 20 normal controls

Region group (N)	mean FMZ-V_d (SD) before VPA	mean FMZ-V_d (SD) after VPA	Δ % FMZ-V_d (SD) after / before VPA
Cerebral Cortex:			
IGE total (10)	*4.79 (0.39)	4.84 (0.49)	+ 1.0 (6.1)
JME (5)	4.73 (0.32)	4.65 (0.11)	- 1.7 (6.2)
CAE/JAE (5)	4.85 (0.49)	5.04 (0.67)	+ 3.9 (5.2)
Controls (20)	4.33 (0.28)		
Thalamus:			
IGE (10)	•2.50 (0.40)	2.65 (0.41)	+ 6.0 (12.6)
JME (5)	2.37 (0.34)	2.51 (0.19)	+ 5.9 (12.1)
CAE/JAE (5)	2.62 (0.46)	2.79 (0.53)	+ 6.5 (16.5)
Controls (20)	2.19 (0.26)		
Cerebellum:			
IGE (10)	+4.16 (0.78)	4.17 (0.77)	+ 0.02 (10.2)
JME (5)	4.02 (0.76)	3.79 (0.65)	- 5.6 (5.8)
CAE/JAE (5)	4.30 (0.87)	4.56 (0.73)	+ 6.0 (10.3)
Controls (15)	3.63 (0.32)		
White matter:			
IGE (10)	0.82 (0.11)	0.85 (0.11)	+ 5.18 (18.2)
Controls (20)	0.78 (0.11)		

IGE versus normal controls: * p=0.009; • p=0.018; + p=0.027

FMZ-V_d = Flumazenil volume of distribution; SD = standard deviation; Δ = difference; IGE = idiopathic generalised epilpesy; JME = juvenile myoclonic epilepsy; CAE = childhood absence epilepsy; JAE = juvenile absence epilepsy

Generalised spike wave activity occupied less than 1% of the EEG recordings during scanning period in all patients except one (pat. 1) whose EEG recordings showed very frequent irregular spike wave activity (first scan: 33%, second scan: 40%). There was a non-significant difference between amount of spike-wave discharges before and after addition of VPA. Four patients had been completely seizure free at the time of the second scan for more than 4 weeks. Absences still occurred in the remaining six patients, albeit much reduced in frequency. Two patients had a single GTCS more than two weeks prior to their second scan. Mean plasma concentration for VPA was 312 µmol/l at the time of the second scan.

8.4.1. Patients with IGE versus normal controls

^{11}C-FMZ-V_d reflecting cBZR availability was significantly higher in the cerebral cortex (Δ difference = 11%; p = 0.009), thalamus (14%; p=0.018) and cerebellum (15%; p=0.027) in patients with IGE compared with control subjects with no significant differences in ^{11}C-FMZ binding within white matter (**Table 11**). The number of voxels allocated to each ROI was not significantly different between patients and controls (within 4.9% for cortex, 2.5% for thalamus, and 3.7% for cerebellar cortex). Subgroup analysis within each of the three anatomical regions also showed significant increases of ^{11}C-FMZ-V_d comparing each patient subgroup with controls except for JME patients versus controls within the thalamus. Comparing the five patients with JME with the 20 control subjects using SPM, accentuated focal increases bilaterally in the dorsolateral prefrontal cortex (DLPFC) and ventral premotor area (**Figure 16**).

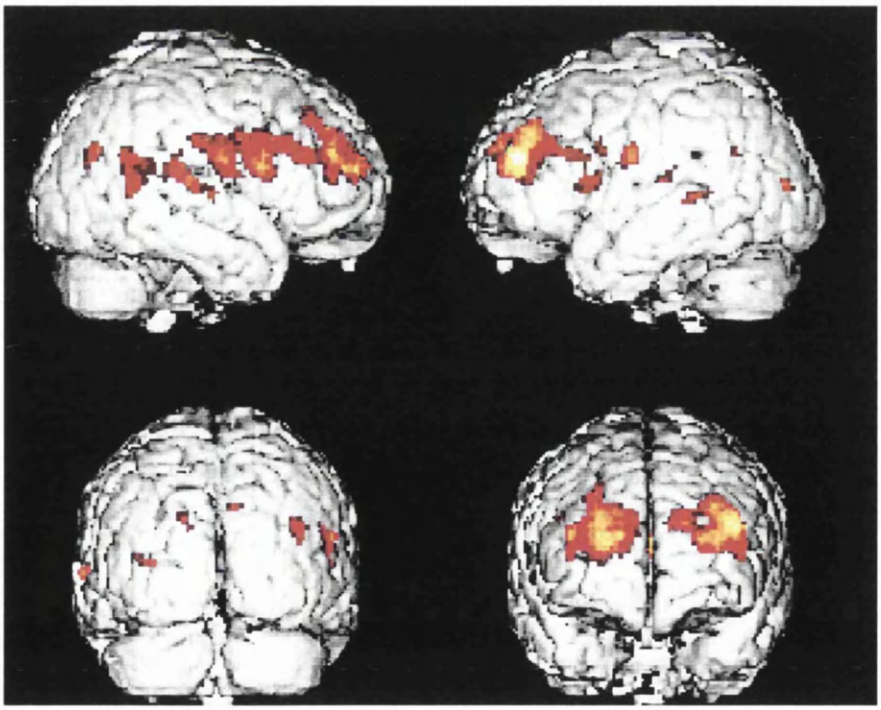

Figure 16: Comparison of five patients with JME versus 20 controls using SPM

These focal accentuations were not seen when comparing the 5 remaining IGE patients with 20 controls. None of the covariates of interest: age of onset of habitual epilepsy, treatment response, VPA serum concentration, and scan interval had any effect on ^{11}C-FMZ-V_d.

8.4.2. Patients with IGE before VPA versus after VPA

Comparison of each patient with IGE before and after taking VPA using the ROI based analysis showed that mean ^{11}C-FMZ-V_d was non-significantly increased by 6 % in the thalamus with no change in the cerebral and cerebellar cortex (**Table 11**). The ROIs segmented by gaussian clustering were essentially identical in size before and after VPA treatment. There was no significant region by time interaction. Patients with JME were not different in their response to VPA treatment than the other patients with IGE (**Figure 17**).

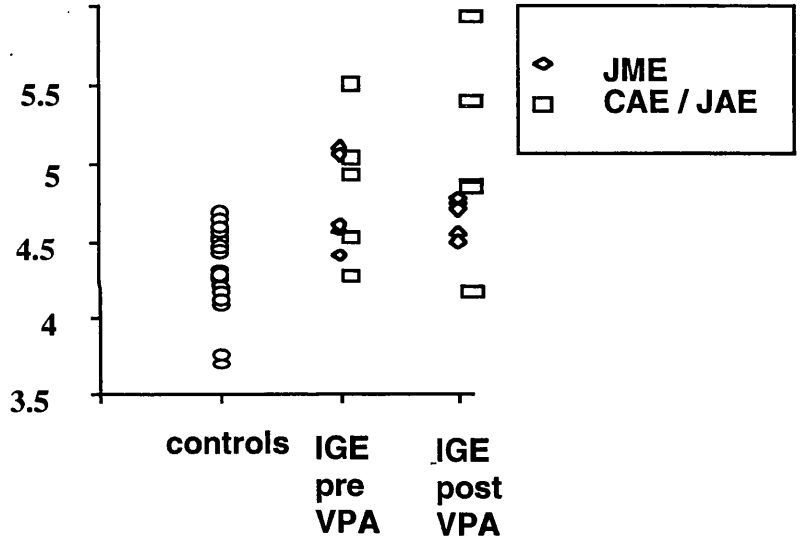

Figure 17: ^{11}C-FMZ-V_d in cerebral cortex of 20 controls compared with 10 patients with IGE before and after treatment with VPA

There were no relationships between patients' age, age at onset of habitual epilepsy, and ^{11}C-FMZ binding. The change in ^{11}C-FMZ-V_d between the two scans were unrelated to the serum concentration, duration or treatment response of VPA therapy, or the interval between scans.

8.5. Discussion

The main finding of this study was that binding of ^{11}C-FMZ to cBZR in 10 patients with IGE not treated with VPA was significantly higher in cerebral cortex, thalamus and cerebellum by 11% to 15%, compared to 20 normal subjects. Our finding is in

contrast to previous reports (Savic, 1990; Savic, 1994; Prevett, 1995a) describing either a reduction or no change of cBZR in IGE. Savic *et al.* (Savic, 1990) studied a heterogeneous group of patients with generalised seizures and used non-pathological areas in patients with focal epilepsy as a control. In a recent study using a computerised anatomical brain atlas no significant changes of ^{11}C-FMZ binding were found in the cerebral cortex of eight patients with IGE in comparison to eight normal subjects, but binding was significantly increased in the cerebellar nuclei and decreased in the thalamus (Savic, 1994). Prevett *et al.* found a tendency towards increased ^{11}C-FMZ binding in the occipital lobe and thalamus when comparing eight patients with eight normal controls using a template of 155 regions of interest (Prevett, 1995a).

8.5.1. Methodological considerations

A number of methodological issues are of importance to explain discrepancies of results between this study and previous reports. All our scans were acquired in 3D, which is about six times more sensitive than the usual 2D acquisition (Spinks, 1991). The numbers of patient and control scans in our study were bigger than in any previous investigation. Furthermore we used entirely objective methods of data analysis, with ROI defined by gaussian clustering, to assess global differences in FMZ-V_d, and SPM for focal changes.

Gaussian clustering is well established for segmentation of MR images using T1 and T2 weighted images. This is the first time this method has been applied to ROI analysis of PET data and has several advantages over standard ROI analysis (Henry, 1990), be it a template or anatomically configured. Gaussian clustering avoids any observer-bias during ROI placement. Threshold-defined, anatomically configured ROIs skew the results, depending on the threshold chosen. Gaussian clustering takes into account individual anatomical differences and minimises partial volume effects by excluding white matter. The efficacy of our segmentation is underlined by the essentially identical size of ROIs before and after VPA treatment.

We measured ^{11}C-FMZ-V_d without using a reference region and found a globally increased FMZ-V_d in 10 patients with IGE compared to 20 normal subjects. In contrast, Savic *et al.* (Savic, 1994) reported no differences of ^{11}C-FMZ binding in the cerebral cortex between eight patients and eight controls. They used white matter as a reference region, assuming that this area is devoid of cBZR. As there is a small degree of specific binding of ^{11}C-FMZ to white matter, which was about 5% higher in our patients compared to controls, this may have led to an underestimate of patients' values in the Savic et al. study and could explain the differences seen in cortical mean ^{11}C-FMZ-V_d between that and the current investigation.

We cannot comment in our study on any changes in the deep cerebellar nuclei as have been reported previously (Savic, 1994), as they were not reliably identifiable in all our scans. SPM detected significant global increases of ^{11}C-FMZ-V_d in the cerebellum including the cerebellar nuclei, but did not reveal any additional focal cortical or subcortical abnormalities in any structure. Conclusions drawn from this part of the analysis, however, are limited due to significant differences in global means between the groups of patients and normal controls. Our patients had a relative, but not significantly, lower ^{11}C-FMZ-V_d in the thalamus before compared to after starting on VPA treatment, which is similar to the pattern of reduced ^{11}C-FMZ binding in the thalamus described previously (Savic, 1994).

All the patients in our study had CAE, JAE or JME. No differences were observed between patients with JME and CAE/JAE. However, the number of patients investigated within each patient group was too small for meaningful statistical analysis. The only feature that might be considered unusual about these patients was the persistence of seizures into adulthood. The results of this study therefore may not necessarily be applicable to children in whom seizures subsequently remit.

The differences in methodology and patient selection might partly explain the differences found in contrast to previous studies. Other factors, however, such as different age, treatment with AED and epileptic seizures itself need consideration. Patients with IGE and normal volunteers were well matched for age. Regression analysis showed no effect of age on cBZR density, either in the whole group of 30 subjects or in analysis of patient subgroups. ^{11}C-FMZ-V_d was significantly reduced only in the area of hippocampal sclerosis (see chapter IV). The lack of differences of ^{11}C-FMZ-V_d in the cerebral neocortex, thalamus and cerebellum between patients with mTLE and normal subjects suggest that partial and secondary generalised seizures and AEDs do not affect cBZR density in these structures, and that the findings of our present study relate to the pathophysiology of IGE.

In the current study one patient was treated with GBP which can increase cerebral GABA concentrations (Petroff, 1996). Treatment with GBP, therefore, theoretically could affect global $GABA_A$/cBZR density due to increased cerebral GABA concentrations in these four patients. ^{11}C-FMZ-V_d in the cerebral cortex, thalamus and cerebellum of this patient taking GBP, however, was not significant different from the other patients indicating that this drug did not affect cBZR. The input function used for spectral analysis was the time course of the total plasma tracer in plasma after correction for radiolabelled metabolites. The free fraction of FMZ (i.e. FMZ not bound to plasma protein) was not determined. Theoretically differences in this free fraction between patients and controls due to anticonvulsant therapy could therefore contribute

to the observed global differences between IGE patients and controls in the V_d of ^{11}C-FMZ in the tissue. However the lack of differences between controls and mTLE patients, who were also on anticonvulsant therapy, would argue against this explanation.

Treatment with VPA did not change ^{11}C-FMZ binding, neither did the concomitant reduction in seizures. The duration of VPA treatment, however, was relatively short (median duration 3 months) and only 40% of patients were completely seizure free at the time of the second scan. These differences in duration of and response to VPA treatment might be of importance to explain, why we could not repeat our previous findings of reduced ^{11}C-FMZ-V_d binding on VPA treatment. However, we re-scanned three patients one year after the second ^{11}C-FMZ PET scan with no change between the second and third scan in those three patients.

8.5.2. Pathophysiological considerations

^{11}C-FMZ-V_d is a combined measure of specific and non-specific binding and proportional to cBZR density (B_{max}) / receptor affinity (K_d). A change of specific binding will therefore result in a proportionally smaller change in V_d than in B_{max}. No previous studies have found a change in FMZ-K_d in studies of patients, making this a very unlikely explanation for the results.

Structural imaging is usually normal in IGE and was so in all our cases. More sophisticated, quantitative MRI analysis, as reported recently in a different group of IGE patients (Woermann, 1998a), has not been performed in our patients. Woermann *et al.* found increased cortical grey matter volumes in patients with various IGE syndromes, and those increases could have contributed to the observed increase of FMZ binding. Regional abnormalities of cortical grey matter volumes were mainly detected in medial frontal areas (Woermann, 1998b), whereas regional accentuations of increased FMZ-V_d were detected in the DLPFC bilaterally using the same technique of SPM. In view of these recent structural findings, future studies need to compare directly structural MRI and functional PET informations with the possibility of correcting PET data for partial volume effects.

Our finding of an increased cBZR density in cerebral cortex, thalamus and cerebellum in IGE is of great interest in comparison with pathological reports of microdysgenesis in JME. Meencke and Janz (Meencke, 1984) reported that 14 of 15 patients with IGE had evidence of abnormal neuronal migration with an increase in dystopic neurons in the stratum moleculare, white matter, hippocampus and cerebellar cortex. Quantification of these changes has been difficult and these findings have been

criticised (Lyon, 1985). However, although these changes can be seen in normal subjects, they were reported to be more severe and more frequent in patients with IGE than in control subjects (Meencke, 1985b). Meencke (Meencke, 1985a) found that neuron density of layer 1 in the frontal lobe in IGE patients was significantly increased compared with age-matched subjects. ^{11}C-FMZ acts as a marker of cBZ / $GABA_A$ receptor bearing neurons and therefore the observed increase of available cBZR in patients with IGE may reflect increased neuronal density.

A further theoretical possibility is that increased ^{11}C-FMZ binding may reflect decreased cBZR occupancy by endogenous ligands. There is evidence from animal experiments and in-vitro studies for endogenous benzodiazepine-like substances (endozepines) (Rothstein, 1992) implying that such compounds have a role in the neurochemical regulation of behaviour (Nutt, 1990). Endozepines may have a modulatory role in the pathophysiology of seizures. Release of endozepines has been very difficult to study non-invasively. However, in an investigation of changes of ^{11}C-FMZ binding during and after hyperventilation induced absences we did not find direct evidence for release of endozepines (Prevett, 1995b). Cerebral binding of ^{11}C-FMZ, was not affected by flurries of absences in any area of neocortex or the thalamus implying that binding to this part of the $GABA_A$-BZR was not involved in the pathophysiology of absences. It is not possible to be certain at present, whether the observed increase of cBZ / $GABA_A$ receptors is due to an increase in neuronal density, is part of a functional pathogenic process underlying IGE, or is a secondary, adaptive phenomenon. Correlative quantitative neuropathology and autoradiographic studies based on autopsy material are needed to resolve this issue.

Our additional finding in patients with JME of accentuated focal increases bilaterally in the dorsolateral prefrontal cortex (DLPFC) and ventral premotor area is of special interest in view of recent neuropsychological reports. These bi-frontal changes could be the pathological substrate for the anecdotally reported behavioural disturbances in JME, which are reminiscent of a frontal lobe personality with emotional instability, lack of discipline and a tendency to jump from one place to another (Janz, 1969). These findings of abnormalities within the GABAergic system are very similar in location to the changes found in a recent ^{18}F-FDG PET study (Swartz, 1997). The authors examined relative regional changes in FDG uptake during a visual working memory paradigm in patients with JME. At rest, JME patients and controls could be discriminated by changes in the ventral premotor area with relative decreases of glucose metabolism in JME patients. The working memory task appeared to enhance and expand these differences between the controls and JME patients in the premotor and prefrontal areas. In the JME patients, unlike control subjects, increased activity was not found during the working memory task in the DLPFC with the ventral premotor area

being highly associated. Together these two PET studies suggest that patients with JME may suffer from cortical functional disorganisation that affects both the epileptogenic potential and cognitive frontal lobe functioning.

8.5.3. Effect of sodium valproate

Our longitudinal study suggested that VPA does not have a significant direct effect on the numbers of cBZR available for binding. Our finding of a 1% increase in the cerebral cortex, 5% increase in the white matter and 6% increase in the thalamus after treatment with VPA lies within the range of inter scan variability (mean 5%).

We did not confirm our initial hypothesis that treatment with VPA would be associated with a down-regulation of cBZR. In a previous cross-sectional study, Prevett et al. (Prevett, 1995a) showed a significant 9% decrease of cerebral ^{11}C-FMZ-V_d in patients taking VPA compared to controls and patients not taking VPA, using a template of geometric ROIs. The longitudinal design of the current study and methodological advances, however, are more powerful to determine an effect of VPA treatment on the amount of available cBZR. VPA is effective in reducing or blocking spontaneous thalamo-cortical oscillations. The exact mode of action of VPA remains uncertain. Although VPA is a weak GABA transaminase inhibitor, it may predominantly act independently from postsynaptic GABA receptors (Johnston, 1984), for example to reduce T-currents in primary afferent neurons (Kelly, 1990).

Chapter IX ^{11}C-Diprenorphine PET in Reading Epilepsy

9.1. Summary

Background: Animal studies implicate endogenous release of opioid peptides as a mechanism for terminating partial and generalised seizures.
Rationale: To localise dynamic changes of opioid neurotransmission during partial seizures and higher cognitive functions
Methods: Three male and two female patients who had primary RE with seizures selectively induced by reading, and six male volunteers, received two ^{11}C-diprenorphine (DPN) PET scans to detect reduced DPN binding to opioid receptors during reading induced seizures. Using SPM we compared the differences between reading induced seizures and rest in patients with RE, taking the physiological effects of reading on the DPN binding in healthy volunteers into account.
Findings: DPN binding to opioid receptors was significantly reduced ($Z=5.22$, $P < 0.001$) in the left parieto-temporo-occipital cortex (Brodman Area (BA) 37) in RE patients during and following reading-induced partial seizures compared to healthy volunteers. Other areas, that showed a reduced DPN binding at a lower level of significance included the left middle temporal gyrus (BA 21, $Z=3.51$) and the posterior parieto-occipital junction (BA 40, $Z=4.12$), regions also known to be involved in word processing.
Conclusions: These findings provide *in-vivo* evidence for localised endogenous opioid peptide release and demonstrate the potential of PET to image neurotransmitter fluxes in response to brain activity in specific cerebral areas *in-vivo*.
(published in ***Lancet*** 1998; 352: 952-55)

9.2. Introduction

Regional cerebral blood flow (rCBF) and rCMRglu reflect local synaptic activity and H_2O and FDG PET activation studies have greatly increased our understanding of the functional anatomy of the brain in health and disease. Neurotransmitters are responsible for mediating human neuronal activity and, until now, PET studies of specific ligands have largely been limited to quantitation of receptor binding and availability under resting conditions (Frost, 1993). Endogenous neurotransmitter release is a pivotal event in neuroregulation, but has been very difficult to study non-invasively *in-vivo* in man (Morris, 1995). To date, PET studies of neurotransmitter release in humans have concentrated on pharmacological manipulations and measured changes in receptor availability to radioligands (Dewey, 1993; Dewey, 1995).

There is evidence from experimental studies that opioid peptide release is involved in the termination of seizures (Bajorek, 1986; Tortella, 1988b; Ramabadran, 1990). Animal studies measuring changes in opioid receptors following seizures have demonstrated increases in ∂-opioid receptor occupation (Tortella, 1988a). Increased levels of Leu-enkepalin in the CSF of epilepsy patients gave indirect evidence of an opiate-receptor mediated endogenous anticonvulsant system in human epilepsy (Jianguo, 1990). In humans, interictal PET studies have shown elevated μ-opiate receptor binding in the lateral temporal neocortex overlying mesial temporal foci, suggesting focal epilepsy may be associated with abnormal opioid transmission (Mayberg, 1991). Cerebral opioid release, as evidenced by displacement of DPN binding, has been observed in the cerebral neocortex as a whole following serial absences (Bartenstein, 1993), but without any anatomical precision.

RE is a localisation-related reflex epilepsy in which seizures characteristically consist of reading-induced myoclonic jerks restricted to the jaw or throat (Bickford, 1956). RE is, therefore, an ideal model to study dynamic neurotransmitter changes in specific brain areas in relation to epileptic seizures. The biochemical and anatomical bases of RE are not well understood (Wolf, 1992). Ictal EEG findings predominantly occur in the temporo-parietal cortex of the language dominant hemisphere but are also found in other cortical areas that are functionally activated by reading (Radhakrishnan, 1995)

.

Recent developments in scanner sensitivity and PET image analysis now allow measurement not only the regional neuroanatomical distribution of opioid receptors but also, for the first time, to localise endogenous neurotransmitter release *in vivo* at high resolution, in response to focal epileptic activity and specific cognitive activation in man. We have used DPN PET studies to investigate acute changes in cerebral opioid receptor occupancy with reading induced seizures, studying the neural networks and neurotransmitter release underlying this form of epilepsy and its specific trigger: reading.

9.3. Methods

9.3.1. Subjects

Five right-handed patients with RE and six, age-matched, right-handed, healthy male volunteers without a previous history of neurological or psychiatric diseases. Written informed consent was obtained in all cases (approved by the Hammersmith Hospital and National Hospital for Neurology and Neurosurgery Ethics Committees and ARSAC (UK)). Patient details are provided in **Table 12**. Prior to PET all RE patients were

studied with video-EEG monitoring and the localisation and reproducibility of reading-induced seizure activity were verified.

We studied six patients (4 male, 2 female) with reading-induced seizures. The diagnosis was based on the patients' own account that reading was the single or the main seizure-triggering stimulus, and was confirmed by reproducing the habitual clinical seizures through reading provocation under continuous video-EEG monitoring. Few unprovoked, nocturnal seizures were decided as compatible with the diagnosis (Wolf, 1992). The median age at onset was 14 years (range 11 to 19 years). The median age at diagnosis 24 years (range 12 to 30 years) and the median time from the first reading-induced seizure until the diagnosis of reading epilepsy was made was 5 years (range 1 to 15 years). No risk factors for epileptic seizures such as prolonged early childhood convulsions or head trauma were found. Neurologic examination and intellect were normal in all subjects.

One patient (pat. 1) had a younger brother also suffering from RE and another brother who had difficulties with learning to read, but myoclonic seizures have never been noticed. Another sister is completely symptom-free. They have two further step-brothers and one step-sister, at an age below the usual age of onset of RE. There are also two half-brothers with an age similar to the age of symptom onset. The brother of another patient 2 gave a similar description of reading induced myoclonic seizures with secondary generalisation. Two brothers of patient 3 had a history of febrile convulsions but did not develop epileptic seizures thereafter. The family history of patient 4 (adopted) is not known. Brain MRI was normal in all except one, who showed a left temporal, probably perinatal, infarct.

9.3.2. PET methodology

PET scans were performed at the MRC Cyclotron Unit at the Hammersmith Hospital on a ECAT 953b scanner (CTI Siemens, Knoxville, TN) which acquires 31 simultaneous slices and has a resolution of 4.8 x 4.8 x 5.2 mm (at FWHM). Subjects were positioned with the glabella-inion line parallel to the detector rings so that the directly obtained transaxial images were parallel to the intercommissural line (AC-PC line). Correct positioning of the patient in the scanner was verified with a two minute transmission scan. We used DPN PET to image μ, k and ∂ opiate receptor binding on two occasions. Subjects received a total dose of 20 mCi (740 MBq) ^{11}C-DPN divided into two scans on consecutive days. A dynamic 3D series, consisting of 27 frames over 90 minutes (with two minute frames from 30 to 60 minutes post injection) was acquired over the full brain volume.

Table 12: Clinical and EEG data of 5 patients with RE

Age / gender	Age at onset (years)	Age at diagnosis (years)	Triggers other than reading (history)	type of seizures	associated symptoms	Family history	AED	EEG-characteristics inter-ictal	ictal
34 / F	19	24	writing, talking, shorthand	MJ 2 GTCS	stuttering, tightening of throat	no	CBZ VPA	occ. theta bilaterally	spike-wave/sharp-wave left fronto-central + temporal
25 / M	11	12	reading conversation	MJ GTCS	tightening of throat	no	CBZ VPA	bitemp slow waves	spike-waves at Cz and Pz
35 / M	15	30	writing, reading talking	MJ GTCS	shock-like feeling	not known	none	occ. theta bilaterally	sharp wave at Cz
57 / F	13	*25*	talking, reading shorthands	MJ GTCS	none	no	PHB PHT	occ. theta bilaterally	sharp and slow wave bilateral centro-parietal (L>R)
24 / M	14	16	writing, reading talking	MJ GTCS	stummering	brother	CZP Clob	bilateral μ-rhythms	spike-wave bilaterally fronto-temporal (L>R)

AED = anti-epileptic drugs; F = female; M = male; L = left; R = right; MJ = myoclonic jaw jerks; GTCS = generalsied tonic clonic seizures; CBZ = carbamazepine; VPA = sodium valproate; CZP = clonazepam; PHT = phenytoin; Clob = clobazam

During the first (activation) scan, subjects were asked to read aloud a complex scientific text from 30 to 60 minutes after injection of the radiotracer. Subjects were observed continuously and patients indicated whenever they experienced a partial seizure. An eight-channel EEG was recorded throughout the PET studies. Reading induced frequent partial seizures (>20 seizures over 30 minutes) in two patients, less frequent seizures (< 10 seizures) in two patients and no visible or self-reported seizures in one patient. During the control scan subjects were asked to silently inspect random strings of meaningful and meaningless symbols. Compliance with this task was controlled by direct observation and through detecting eye movements on the EEG trace. No seizure activity was reported by the patients, nor observed on the EEG, during the control scans.

Voxel-by-voxel parametric images were produced from the brain uptake and plasma input functions using spectral analysis (Cunningham, 1993) for all conditions with the analysis based on the unit impulse response function (IRF) at 60 minutes. These IRF_{60} parametric images are dominated by binding, reflect regional concentration of opioid receptor sites and are relatively insensitive to regional differences in CBF and delivery of DPN (Tadokoro, 1993).We calculated parametric images of DPN binding, reflecting the regional concentration of opioid receptors, for both scans. A significant localised reduction of DPN binding in RE patients when reading compared to the control scan implies displacement of ^{11}C-DPN during focal seizure activity due to endogenous release of opioids. Using SPM regional differences in DPN binding during reading with seizures, compared with looking at symbols without seizures, by the patients were contrasted with regional differences of DPN binding between these two conditions in the healthy volunteers.

9.4. Results

9.4.1. Effect of reading on ^{11}C-DPN binding

There were no areas of significantly increased DPN binding in association with reading induced seizures compared with inspection of symbols and no differences in cortical DPN binding between patients and controls for the inspection of symbols condition alone. The group of healthy controls showed no significant differences in DPN binding when reading text compared with looking at strings of symbols.

9.4.2. Effect of reading-induced seizures on ^{11}C-DPN binding

Significant reductions in DPN binding corrected for multiple comparisons ($Z=5.22$, $P < 0.001$ uncorrected) were observed in the left parieto-temporo-occipital cortex (Brodman

Area (BA) 37) (**Figure 18**) when comparing the interaction of activation (=reading text) minus control (=looking at strings of symbols) between the patient and the control groups. DPN binding was relatively reduced in patients with RE when reading with reading-induced seizures compared with the control state, but relatively increased in healthy subjects.

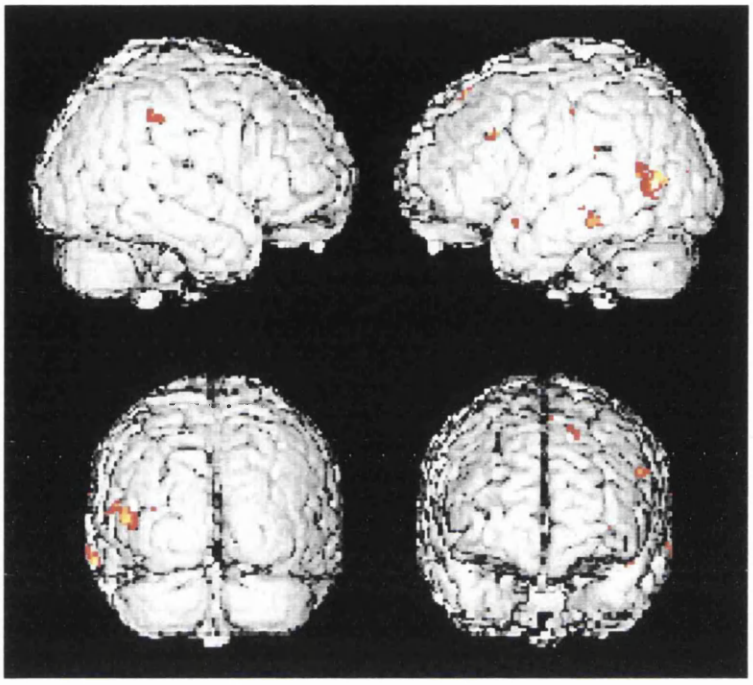

Figure 18: Result of SPM analysis
A statistical parametric map (SPM) showing significant activation of the left parieto-temporo-occipital cortex (BA 37). Significant areas of activation (uncorrected $P < 0.001$, corrected for multiple comparisons $P < 0.05$) are mapped in yellow onto a normalised MR image of the brain. Additional areas (uncorrected $P < 0.001$ but not significant for multiple comparisons) are shown in red.

Other areas, that were not significant when t-maps were corrected for multiple comparisons, included the left middle temporal gyrus (BA 21; Z=3.51) and the posterior parieto-occipital junction (BA 40; Z=4.12). The coordinates (x, y, z) in relation to the AC-PC line and Z-scores for these significant interactions are detailed below.

Table 13: Regions of significant endogenous opioid release

Area	Co-ordinates (x, y, z)	Z Score
Left parieto-temporo-occipital (BA37)	-42, -64, 2	5.22
Right parietal inferior (BA 40)	50, -36, 42	4.12
Left superior temporal gyrus (BA 38)	-44, 8, -14	4.02
Left middle temporal gyrus (BA 21)	-64, -34, -14	3.51
Left temporo-parietal (BA 40)	-68, -34, 24	3.37

9.4.3. Individual analysis

Analysis of individual cases revealed the same pattern of significant left temporo-parietal reduction of DPN binding in four out five RE patients. The fifth patient produced few reading induced partial seizures (< 10 seizures / 30 minutes) and showed sub-threshold ($P < 0.05$, uncorrected) abnormalities at the same location. One of the other patients showed additional reduced DPN binding in both frontal lobes. The spatial extent of abnormalities did not correlate with the duration of induced seizure activity. Reading induced frequent partial seizures (>20 seizures over 30 minutes) in two patients, less frequent seizures (< 10 seizures) in two patients and no visible or self-reported seizures in one patient. Video-EEG telemetry carried out prior to the PET scanning revealed, only during reading, bilateral symmetric paroxysmal abnormalities in the central regions in two patients, generalised spike-wave discharges with left-sided predominance in two patients and in one patient focal spike-wave discharges that were left fronto-central and temporal. The multi-focal EEG changes of the last patient were co-localised with her PET abnormalities .

9.5. Discussion

9.5.1. Methodological considerations

We have demonstrated dynamic properties of the opioid neurotransmitter system in RE patients and the localised release of endogenous opioids in a specific neuronal network that is involved in reading and visual processing and recognition of words (Petersen, 1990; Price, 1994). This is the first time that focal release of neurotransmitters in response to specific brain activity has been demonstrated in man, *in vivo*.

The relative increases in DPN binding of healthy volunteers whilst reading can be explained by either reduced release of endogenous opioids during cognitive activation, or a physiological shift of the opiate receptors to a higher affinity state (Seeger, 1984). There is evidence from animal research that the release of dynorphin is reduced during cognitive tasks (Theodore, 1996). In order to eliminate physiological effects of reading on the availability or the affinity of opioid receptors, we compared the differences between activation and rest in patients with those in healthy volunteers. In contrast to the healthy volunteers, the reductions of DPN binding to opioid receptors found in patients with RE patients during reading were suggestive of endogenous opioid release. Nevertheless, simultaneous decreases in receptor affinity and increased endogenous opioid release cannot be ruled out. Seizures might also change coupling of the opiate receptors to proteins that modulate its affinity leading to reduced DPN binding.

Increased rCBF could theoretically lead to increased tracer washout or decreased DPN binding and thereby mimic the effect of endogenous opioid release. From 30 to 60 minutes after tracer injection, however, we can discount an increase in rCBF associated with the seizure activity as the cause of decreased DPN binding; simulation studies have indicated that at least a 10-fold increase in rCBF would be required to sufficiently raise tracer washout (Bartenstein, 1993) whereas CPS increased rCBF in temporal lobes by only 70-80%. Reading over 30 minutes can be expected to be a more powerful stimulus to increase rCBF than the very short lasting myoclonic jerks. In healthy volunteers we found increased opioid binding reflecting decreased tracer washout, which further supports our view that any increases in rCBF 30 minutes after tracer injection will not have an effect on DPN binding. It is also highly unlikely that the patients' antiepileptic drug treatment could have led to such localised effects on dynamic changes in regional opioid binding.

9.5.2. Pathophysiological considerations

The left posterior temporal and the left inferior parietal cortex have recently been shown to be associated with word processing. Activation studies on reading words versus false font or letters found significantly raised regional CBF in similar areas (Price, 1994) as we report in our current study of neurotransmitter release (**Table 13**). Wernicke's Area (BA 22) did not show any endogenous opioid release during reading induced seizures and this is consistent with the view that visual and auditory perceptions of a word are processed independently by modality-specific pathways that have independent access to Broca's area and to association cortex concerned with the meaning and expression of language. This might explain why reading rather than listening is the most effective trigger in RE. However, after sensitisation through repeated reading-induced partial seizures, other language-related activities, such as writing and even talking, can generate regional epileptic activity in these patients (Brooks, 1971). Eye movements mimicking reading saccades were also found to be provocative in a few early case reports (Alajouanine, 1959) whilst others reported the importance of comprehension as seizure-precipitating factor (Kartsounis, 1988).

Recent advances in the understanding of the physiology of reading helps us to interpret our findings of localised endogenous opioid release in RE patients in response to the cognitive stimulus. Conversely, investigating the mechanism of this reflex epilepsy by comparing reading text with scanning symbols provides indirect evidence that the "ventral and dorsal streams" are both involved in the physiological processing of reading. The "dorsal stream" of projections from the striate cortex to the posterior parietal regions has been suggested to program saccadic eye movements (Andersen, 1989) and is therefore likely to be involved in encoding the spatial co-ordinates of

words and sentences. Projections along the "ventral stream" to the left inferotemporal cortex have been associated with complex semantic judgement and sentence comprehension (Goodale, 1992; Bottini, 1994). The involvement of both areas in RE suggest that both reading saccades and semantic comprehension may act as trigger mechanisms in RE.

Using this novel approach of dynamic neurotransmitter activation we were able to image an endogenous anticonvulsant mechanism modulated by opioid-like substances which, most likely, had been released to terminate seizure activity. Opioid peptides are only released during high frequency neuronal firing as mediators of use-dependant synaptic activity. There is evidence from hippocampal slice preparations that opioid peptides have an important role in the regulation of long term potentiation (LTP) of synaptic activity. Enkephalin promotes the development of LTP while dynorphin suppresses it. DPN labels all opioid receptors with similar affinity and is easier displaceable by endogenous opioids than subtype-specific ligands. The disadvantage of using DPN is that we cannot determine which opioid-subtypes are specifically involved in terminating partial seizures. Evidence for endogenous opioid release has previously been shown during hyperventilation induced absences in a non-specific fashion without any anatomical precision (Bartenstein, 1993). The pathophysiology of absences, however, is quite different from partial seizures. Release of opioids enhances the occurrence of absences, but are released as a response to focal seizure activity, and are antiepileptic. The finding of significant opioid release in the patient without overt seizure activity is consistent with the argument for an endogenous anticonvulsant mechanism. It is possible that this patient had subclinical, undetected epileptic activity during the activation scan, which was efficiently suppressed by endogenous opioid release. It is likely that clinically overt seizure activity was the "tip of the iceberg" of subclinical abnormal activity within cortical and subcortical networks and this was further underlined by our observation that there was no correlation between duration and frequency of seizures and endogenous opioid release. The bilateral EEG findings are characteristic of RE and support the view of multiple cortical and subcortical areas of hyperexcitability in this localisation-related epilepsy syndrome.

CHAPTER X Discussion

10.1. Summary of main findings

The main findings in patients with mesial temporal lobe epilepsy (mTLE) due to unilateral hippocampal sclerosis (HS) were:

- Binding of ^{11}C-flumazenil (FMZ) to central benzodiazepine receptors (cBZR) is reduced in the sclerotic hippocampus with no further decreases or increases elsewhere in the cerebral cortex.
- Reduction in ^{11}C-FMZ binding in mTLE is over and the above the loss of hippocampal tissue.
- *In-vivo* measurements of ^{11}C-FMZ binding using PET correlated with *ex-vivo* ^{3}H-FMZ autoradiography. Quantitative neuropathology and saturation autoradiography of resected sclerotic hippocampi showed loss of cBZR that exceeded that due to neurone loss, in the CA1 subregion.
- Partial volume effect corrected ^{11}C-FMZ-PET revealed bilateral abnormalities in one third of patients with mTLE and unilateral or markedly asymmetrical bilateral HS.

The main findings in patients with idiopathic generalised epilepsy (IGE) were:

- Binding of ^{11}C-FMZ to cBZR was significantly higher in cerebral cortex, thalamus and cerebellum compared to healthy controls as well as compared to patients with mTLE.
- Patients with JME show accentuations of increased ^{11}C-FMZ binding to cBZR in the DLPFC bilaterally.
- Treatment with VPA treatment did not change ^{11}C-FMZ binding, neither did the concomitant reduction in seizures.

The main finding in patients with reading epilepsy (RE) was:

- Binding of ^{11}C-diprenorphine (DPN) to opioid receptors was increased during reading in controls and reduced during reading-induced seizures in patients with RE
- These changes occurred within a network of cortical areas involved in reading.

10.2 Neurobiological implications

Recent developments in absolute PET quantification allowing correction for partial volume effect have now made direct comparisons of *in-vivo* and *ex-vivo* measurements of cBZR binding possible. We have used autoradiography to validate the use of ^{11}C-

FMZ PET coregistered with high quality MRI and corrected for partial volume effect for quantitatively and objectively delineating cBZR binding abnormalities in the hippocampi of patients with mTLE. This project validated *in-vivo* functional imaging and demonstrated receptor abnormalities underlying hippocampal epilepsy. Identification of functional abnormalities, over and above structural abnormalities, has profound implications for the investigation of patients with refractory seizures, who are candidates for surgical treatment and in whom MRI does not reveal a relevant underlying lesion.

Our data showed that partial volume effect correction is necessary to detect and quantitate dysfunction in areas of abnormalities with PET in small structures such as the hippocampus. We have shown how this may be done to obtain PET data from multiple hippocampal regions. We demonstrated for the first time the regional cBZR density in the hippocampus *in-vivo*, and loss of cBZR over and above the loss of volume along the length of the hippocampus in patients with mTLE and HS. As found in MRI studies bilateral involvement commonly affected the anterior hippocampus.

The lack of correlation with neuronal densities and hippocampal volumes suggests that the observed reductions of hippocampal volumes and neuronal loss do not explain the reduction of cBZR binding in HS. This implies a functional abnormality in abnormal tissue. We have also shown in an more detailed autoradiographic and quantitative neuropathological analysis of hippocampal subregions that this is in fact the case with a reduction of cBZR density in HS by 50% on surviving neurons of the CA1 subregion. The loss of inhibitory receptors may be relevant to the pathophysiology og TLE in HS.

Increased ^{11}C-FMZ binding in patients with IGE could reflect the neurochemical abnormality underlying cortical hyperexcitability. Cortical hyperexcitability may result from decreases of inhibitory neurotransmitters, such as GABA. In contrast $GABA_A$ agonists such as muscimol and GABA-mimetics, such as γ-vinyl GABA, an inhibitor of GABA transaminase, exacerbate absence seizures through action at the thalamic relay nuclei. It is possible that the observed increased ^{11}C-FMZ binding in our patients with IGE might be the result of a widespread GABA deficiency resulting in receptor upregulation.

It is possible that increased ^{11}C-FMZ binding in patients with IGE reflects the neurochemical abnormality underlying cortical hyperexcitability. Cortical hyperexcitability may result from decreases of inhibitory neurotransmitters, such as GABA. In contrast $GABA_A$ agonists such as muscimol and THIP and GABA-mimetics, such as γ-vinyl-GABA, an inhibitor of GABA transaminase, exacerbate absence seizures through action at the thalamic relay nuclei (Marescaux, 1992). It is

possible that the observed increased ^{11}C-FMZ binding in our patients with IGE might be the result of a widespread GABA deficiency resulting in receptor upregulation.

An upregulation of $GABA_A$ receptors may perturb the functioning of dynamic thalamic circuits, facilitating synchronisation of discharges. An increase in $GABA_A$ receptors in the thalamic relay nuclei could contribute to a tendency to absences, although $GABA_B$ receptors have a major role in this process. In animal models of absence seizures, GABAergic transmission within the thalamus influences spike-wave activity through an interaction between $GABA_A$ and $GABA_B$ receptors of the relay and reticular nuclei. The nature of this interaction has not been fully established and is complicated by the presence of GABAergic interneurons and autoreceptors. It is possible that an imbalance or abnormal sensitivity of $GABA_A$ or $GABA_B$ receptors facilitates the generation of spike-wave activity. An increase in $GABA_A$ receptors in the cerebral cortex would not be a tenable primary explanation for cortical hyperexcitability, but could be an adaptive response.

Analogous to the idea of a hyperexcitable cortex in IGE, ictogenesis in reading or language-induced epilepsy may be based on the reflex activation of a hyper-excitable network that subserves the function of speech and extends over multiple cerebral areas on both hemispheres, by language-related stimuli. This network hyperexcitability could be genetically determined and its clinical expression is age-related. It is well established that endogenous opioids have the opposite effects in generalised and partial seizures. This situation is analogous to the differential effects of GABA on absences and GTCS and emphasises that different mechanisms underlie these two types of seizures. Observation following systemic administration of opioids, whilst of possible therapeutic significance, provide only limited information regarding pathogenic mechanisms, different areas of the brain contain varying proportions of μ-, ∂- and k-receptors.

The effect of opioids at any given site will depend on the predominant receptor type and the class of opioid. There is also evidence for receptor subtype heterogeneity (μ1 and μ2, ∂1 and ∂2, k1-3) (Pasternak, 1993). Neuronal circuitry adds a further level of complexity. Pyramidal neuron excitability is increased following opioid application. However, no direct effects of opioids on CA1 pyramidal cells themselves have been reported. This paradoxical effect was explained via a mechanism of "disinhibition" in which opiates were acting directly via μ- or ∂-receptors to inhibit GABA release on inhibitory interneurons, resulting in excitation of the pyramidal neurons. Disinhibition has also been proposed to be the underlying mechanism by which μ-receptors facilitate longterm-potentiation (LTP) in the mossy fibers. In contrast to disinhibition resulting from reduction of GABA release, k-opioid agonists were found at the perforant path-

granule cell synapse to act presynaptically inhibiting excitatory glutamate release in the dentate molecular layer. Consistent with these effects k-opioids can have an inhibitory effect on LTP induction in the dentate gyrus. LTP can be described simply as a longlasting enhancement of synaptic response following an appropriate, typically high frequency stimuli, conditions which also favor release of endogenous opioids. If one assumes that LTP is representative of learning and/or memory mechanisms, then by analogy with their interactions with LTP, endogenous opiates should potentially effect these processes as well.

10.3 Future Studies

The abnormal electrical discharge and accompanying seizure activity that characterise epilepsy in humans reflect excessive neuronal activity. Increasingly sensitive measures of anatomy and physiology can demonstrate these alterations and have a high correlation with the location of the EEG manifestations of the process. Structural abnormalities are highly correlated but not synonymous with the epileptogenic zone. Therefore, MRI cannot be used alone to define an epileptogenic process. SPECT and PET, because of lesser anatomic resolution are dependent on co-registration with MRI for precise anatomic correlations.

The partial volume correction techniques we implemented will have wide application in the evaluation of PET data from cerebral structures, particularly if there is associated atrophy. Correction for partial volume effect will have important general applications to assess functional abnormalities in PET data within small structures such as the basal ganglia or the cortical ribbon, particularly in conditions in which atrophy is part of the pathological process, e.g. Huntingdon's Disease or Alzheimer's Disease.

In clinical terms our studies suggest that cBZR changes reflect functional changes in the epileptogenic zone in addition to localised neuronal loss and FMZ PET may visualise such abnormalities in patients with normal MRI. ^{11}C-FMZ-PET may be a clinical useful tool in a multidisciplinary, preoperative epilepsy evaluation when quantitative MRI reveals equivocal or no abnormalities. Serial and postoperative follow-up studies will give further insight into the neurobiology of mTLE with HS.

Alterations in cerebral blood flow and cerebral metabolic rate of glucose accompany the epileptic process; the alterations in metabolism may be more profound. They may be multifocal, diffuse or regional, but the epileptogenic zone is highly likely to be located within the area of defined functional alteration. The ability to use different tracers to measure various functional disturbances and to perform quantitative data

analysis, as well as the superior resolution of PET, are distinct advantages. The recent development of high-sensitivity PET scanners will allow to perform multiple tracer experiments in the same individual, enabling a cross-correlation between changes in different systems and the impact of changes in seizure frequency. Elucidation of the neurochemical and functional abnormalities underlying seizures will assist the design of new antiepileptic drugs and is a necessary prerequisite to the development of local drug delivery systems.

The rare syndrome of RE served as an ideal model to study dynamic neurotransmitter changes underlying both focal seizure activity and higher cognitive activity. This novel PET approach for measuring focal dynamic neurotransmitter changes associated with brain activity has far reaching implications, not only for the understanding of the neurobiology and neuropharmacology of partial seizures, but also providing a framework (Koepp, 1998a) for the future anatomical localisation of neurotransmitters and the circuitry involved in cognitive processing leading to a true "functional neurochemistry of cognition and behaviour".

BIBLIOGRAPHY

Abadie P, Baron JC, Bisserbe JC, *et al.* Central benzodiazepine receptors in human brain: estimation of regional Bmax and Kd values with positron emission tomography. Eur J Pharmacol 1992;213:107-15.

Abou-Khalil BW, Siegel GJ, Sackellares JC, *et al.* Positron emission tomography studies of cerebral glucose metabolism in chronic partial epilepsy. Ann Neurol 1987;22:480-6.

Adam C, Baulac M, Sainte Hilaire JM, *et al.* Value of magnetic resonance imaging-based measurements of hippocampal formations in patients with partial epilepsy. Arch Neurol 1994;51:130-8.

Adams CBT, Anslow P, Molyneux A. Radiological detection of surgically treatable pathology. In: Engel JJ, ed. Surgical treatment of the epilepsies. New York: Raven Press, 1987:213-33.

Aicardi J. Status epilepticus in infants and children: consequences and prognosis. Int Pediatr 1987;2:189-95.

Alajouanine TH, Nehlil J, Gabersek V. A propos d'un cas d'épilepsie déclenché par la lecture. Rev Neurol 1959;101:463-367.

Andersen RA. Visual and eye movement functions of the posterior parietal cortex. Ann Rev Neurosci 1989;12:377-403.

Annegers JF, Hauser WA, Shirts SB, Kurland LT. Factors prognostic of unprovoked seizures after febrile convulsions. N Engl J Med 1987;316:439-98.

Avanzini G, de Curtis M, Marescaux C, *et al.* Role of the thalamic reticular nucleus in the generation of rhythmic thalamo-cortical activities subserving spike and waves. J Neural Transm 1992;35 (Suppl):85-95.

Avanzini G, Vergnes M, Spreafico R, Marescaux C. Calcium-dependent regulation of genetically determined spike and waves by the reticular thalamic nucleus of rats. Epilepsia 1993;34:1-7.

Avoli M, Gloor P, Kostopoulos G, Gotman J. An analysis of penicillin-induced generalised spike and wave discharges using simultaneous recordings of cortical and thalamic single neurons. J Neurophysiol 1983;50:819-37.

Babb TL, Brown WJ, Pretorius J, *et al.* Temporal lobe volumetric cell densities in temporal lobe epilepsy. Epilepsia 1984a;25:756-62.

Babb TL, Lieb JP, Brown WJ, Pretorius J, Crandall PH. Distribution of pyramidal cell density and hyperexcitability in the epileptic human hippocampal formation. Epilepsia 1984b;25:721-8.

Babb TL, Brown WJ. Pathological findings in epilepsy. In: Engel JJ, ed. Surgical Treatment of the Epilepsies. New York: Raven Press, 1987:511-40.

Babb TL, Pretorius JK, Kupfer WR, Crandall PH. Glutamate decarboxylase-immunoreactive neurons are preserved in human epileptic hippocampus. J Neurosci 1989;9:2562-74.

Bailey DL. 3D acquisition and reconstruction in positron emission tomography. Ann Nuc Med 1992;6:121-30.

Bajorek JG, Lee RL, Lomax P. Neuropeptides: Anticonvulsant and convulsant mechanisms in epileptic model systems and in humans. Adv Neurol 1986;44:489-500.

Bancaud J, Talairach J, Morel P, *et al.* "Generalised" epileptic seizures elicited by electrical stimulation of the frontal lobe in man. Electroenceph Clin Neurophysiol 1974;37:275-82.

Bartenstein PA, Duncan JS, Prevett MC, *et al.* Investigation of the opioid system in absence seizures with positron emission tomography. J Neurol Neurosurg Psychiatry 1993;56:1295-302.

Bekenstein JW, Lothman EW. Dormancy of inhibitory interneurons in a model of temporal lobe epilepsy. Science 1993;259:97-100.

Ben-Ari Y, Tremblay E, Ottersen OP, Meldrum BS. The role of epileptic activity in hippocampal and "remote" cerebral lesions induced by kainic acid. Brain Res 1980;191:79-97.

Ben-Ari Y, Represa A. Brief seizure episodes induce long-term potentiation and mossy fibre sprouting in the hippocampus. Trends Neurosci 1990;13:321.

Berkovic SF, Andermann F, Andermann E, Gloor P. Concepts of absence epilepsies: Discrete syndromes or a biological continuum? Neurology 1987;37:993-1000.

Berkovic SF, Newton MR, Chiron C, Dulac O. SPECT. In: Engel JJ, ed. Surgical treatment of the epilepsies. 2nd ed. New York: Raven Press, 1993:233-43.

Bernardi S, Trimble MR, Frackowiack RSJ, Wise RJS, Jones T. An interictal study of partial epilepsy using positron emission tomography and the oxygen-15 inhalation technique. J Neurol Neurosurg Psychiatry 1983;46:175-82.

Bickford RG, Whelan JL, Klass DW, Corbin KB. Reading epilepsy: clinical and electroencephalographic studies of a new syndrome. Trans Am Neurol Assoc 1956;81:100-2.

Bland MJ, Altman DG. Statistical methods for assessing agreement between two methods of clinical measurement. Lancet 1986;327:307-10.

Bottini G, Corcoran R, Sterzi R, *et al.* The role of the right hemisphere in the interpretation of figurative aspects of language. A positron emission tomography activation study. Brain 1994;117:1241-53.

Bowery NG. $GABA_B$ receptors and their significance in mammalian pharmacology. Trends Pharmacol Sci 1989;10:401-7.

Brodie MJ. Lamotrigine. Lancet 1992;339:1397-400.

Brooks JE, Jirauch PM. Primary reading epilepsy: a misnomer. Arch Neurol 1971;25:97-104.

Brooks-Kayal AR, Shumate MD, Jin H, Rikhter TY, Coulter DA. Selective changes in single cell GABAA receptor subunit expression and function in temporal lobe epilepsy. Nature Medicine 1998; 4: 1166-1172

Brown SD. Topiramate. Epilepsia 1993;34 (Suppl 2):122-3.

Browning RA. Role of the brainstem reticular formation in tonic-clonic seizures: lesion and pharmacological studies. Fed Proc 1985;44:2425-31.

Burdette DE, Sakurai SY, Henry TR, *et al.* Temporal lobe central benzodiazepine binding in unilateral mesial temporal lobe epilepsy. Neurology 1995;45:934-41.

Buzsáki G. The thalamic clock: Emergent network properties. Neuroscience 1991;41:351-64.

Cavazos J, Sutula T. Progressive neuronal loss induced by kindling: a possible mechanism in mossy fibre reorganisation and hippocampal sclerosis. Brain Res 1990;527:1-6.

Cavenini M, Mai R, Di Marco C, et al. Juvenile myoclonic epilepsy of Janz: clinical observations in 60 patients. Seizure 1992;1:291-8.

Chadwick DW. Gabapentin and felbamate. In: Duncan JS, Panayiotopoulos CP, eds. Typical absences and related epileptic syndromes. London: Churchill Livingstone, 1995:376-80.

Coenen AML, Drinkenburg WHIM, Inoue M, van Luijtelaar ELJM. Genetic models of absence epilepsy, with emphasis on the WAG/R1J strain of rats. Epilepsy Res 1992;12:75-86.

Cohn R. A neuropathological study of a case of petit mal epilepsy. Electroenceph Clin Neurophysiol 1968;24:282.

Commision for the Classification and Terminology of the International League against Epilepsy. Proposal for revised classification of epilepsies and epileptic syndromes. Epilepsia 1989;30:389-99.

Cook MJ, Fish DR, Shorvon SD, Straugham K, Stevens JM. Hippocampal volumetric and morphometric studies in frontal and temporal lobe epilepsy. Brain 1992;115:1001-15.

Corsellis JAN, Bruton CJ. Neuropathology of status epilepticus in humans. In: Delgado-Escueta AV, Wasterlain DM, Treiman DM, Porter RJ, eds. Status epilepticus - Advances in neurology. New York: Raven Press, 1983:129-39.

Coulter DA. Topiramate. Epilepsia 1993;34 (Suppl 2):123.

Crunelli V, Leresche N. A role for $GABA_A$ receptors in excitation and inhibition of thalamocortical cells. Trends Neurosci 1991;14:18-21.

Cunningham VJ, Hume SP, Price GR, *et al.* Compartmental analysis of diprenorphine binding to opiate receptors in the rat in vivo and its comparison with equilibrium data in vitro. J Cereb Blood Flow Metab 1991;11:1-9.

Cunningham VJ, Jones T. Spectral analysis of dynamic PET data. J Cereb Blood Flow Metab 1993;13:15-23.

Daly RF, Forster FM. Inheritance of Reading Epilepsy. Neurology 1975;25:1051-4.

Dam AM. Epilepsy and neuronal loss in the hippocampus. Epilepsia 1980;21:617-29.

de Lanerolle NC, Kim JH, Robbins RJ, Spencer DD. Hippocampal interneuron loss and plasticity in human temporal lobe epilepsy. Brain Res 1989;495:387-95.

Depaulis A, Vergnes M, Liu Z, Kempf E, Marescaux C. Involvement of the nigral output pathways in the inhibitory control of the substantia nigra over generalised nonconvulsive seizures in the rat. Neuroscience 1990;39:339-50.

Dewey SL, Smith GS, Logan J, *et al.* GABAergic inhibition of endogenous dopamine release measured in vivo with ^{11}C-raclopride and positron emission tomography. J Neurosci 1992;12:3773-80.

Dewey SL, Smith GS, Logan J, *et al.* Effects of central cholinergic blockade on striatal dopamine release measured with positron emission tomography in normal human subjects. Proc Natl Acad Sci USA 1993;90:11816-20.

Dewey SL, Smith GS, Logan J, *et al.* Serotonergic modulation of striatal dopamine measured with positron emission tomography (PET) and in vivo microdialysis. J Neurosci 1995;15:821-9.

Duncan JS, Sagar HJ. Seizure characteristics, pathology, and outcome after temporal lobectomy. Neurology 1987;37:405-9.

Duncan JS, Shorvon SD, Fish DR. Clinical Epilepsy. London: Churchill Livingstone 1995;125-132

During MJ, Spencer DD. Extracellular hippocampal glutamate and spontaneous seizure in the conscious human brain. Lancet 1993;341:1607-10.

Ebner A. Lateral (neocortical) temporal lobe epilepsy. In: Wolf P, ed. Epileptic seizures and syndromes. London: John Libbey, 1994:375-82.

Engel JJ, Kuhl DE, Phelps ME, Rausch R, Nuwer M. Local cerebral metabolism during partial seizures. Neurology 1983;33:400-13.

Engel JJ, Lubens P, Kuhl DE, Phelps ME. Local cerebral metabolic rate for glucose during petit mal absences. Ann Neurol 1985:121-8.

Engel JJ, Caldecott-Hazard S, Bandler R. Neurobiology of behavior: anatomic and physiologic implications related to epilpesy. Epilepsia 1986;27 (Suppl 1.2):3-13.

Engel JJ. Outcome with respect to seizures. In: Engel JJ, ed. Surgical treatment of the Epilepsies. New York: Raven Press, 1987:553-72.

Engel JJ, Henry TR, Risinger MW, *et al.* Presurgical evaluation for partial epilepsy: relative contributions of chronic depth-electrode recordings versus FDG-PET and scalp-sphenoidal ictal EEG. Neurology 1990;40:1670-7.

Engel JJ. Recent advances in surgical treatment of temporal lobe epilepsy. Acta Neurol Scand 1992;86 (Suppl 5):71-80.

Falconer MA, Serafetinides EA, Corsellis JA. Etiology and pathogenesis of temporal lobe epilepsy. Arch Neurol 1964;10:233-48.

Falconer MA. Mesial temporal (ammon's horn) sclerosis as a common cause of epilepsy: aetiology, treatment and prevention. Lancet 1974;2:767-70.

Fariello RG, Ticku MK. The perspective of GABA replenishment therapy in the epilepsies: a critical evaluation of hopes and concerns. Life Sci 1983;33:1629- 40.

Feeney DM, Baron JC. Diaschisis. Stroke 1986;17:817-30.

Fisher RS, Frost JJ. Epilepsy. J Nucl Med 1991;32:651-9.

Forster FM, Daly RF. Reading Epilepsy in identical twins. Trans Am Neurol Ass 1973;98:186-8.

Frackowiak RSJ, Jones T. PET scanning. BMJ 1989;298:693-4.

Franceschi M, Lucignani G, Del Sole A, *et al.* Increased interictal cerebral glucose metabolism in a cortical-subcortical network on drug-naive patients with cryptogenic temporal lobe epilepsy. Epilepsia 1997.

Franck JE, Kunkel DD, Baskin DG, Schwartzkroin PA. Inhibition in kainate-lesioned hyperexcitable hippocampi: physiologic, autoradiographic, and immunocytochemical observations. J Neurosci 1988;8:1991-2002.

Fraser D, Duffy S, Angelides K. GABAA/Benzodiazepine receptors in acutely isolated hippocampal astrocytes. J Neurosci 1995;15:2720-32.

Frederickson CCA, Geary LE. Endogenous opioid peptides: review of physiological, pharmacological and epileptic properties. Prog Neurobiol 1982;19:19-69.

Free SL, Bergin PS, Fish DR, *et al.* Proposed methods for normalisation of hippocampal volumes measured with MR. Am J Neuroradiol 1995;16:637-43.

Frey KA, Holthoff VA, Koeppe RA, *et al.* Parametric in vivo imaging of benzodiazepine receptor distribution in human brain. Ann Neurol 1991;30:663-72.

Fried I, Kim JH, Spencer DD. Hippocampal pathology in patients with intractable seizures and temporal lobe masses. J Neurosurg 1992;76:735-40.

Friston KJ, Frith CD, Liddle PF, *et al.* The relationship between global and local changes in PET scans. J Cereb Blood Flow Metab 1990;10:458-66.

Friston KJ, Frith CD, Liddle PF, Frackowiak RSJ. Plastic transformation of PET images. J Comput Assist Tomogr 1991;15:634-9.

Friston KJ, Ashburner J, Poline JB, Frackowiak RSJ. Spatial registration and normalisation of images. Human Brain Mapping 1995a;2:165-89.

Friston KJ, Holmes AP, Worsley KJ, *et al.* Statistical parametric maps in functional imaging: A general linear approach. Human Brain Mapping 1995b;2:189-210.

Frost JJ, Mayberg HS, Fisher RS, *et al.* Mu-opiate receptors measured by positron emission tomography are increased in temporal lobe epilepsy. Ann Neurol 1988;23:231-7.

Frost JJ. Receptor imaging by PET and SPECT: focus on the opiate receptor. J Receptor Res 1993;13:39-53.

Fulton JF. Discussion of Gastaut, H.: So-called 'psychomotor" and "temporal" epilepsy. Epilepsia 1953;2:77.

Gaillard WD, Bhatia S, Bookheimer SY, *et al.* FDG-PET and volumetric MRI in the evaluation of patients with partial epilepsy. Neurology 1995;45:123-6.

Gale K. Progression and generalisation of seizure discharge. Anatomical and neurochemical substrates. Epilepsia 1988;29(Suppl 2):15-34.

Geddes JW, Cahan LD, Cooper SM, *et al.* Altered distribution of excitatory amino acid receptors in temporal lobe epilepsy. Exp Neurol 1990;108:214-20.

Giaretta D, Avoli M, Gloor P. Intracellular recordings in pericruciate neurons during spike and wave discharges of feline generalised penicillin epilepsy. Brain Res 1987:68-9.

Gibbs FA, Gibbs EL. Atlas of electroencephalography. Cambridge: AddisonWesley, 1952.

Gloor P, Testa G. Generalised penicillin epilepsy in the cat. Effects of intracarotid and intravertebral pentylenetetrazol and amobarbital injection. Electroenceph Clin Neurophysiol 1974;36:499-515.

Gloor P, Quesney LF, Zumstein H. Pathophysiology of generalised penicillin epilepsy in the cat: The role of cortical and subcortical structures. II. Topical application of penicillin to the cerebral cortex and to subcortical structures. Electroenceph Clin Neurophysiol 1977;43:79-94.

Gloor P. Generalised epilepsy with spike-and-wave discharge: A reinterpretation of its electrographic and clinical manifestations. Epilepsia 1979;20:571-88.

Gloor P. Experiential phenomena of temporal lobe epilepsy. Brain 1990;113:1673-94.

Goodale MA, Milner AD. Separate visual pathways for perception and action. TINS 1992;15:20-5.

Griffiths RG, Evans MC, Meldrum BC. Intracellular calcium accumulation in rat hippocampus during seizures induced by bicuculline or L-allylglycine. Neuroscience 1983;10:385-95.

Grootoonk S, Spinks TJ, Bloomfield PM, Sashin D, Jones T. The practical implementation and accuracy of dual window sactter corection in a neuro PET scanner with the septa retracted. IEEE Med Imaging Conference Records 1993;5:942-4.

Grünewald RA, Jackson GD, Connelly A, Duncan JS. MRI detection of hippocampal pathology in epilepsy: factors influencing T2 relaxation time. Am J Neuroradiol 1994;15:1149-56.

Guberman A, Gloor P, Sherwin AL. Response of generalised penicillin epilepsy in the cat to ethosuximide and diphenylhydantoin. Neurology 1975;25:758-64.

Haefely W. Benzodiazepines: mechanisms of action. In: Levy R, Mattson R, Meldrum B, Penry JK, Dreifuss FE, eds. Antiepileptic drugs. 3rd ed. New York: Raven Press, 1989:721-34.

Haffmans J, Dzoljic MR. Effects of delta opioid antagonists on enkephalin induced seizures. Pharmacology 1987;34:61-5.

Hajek M, Antonini A, Leenders KL, Wieser HG. Mesiobasal versus lateral temporal lobe epilepsy: metabolic differences shown in the temporal lobe by interictal ^{18}F-FDG positron emission tomography. Neurology 1993;43:79-86.

Hajek M, Wieser HG, Khan N, *et al.* Preoperative and postoperative glucose consumption in mesiobasal and lateral temporal lobe epilepsy. Neurology 1994;44:2125-32.

Hall JH, Marshall PC. Clonazepam therapy in reading epilepsy. Neurology 1980;30:550-1.

Hand KSP, Baird VH, Van Paesschen W, *et al.* Central benzodiazepine receptor autoradiography in hippocampal sclerosis. Brit J Pharmacology 1997;122:358-364

Handforth A, Cheng JT, Mandelkern MA, Treiman DA. Markedly increased mesiotemporal lobe metabolism in a case with PLEDs: further evidence that PLEDs are a manifestation of partial status epilepticus. Epilepsia 1994;35:648-57.

Hariton C, Ciesielski L, Cane JP, Mandel P. Studies on benzodiazepine receptor subtypes in a model of chronic spontaneous petit mal-like seizures. Neurosci Lett 1988;84:97-102.

Hartigan JA. Clustering Algorithms. New York: John Wiley & Sons, Inc., 1975.

Haycock KA, Roth J, Gagnon J, Finzer WF, Soper C. Abacus Concepts, StatView. Berkeley, CA: Abacus Concepts, Inc., 1992:

Henry TR, Mazziotta JC, Engel JJ, *et al.* Quantifying interictal metbaolic activity in human temporal lobe epilpsy. J Cereb Blood Flow Metab 1990;10:748-57.

Henry TR, Sutherling WW, Engel JJ, *et al.* Interictal cerebral metabolism in partial epilepsies of neocortical origin. Epilepsy Res 1991;10:174-82.

Henry TR, Frey KA, Sackellares JC, *et al.* In vivo cerebral metabolism and central benzodiazepine-receptor binding in temporal lobe epilepsy. Neurology 1993;43:1998-2006.

Henry TR, Babb TL, Engel JJ, *et al.* Hippocampal neuronal loss and regional hypometabolism in temporal lobe epilepsy. Ann Neurol 1994;36:925-7.

Hill DR, Bowery NG. ^{3}H-baclofen and ^{3}H-GABA bind to bicuculline-insensitive GABAR sites in rat brain. Nature 1981;290:149-52.

Hirsch LJ, Spencer SS, Williamson PD, Spencer DD, Mattson RH. Comparison of bitemporal and unitemporal epilepsy defined by electroencephalography. Ann Neurol 1991;30:340-6.

Hoffman EJ, Huang SC, Phelps ME. Quantitation in positron emission computed tomography: 1. Effect of object size. J Comput Assist Tomogr 1979;3:299-308.

Hoffman EJ, Huang SC, Phelps ME, Kuhl DE. Quantitation in positron emission computed tomography: 4. Effect of accidental coincidences. J Comput Assist Tomogr 1981;5:391-400.

Hosford DA, Clark S, Cao Z, *et al.* Role of $GABA_A$ receptor activation in absence seizures of lethargic (Ihllh) mice. Science 1992;257:398-401.

Houser CR, Miyashiro JE, Swartz BE, *et al.* Altered patterns of dynorphin immunoreactivity suggest mossy fiber reorganisation in human hippocampal epilepsy. J Neurosci 1990;10:267-82.

Houser CR, Olsen RW, Richards JG, Möhler H. Immunohistochemical localisation of benzodiazepine/$GABA_A$ receptors in the human hippocampal formation. J Neurosci 1988;8:1370-83.

Hunkeler W, Möhler H, Pieri L, *et al.* Selective antagonists of benzodiazepines. Nature 1981;290:514.

Isokawa-Akesson M, Wilson CL, Babb TL. Inhibition in synchronously firing human hippocampal neurons. Epilepsy Res 1989;3:236-47

Isokawa-Akesson M, Avanzini G, Finch DM, Levesque MF. Physiological properties of human dentate granule cells in slices prepared from epileptic patients. Epilepsy Res 1991;9:242-250.

Jack CR, Sharbrough FW, Twomey CK, *et al.* Temporal lobe seizures: lateralization with MR volume measurements of the hippocampal formation. Radiology 1990;175:423-9.

Jack CR, Sharbrough FW, Cascino GD, *et al.* Magnetic resonance image-based hippocampal volumetry: correlation with outcome after temporal lobectomy. Ann Neurol 1992;31:138-46.

Jackson GD, Berkovic S, Tress B, *et al.* Hippocampal sclerosis can be reliably detected by magnetic resonance imaging. Neurology 1990;40:1869-75.

Jackson GD, Berkovic SF, Duncan JS, Connelly A. Optimizing the diagnosis of hippocampal sclerosis using MR imaging. Am J Neuroradiol 1993a;14:753-62.

Jackson GD, Connelly A, Duncan JS, Grunewald RA, Gadian DG. Detection of hippocampal pathology in intractable partial epilepsy: increased sensitivity with quantitative magnetic resonance T2 relaxometry. Neurology 1993b;43:1793-9.

Jackson JH, Beevor CE. Case of tumour of the right temporo-sphenoidal lobe bearing on the localisation of the sense of smell and on the interpretation of a particular variety of epilepsy. Brain 1889;21:580-90.

Janz D, Neimanis G. Clinico-anatomical study of a case of idiopathic epilepsy with impulsive petit mal and grand mal on awakening. Epilepsia 1961;2:251-69.

Janz D. Die Epilepsien. Stuttgart, Germany: George Thieme, 1969.

Janz D. Juvenile myoclonic epilepsy. Epilepsy with impulsive petit mal. Cleve Clin J Med 1989;56 (Suppl 1):23-33.

Jasper HH, Droogleever-Fortuyn J. Experimental studies on the functional anatomy of petit mal epilepsy. Assoc Res Nerv Ment Dis 1947;26:272-98.

Jianguo C, Xuekong X. A study on opioid peptides in CSF of patients with epilepsy. Epilepsy Res. 1990;6:141-5.

Johnson EW, de Lanerolle NC, Kim JH, *et al.* "Central" and "peripheral" benzodiazepine receptors: opposite changes in human epileptogenic tissue. Neurology 1992;42:811-5.

Johnston D. Valproic acid: update on its mechanism of action. Epilepsia 1984;25 (Suppl 1):1-9.

Jones AKP, Luthra SK, Maziere B, al. e. Regional cerebral opioid receptor studies with ^{11}C-diprenorphine in normal volunteers. J Neurosci Methods 1988;23:121-9.

Kamphuis W, Wadman WJ, Buijs RM, Lopes Da Silva SH. Decrease in number of hippocampal gamma-aminobutyric acid (GABA) immunoreactve cells in the rat kindling model of epilepsy. Exp Brain Res 1986;64:491-5.

Kamphuis W, Gorter JA, da Silva FL. A long-lasting decrease in the inhibitory effect of GABA on glutamate responses of hippocampal pyramidal neurons induced by kindling epileptogenesis. Neuroscience 1991;41:425-31.

Kamphuis W, De Rijk TC, Lopes da Silva FH. Expression of $GABA_A$ receptor subunit mRNAs in hippocampal pyramidal and granular neurons in the kindling model of epileptogenesis: an in situ hybridisation study. Mol Brain Res 1995;31:33-47.

Kartsounis LD. Comprehension as the effective trigger in a case of primary reading epilepsy. J Neurol Neurosurg Psychiatr 1988;51:128-30.

Kelly KM, Gross RA, Macdonald RL. Valproic acid selectively reduces the low-threshold (T) calcium in rat nodose neurons. Neurosci Lett 1990;116:233-8.

Kennedy AM, Newman SK, Frackowiak RSJ. Chromosome 14 linked familial Alzheimer's disease. A clinico-pathological study of a single pedigree. Brain 1995;118:185-205.

Kerwin RW, Tabener PV. The mechanism of action of sodium valproate. Gen Pharmacol 1981;12:70.

Kessler RM, Ellis JR, Edden M. Analysis of emission tomographic scan data: Limitations imposed by resolution and background. J Comput Assist Tomogr 1984;8:514-22.

King A. Effects of systemically applied GABA agonists and antagonists on wave-spike ECoG activity in rat. Neuropharmacology 1979;18:47-55.

Knight AR, Bowery NG. GABA receptors in rats with spontaneous generalised non-convulsive epilepsy. J Neural Transm 1992;35 (Suppl):189-96.

Knowles WD, Awad IA, Nayel MH. Differences of in vitro electrophysiology of neurons from epileptic patients with mesiotemporal sclerosis versus structural lesions. Epilepsia 1992;33:601-9.

Koe BK. Enhancement of benzodiazepine binding by progabide (SL 76002) and SL 75102. Drug Dev Res 1983;3:421-32.

Koepp MJ, Richardson MP, Brooks DJ, *et al.* Cerebral benzodiazepine receptors in hippocampal sclerosis: an objective in vivo analysis. Brain 1996a;119:1677-87.

Koepp MJ, Richardson MP, Brooks DJ, Van Paesschen W, Duncan JS. ^{11}C-Flumazenil PET in temporal lobe epilepsy with normal or nondiagnostic MRI. Epilepsia 1996b;37 (Suppl. 4):153.

Koepp MJ, Richardson MP, Labbé C, *et al.* ^{11}C-Flumazenil PET, volumetric MRI and quantitative pathology in mesial Temporal Lobe Epilepsy. Neurology 1997a;49:764-73.

Koepp MJ, Labbé C, Brooks DJ, *et al.* Regional hippocampal 11C Flumazenil PET in Temporal Lobe Epilepsy with unilateral and bilateral hippocampal sclerosis. Brain 1997b;120:1865-76.

Koepp MJ, Gunn RN, Lawrence AD, *et al.* Evidence for striatal dopamine release during a video game. ***Nature*** 1998a; 393: 266-26

Koepp MJ, Hand KSP, Labbé C, *et al.* Flumazenil-PET correlates with ex-vivo ^{3}H-Flumazenil Autoradiography in Hippocampal Sclerosis. ***Annals of Neurology*** 1998b; 43: 618-626

Koepp MJ, Richardson MP, Brooks DJ & Duncan JS. Focal cortical release of endogenous opioids during reading induced seizures. ***Lancet*** 1998c; 352: 952-55

Koeppe RA, Holthoff VA, Frey KA, Kilbourn MR, Kuhl DE. Compartmental analysis of ^{11}C-flumazenil kinetics for the estimation of ligand transport rate and receptor distribution using positron emission tomography. J Cereb Blood Flow Metab 1991;11:735-44.

Kostopoulos G, Gloor P, Pellegrini A, Siatitsas I. A study of the transmission from spindles to spike wave discharge in feline generalised penicillin epilepsy: microphysiological features. Exp Neurol 1981;73:43-54.

Kostopoulos G, Avoli M, Gloor P. Participation of cortical recurrent inhibition in the genesis of spike wave discharges in feline generalised penicillin epilepsy. Brain Res 1983;267:101-13.

Kotagal P, Lüders H, Morris HH, *et al.* Dystonic posturing in complex partial seizures of temporal lobe onset: a new lateralizing sign. Neurology 1989;39:196-201.

Kreindler A, Zuckermann E, Steriade M, Chimion J. Electroclinical features of convulsions induced by stimulation of the brainstem. J Neurophysiol 1958;21:430-6.

Krnjevic K. Chemical nature of synaptic transmission in vertebrates. Physiol Rev 1974;54:418-540.

Kumlien E, Hilton-Brown P, Spannare B, Gillberg PG. In vitro quantitative autoradiography of ^{3}H-L-deprenyl and ^{3}H-PK 11195 binding sites in human epileptic hippocampus. Epilepsia 1992;33:610-7.

Kumlien E, Bergstrom M, Lilja, A, *et al.* Positron emission tomography with [11C]deuterium deprenyl in temporal lobe epilepsy. Epilepsia 1995;36:712-21

Kuzniecky R, de la Sayette V, Ethier R, *et al.* Magnetic resonance imaging in temporal lobe epilepsy: pathological correlations. Ann Neurol 1987;22:341-7.

Kuzniecky R, Bilir E, Gilliam, F, *et al.* Multimodality MRI in mesial temporal sclerosis: Relative sensitivity and specificity. Neurology 1997; 49:774-778.

Labbé C, Froment JC, Kennedy A, Ashburner J, Cinotti L. Positron Emission Tomography metabolic data corrected for cortical atrophy using Magnetic Resonance Imaging. Alzheimer Dis Assoc Disorders 1996;10:141-170.

Labbé C, Koepp MJ, Ashburner J, *et al.* Absolute PET quantification with correction for partial volume effect within cerebral structures. In: Carsson R, Daube-Witherspoon M, Herscovitch P (eds). Quantitative functional brain imaging with positron emission tomography. San Diego: Academic Press 1998 *in press*

Lacaille JC, Schwartzkroin PA. Stratum lacunosum - molecular interneurons of the hippocampal CA1 region II. Intrasomatic and intradendritic recordings of local circuit synaptic activity. J Neurosci 1988;8:1411-24.

Lammertsma AA, Bench CJ, Price GW, *et al.* Measurement of cerebral monoamine oxidase B activity using L-^{11}C-deprenyl and dynamic positron emission tomography. J Cereb Blood Flow Metab 1991;11:545-56.

Lammertsma AA, Lassen NA, Prevett MC, *et al.* Quantification of benzodiazepine receptors in vivo using ^{11}C-flumazenil: application of the steady state principle. In: Uemura K, ed. Quantification of brain function. Tracer kinetic and image analysis in brain PET. Elsevier Science Publishers, 1993:303-11.

Lammertsma AA, Hume SP. Simplified reference tissue model for PET receptor studies. NeuroImage 1996;4:153-8.

Lason W, Przewlocka B, Przewlocki R. The effect of gamma-hydroxybutyrate and anticonvulsants on opioid peptide content in the rat brain. Life Sci 1983;33:599-602.

Lee RJ, McCabe RT, Walmsley JK, Olsen RW, Lomax P. Opioid receptor alterations in a genetic model of generalised epilepsy. Brain Res 1986;380:76-82.

Leiderman DB, Balish M, Bromfield EB, Theodore WH. Effect of Valproate on Human Cerebral Glucose Metabolism. Epilepsia 1991;32:417-22.

Leidermann DB, Balish M, Sato S, *et al.* Comparison of PET measurements of cerebral blood flow and glucose metabolism for the localisation of human epileptic foci. Epilepsy Res 1992;13:153-7.

Levesque MF, Nakasato N, Vinters HV, Babb TL. Surgical treatment of limbic epilepsy associated with extrahippocampal lesions: the problem of dual pathology. J Neurosurg 1991;75:364-70.

Lieb JP, Engel JJ, Babb TL. Interhemispheric propagation time of human hippocampal seizures. Relationship to surgical outcome. Epilepsia 1986;27:286-93.

Lin F, Cao Z, Hosford DA. Increased number of $GABA_B$ receptors in the lethargic (Ihllh) mouse model of absence epilepsy. Brain Res 1993;608:101-6.

Lindsay J, Glaser G, Richards P, Ounstedt C. Developmental aspects of focal epilepsies of childhood treated by neurosurgery. Dev Med Child Neur 1984;26:574-87.

Liu Z, Vergnes M, Depaulis A, Marescaux C. Evidence for a critical role of GABAergic transmission within the thalamus in the genesis and control of absence seizures in the rat. Brain Res 1991;545:1-7.

Lloyd KG, Dreksler S. An analysis of ^{3}H-γ-aminobutyric acid (GABA) binding in the human brain. Brain Res 1979;163:77-87.

Login JS, Kolakovich TM. Successful treatment of primary reading epilepsy with clonazepam. Ann. Neurol. 1978;4:155-6.

Lorente de No R. Studies on the structure of the cerebral cortex. II: Continuation of the study of the Ammonic system. J Psychol Neurol 1934;46:113-77.

Löscher W. Comparative assay of anticonvulsant and toxic potencies of sixteen GABAmimetic drugs. Neuropharmacology 1982;21:803-10.

Löscher W, Siemes H. Valproic acid increases gamma-aminobutyric acid in CSF of epileptic children. Lancet 1984;2:225.

Löscher W, Siemes H. Cerebrospinal fluid y-aminobutyric acid levels in children with different types of epilepsy: effect of anticonvulsant treatment. Epilepsia 1985;26:314-9.

Löscher W, Jackel R, Czuczwar SJ. Is amygdala kindling in rats a model for drug-resistant partial epilepsy? Exp Neurol 1986;93:211-6.

Lothman EW, Bertram EH, Kapur J, Stringer JL. Recurrent spontaneous hippocampal seizures in the rat as a chronic sequela to limbic status epilepticus. Epilepsy Res 1990;6:110-8.

Luna D, Dulac O, Pajot N, Beaumont D. Vigabatrin in the treatment of childhood epilepsies: a single blind placebo-controlled study. Epilepsia 1989;30:430-7.

Luthra SK, Osman S, Turton DR, *et al.* An automated system based on solid phase extraction and HPLC for the routine determination in plasma of unchanged ^{11}C-L-deprenyl,; ^{11}C-diprenorphine; ^{11}C-raclopride; and ^{11}C-Scherring 23390. J Label Compds and Radiopharm 1993;32:518-20.

Lyon G, Gastaut M. Considerations on the significance attributed to unusual cerebral findings recently described in eight patients with primary generalised epilepsy. Epilepsia 1985;26:365-7.

Madar I, Lesser RP, Krauss G, *et al.* Imaging of ∂- and μ-opioid receptors in temporal lobe epilepsy by positron emission tomography. Ann Neurol 1997;41:358-67.

Manno EM, Sperling MR, Ding X, *et al.* Predictors of outcome after anterior temporal lobectomy: positron emission tomography. Neurology 1994;44:2331-6.

Marangos PJ, Patel J, Boulenger J, Clark-Rosenberg R. Characterisation of the peripheral-type benzodiazepine binding site in brain using ^{3}H-Ro5-4864. Mol Pharmacol 1982;22:26-32.

Marcus EM, Watson CW, Simon SA. An experimental model of some varieties of petit mal epilepsy. Epilepsia 1968;9:233-48.

Marescaux C, Micheletti G, Vergnes M, Rumbach L, Warter JM. Diazepam antagonises GABAmimetics in rats with spontaneous petit mal-like epilepsy. Eur J Pharmacol 1985;113:19-.

Marescaux C, Vergnes M, Depaulis A. Genetic absence epilepsy in rats from Strasbourg: a review. J Neural Transmission 1992;35 (Suppl):37-69.

Margerison JHM, Corsellis JAN. Epilepsy and the temporal lobes. A clinical, electroencephalographic and neuropathological study of the brain in epilepsy. Brain 1966;89:479-530.

Martin D, McNamara JO, Nadler JV. Kindling enhances sensitivity of CA3 hippocampal pyramidal cells to NMDA. J Neurosci 1992;12:1928-35.

Masukawa LM, Higashima M, Kim JH, Spencer DD. Epileptiform discharges in hippocampal brain-slices from epileptic patients. Brain Res 1989;493:168-174.

Mayberg HS, Sadzot B, Meltzer CC, *et al.* Quantification of μ and non-μ receptors in temporal lobe epilepsy using positron emission tomography. Ann Neurol 1991;30:3-11.

Mazziotta JC, Phelps ME, Plummer D, Kuhl DE. Quantitation in positron mission tomography: 5. Physical-anatomical effects. J Comput Assist Tomogr 1981;3:299-308.

McDonald JW, Garofalo EA, Hood T, *et al.* Altered excitatory and inhibitory amino acid receptor binding in hippocampus of patients with temporal lobe epilepsy. Ann Neurol 1991;29:529-41.

McLean MJ, Macdonald RL. Sodium valproate, but not ethosuximide, produces use- and voltage-dependent limitation of high frequency repetitive firing of action potentials of mouse central neurons in cell culture. J Pharmacol Exp Ther 1986;237:1001-11.

McNamara JO. Kindling: an animal model of complex partial epilepsy. Ann Neurol 1984;16 Suppl:S72-6.

Meencke HJ, Janz D. Neuropathological findings in primary generalised epilepsy: A study of eight cases. Epilepsia 1984;25:8-21.

Meencke HJ, Janz D. The significance of microdysgenesis in primary generalised epilepsy: An answer to the consideration of Lyon and Gastaut. Epilepsia 1985a;26:368-71.

Meencke HJ. Neuron density in the Molecular Layer of Frontal Cortex in Primary Generalsied Epilepsy. Epilepsia 1985b;26:368-71.

Meldrum BS, Horton RW, Brierley JB. Epileptic brain damage in adolescent baboons following seizures induced by allylglycine. Brain 1974;97:407-18.

Meldrum BS. Metabolic factors during prolonged seizures and their relation to nerve cell death. In: Delgado-Escueta AV, Wasterlain DM, Treiman DM, Porter RJ, eds. Status epilepticus - Advances in neurology. New York: Raven Press, 1983:261-75.

Meldrum BS, Chapman AG. Benzodiazepine receptors and their relationship to the treatment of epilepsy. Epilepsia 1986;27 (Suppl):3-13.

Meldrum BS. Update on the mechanism of action of antiepileptic drugs. Epilepsia 1996;37 (Suppl 6):S4-S11.

Meltzer CC, Leal JP, Mayberg HS, Wagner HJ, Frost JJ. Correction of PET data for partial volume effects in human cerebral cortex by MR imaging. J Comput Assist Tomogr 1990;14:561-70.

Meltzer CC, Zubieta JK, Brandt J, *et al.* Regional hypometabolism in Alzheimer's disease as measured by positron emission tomography after correction for effects of partial volume averaging. Neurology 1996a;47:454-61.

Meltzer CC, Zubieta JK, Links JM, *et al.* MR-based correction for brain PET measurements for heterogenous gray matter radioactivity distribution. J Cereb Blood Flow Metab 1996b;16:650-8.

Miller LA, Munoz DG, Finmore M. Hippocampal sclerosis and human memory. Arch Neurol 1993;50:391-4.

Minamato Y, Itano T, Tokuda M, *et al.* In vivo microdialysis of amino acid neurotransmitters in the hippocampus of amygdaloid kindled rats. Brain Res 1992;573:343-8.

Mody I, Heinemann I. NMDA receptors of dentate gyrus granule cells participate in synaptic transmission following kindling. Nature 1987;326:701-4.

Möhler H, Richards JG. Agonist and antagonist benzodiazepine receptor interaction in vitro. Nature 1981;294:763-5.

Molaie M, Kadzielawa K. Effect of naloxone infusion on the rate of epileptiform discharges in patients with complex partial seizures. Epilepsia 1989;30:194-200.

Moore SD, Madamba SG, Schweitzer P, Siggins GR. Voltage-dependent effects of opioid peptides on hippocampus CA3 pyramidal neurons in vitro. J Neurosci 1994;14:809-20.

Morell F. Secondary epileptogenesis in man. Arch Neurol 1985;42:318-35.

Morimoto K, Sanei T, Sato K. Comparative study of the anticonvulsant effect of gamma-aminobutyric acid agonists in the feline kindling model of epilepsy. Epilepsia 1993;34:1123-9.

Morris ED, Fisher RE, Alpert NM, Rauch SL, Fischman AJ. In vivo imaging of neuromodulation using positron emission tomography: optimal ligand characteristics and task length for detection of activation. Human Brain Mapping 1995;3:35-55.

Mott DD, Bragdon AC, Lewis DV, Wilson WA. Baclofen has a proepileptic effect in the rat dentate gyrus. J Pharmacol Exp Ther 1989;249:721-5.

Müller-Gärtner HW, Links JM, Prince JL, *et al.* Measurement of radiotracer concentration in brain gray matter using positron emission tomography: MRI-based correction for partial volume effects. J Cereb Blood Flow Metab 1992;12:571-83.

Murphy MJ, Yamada T. Clonazepam therapy in reading epilepsy. Neurology 1981;31:233.

Naquet R, Meldrum BS. Photogenic seizures in baboon. In: Purpura DP, Penry JK, Woodbury DM, Tower DB, Waiter RD, eds. Experimental models of epilepsy - A manual for the laboratory worker. New York: Raven, 1972:373-406.

Nehlig A, Vergnes M, Marescaux C, Boyet S. Mapping of cerebral energy metabolism in rats with genetic generalised nonconvulsive epilepsy. J Neural Transm 1992;35 (Suppl):141-53.

Nehlig A, Vergnes M, Marescaux C, Boyer S. Cerebral energy metabolism in rats with genetic absence epilepsy is not correlated with the pharmacological increase or suppression of spike-wave discharges. Brain Res 1993;618:1-8.

Neumaier JF, Chavkin C. Release of endogenous opioid peptides displaces. 3H diprenorphine binding in rat hippocampal slices. 1989;493:292-302.

Newton MR, Berkovic SF, Austin MC, *et al.* Dystonia, clinical lateralisation, and regional blood flow changes in temporal lobe seizures. Neurology 1992;42:371-7.

Niedermeyer E, Laws ER, Walker AE. Depth EEG findings in epileptics with generaiised spike-wave complexes. Arch Neurol 1969;21:51-8.

Nutt DJ, Cowen PJ, Little HJ. Unusual interactions of benzodiazepine receptor antagonists. Nature 1982;295:426-38.

Nutt DJ, Glue P, Lawson CSW. Flumazenil provocation of panic attacks. Arch Psychol 1990;47:917-25.

Ochs RF, Gloor P, Tyler JL, *et al.* Effect of generalised spike-and-wave discharge on glucose metabolism measured by positron emission tomography. Ann Neurol 1987;21:458-64.

Olsen RW, McGabe RT, Wamsley JK. $GABA_A$ receptor subtypes: autoradiographic comparison of GABA, benzodiazepine and convulsant binding sites in rat central nervous system. J Chem Neuroanat 1990;3:59-76.

Onishi H, Koide S, Yamagami S, Kawakita Y. Developmental and regional alteration of methionine enkephalin-like immunoreactivity in siezure-susceptible E1 mouse brain. Neurochem Res 1990;15:83-7.

Ortiz JG, Negron AE, Thomas AP, *et al.* GABAergic neurotransmission in the C57BW10 sps/sps mouse mutant: a model of absence seizures. Exp Neurol 1991;113:338-43.

Panayiotopoulos CP, Obeid T, Waheed G. Differentiation of typical absence seizures in epileptic syndromes. A video EEG study of 224 seizures in 20 patients. Brain 1989; 112: 1039-56.

Panayiotopoulos CP, Chroni E, Daskopoulos C, *et al.* Typical absence seizures in adults: clinical, EEG, video-EEG findings and diagnostic/syndromic considerations. J Neurol Neurosurg Psychiat 1993;55:1002 - 8.

Panayiotopoulos CP, Obeid T. Juvenile myoclonic epilepsy: a 5-years prospective study. Epilepsia 1994;35:285-96.

Pasternak GW. Pharmacological mechanisms of opiate analgesics. Clinical Neuropharmacology 1993;16:1-18.

Penfield W, Jasper HH. Epilepsy and the functional anatomy of the brain. Boston: Little, Brown and Company, 1954:896.

Perry CB, Mullis KB, Oie S, Sadee W. Opiate antagonist receptor binding in vivo: evidence for a new receptor model. Brain Res 1980;199:49.

Pert CB, Kuhar MJ, Snyder SH. Autoradiographic localisation of the opiate receptor in rat brain. Life Sci 1975;16:1849-54.

Peters BWMM, Van Rijn CM, Vossen JHM, Coenen AML. Effects of GABAergic agents on spontaneous non-convulsive epilepsy, EEG and behaviour in the WAG/Rij strain. Life Sci 1989;45:1171-6.

Petersen SE, Fox PT, Snyder AZ, Raichle ME. Activation of extrastriate and frontal cortical areas by visual words and word-like stimuli. Science 1990;249:1041-4.

Petroff OAC, Rothman DL, Behar KL, Mattson RH. Initial observations on the effect of gabapentin on brain GABA in patients with epilepsy. Ann Neurol 1996;39:95-9.

Pfeiffer A, Pasi A, Mehraein P, Herz A. Opiate receptor binding sites in human brain. Brain Res 1982;248:87-96.

Phelps ME. Positron emission tomography. In: Mazziotta JC, Gilman S, eds. Clinical brain imaging: principles and applications. 39th ed. Philadelphia: F.A.Davis, 1993:71-107.

Piguet P. $GABA_A$- and $GABA_B$-mediated inhibition in the rat dentate gyrus in vitro. Epilepsy Res 1993;16:111-22.

Pleuvrey BJ. Opioid receptors and their ligands: natural and unnatural. Br J Anaesth 1991;66:370-80.

Press WH, Flannery BP, Teukolsky SA, Vetterling WT. Modeling of data: Non linear models. Cambridge, New-York: 1988.

Prevett MC, Duncan JS, Jones T, Fish DR, Brooks DJ. Demonstration of thalamic activation during typical absence seizures using H_20-0-15 and PET. Neurology 1995a;45:1396-1402.

Prevett MC, Lammertsma AA, Brooks DJ, *et al.* Benzodiazepine-$GABA_A$ receptors in idiopathic generalised epilepsy measured with ^{11}C-flumazenil and positron emission tomography. Epilepsia 1995b;36:113-21.

Prevett MC, Lammertsma AA, Brooks DJ, *et al.* Benzodiazepine-$GABA_A$ receptor binding during absence seizures. Epilepsia 1995c;36:592-9.

Price CJ, Wise RJS, Watson JDG, *et al.* Brain activity during reading - the effects of exposure duration and task. Brain 1994;117:1255-69.

Pritchett DB, Sontheimer H, Shivers ED. Importance of a novel $GABA_A$ receptor subunit for benzodiazepine pharmacology. Nature 1989;338:582-5.

Quesnay LF, Risinger MW, Shewmon AD. Extracranial EEG evaluation. In: Engel JJ, ed. Surgical treatments of the epilepsies. 2nd ed. New York: Raven Press, 1993:173-95.

Radhakrishnan K, Silbert PL, Klass DW. Reading epilepsy - an appraisal of 20 patients diagnosed at the Mayo Clinic, Rochester, Minnesota, between 1949 and 1989, and delineation of the epileptic syndrome. Brain 1995;118:75-89.

Raichle ME. Circulatory and metabolic correlates of brain function in normal humans. In: Plum F, ed. Handbook of physiology: the nervous system. New York: American Physiological Society-Oxford UP, 1987:643-74.

Rainnie DG, Asprodini EK, Shinnickgallagher P. Kindling-induced long-lasting changes in synaptic transmission in the basolateral amygdala. J Neurophysiol 1992;67:443-54.

Ramabadran K, Bansinath M. Endogenous opioid peptides and epilepsy. Int J Clin Pharmacol Ther Toxicol 1990;28:47-62.

Ranicar ASO, Williams CW, Schnorr L, *et al.* The on-line monitoring of continuously withdrawn arterial blood during PET studies using a single BGO/photomultiplier assembly and non-stick tubing. Medical Progress Through Technology 1991;17:259-64.

Raymond AA, Fish DR, Stevens JM, *et al.* Association of hippocampal sclerosis with cortical dysgenesis in patients with epilepsy. Neurology 1994;44:1841-5.

Reigel CE, Jobe PC, Dailey JW, Stewart JJ. Responsiveness of genetically epilepsy prone rats to intracerebroventricular morphine-induced seizures. Life Sci 1988;42:1743-9.

Rho JM, Donevan SD, Rogawski MA. Mechanism of action of the anticonvulsant felbamate: opposing effects on N-methyl-D-Aspartate and y-amino butyric acid A receptors. Ann Neurol 1994;35:229-34.

Rice A, Rafiq A, Shapiro SM, Jakoi ER, Coulter DA, DeLorenzo RJ. Long-lasting reduction of inhibitory function and g-aminobutyric acid type A receptor subunit mRNA expression in a model of temporal lobe epilepsy. Proc Natl Acad Sci USA 1996;93:9665-9669

Richards JG, Miihler H. Benzodiazepine receptors. Neuropharmacology 1984;23:233-42.

Richardson MP, Koepp MJ, Brooks DJ, Fish DF, Duncan JS. Benzodiazepine receptors in focal epilepsy with cortical dysgensis: an 11C-Flumazenil PET study. Ann Neurol 1996;40:188-98.

Richardson MP, Koepp MJ, Brooks DJ, Duncan JS. ^{11}C-Flumazenil PET in neocortical epilepsy. ***Neurology*** 1998;51:485-492.

Risinger MW, Engel JJ, Van Ness PC, Henry TR, Crandall PH. Ictal localisation of temporal lobe seizures with scalp/sphenoidal recordings. Neurology 1989;39:1288-93.

Robb RA, Hanson DP. ANALYZE: A software system for biomedical image analysis. First Conference on Visualisation in Biomedical Computing. Atlanta, 1990:507-18.

Rocca WA, Sharbrough FW, Hauser WA, Annegers JF, Schoenberg BS. Risk factors for complex partial seizures: a population based case-control study. Ann Neurol 1987;21:22-31.

Rogawski MA, Porter RJ. Antiepileptic drugs: Pharmacological mechanisms and clinical efficacy with consideration of promising developmental stage compounds. Pharmacological Reviews 1990;42:223-86.

Rooneengstrom E, Hillered L, Flink R, *et al.* Intracerebral microdialysis of extracellular amino acids in human epileptic focus. J Cereb Blood Flow Metab 1992;12:873-6.

Rothstein JD, Garland W, Puia G, *et al.* Purification and characterization of naturally occuring benzodiazepine receptor ligands in rat and human brain. J Neurochem 1992;58:2102-15.

Rousset OG, Ma Y, Marenco S, Wong DF, Evans AC. In vivo correction for partial volume effects in PET: accuracy and precision. NeuroImage 1995;2:33.

Rowe CC, Berkovic SF, Austin MC, *et al.* Visual and quantitative analysis of interictal SPECT with technetium-99m HMPAO in temporal lobe epilepsy. J Nucl Med 1991;32:1688-94.

Sadzot B, Price JC, Mayberg HS, *et al.* Quantification of human opiate receptor concentration and affinity using high and low specific activity ^{11}C-diprenorphine and positron emission tomography. J Cereb Blood Flow Metab 1991;11:204-19.

Sadzot B, Debets RM, Delfiore G, *et al.* ^{11}C-Flumazenil positron emission tomography: an in vivo marker of neuronal loss in temporal lobe epilepsy. Epilepsia 1994;35(Suppl 7):29.

Sato S, White BG, Penry JK, *et al.* Valproic acid versus ethosuximide in the treatment of absence seizures. Neurology 1982;32:157-63.

Savage DD, Mills SA, Jobe PC, Reigel CE. Elevation of naloxone sensitive ^{3}Hdihydromorphine binding in hippocampal formation of genetically epilepsy prone rats. Life Sci 1988;43:239-46.

Savic I, Persson A, Roland P, *et al.* In-vivo demonstration of reduced benzodiazepine receptor binding in human epileptic foci. Lancet 1988;2:863-6.

Savic I, Widen L, Thorell JO, *et al.* Cortical benzodiazepine receptor binding in patients with generalised and partial epilepsy. Epilepsia 1990;31:724-30.

Savic I, Ingvar M, Stone Elander S. Comparison of ^{11}C-flumazenil and ^{18}F-FDG as PET markers of epileptic foci. J Neurol Neurosurg Psychiatry 1993;56:615-21.

Savic I, Pauli S, Thorell JO, Blomqvist G. In vivo demonstration of altered benzodiazepine receptor density in patients with generalised epilepsy. J Neurol Neurosurg Psychiatry 1994;57:797-804.

Savic I, Thorell JO, Roland P. ^{11}C-Flumazenil positron emission tomography visualises frontal epileptogenic regions. Epilepsia 1995;36:1225-32.

Savic I, Svanborg E, Thorell JO. Cortical benzodiazepine receptor changes are related to frequency of partial seizures: a positron emission tomography study. Epilepsia 1996;37:236-44.

Saygi S, Spencer SS, Scheyer R, *et al.* Differentiation of temporal lobe ictal behavior associated with hippocampal sclerosis and tumors of temporal lobe. Epilepsia 1994;35:737-42.

Schmidt D, Tsai J, Janz D. Febrile seizures in patients with complex partial seizures. Acta Neurol Scand 1985;72:68-71.

Schneidemann JH, Sterling CA, Luo R. Hippocampal plasticity following epileptiform bursting produced by $GABA_A$ antagonists. Neuroscience 1994;59:259-73.

Seeger TF, Sforzo GA, Pert CB, Pert A. In vivo autoradiography: visualisation of stress-induced changes in opiate receptor occupancy in the rat brain. Brain Res 1984;305:303-11.

Semah F, Baulac M, Hasboun D, *et al.* Is interictal temporal hypometabolism related to mesial temporal sclerosis? A Positron Emission Tomgraphy / Magnetic Resonance Imaging confiontation. Epilepsia 1995;36:447-56.

Shields WD, Saslow E. Myoclonic, atonic, and absence seizures following institution of carbamazepine therapy in children. Neurology 1983;33:1487-9.

Shin C, Rigsbee LC, McNamara JO. Anti-seizure and anti-epileptogenic effect of gamma-vinyl gamma-aminobutyric acid in amygdaloid kindling. Brain Res 1986;398:370-4.

Sieghart W. $GABA_A$ receptors: ligand-gated Cl- ion channels modulated by multiple drug binding sites. Trends Pharmacol Sci 1992;13:446-50.

Sieghart W. Multiplicity of $GABA_A$-benzodiazepine receptors. Trends Pharmacol Sci 1989;10:407-11.

Sivilotti L, Nistri A. GABA receptor mechanisms in the central nervous system. Frog Neurobiol 1991;36:35-92.

Sloviter RS. Decreased hippocampal inhibition and a selective loss of interneurons in experimental epilepsy. Science 1987;235:73-6.

Sloviter RS. Permanently altered hippocampal structure, excitability, and inhibition after experimental status epilepticus in the rat: the "dormant basket cell" hypothesis and its possible relevance to temporal lobe epilepsy. Hippocampus 1991;1:41-66.

Sloviter RS. The functional organisation of the hippocampal dentate gyrus and its relvance to the pathogenesis of temporal lobe epilepsy. Ann Neurology 1994;35:640-54.

Snead OC, Bearden LJ. Anticonvulsants specific for petit mal antagonise epileptogenic effect of leucine enkephalin. Science 1980;210:1031-3.

Snead OC, Hosey LC. Exacerbation of seizures in children by carbamazepine. New Engl J Med 1985;313:916-21.

Snead OC. Gamma-hydroxybutyrate model of generalised absence seizures: further characterisation and comparison with other absence models. Epilepsia 1988;29:361-8.

Snead OC. Pharmacological models of generaiised absence seizures in rodents. J Neural Transm 1992a;35 (Suppl):7-19.

Snead OC, Depaulis A, Banerjee PK, Hechler V, Vergnes M. The GABAA receptor complex in experimental absence seizures in rat: an autoradiographic study. Neurosci Lett 1992b;140:9-12.

Snead OC, Liu CC. $GABA_A$ receptor function in the y-hydroxybutyrate model of generalised absence seizures. Neuropharmacology 1993;32:401-9.

So N, Quesney LF, Jones-Gotman M, Olivier A, Anderman F. Depth electrode investigations in patients with bitemporal epileptiform abnormalities. Ann Neurol 1989;25:423-31.

Spencer SS. The relative contribution of MRI, SPECT and PET imaging in epilepsy. Epilepsia 1994;35 (Suppl 6):72-89.

Spinks TJ, Jones T, Bailey DL, *et al.* Physical performance of a new positron tomograph with retractable septa. IEEE Med Imag Conf Rec 1991;38:1313-7.

Spreafico R, Mennini T, Danober L, *et al.* $GABA_A$ receptor impairment in the genetic absence epilepsy rats from Strasbourg (GAERS): an immunocytochemical and receptor binding auroradiographic study. Epilepsy Res 1993;15:229-38.

Stefan H, Plouin P, Fichsel H, Jalin C, Burr W. Progabide for previously untreated absence epilepsy. Epilepsy Res 1988;2:132-6.

Sutula T, Xiao-Xian H, Cavazos J, Scott G. Synaptic reorganisation in the hippocampus induced by abnormal functional activity. Science 1988;239:1147-50.

Sutula T. Experimental models of temporal lobe epilepsy: new insights from the study of kindling and synaptic reorganisation. Epilepsia 1990;31:45-54.

Sutula TP. Reactive changes in epilepsy: cell death and axon sprouting induced by kindling. Epilepsy Res 1991:62-70.

Swanson TH. The pathophysiology of human mesial temporal lobe epilepsy. J Clin Neurophysiol 1995;12:2-22.

Swartz BE, Simpkins F, Halgren E, *et al.* Visual working memory in primary generalized epilepsy: an ^{18}FDG-PET study. Neurology 1997; 47: 1203-12

Szelies B, Weber-Luxenberger G, Pawlik G, *et al.* Focus detection in temporal lobe epilepsy by MRI coregistered quantitative flumazenil and FDG PET. NeuroImage 1996;3:109-18.

Tadokoro M. Parametric images of 11C-diprenorphine binding using spectral analysis of dynamic PET images acquired in 3D. In: Umeura K, ed. Quantification of Brain Function. Tracer Kinetics and Image Analysis in Brain PET. Amsterdam: Elsevier Science Publishers, 1993:281-98.

Tanska E, North RA. Opioid actions on rat anterior cingulate cortex neurons in vitro. J Neurosci 1994;14:1106-13.

Tauck DL, Nadler JV. Evidence of functional mossy fiber sprouting in hippocampal formation of kainic acid treated rats. J Neurotox 1985:1016-22.

Theodore WH, Newmark ME, Sato S, *et al.* ^{18}F-fluorodeoxyglucose positron emission tomography in refractory complex partial seizures. Ann Neurol 1983;14:429-37.

Theodore WH, Brooks R, Margolin R, *et al.* Positron emission tomography in generalised seizures. Neurology 1985;35:684-90.

Theodore WH, Fishbein D, Dubinsky R. Patterns of cerebral glucose metabolism in patients with partial seizures. Neurology 1988;45:1201-6.

Theodore WH, Carson RE, Andreasen P, *et al.* PET imaging of opiate receptor binding in human epilepsy using ^{18}F-cyclofoxy. Epilepsy Res 1992;13:129-39.

Theodore WH, Gaillard WD, Sato S, Kufta C, Leiderman DB. Measurement of cerebral blood flow and temporal lobectomy. Ann Neurol 1994;36:241-4.

Theodore WH. Effect of seizures on cerebral blood flow measured with ^{15}O-H_2O and positron emission tomography. Epilepsia 1996;37:796-802.

Tietz EI, Chui TH. GABA-stimulated chloride uptake in amygdala kindled rats. Neurosci Lett 1991;123:269-72.

Timmings FL, Richens A. Lamotrigine in primary generalised epilepsy. Lancet 1992;339:1300-1.

Tortella FC, Long JB. Endogenous anticonvulsant substance in rat CSF after a generalised seizure. Science 1985;228:1106-8.

Tortella FC. Endogenous opioid peptides and epilepsy: quieting the seizing brain? TIPS 1988a;9:366-72.

Tortella FC. Opioid peptides: possible physiological role as endogenous anticonvulsants. In: Ferrendelli JA, Collins RC, Johnson EM, eds. Neurobiology of amino acids, peptides and trophic factors. New York: Kluwer Academic Publishers, 1988b:163-79.

Urca G, Frenk H, Liebesking JC, Taylor AN. Morphine and enkephalin: analgesic and epileptic properties. Science 1977;197:83-6.

Van Paesschen W, Sisodiya S, Connelly A, *et al.* Quantitative hippocampal MRI and intractable temporal lobe epilepsy. Neurology 1995;45:2233-40.

Van Paesschen W, Connelly A, King MD, Jackson GD, Duncan JS. The spectrum of hippocampal sclerosis: a quantitative magnetic resonance imaging study. Annals of Neurology 1997a;41:41-51.

Van Paesschen W, Revesz T, Duncan JS, King MD, Connelly A. Quantitative neuropathology and quantitative magnetic resonance imaging of the hippocampus in temporal lobe epilepsy. Ann Neurol 1997b;42:756-66.

Vanderzant C, Fitz R, Holmes G, Greenberg HS, Sackellares JC. Treatment of primary reading epilepsy with valproic acid. Arch Neurol 1982;39:452-3.

Velasco M, Velasco F, Velasco AL, Lujrin M, Velasquez del Mercado J. Epileptiform EEG activities of the centromedian thalamic nuclei in patients with intractable partial motor, complex partial, and generalised seizures. Epilepsia 1989;30:295-306.

Verdoorn TA, Draguhn A, Ymer S, Seeburg PH, Sakmann B. Functional properties of recombinant rat $GABA_A$ receptors depend upon subunit composition. Neuron 1990;4:919-28.

Vergnes M, Marescaux C, Micheletti G, *et al.* Spontaneous paroxysmal electroclinical patterns in rat: a model of generalised non-convulsive epilepsy. Neurosci Lett 1982;33:97-101.

Vergnes M, Marescaux C, Micheletti G, *et al.* Enhancement of spike and wave discharges by GABAmimetic drugs in rats with spontaneous petit mal-like epilepsy. Neurosci Lett 1984;44:91-4.

Vergnes M, Marescaux C, Depaulis A, Micheletti G, Warter JM. Spontaneous spike-and-wave discharges in thalamus and cortex in a rat model of genetic petit mal like seizures. Exp Neurol 1987;96:127-36.

Vergnes M, Marescaux C. Cortical and thalamic lesions in rats with genetic absence epilepsy. J Neural Transm 1992;35 (Suppl):71-83.

von Krosigk M, Bal T, McCormick DA. Cellular mechanisms of a synchronised oscillation in the thalamus. Science 1993;261:361-4.

Walczack TS. Neocortical temporal lobe epilepsy. Epilepsia 1995;36:633-5.

Wallace SJ. Prognosis for non-febrile seizures. In: Wallace SJ, ed. The child with febrile seizures. London: Butterworth, 1988:109-26.

Watson C, Andermann F, Gloor P, *et al.* Anatomic basis of amygdaloid and hippocampal volume measurement by magnetic resonance imaging. Neurology 1992;42:1743-50.

Weeks RA, Cunningham VJ, Piccini P, Waters S, Harding AE, Brooks DJ. ^{11}C-diprenorphine binding in Huntington's disease: A comparison of region of interest analysis with statistical parametric mapping. J Cereb Blood Flow Metab 1997; 17:943-949.

Wieser HG. Temporal lobe or psychomotor status epilepticus. Electroenceph Clin Neurophysiol 1980;48:558-72.

Wieser HG. Psychomotor seizures of hippocampal-amygdalar origin. In: Pendley TA, Meldrum BS, eds. Recent advances in epilepsy. Edingburgh: Churchill Livingstone, 1986:57-79.

Wieser HG. The phenomenology of limbic seizures. In: Wieser HG, Speckmann EJ, Engel JJ, eds. The epileptic focus. London, Paris: John Libbey, 1987:113-36.

Wieser HG, Engel JJ, Williamson PD, Babb TL, Gloor P. Surgically remediable temporal lobe syndromes. In: Engel JJ, ed. Surgical treatment of the Epilepsies. 2nd ed. New York: Raven Press, 1993:49-64.

Williams D. A study of thalamic and cortical rhythms in petit mal. Brain 1953;76:50-69.

Williams RW, Rakic P. Three-dimensional counting: an accurate and direct method to estimate numbers of cells in sectioned material. J Comp Neurol 1988;278:344-52.

Wisden W, Laurie DJ, Monyer H, Seeburg PH. The distribution of 13 GABAA receptor subunit mRNAs in the rat brain. 1. Telencephalon,diencephalon , mesencephalon. J Neurosci 1992;12:1040-62.

Woermann FG, Sisodiya SM, Free SL, Duncan JS. Quantitative MRI in patients with idiopathic generalised epilepsy - Evidence of widespread cerebral structural changes. Brain 1998a;121:1661-1667

Woermann FG, Free SL, Koepp MJ, Sisodiya SM, Duncan JS. Quantitative MRI in patients with juvenile myoclonic epiplepsy (JME): an objective voxel-based comparison of structural imaging data. NeuroImage 1998b;7:S502.

Wolf HK, Spänle M, Müller MB, *et al.* Hippocampal loss of the $GABA_A$ receptor $\alpha 1$ subunit in patients with chronic pharmacoresistant epilepsies. Acta Neuropathol 1994;88:313-9.

Wolf P, Inoue Y. Therapeutic response of absence seizures in patients of an epileptic clinic for adolescents and adults. J Neurol 1984;231:2225-229.

Wolf P. Reading epilepsy. In: Roger J, Bureau M, Dravet C, *et al.*, eds. Epileptic syndromes in infancy, childhood and adolescence. 2nd ed. London: John Libbey, 1992:281-98.

Woods RP, Mazziotta JC, Cherry SR. MRI-PET registration with automated algorithm. J Comp Assist Tomogr 1993;17:536-46.

Worsley KJ, Evans AC, Marrett S, Neelin P. A three-dimensional statistical analysis for rCBF activation studies in human brain. J Cereb Blood Flow Metab 1992;12:900-18.

Zezula J, Cortes R, Probst A, Palacios JM. Benzodiazepine receptor sites in the human brain: Autoradiographic mapping. Neuroscience 1988;25:771-95.

Zieglgänsberger W, French ED, Siggins GR, Bloom FE. Opioid peptides may excite hippocampal pyramidal neurons by inhibiting adjacent inhibitory interneurons. Science 1979;205:415-6.